2009

PALEOGEOGRAPHIC RECONSTRUCTUION OF THE ST. LAWRENCE PROMONTORY, WESTERN NEWFOUNDLAND

John Stefan Allen
University of Kentucky, john-allen@uky.edu

PALEOGEOGRAPHIC RECONSTRUCTUION OF THE ST. LAWRENCE PROMONTORY, WESTERN NEWFOUNDLAND

ABSTRACT OF DISSERTATION

A dissertation submitted in partial fulfillment of the
Requirements for the degree of Doctor of Philosophy in the
College of Arts and Sciences at
the University of Kentucky

By
John Stefan Allen

Lexington, Kentucky

Director: Dr. William A. Thomas, Professor of Geology

Lexington, Kentucky

2009

ABSTRACT OF DISSERTATION

John Stefan Allen

The Graduate School

University of Kentucky

2009

ABSTRACT OF DISSERTATION

PALEOGEOGRAPHIC RECONSTRUCTUION OF THE ST. LAWRENCE PROMONTORY, WESTERN NEWFOUNDLAND

Neoproterozoic-Early Cambrian continental rifting related to the breakup of the supercontinent Rodinia framed the continental margin of eastern Laurentia and the departing cratons around the opening Iapetus Ocean. The result of continental extension was the production of a zig-zag set of promontories and embayments on the eastern Laurentian margin defined by northeast-trending rift segments offset by northwest-trending transform faults.

The St. Lawrence promontory defines the Laurentian margin in western Newfoundland. There, Neoproterozoic-Carboniferous clastic, volcanic, and carbonate successions record protracted continental rifting and passive-margin thermal subsidence followed by destruction of the margin during the early, middle, and late Paleozoic Appalachian orogenic cycles. Palinspastic restoration of deformed Paleozoic strata by a set of balanced cross sections resolves the structure, stratigraphy, and timing of Paleozoic tectonic events on the St. Lawrence promontory. Synrift and post-rift subsidence profiles, as well as abrupt along-strike variations in the age, thickness, facies, and the palinspastically restored extent of synrift and post-rift stratigraphy, indicate the St. Lawrence promontory was founded upon a low-angle detachment rift system. Upper-plate margins, lower-plate margins, and transform faults that bound zones of oppositely dipping low-angle detachments are recognized along specific segments of the promontory.

A detailed U-Pb and Lu-Hf isotopic detrital zircon study elucidates the identity of specific cratons conjugate to the St. Lawrence promontory in the pre-rift configuration of Rodinia. Approximately 510 zircons from 9 samples collected from basement and overlying Early Cambrian synrift rocks in Newfoundland were analyzed by LA-ICP-MS for U-Pb ages and Hf isotopic ratios. Synrift samples yielded ages ranging from 3605 Ma to 544 Ma with maximum age frequencies of 1000-1200 Ma (Grenville), 1350-1450 Ma (Pinware), and 2650-2800 Ma (Superior), while two basement samples yielded U-Pb ages of 1044 Ma and 1495 Ma. $^{177}Hf/^{176}Hf$ isotopic ratios of ca.1000 Ma, 1200 Ma, and 1400-1600 Ma zircons from Newfoundland basement and synrift rocks are a close match to

reported $^{177}Hf/^{176}Hf$ ratios for Baltican zircons of the same vintage, suggesting that Baltica was conjugate to the St. Lawrence promontory.

KEYWORDS: Appalachian orogen, Laurentian margin, Humber zone, St. Lawrence promontory, western Newfoundland

_____

Student's Signature

_____

Date

PALEOGEOGRAPHIC RECONSTRUCTUION OF THE ST. LAWRENCE PROMONTORY, WESTERN NEWFOUNDLAND

By

John Stefan Allen

_____

Director of Dissertation

_____

Director of Graduate Studies

_____

RULES FOR THE USE OF DISSERTATIONS

Unpublished dissertations submitted for the Doctor's degree and deposited in the University of Kentucky Library are as a rule open for inspection, but are to be used only with due regard to the rights of the authors. Bibliographical references may be noted, but quotations or summaries of parts may be published only with the permission of the author, and with the usual scholarly acknowledgments.

Extensive copying or publication of the dissertation in whole or in part also requires the consent of the Dean of the Graduate School of the University of Kentucky.

A library that borrows this dissertation for use by its patrons is expected to secure the signature of each user.

Name	Date

DISSERTATION

John Stefan Allen

The Graduate School

University of Kentucky

2009

PALEOGEOGRAPHIC RECONSTRUCTUION OF THE ST. LAWRENCE PROMONTORY, WESTERN NEWFOUNDLAND

DISSERTATION

A dissertation submitted in partial fulfillment of the
Requirements for the degree of Doctor of Philosophy in the
College of Arts and Sciences at
the University of Kentucky

By
John Stefan Allen

Lexington, Kentucky

Director: Dr. William A. Thomas, Professor of Geology

Lexington, Kentucky

2009

To my parents,
To my sister,
To my friends and family…

…and to all those foolish enough to dream,
and stubborn enough to make their dreams a reality…

ACKNOWLEDGEMENTS

I wish to begin by conveying my deepest respect and gratitude to Dr. William A. Thomas, who is my faculty advisor, dissertation committee chair, and good friend. Dr. Thomas believed in me long before this project manifest itself and gave me that opportunity to pursue a Ph.D. when others would not. Thank you. I would also like to thank the members of my dissertation committee: Dr. Edward Woolery, Dr. Kieran O'Hara, Dr. Richard Sweigard, and Dr. Alice Turkington. Your classes prepared me for the tough work necessary to complete my degree and your constructive criticism more than helped to improve the quality of the research in my dissertation, as well as its presentation herein. I consider you all friends, as well as colleagues.

Next I would like to extend my gratitude to Dr. Denis Lavoie and Dr. Cees van Staal at the Geological Survey of Canada, who approached Dr. Thomas and myself with the idea for this research in the spring of 2006, as well as acquired the necessary funding for field work through various government grants. Thank you for believing in me. With out your help and expertise, this dissertation would literally not have happened. I would also like to thank Dr. John Waldron, Dr. Ian Knight, and Dr. Doug Boyce for all of there help, suggestions, and criticism concerning the geology of western Newfoundland.

I want to extend my deepest thanks to all of the friends that I made in my three years in Lexington. Without your support and friendship, I would not have been able to complete this dissertation. So, to Matt Bahm, Dr. Rick Bowersox, Joe Chase, Trish Coakley, Brian Cook, Liz Dodson, Jennifer Gifford, Estifanos Haile, John Hickman, Dr. George Kamenov, Carrie Kidd, Dr. Ken MacPherson, Sarah Mardon, John May, Amy Murphy, Terry Randell, Josh Sexton, Dr. James and Katy Ward, John Wardon, Brent Wilhelm, James Whitt, Devi, Lisa, Marilyn and James, and anyone I may have missed, thank you.

Finally, I would like to thank my Mom and Dad, Drs. Kathleen and Tom Allen, for all of the love and support they have given me throughout my entire graduate school experience, from NC State to UK. It's been a long trip, and thank you for putting up with three more years of grad school. I also want to thank my sister Kara for putting up with a geologist brother. Believe it or not you helped me through grad school, as well. And thank you to all of my family for being there for me when I needed you most. Thank you.

TABLE OF CONTENTS

LIST OF TABLES

LIST OF FIGURES

LIST OF PLATES

CHAPTER 1 - PREAMBLE

1.1 INTRODUCTION, PROBLEM STATEMENTS, HYPOTHESES, AND OBJECTIVES OF STUDY

Continental rifting and final breakup of the supercontinent Rodinia at the end of the Neoproterozoic framed the continental margin of eastern Laurentia and the departing cratons around the opening Iapetus Ocean (e.g., Hoffman, 1991; Dalziel, 1997; Cawood et al., 2001). Continental extension related to the breakup of Rodinia produced promontories and embayments on the eastern Laurentian margin defined by an orthogonally zig-zag set of northeast-trending rifts offset by northwest-trending transform faults (Thomas, 1977; 1991). Geology of the St. Lawrence promontory in western Newfoundland represents the northernmost expression of this ancient continental rift system, elements of which are still preserved in the North American Appalachian mountain belt. Exposed along the shorelines and coastal lowlands of western Newfoundland, Neoproterozoic and Paleozoic rocks provide an outstanding record of protracted continental rifting related to the opening of the Iapetus Ocean followed by the formation of an extensive carbonate passive margin that was later deformed by multiple westward progressing Paleozoic thrust belts and foreland basins (e.g. Williams and Hiscott, 1987; Williams, 1995; Cawood et al., 2001; Lavoie et al., 2003; van Staal, 2005).

While the general geologic history of the Paleozoic eastern Laurentian margin in the northern Appalachians, including the St. Lawrence promontory, is now well known and accepted several important questions remain unresolved. What is the structural architecture of the eastern Laurentian rifted margin on the St. Lawrence promontory? Is the architecture of the Neoproteoroizc-Paleozoic rift and passive margin expressed in western Newfoundland consistent across the entire northern Appalachian orogen? What are the specific matches of conjugate cratons to the St. Lawrence promontory in the pre-rift supercontinent Rodinia configuration? The primary goal of this dissertation is to answer these questions, as well as, present an accurate and detailed structural and stratigraphic history for the St. Lawrence promontory that spans the 1350 million year time span between the Mesoproterozoic and the late Paleozoic.

Problem Statement 1: The St. Lawrence promontory in western Newfoundland is part of an extensive continental rift system that was active during the Neoproterozoic and early Paleozoic (e.g., Rankin, 1976; Thomas, 1977; 1991; 2006; Cawood et al. 2001). Structural and stratigraphic observations from the Laurentian margin preserved in the southern Appalachian-Ouachita orogen highlight an underlying continental rift that evolved as a simple-shear, low-angle detachment rift system (Thomas, 1993; Thomas and Astini; 1999). This model illustrated the need for palinspastic reconstruction of a rifted margin that is now dispersed in an orogenic belt. The model of Thomas and Astini (1999) did not extend to the northern Appalachians, however, leaving a substantial gap in our understanding of the four-dimensional development of the eastern Laurentian rifted margin, including the St. Lawrence promontory. No comprehensive study to date has attempted to demonstrate the four-dimensional tectonic history of the Laurentian margin exposed in the northern Appalachians, nor has there been an attempt to test alternative hypotheses.

Hypothesis 1: The Neoproterozoic-early Paleozoic eastern Laurentian margin in the northern Appalachians, with specific reference to the St. Lawrence promontory of western Newfoundland, developed from a simple-shear, low-angle detachment rift system.

Objective A: Determine if regional lateral variations in the age, thickness, facies, composition, and geophysical attributes of synrift and post-rift successions distributed along the deformed northern Appalachian margin conform to proposed models for a low-angle detachment rift model.

Objective B: Palinspastically reconstruct the St. Lawrence promontory to test if the distribution of synrift and post-rift sediments and structures fit a low-angle detachment model for this segment of the eastern Laurentian margin.

Summary of results:

The first objective of the dissertation is to determine if regional stratigraphic and structural observations from the northern Appalachians conform to any specific model for the development and evolution of a continental rift system. The function of Objective A is to produce a working hypothesis for the evolution of the eastern Laurentian continental rift and passive margin that can later be tested more rigorously with the geology exposed in western Newfoundland. A synthesis of along-strike variations in the age, facies, and thickness of synrift and post-rift stratigraphy suggest an asymmetrical basement structure along the eastern Laurentian continental margin in the northern Appalachians, consistent with a low-angle detachment rift system. The results of this part of the dissertation are presented in Chapter 2. A concise version of Chapter 2 has been published in the April 2009 edition of the journal *Geology*. A more complete version of this Chapter is currently in review for publication in an up coming *Geological Society of America Memoir*, which focuses on recent research in the Appalachian orogen.

The purpose of Objective B is to test if the distribution and subsidence history of synrift and early post-rift stratigraphic elements on the St. Lawrence promontory conform to proposed models for a low-angle detachment continental rift system. To accomplish this objective, nine balanced cross sections were constructed across the deformed Paleozoic successions exposed in western Newfoundland. Restored sections illustrate the palinspastic distribution of Neoproterozoic and early Paleozoic strata on the promontory. The along-strike distribution of palinspastically restored rift sediments is best explained by continental rifting and synrift sediment dispersal into upper- and lower-plate domains of an asymmetric, low-angle detachment rift system. Subsidence curves generated by backstripping early Paleozoic stratigraphic successions highlight along-strike asymmetry in the tectonic subsidence record for the St. Lawrence promontory, which is also consistent with a low-angle detachment rift. The results accomplished under Objective B go beyond the scope of a rifted margin by demonstrating the tectonic effect of a low-angle detachment continental margin on the evolution of a subsequent collisional orogen. Results of Objective B produce a detailed structural, stratigraphic, and temporal report for the St. Lawrence promontory in western Newfoundland, spaning the entire Paleozoic. Data and results related to Objective B are presented in Chapter 3 and are planned for

submission for publication as an official report through the Geological Survey of Canada and as a paper in *GSA Bulletin*.

Problem Statement 2: Breakup of the supercontinent Rodinia during the latest Neoproterozoic to Early Cambrian dispersed neighboring cratons away from the newly formed eastern Laurentian margin as the Iapetus Ocean basin opened. Although this scenario is generally accepted (e.g., Hoffman, 1991; Dalziel, 1997; Karlstrom et al., 1999; Cawood et al. 2001; Meert and Torsvik, 2003), alternatives for the identity of the specific conjugate cratons remain unresolved, including the positions of various cratonic elements relative to specific segments of the Laurentian margin (i.e., St. Lawrence promontory) (e.g., Dalziel, 1994; Lowey et al., 2003; Tohver et al., 2002; Hatcher et al., 2004a). Further compounding this problem is the recognition that Wilson cycles are more complex than the process originally envisioned by Tuzo Wilson (Wilson, 1966). Thus, conjugate cratons to the modern Atlantic margin of eastern North America are not necessarily the same conjugate cratons to the early Paleozoic eastern Laurentian margin.

Hypothesis 2: During the breakup of Rodinia and opening of the Iapetus Ocean, departing conjugate cratons may have left a geochemical fingerprint on the eastern Laurentian margin in the synrift sedimentary detritus, which is currently exposed as a result of the Appalachian orogenic cycle. Thus, isotopic tracers in detrital zircon deposited as part of the synrift sedimentary system on the St. Lawrence promontory can be used to identify Proterozoic conjugate cratons to the eastern Laurentian margin in that region.

Objective C: Conduct modern isotopic analyses (i.e., U-Pb ages and Lu/Hf ratios) of detrital zircons from synrift sediments to test the alternatives for provenance in the context of conjugate cratons to the St. Lawrence promontory.

Summary of results:

Approximately 510 zircons from 9 samples collected from Mesoproetozoic basement and the overlying Early Cambrian synrift succession in Newfoundland were

analyzed by laser ablation microprobe inductively coupled plasma mass spectrometry (LAM-ICP-MS) at the University of Florida for U-Pb ages and Hf isotopic ratios. The purpose of this objective was to compare the distribution of U-Pb ages and Lu/Hf ratios in detrital zircon through a vertical rift section to discover changes in provenance through time and to determine if a craton exotic to Laurentia was providing sediment into the Iapetan rift. Seven samples collected from the Iapetan synrift succession in Newfoundland yielded ages that range from 544 Ma to 3605 Ma with maximum age frequencies of 1000-1200 Ma (Grenville), 1350-1450 Ma (Pinware), and 2650-2800 Ma (Superior). Analysis of the Newfoundland dataset indicates that the Hf isotopic ratios of ca.1000 Ma, 1200 Ma, and 1400-1600 Ma detrital zircons from the Laurentian synrift succession are a close match to reported Hf ratios from Baltican zircons of the same vintage, suggesting that Baltica was the conjugate to the St. Lawrence promontory. Data and results of Object C are in Chapter 4, which will be submitted for future publication in the *Journal of Precambrian Research*.

1.2 RESEARCH LOCATIONS AND TIMELINE

The Island of Newfoundland located off the northeastern coast of North America (Figure 1.1) makes up a part of the Canadian province of Newfoundland and Labrador. The dissertation study area consists of nearly the entire western coastal and inland regions of the Island of Newfoundland, where Laurentian margin rocks are chiefly exposed. Approximately 12 consecutive weeks during the late spring and summer months of 2007, starting on May 21st and ending on August 17th, were spent in the field in western Newfoundland collecting the requisite stratigraphic and structural data for balanced cross sections, as well as samples of Laurentian crystalline basement and synrift sedimentary rock for the detrital zircon study.

Between May 21st and June 4th, the author was in southwestern Newfoundland completing traverses across Port au Port peninsula and examining the local geology north of the town of Stephenville (Figure 1.2). From June 4th to July 21st, the author was in residence at Grenfell College in the town of Corner Brook, where he investigated important stratigraphic and structural relationships within the Humber Arm allochthon at the type locality around the Bay of Islands, as well as examined highly deformed and

metamorphosed rocks in the Corner Brook Lake terrane. Between June 5th and June 8th, the author attended the "2nd International Symposium on Oil and Gas Resources in Western Newfoundland" hosted by the Greater Corner Brook Board of Trade, where he was able to meet with top geoscientists in the field of western Newfoundland geology (Dr. Denis Lavoie, Dr. Ian Knight, Dr. John Waldron, Dr. Doug Boyce) and discuss his current research. This was followed by an a recorded radio interview with the Canadian Broadcast Corporation (CBC) in early July, in which he and his advisor (Dr. William Thomas) discussed and answered questions concerning the relevance of western Newfoundland geology in the context of the entire Appalachian orogen. The span of time between July 21st and August 2nd was spent around the area of Deer Lake. For 7 days between July 26th and August 1st, Dr. William A. Thomas (Committee Chair) accompanied the author in the field. Their time was spent examining the geology on the southern limb of the Long Range massif, as well as collecting detrital zircon samples from basement-cover rocks along White Bay on the eastern shore of the Great Northern Peninsula. August 2nd through August 17th was spent completing traverses across the western coastal regions of the Great Northern Peninsula.

The detrital zircon aspect of this investigation was conducted primarily at the Department of Geological Sciences, University of Florida (UF) in Gainesville, Florida, under the direction of Dr. Paul A. Mueller and Dr. George Kamenov. Transportation of samples and sample prep work were completed over a four week period at UF, split between two weeks in December 2007 (December 2nd to 14th) and two weeks in March 2008 (March 17th to 28th). Final sample prep work and analyses of individual zircon grains by LAM-ICP-MS were conducted by the author over a course of several days in June 2009 with the assistance of Leeanna Hyacinth (at present, a high school summer foreign exchange student at the Department of Geological Sciences at UF) and Jennifer Gifford (at present, a Ph.D. student in the Department of Geological Sciences at UF).

1.3 OUTLINE OF DISSERTATION

This dissertation is divided into an introductory chapter (this chapter), three chapters that address specific questions and objectives of this research (Chapters 2 to 4), and a final chapter (Chapter 5) with a summary of the principal conclusions of the

research. With the exception of Chapter 5, each of the subsequent chapters is formatted to reflect a scientific paper as it would appear in a professional journal. The narratives within Chapters 2 through 4 are independent with respect to each other, and do not rely heavily on results from other chapters.

For dissertation purposes, the major goal of Chapter 2 is to address the underlying basement architecture of the eastern Laurentian margin in the northern Appalachians. A detailed synthesis of current stratigraphic, structural, and geochronologic observations and ideas concerning the eastern Laurentian rift and passive margin in New England, Maritime Canada, and western Newfoundland is presented along with important interpretations and implications for tectonic development of the margin. Disparities in the geochronologic and paleomagnetic data set for eastern Laurentia around the end of the Neoproterozoic require a multi-stage continental rift system. Chapter 2 concludes by proposing a general model for the geologic evolution of the eastern Laurentian continental margin from the Neoproterozoic through the early Paleozoic, using models for continental rifting by a simple-shear, low-angle detachment system.

Chapter 3 attempts to test the model proposed in Chapter 2 by palinspastically restoring the deformed continental margin of eastern Laurentia on the St. Lawrence promontory in western Newfoundland. Western Newfoundland was chosen for this investigation because nowhere else in the northern Appalachian orogen is the stratigraphy and structure of the Laurentian margin better exposed and documented. This chapter relies heavily on the field work of previous investigators, as well as 3 months of field work by the author during the summer of 2007. Palinspastic restoration of the deformed continental margin highlights along-strike variation in the stratigraphy of the St. Lawrence promontory, as well as the Paleozoic structure of the Appalachian orogen. The difference in deformational styles between the various along-strike segments of the margin is best explained by along-strike variation in the underlying continental margin in the form of upper- and lower-plate rift segments in a low-angle detachment system offset by transform faults.

Chapter 4 goes beyond the architecture of the rifted margin on the St. Lawrence promontory to address the question of what lay on the other side of the eastern Laurentian

rift prior to rifting at the end of the Neoproterozoic. Previous paleomagnetic investigations have narrowed candidates to either Baltica or Amazonia and either of these cratons may have left a geochemical finger print on the St. Lawrence promontory preserved in the form of U-Pb ages and Lu-Hf isotopes in detrital zircon deposited as part of the synrift sedimentary record. Because deep synrift basins developed on the promontory as a result of the low-angle detachment rift system, the likelihood that exotic sedimentary detritus was shed onto the St. Lawrence promontory from a conjugate craton is greater than elsewhere along the margin in the northern Appalachians.

The final chapter in this dissertation (Chapter 5) draws heavily from all previous chapters by readdressing the problems stated herein and synthesizing the primary results of Chapters 2 through 4 into a complete geologic history for the St. Lawrence promontory. Chapter 5 concludes with new questions uncovered by the author's interpretations followed by potential avenues of future research to answer those new questions.

Figure 1.1. General map illustrating the geographic location of the Island of Newfoundland.

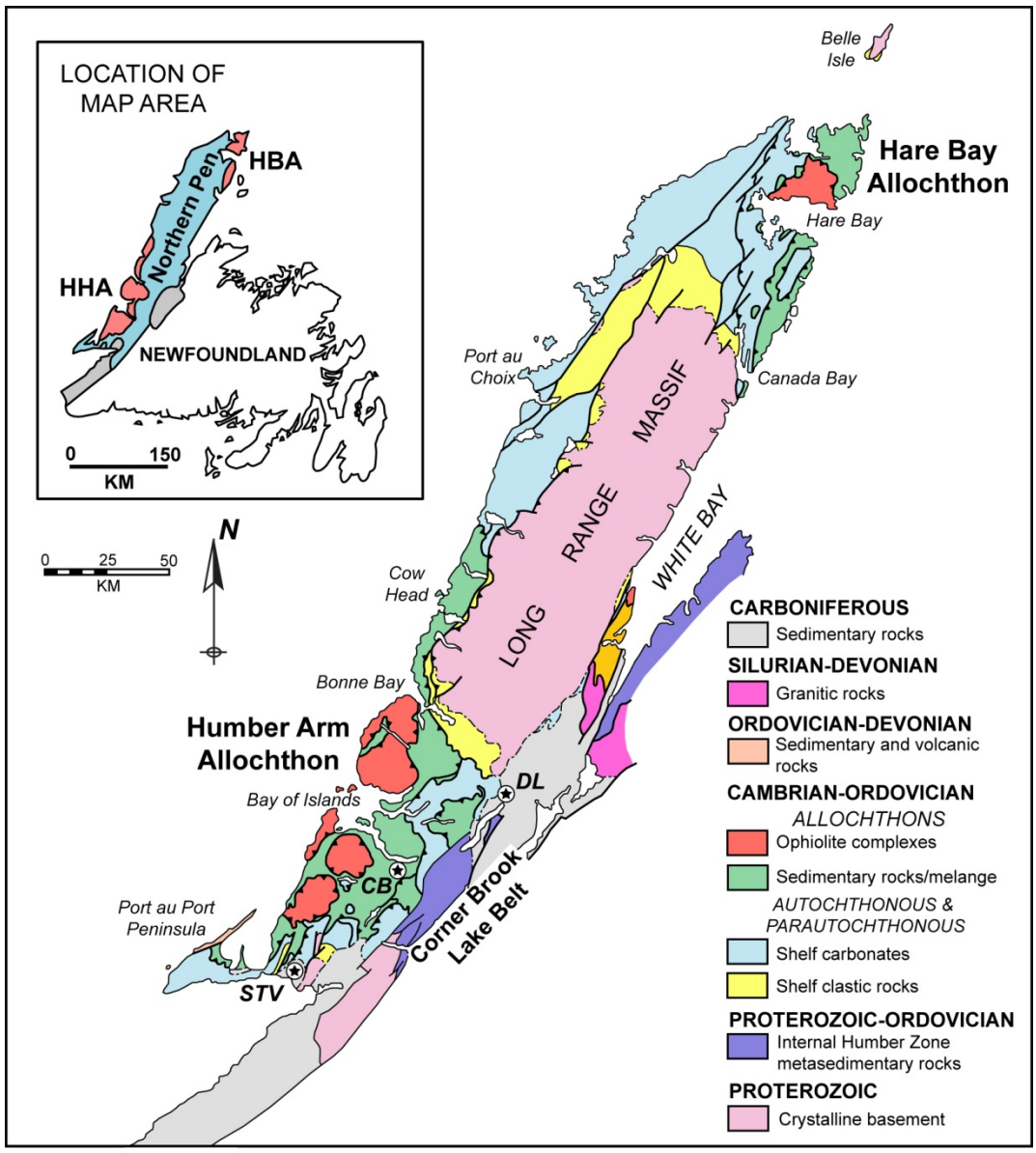

Figure 1.2. Generalized geologic map of the Laurentian margin geology in western Newfoundland. Locations of the Humber Arm allochthon (HHA) and the Hare Bay allochthon (HBA) are also shown. Abbreviations: CB = City of Corner Brook; DL = City of Deer Lake; STV = City of Stephenville.

CHAPTER 2 - THE LAURENTIAN MARGIN OF NORTHEASTERN NORTH AMERICA

2.1 INTRODUCTION

Neoproterozoic-early Paleozoic continental rifting related to the opening of the Iapetus Ocean produced promontories and embayments on the eastern Laurentian continental margin defined by northeast-trending rifts offset by northwest-trending transforms (Thomas, 1977, 1991). In the Appalachians of northeastern North America, vestiges of the Laurentian rift and passive margin are preserved in stratigraphic successions and in anorogenic magmatic suites. Previous studies in the southern Appalachian-Ouachita orogen define a complex and diachronous rift and passive margin that highlight an underlying continental margin architecture that developed as simple-shear, low-angle detachment rift system (Thomas, 1993; Thomas and Astini, 1999). These studies of the eastern Laurentian margin, however, extend northward only as far as southern New York, leaving a significant gap in our understanding of the evolution of the eastern Laurentian continental margin in the northern Appalachians. Previous studies have documented the stratigraphy, geochemistry, age, and geophysical attributes of Laurentian synrift and passive-margin deposits preserved in the northern Appalachians (e.g., Williams, 1995; Waldron et al., 1998; Cawood et al., 2001; Lavoie et al., 2003 and references therein). This article synthesizes recent work in the Neoproterozoic-early Paleozoic synrift and post-rift stratigraphy, structures, and magmatic suites in northeastern North America. A revised model for the development of the Laurentian margin in the northern Appalachians is based on a low-angle detachment rift system that, when coupled with the previous work in the southern Appalachians, provides an orogen-wide working hypothesis for the four-dimensional architecture of the eastern Laurentian continental margin.

2.2 REGIONAL GEOLOGY OF THE NORTHERN APPALACHAIN MARGIN

The curvature of salients and recesses in the Appalachian thrust belt outline promontories and embayments, which formed along the eastern Laurentian continental

margin as the Iapetus Ocean opened and were later overprinted by the Appalachian orogenic cycle (Thomas, 1977, 1991). A simple first-order comparison reveals that, in general, recesses are marked by a thin Paleozoic stratigraphic succession, a narrow thrust belt, and complexly deformed internal and external basement massifs, consistent with the presence of a continental promontory. Salients, on the other hand, tend to have thicker stratigraphic successions, a wider foreland thrust belt, and fewer exposed basement massifs, which reflects a continental embayment. In the northern Appalachians, the geology of the present day New York and St. Lawrence recesses and the Quebec salient fit this generalization (Figure 2.1), which led to the recognition of the New York promontory, the Quebec embayment, and the St. Lawrence promontory on the eastern Laurentian margin (Figure 2.2) (Thomas, 1977).

In the northern Appalachians, elements of the eastern Laurentian margin can be grouped into three fundamental geologic units that overlie ca. 1.0 Ga and older Laurentian basement: 1) a Neoproterozoic-Early Cambrian synrift clastic-magmatic succession, 2) Cambrian-Ordovician carbonate passive-margin and associated off-shelf facies, and 3) polydeformed and metamorphosed internal basement massifs with a lithodemic stratigraphy that matches the synrift and passive-margin successions. The early Paleozoic Appalachian continental-margin succession is not laterally uniform. Significant along- and across-strike variations in facies, composition, thickness, and age of sedimentary succession mark discrete rift zones within the New York promontory, Quebec embayment, and the St. Lawrence promontory (Figure 2.2). A transition in the age and facies of Laurentian stratigraphy from central New York to Vermont allows for the recognition of the New England rift zone (e.g., Thomas, 1993; Cherichetti et al., 1998). Lateral variations in the early Paleozoic stratigraphy within the Quebec embayment indicate the development of two independent rift zones; the more southerly Quebec rift zone, named after Quebec City where the regional geology of the rift zone is best exposed, and the more northerly Gaspé rift zone, named after Gaspé Peninsula where important Laurentian margin geology is exposed (e.g., Cousineau and Longuépée, 2003). Finally, the Long Range rift zone comprises the entire length of the St. Lawrence promontory and is named after the Long Range Mountains of western Newfoundland where important basement and Paleozoic cover relationships are preserved.

2.2.1 Synrift Rocks and Structures

The stratigraphically oldest formations along the length of the Appalachian orogen consist of a mixed clastic-volcanic succession, which was deposited in extensional basins that opened as Laurentia rifted out of the Rodinia supercontinent (Thomas, 1977; Hoffman, 1991; Dalziel, 1997; Cawood et al., 2001). Synrift stratigraphy in the northern Appalachians is characterized by abrupt lateral changes in thickness and facies that contrasts sharply with the uniform stratigraphy, uniform thickness and broad lateral continuity of overlying passive-margin formations (Thomas, 1977; Williams and Hiscott, 1987). Lateral variation in the facies, thickness, age, and composition of synrift sedimentary and magmatic accumulation reflect individual rift zones along the margin and illumine the structural architecture of the eastern Laurentian rift (Thomas, 1991; 1993; Thomas and Astini, 1999).

In the New England rift zone on the New York promontory (Figure 2.2), Neoproterozoic-Lower Cambrian synrift clastic rocks of the Pinnacle Formation consist of alluvial-fan deposits that are geographically extensive and have a thickness of 2000-3500 m (Cherichetti et al., 1998). Sandstone and shale of the Pinnacle Formation in northern Vermont underlie and are interlayered with metabasalt of the Tibbit Hill Formation (Coish et al., 1985), which has been dated at 554 +4/-2 Ma in southern Quebec (Kumarapeli et al., 1989), suggesting that synrift deposition in the New England rift zone predates the latest Neoproterozoic. Northward into southern Quebec, the Pinnacle Formation thins abruptly (Figure 2.3A) and displays a facies transition to shallow-marine coastal deposits (Marquis and Kumarapeli, 1993; Cherichetti et al., 1998). Synrift clastic deposits pinch out southward into Green Mountains and Berkshires (Stanley and Ratcliffe, 1985; Rankin et al., 1989) and are locally interlayered with volcanic rocks of the Pinney Hollow Formation, which have been dated at 571±5 Ma (Walsh and Aleinikoff, 1999).

Into southern Quebec, Iapetan synrift stratigraphy along the Quebec rift zone (Figure 2.2) is preserved in both shelf and slope deposits that are distributed between several nappes in southern Quebec. On the shelf, shallow-marine synrift clastic deposits of the Pinnacle Formation are thin (140-250 m) and conformably overlie bimodal volcanic deposits of the ca. 554 Ma Tibbit Hill Formation (Figure 2.3A) (Marquis and

Kumarapeli, 1993; Cousineau and Longuépée, 2003), indicating that the Pinnacle Formation in southern Quebec is younger than the synrift succession in northern New England. Felsites in the Tibbit Hill Formation have trace and rare earth element chemistries that resemble within-plate granites associated with thick continental crust (Kumarapeli et al., 1989). On the Laurentian slope in southern Quebec, synrift deposits of the lower Armagh Formation and the Green Sandstone unit (Lavoie et al., 2003) have an estimated thickness of 600 m, overlie rift basalts of the 550±7 Ma Mt. St.-Anselme Formation (Hodych and Cox, 2007), and contain late-Early Cambrian macrofuana and acritarchs. Reprocessed seismic reflection profiles across southern Quebec reveal that the top of Laurentian basement beneath the Appalachian allochthon dips from the near surface to below 4.0 sec TWTT (~10 km at 5 km/sec) over an across-strike distance of 70 km and is broken by a stair-step system of basement faults that dip steeply southeast (Figure 2.3B) (Castonguay et al., 2006).

Along the Gaspé Peninsula of eastern Quebec (Figure 2.2), Laurentian shelf deposits are buried beneath the Appalachian allochthon except along the St. Lawrence Estuary where seismic profiles indicate platform strata beneath the estuary (Pinet et al., 2008). Appalachian thrust sheets on the Gaspé Peninsula are dominated by Laurentian slope deposits. There, synrift sediments in the Gaspé rift zone (St-Roch and Shickshock Groups) were deposited on a steep continental slope (Cousineau and Longuépée, 2003) and are interlayered with rift basalts of the Lac Matapédia suite, which were dated at 565 ± 6 Ma and 556 ± 7 Ma (Figure 2.4) (Hodych and Cox, 2007). The latter age is statistically indistinguishable from volcanics in the Tibbit Hill Formation; however, the ca. 565 Ma age is unique to the Gaspé rift zone suggesting that synrift deposition in Gaspé began prior to synrift deposition in the Quebec rift zone. A separate suite of rift basalts (Shickshock Group) has geochemical signatures that indicate magmatic interaction with highly attenuated continental crust (Camire et al., 1995).

The Saguenay-Montmorency transform (Figure 2.2) is proposed herein to separate the Quebec and Gaspé rift zones. Northwest of the transform is the Saguenay graben, which is an extensional structure that extends into the continent perpendicular to the strike of the margin and contains two known Neoproterozoic synrift igneous complexes (Kumarapeli, 1985). The intersection of the transform and the Quebec rift zone forms the

second-order Montmorency promontory, which is recognized as an asymmetric structural and stratigraphic high with a steep northeast gradient within the Quebec embayment (e.g., Cousineau and Longuépée, 2003). Sedimentary deposits along the Montmorency promontory consist of thin (200–800 m), late Early to Middle Cambrian glauconite-bearing sandstones of the Anse Maranda Formation, which is interpreted to represent a narrow sediment-starved shelf (Longuépée and Cousineau, 2005). Southwest of the transform, the Anse Maranda Formation is overlain by sparse Middle to Late Cambrian conglomerates of the Lauzon Formation. Along strike to the northeast across the transform into the Gaspé rift zone, conglomeratic beds of the Saint-Damase Formation are more abundant and contain boulder-sized clasts of platform carbonate, rift basalt, and basement gneiss (Lavoie et al., 2003).

The Sept-Iles transform defines the northern boundary of the Quebec embayment and offsets the trace of the Iapetan rift by ~500 km from the Quebec embayment to the St. Lawrence promontory (Figure 2.2). North of the transform on the Anticosti platform, thin (<855 m), autochthonous Lower Ordovician shelf carbonates of the Romaine Formation lie unconformably on crystalline basement (Figure 2.4) (Lavoie et al., 2005). In contrast, south of the transform on Gaspé Peninsula, deep-water Cambrian clastic deposits of the Orignal Formation are overlain by distinctive deep-marine conglomerates (Saint-Damase Formation) (Lavoie et al., 2003). Northwest along strike of the transform is the large, ca. 565 Ma rift-related Sept-Iles layered mafic intrusion (SILMI) (Figure 2.2) (Higgins and van Breeman, 1998). Geochemical and isotopic data indicate that magmas in the SILMI were derived from an upper mantle source and that they did not interact with continental crust. A possible explanation is that fracture systems related to the Sept-Iles transform tapped the upper mantle and channeled SILMI magmas through the crust.

The St. Lawrence promontory along the northernmost Appalachian orogen comprises the entire length of the Long Range rift zone (Figure 2.2). The southwestern corner of the promontory is commonly inferred to lie near the northwestern tip of Cape Breton Island where an isolated, fault-bounded inlier of Mesoproterozoic Laurentian basement, termed the Blair River inlier, is exposed (Miller and Barr, 2000). Some of the oldest rift-related magmatic ages in northeastern North America come from the St. Lawrence promontory and the nearby craton in eastern Labrador (Figure 2.2). There,

Laurentian basement is intruded by tholeiitic dikes of the Long Range swarm, for which $^{40}Ar/^{39}Ar$ and U-Pb baddeleyite ages indicate a ca. 605 Ma crystallization age (Stukas and Reynolds, 1974; Kamo et al., 1989). Farther south on the St. Lawrence promontory, the alkalic Hare Hill granite cuts ca. 1.0 Ga basement in the Steele Mountain inlier and is dated at 617±8 Ma (van Berkel and Currie, 1988). Other rift-related plutonic complexes include the Round Pond granite dated at 602 Ma (Williams et al., 1985) and the Lady Slipper pluton dated at 555 Ma (Cawood and van Gool, 1998), both of which unconformably underlie synrift metaclastic rocks. Volcanic rocks of the Skinner Cove Formation in the Humber Arm allochthon have an U-Pb zircon age of 550 Ma (Cawood et al., 2001).

Stratigraphic elements of the Laurentian margin in western Newfoundland are divided into a parautochthonous footwall that consists of mildly deformed late-Neoproterozoic to Middle Ordovician synrift and passive-margin shelf successions, and an allochthonous hanging wall (Humber Arm and Hare Bay allochthons) of coeval slope deposits that are polydeformed and mildly metamorphosed (e.g., James and Stevens, 1986; Williams and Hiscott, 1987; Williams, 1995; Waldron et al., 1998). Parautochthonous Neoproterozoic-Lower Cambrian synrift successions in western Newfoundland structurally underlie slope deposits in the Hare Bay and Humber Arm allochthons (Figure 2.5). The stratigraphic base of the sedimentary cover is preserved within the siliciclastic deposits of the Labrador Group (Figures 2.3C & 2.3D). The lower Labrador Group consists of an early rift succession of fault-bounded conglomerates and arkoses (Bateau Formation) cross-cut by Neoproterozoic tholeiitic basalts (Lighthouse Cove Formation), which are commonly correlated with the ca. 615 Ma Long Range dike swarm (Williams and Hiscott, 1987; Kamo et al., 1989; Williams, 1995). These same dikes and basalt flows are truncated by a regional unconformity, above which are Early Cambrian clastic rocks and limestones of the upper Labrador Group indicating a substantial hiatus (50-70 m.y.) between the upper and lower divisions of the Labrador Group on Belle Isle (Cawood et al., 2001). Unconformably above the lower rift succession, a Lower Cambrian clastic succession consists of a basal immature, fluvial and shallow-marine sandstone of the Bradore Formation, which grade into into fine-grained clastic rocks and archaeocyathid-rich mud bank limestones of the Forteau Formation

followed by overlying passive-margin sandstones of the Hawkes Bay Formation (e.g., Williams and Hiscott, 1987; Cawood et al., 2001).

Although most studies allude to uniformity of early Paleozoic shelf deposits in western Newfoundland, several previous investigations demonstrate important along-strike contrasts within the synrift shelf stratigraphy. East of Port au Port peninsula, only the Bradore, Forteau, and Hawkes Bay Formations (i.e., upper Labrador Group) are present in outcrop and are relatively thin (~240-260m) (Williams and Hiscott, 1987; Knight, 2003). Outcrop and geophysical well data indicate that sandstones of the Bradore Formation increase abruptly in thickness in the hanging walls of synrift basement faults (Figures 2.3C & 2.5) (e.g., Cooper et al., 2001; Stockmal et al., 2004). Between Bonne Bay and Canada Bay on the Northern Peninsula, the Labrador Group also consists predominantly of the upper clastic section. Here, the basal Bradore Formation ranges in thickness from <10m to >175m, is thickest in the hangingwall of basement faults, and consists of red, immature, partly sub-aerial sandstones (e.g., Bostock, 1983; Williams and Hiscott, 1987; Knight, 1991).

Synrift successions are also preserved within the Humber Arm and Hare Bay allochthons (Figure 2.5) (e.g. Williams and Cawood, 1989; Williams, 1995; Waldron et al., 1998). Neoproterozoic(?)-Early Cambrian synrift deposits of the Summerside and Irishtown Formations (i.e., Curling Group) at the base of the Humber Arm allochthon east of the Bay of Islands consist of a coarse siliciclastic succession with a minimum measured thickness of 1840 m (Figure 2.3D) (Waldron and Palmer, 2000; Palmer et al., 2001). The top of the Irishtown is marked locally by massive conglomerates that contain large rounded blocks of shelf carbonate and crystalline basement. In contrast to the Bay of Islands region, the Humber Arm allochthon north of Bonne Bay around Cow Head and around Port au Port peninsula to the south (Figure 2.5) contains no Early Cambrian strata (e.g., Lavoie et al., 2003). Here, the allochthon consists of coarse Middle Cambrian passive-margin carbonate debris flows and background hemipelagic sedimentation of the Cow Head Group (James and Stevens, 1986; Cawood and Botsford, 1991). The lack of Neoproteroizoic-Early Cambrian in outcrop in the Humber Arm allochthon in these two regions suggests little or no synrift deposition on the Laurentian slope along the distal margin east of Port au Port peninsula and Cow Head.

The Hare Bay allochthon north of Canada Bay is less well studied but appears to be stratigraphically similar to the Humber Arm allochthon. There, the Lower Cambrian Maiden Point Formation consists of synrift coarse sandstone, greywacke, and conglomerate containing metamorphic and granitic basement, which is intercalated with alkalic, rift volcanics (e.g., Williams, 1995). South of Hare Bay, the Maiden Point Formation is measured at 2000 m thick (Tuke, 1968).

2.2.2 Rift-to-Passive-Margin Transition

Along the New England rift zone, sandstones of the Early Cambrian Cheshire Formation are the oldest stratigraphic units that contain a macrofossil assemblage (Osberg, 1969). Regionally overlying sandstones in the Cheshire Formation are carbonate shelf deposits of the Dunham Formation, which also bear an Early Cambrian fossil assemblage (Rankin et al., 1989). In the New England rift zone, both the Cheshire and Dunham Formations are regionally extensive and have a combined thickness of 750 to 850 m (Figure 2.3A) (Osberg, 1969). In northern Vermont near the international border, sandstones of the Cheshire Formation lie conformably over synrift deposits of the Pinnacle Formation and its correlatives (Cherichetti et al., 1998). Southward into the Green Mountains and the Berkshires, however, the Pinnacle Formation pinches out completely and the Cheshire Formation thins and lies directly on Precambrian Laurentian basement (Rankin et al., 1989). Thus, in a regional context, the Cheshire Formation overlies both basement and synrift clastic deposits in different locations, and underlies an extensive Cambrian-Ordovician carbonate bank, indicating that the Early Cambrian Cheshire Formation represents the rift-to-passive-margin transition in the New England rift zone.

The transition from rift to passive margin in the Quebec embayment is less well constrained, in part because of a lack of exposure and because of intense deformation and structural imbrication of shallow-marine platform facies between the nappes of the Quebec Appalachians. Further compounding the problem is the recognition that there is no unequivocal preserved record of Early Cambrian sedimentation on the autochthonous St. Lawrence platform. The Covey Hill Formation of the Potsdam Group unconformably overlies ca. 1.0 Ga Laurentian basement and has been assigned an Early Cambrian age

(Sanford, 1993), but without any supporting faunal evidence. In the eastern nappes in the Quebec embayment, sandstones in the Cheshire Formation of the Oak Hill Group overlie synrift deposits and contain an Early Cambrian fauna (Clark, 1934). Deposits in the Cheshire Formation and the overlying Dunham Formation do not exceed 600 m in total thickness, indicating that the rift-to-passive-margin transition thins from the New England rift zone into the Quebec rift zone (Osberg, 1969; Marquis and Kumarapeli, 1993). Farther outboard of the Oak Hill Group, the Green Sandstone Unit, which contains blocks of rift volcanics and a late-Early Cambrian faunal assemblage, may overlap with the rift-to-passive-margin transition (Lavoie et al., 2003). Thus, the stratigraphic evidence suggests an Early to late-Early Cambrian transition from rift to passive margin in the Quebec embayment.

Outside the extent of synrift sedimentary and volcanic accumulations on the St. Lawrence promontory, sandstones in the Bradore Formation (upper Labrador Group) lie unconformably on Laurentian basement (Williams and Hiscott, 1987). On Belle Isle, the Bradore Formation unconformably overlies rift-related sediments in the Bateau Formation and basalt dikes and flows of the Lighthouse Cove Formation (Bostock, 1983). Sparse biostratigraphic data from the Bradore Formation in southern Labrador suggest an Early Cambrian age, and the overlying limestone and shale in the Forteau Formation contain abundant trilobite and archeocyathan fauna of late-Early Cambrian age (Williams and Hiscott, 1987).

The unconformity at the base of the Bradore Formation has previously been interpreted to mark the transition from rift to passive margin (e.g., Cawood et al., 2001). Stratigraphic sections and deep well data indicate that the Bradore Formation ranges in thickness from ≤5m to 175m (Bostock, 1983; Williams and Hiscott, 1987; Knight, 1991; 2003; Copper et al., 2001). Depositional facies indicate that the early part of the Bradore Formation was deposited in a subaerial, high-energy environment that later changed into a more passive shallow-marine to deltaic environment, which was followed by an extensive marine transgression represented in the Forteau Formation (Williams and Hiscott, 1987; Knight, 1991). Furthermore, measured sections and deep wells indicate that the Bradore Formation increases in thickness locally in the hanging walls of steep basement faults interpreted as synrift graben (e.g., Waldron et al., 1998; Cooper et al.,

2001). Therefore, we interpret the rift-to-passive-margin transition on the St. Lawrence promontory to lie within the Early Cambrian Bradore Formation, rather than in the unconformity below it.

2.2.3 Passive-Margin Stratigraphy

Clastic deposits of the rift-to-passive-margin transition in the northern Appalachians are overlain by an extensive carbonate bank that ranges in age from middle Early Cambrian to early Middle Ordovician (Rodgers, 1968; Knight and Cawood, 1991; Sanford, 1993; Williams, 1995). Early Paleozoic shallow-water carbonates dominate much of the western autochthonous and parautochthonous rocks of the northern Appalachian orogen, whereas allochthonous thrust slices east of the Laurentian craton contain distal, deep-water shale and carbonate conglomerate facies (Lavoie et al., 2003). Exposure of Cambrian-Ordovician shelf-edge and shelf-break facies are rare in the northern Appalachians (Rodgers, 1968).

In New England, sandstones of the Early Cambrian Cheshire Formation are comformably overlain by a passive-margin succession that displays lateral variation in both thickness and facies (Rankin et al., 1989). The passive margin of east-central New York and western Vermont consists of a shallow-water succession, the lowest part of which includes a late-Early Cambrian cycle of carbonate (Dunham Formation) and clastic (Monkton Formation) shelf deposits, which grade upward into a full-fledged carbonate shelf that persisted through the Early Ordovician (Rankin et al., 1989). The entire Cambrian-Ordovician shelf succession in western Vermont reaches thicknesses in excess of 2000 m, yet thins to less than 700 m southward into Massachusetts (Palmer, 1971; Rankin et al., 1989). The facies boundary between passive-margin shelf and slope deposits cuts northward obliquely across Appalachian structural strike from central Vermont into southern Quebec (Rodgers, 1968). In northern Vermont, carbonate deposits of the Dunham and overlying Winooski Formations are replaced progressively northward by black shale (Parkers Formation) and limestone conglomerate (Woods Corners Group) (Palmer, 1971). Farther east, metamorphosed shale and minor calcareous beds of the Ottauquechee and Sweetsburg Formations are interpreted as distal slope deposits of the Cambrian-Ordovician passive margin (Palmer, 1971).

In the Quebec embayment, autochthonous shelf carbonates on the St. Lawrence platform record the Cambrian-Ordovician passive margin in the Quebec rift zone. There, Late Cambrian clastic deposits in the Potsdam Group lie unconformably beneath Early and early-Middle Ordovician limestones of the Beekmantown Group (Figure 2.3B) (Sanford, 1993; Salad Hersi et al., 2003; Dix et al., 2004). Outer shelf facies are preserved in the northwesternmost nappes of the Quebec Appalachians (e.g., Phillipsburg slice), the stratigraphy of which has recently been revised to correlate with the more proximal shelf on the St. Lawrence platform (Salad Hersi et al., 2007). Passive-margin slope deposits preserved in the nappes of Quebec rift zone include a lower succession of Middle Cambrian sandstone and shale (upper Saint-Roch Group, upper Sillery Group, upper Armagh Formation) that are overlain by distinctive coarse, Late Cambrian conglomeratic units (Saint-Damase Formation and correlatives) (Lavoie et al., 2003). Overlying the Upper Cambrian conglomerates are the uppermost Cambrian to lowermost Ordovician shales of the Rosaire and Kamouraska Formations that grade upward into shale with subordinate sandstone and limestone conglomerate of the Rivière-Ouelle Formation (Lavoie et al., 2003).

The only known exposed carbonate-platform deposit in the Gaspé rift zone is the Middle Cambrian Corner-of-the-Beach Formation, which is limited to a fault bounded sliver located outboard of the deformed continental margin (Lavoie et al., 2003). Allochthonous slope deposits dominate the Gaspé rift zone. Middle Cambrian deep-water sandstones of the Orignal Formation are overlain by Late Cambrian through Early Ordovician deposits consisting of alternate beds of shale and limestone conglomerate (Lavoie et al., 2003). The abundance and distribution of limestone conglomerate in the Gaspé rift zone increases in the St. Lawrence Lowlands toward the proposed Saguenay-Montmorency transform. Distinctive Late Cambrian conglomerates of the Saint-Damase Formation and correlative units contain channel-fill carbonate conglomerates with blocks of Early and Middle Cambrian shelf limestone, along with boulders of rift-related basalt and basement gneiss (Lavoie et al., 2003). Middle to Late Ordovician shallow-marine St. Lawrence platform facies are also found in the Charlevoix area (Lemieux et al., 2003) near the Saguenay-Montmorency transform and significant changes in the thickness and

facies architecture suggest that the transform system was active sporadically during the Late Cambrian and the early-Late Ordovician (Lavoie et al., 2003).

On the St. Lawrence promontory, the onset of passive-margin thermal subsidence is marked by the Forteau Formation of the Labrador Group, which records progressive deepening of the shelf from reef limestones (Devil's Cove member) into deeper water shale (Cooper et al., 2001). On the Northern Peninsula of western Newfoundland, the Forteau Formation consists of a lower shale-dominated member that grades upward into a thick limestone member (Knight, 1991). In southwestern Newfoundland, however, the upper limestone facies in the Forteau Formation is absent and, with the exception of the basal Devil's Cove Member, the formation consists almost entirely of shale and siltstone (Knight, 2003), suggesting further instability along this part of the margin during the late-Early Cambrian. The Hawkes Bay Formation overlies the Forteau Formation and consists predominantly of mature sandstones indicative of a broad marine regression that preceded the establishment of a full-fledged carbonate platform on the promontory (James et al., 1989).

The dominantly siliciclastic early shelf embodied in the uppermost Labrador Group (i.e., Forteau and Hawkes Bay Formations) is overstepped by a Middle to Late Cambrian narrow, high-energy carbonate platform expressed in the Port au Port Group, which is overlain by an Early Ordovician broad, low-energy carbonate platform represented in the St. George Group (James et al., 1989). A Middle Ordovician foundered carbonate bank (Table Head Group) marks the end of the passive margin sequence on the St. Lawrence promontory (Stenzel et al., 1990). Along the length of the St. Lawrence promontory, the Cambrian-Ordovician carbonate shelf consistently ranges in thickness from 1200 to 1500 m (Figure 2.3C & 2.3D) (e.g. Williams, 1995; Waldron et al., 1998). Between Port au Port peninsula and Bonne Bay, passive-margin shelf deposits plunge beneath the Humber Arm allochthon and are hidden from direct observation except where exposed in anticlinal culminations (Figure 2.5). Where it is exposed, the Early Cambrian siliciclastic shelf grades upward into Middle Cambrian phyllite and limestone conglomerate of the Reluctant Head Formation (Figure 2.3D), which is interpreted as a prograding carbonate ramp that in turn grades upward into a Late Cambrian shallow-marine carbonate platform (i.e., upper Port au Port Group) (Knight and Boyce, 1991).

The succession indicates prolonged subsidence during the Early and Middle Cambrian on the shelf along this segment of the promontory that resulted in a deeper water depositional environment.

The record of the passive-margin slope on the St. Lawrence promontory is preserved within the various thrust slices of the Humber Arm allochthon. The Cow Head Group, exposed around Cow Head and Port au Port peninsula, consists of a distinct assemblage of interbedded shale, sandstone, and limestone conglomerate (Figure 2.3C) (James and Stevens, 1986; Cawood and Botsford, 1991). The Northern Head Group, which is exposed around the Bay of Islands, preserves a more distal and condensed slope section of limestone and shale (Figure 2.3D) (Lavoie et al., 2003). Shelf-edge facies are expressed as ribbon limestone, shale, and limestone conglomerate within the Weasel Group (Boyce et al., 1992) and the Pinchgut Lake Group (Knight, 1996), which occupy separate thrust slices within the Humber Arm allochthon.

2.2.4 Internal Basement Massifs

Internal basement massifs are well defined areas along the Appalachian orogen composed of intensely deformed metamorphic rocks that contrast sharply with the surrounding geology. They typically consist of a crystalline core of remobilized, polydeformed and metamorphosed Precambrian Laurentian(?) basement overlain by metaclastic and metacarbonate rocks that are the equivalent, in large part, to the more mildly deformed clastic and carbonate successions found in foreland sedimentary thrust belts. What distinguishes internal basement massifs in the northern Appalachians from the "classic" Laurentian margin succession is that the massifs are tectonically severed from Laurentian margin rocks, lying outboard of Laurentian continental deposits, commonly within in the Iapetan oceanic realm (e.g., Hibbard et al., 2006). The internal basement massifs relevant to this discussion include the Chain Lakes massif of Quebec and Maine; the Maquereau inlier of Gaspé Peninsula; and the Corner Brook Lake terrane, Dashwoods block, and Baie Verte terrane of west central Newfoundland (Figure 2.1).

The Chain Lakes massif is made up of a polymetamorphosed metaclastic assemblage that is distinct from other early Paleozoic successions exposed along strike in Maine and Quebec (Boudette et al., 1989). Rocks in the Chain Lakes massif consist

predominately of poorly stratified polymictic diamictite estimated at 3000 m thick with local inclusions of amphibolite (Boudette et al., 1989; Trzcienski et al., 1992). Crystalline basement is not exposed in the massif, however, geophysical studies suggest that metasedimentary rocks either depositionally or structurally overlie Laurentian crust (Stewart et al., 1993). The metaclastic assemblage in the Chain Lakes massif is tentatively assigned to the Laurentian synrift succession because 1) diamictite and metaconglomerate appear to overlie Laurentian basement at depth (Stewart et al., 1993), 2) detrital zircon populations from the metaclastic assemblage contain both Grenville-age and Iapetan synrift aged zircons (Dunning and Cousineau, 1990), and 3) Pb-isotope ratios in detrital feldspars from the metaclastic assemblage have a Grenville-like signature (Ayuso and Bevier, 1991; cited in Moench and Aleinikoff, 2003).

Fault-bounded rocks in the Maquereau inlier crop out on the southeastern end of Gaspé Peninsula at Chaleur Bay. Volcanic and sedimentary rocks of the Maquereau Group form a significant part of the inlier, and have been folded and metamorphosed to greenschist facies (De Broucker, 1987). The Maquereau Group itself consists of arkosic wacke, sandstone, and conglomerate that are interstratified with tholeiitic basalts, suggesting a Laurentian synrift facies. Although these rocks are unfossiliferous, they are inferred to be of Early Cambrian or late-Neoproterozoic age (De Broucker, 1987) and are interpreted as part of the Laurentian margin succession. The current location of the inlier is likely the result of large-scale Acadian strike-slip faulting (Malo et al., 1992).

On the St. Lawrence promontory, only the Corner Brook Lake terrane (Figure 2.5) is juxtaposed directly against known continental margin successions, allowing for direct correlation with Laurentian stratigraphy (e.g., Knight, 1996; Cawood and van Gool, 1998). Rocks of the Corner Brook Lake terrane comprise a high-grade metaclastic succession (South Brook Formation) and an extensive metacarbonate cover (Breeches Pond Formation). The South Brook Formation consists of polydeformed paragneiss, quartzite, and metaconglomerate that appear to lie unconformably on Mesoproterozoic crystalline basement and synrift magmatic suites (Williams et al., 1985; Hibbard, 1988; Cawood and van Gool, 1998; Cawood et al., 2001). The Breeches Pond Formation consists of calcareous metaconglomerate, marble, and marble breccia (Cawood and van Gool, 1998). These lithodemic rock packages are consistent with a transition from

siliciclastic deposition on eroded basement to carbonate-dominated sedimentation corresponding to a rift-to-passive-margin transition (e.g. Cawood et al., 1996). Metaconglomerates and metagreywackes in the South Brook Formation strongly resemble synrift deposits in the Curling Group in the Humber Arm allochthon, whereas marble breccias and conglomerates in the Breeches Pond Formation are nearly identical to the Pinchgut Lake Group and the Cow Head Group.

The Baie Verte terrane (Figures 2.1 and 2.5) consists of a similar lithodemic stratigraphy as the Corner Brook Lake terrane; however, unlike the Corner Brook Lake terrane, the Baie Verte terrane lies to the east of the Cabot fault, which experienced a significant amount of dextral strike slip displacement during the late Paleozoic (Brem et al., 2003). Infrastructural rocks are grouped into the East Pond Metamorphic Suite, which consists of polydeformed granitic and migmatitic gneiss interpreted as Laurentian basement overlain by a metaclastic succession of paragneiss, quartzite, metaconglomerate, and amphibolite that correlate with synrift clastic and volcanic rocks in the Labrador Group (Hibbard, 1988). Overlying the internal domain infrastructure is an extensive clastic-carbonate cover sequence (Fleur de Lys Supergroup) that appears to have been deposited on an east-facing attenuated continental margin (e.g. Hibbard, 1988). Recent geochronologic studies in the easternmost ultramafic/meta-aluminous mélanges in the Fleur de Lys Supergroup (i.e., Birchy Complex) yield isotopic ages around ca. 558 Ma (van Staal et al., 2009), suggesting that at least part of the Fluer de Lys cover is latest Neoproterozoic in age.

The Dashwoods block is unique in that it appears to incorporate geologic elements of both the eastern Laurentian margin and Iapetan oceanic terranes (Cawood et al., 1995; Waldron and van Staal, 2001). The Dashwoods block is bounded by the Cabot fault system on the west and the Cape Ray fault and the Red Indian line on the east (Figure 2.5). It consists of psammite, pelitic schists, amphibolite, and migmatitic gneiss with minor calcareous bands, which have been correlated with the Fleur de Lys Supergroup (Currie and van Burkel, 1992). The metasedimentary rocks are intruded by a large suite of Ordovician tonalite and granodiorite that have zircons with ca. 1500 Ma inherited ages (Dunning et al., 1989; Dubé et al., 1995) and Nd isotopic signatures indicating derivation from continental crust (Whalen et al., 1997), suggesting that

unexposed Laurentian basement lies at depth beneath the Dashwoods block (Cawood et al., 1995, Waldron and van Staal, 2001).

2.3 INTRACRATONIC RIFT-RELATED STRUCTURES

The Ottawa graben is an eroded structure that extends approximately 700 km orthogonal to the Appalachian orogen into the craton from the southern Quebec embayment (Figures 2.1 & 2.2). Laurentian basement along the graben is intruded by several alkalic and carbonatitic igneous suites dated at ca. 565 Ma (Doig, 1970) and is also intruded by an extensive swarm of tholeiitic dikes (the Grenville dike swarm) that trend roughly parallel to the strike of the graben and range in age from ca. 590 to 577 Ma (Kamo et al., 1995). Within the graben, immature fluvial sandstones of the Covey Hill Formation (lower Potsdam Group) lie directly on Laurentian basement and range in thickness from < 40 m to > 500 m (Marquis and Kumarapeli, 1993). To the northeast of the Ottawa graben, several smaller graben are oriented orthogonal to the rifted margin (Kumarapeli, 1985). The most notable of these is the Saguenay graben, which is a tensional structure that extends into the continent near perpendicular to the strike of the Appalachian orogen (Figures 2.1 & 2.2). The Saguenay graben lacks synrift sedimentary deposits (e.g., Lavoie and Asselin, 1998 and references therein), but it does include two carbonatite complexes, one of which (St. Honore complex) has yielded a K-Ar age of 564 Ma (Doig and Barton, 1968). Ages of the igneous rocks suggest that these intracratonic fault systems are closely related to continental rifting and the opening of the Iapetus Ocean.

The Ottawa graben commonly has been interpreted as the failed arm of a three-arm radial rift triple junction on the basis of *i)* the synrift igneous suites within the graben, *ii)* geometric and spatial relationships with the trace of the Laurentian rifted margin, *iii)* and the relative position of rift basalts of the Tibbit Hill Foramtion and clastic deposits in the Oak Hill Group at the inferred ‘mouth’ of the graben (Kumarapeli, 1985, 1993). While a failed rift arm interpretation appears to satisfy the available data, several points conflict with the current model for the graben. First, volcanic deposits of the Tibbit Hill Formation and sedimentary and accumulations in the Oak Hill Group are interpreted to have been deposited at the mouth the Ottawa graben (e.g., Marquis and Kumarapeli,

1993); however, these rocks are allochthonous and have been transported an unknown but likely substantial distance (Spencer et al., 1989). Second, Marquis and Kumarapeli (1993) proposed that fluvial siliciclastic deposits in the Potsdam Group fed deltaic deposits in the lower Oak Hill Group; however, Upper Cambrian medusae fossils have been reported recently from the upper Potsdam Group (Covey Hill Formation) (Lacelle et al., 2008). Furthermore, an unconformity at the top of the Potsdam Group (Salad Hersi et al., 2002) correlates with a well dated unconformity in the Philipsburg nappe between the Middle-Late Cambrian Missisquoi Group and Early Ordovician School House Hill Group (Salad Hersi et al., 2007). The correlations suggest that most of the Potsdam Group is significantly younger than the Oak Hill Group. Third, Kumarapeli (1985; 1993) proposed that rift basalts of the Tibbit Hill Formation erupted at the center (i.e., plume head) of an RRR triple junction; however, geochemical analysis indicates that the youngest lavas at the top of the Tibbit Hill volcanic pile interacted with thick continental crust (Kumarapeli et al., 1989) and not with attenuated crust, which would be expected at the axis of a major RRR triple junction. Finally, no geophysical report to date indicates that the eastern end of a distinct Ottawa basement graben, which is now buried beneath the Appalachian allochthon, extends out to the edge of attenuated Laurentian crust in the Quebec rift zone.

The hypothesis that the Ottawa graben represents the failed arm of an Iapetan rift triple junction was first introduced by Burke and Dewey (1973) and later expanded by Kumarapeli (1985; 1993). In a later paper, Dewey and Burke (1974) proposed that continental extension results from thermal doming of continental crust over a mantle plume followed by rifting and establishment of oceanic spreading centers along two "successful" arms of a radial rift triple junction. A third "failed" rift arm evolves into an extensive graben system that projects into the craton at the apex of the newly formed continental embayment (Dewey and Burke, 1974). The model of Dewey and Burke (1974) is based primarily on several post-Paleozoic African rifts, most notably the Benue trough of West Africa (Burke and Dewey, 1973; Dewey and Burke, 1974). Several workers have suggested that the Benue trough serves as a modern analogue for the Ottawa graben (Burke and Dewey, 1973; Rankin, 1976; Kumarapeli, 1985). More recent work indicates that the Benue trough system is the direct result of transtension and strike-slip faulting along equatorial transform faults, and not extension resulting from a failed

arm of a radial-rift triple junction (Benkhelil, 1989; Benkhelil et al., 1998). According to Benkhelil (1989), stratigraphic and geophysical evidence indicates that the Benue trough itself is an on-land expression of transform fault fracture systems linked to the Mid-Atlantic Ridge. Furthermore, other discussions have discredited the thermal doming mechanism related to mantle plumes for the initiation of three-armed rift triple junctions (Mohr, 1982; Rosendahl, 1987; Hamilton, 2003).

Numerous studies indicate that continental extension is facilitated by a combination of rift and transform fracture systems (e.g., Francheteau and Le Pichon, 1972; Thomas 1977; 1991; Mascle and Blarez, 1987; Lister et al., 1991; Thomas and Astini; 1999), rather than by radial rifting as a result of thermal doming of continental crust (e.g., Dewey and Burke, 1974). The new working model for the Benue trough (Benkhelil, 1989) concludes that the trough represents propagation of transform faults into the craton and is not a failed arm of a radial rift triple junction. Analogy with the new interpretation of the Benue trough suggests that the Ottawa graben is an intracratonic fracture system parallel with transform faults of the rifted margin (Figure 2.2). Neoproterozic magmatic suites are associated with the graben. In this context, the Ottawa graben is related to transform faults of the rifted margin in the same way as the Southern Oklahoma fault system in the Ouachita embayment of the southern Laurentian margin (Thomas, 1991). Similarly, the Saguenay graben is interpreted to be an intracratonic expression of the Saguenay-Montmorency transform, which separates the Quebec and Gaspé rift zones in the Quebec embayment (Figure 2.2).

2.4 EVOLUTION OF THE EASTERN LAURENTIAN MARGIN

2.4.1 Age of the Rift

Isotopic ages of rift-related magmatic suites (Figure 2.2) suggest diachronous continental rifting along the Laurentian margin in the northern Appalachians. The oldest rift-related magmatism is limited to the St. Lawrence promontory where ca. 620-600 Ma intrusive suites cut basement and are unconformably overlain by synrift deposits. On the New York promontory, synrift intrusive and volcanic rocks are limited in age to ~ 570 Ma. Within allochthonous marginal rocks along the Quebec embayment, a slight contrast in the age of synrift magmatism and sedimentation appears between the Quebec and

Gaspé rift zones. In the Quebec rift zone, rift-related volcanic rocks range in age from ca. 555 to 550 Ma (Kumarapeli et al., 1989; Hodych and Cox, 2007). Rift-related volcanism in the Gaspe rift zone, however, appears to have commenced earlier, ranging from ca. 565 to 555 Ma (Hodych and Cox, 2007). Thus, synrift magmatism in the northern Appalachians can be bracketed into an early pulse (620-600 Ma) consisting principally of plutonic and shallow intrusive suites on the St. Lawrence promontory followed by a later pulse (570-550 Ma) of widespread volcanic and plutonic magmatism. Synrift clastic deposits are interlayered with or underlie synrift volcanic rocks on the New York promontory and Quebec embayment, constraining the age of synrift deposition along those segments of the margin. Transition from rift to passive margin began sometime during the Early Cambrian; by the end of the late-Early Cambrian, the entire length of the Laurentian margin in the northern Appalachians had evolved to a passive-margin environment.

While the isotopic and stratigraphic data suggest diachronous rifting that lasted into the earliest Cambrian, paleomagnetic data indicate that eastern Laurentia had rifted away from the then assembling Gondwanan landmass by 570 Ma and was separated from Gondwana by a wide Iapetus Ocean by ~550 Ma (McCausland and Hodych, 1998; Cawood et al., 2001), implying the development of a passive margin well before the late Early Cambrian. To resolve the disparity between the stratigraphic and paleomagnetic data sets, Cawood et al. (2001) proposed a two-stage rift model with initial break-up of eastern Laurentia from Gondwana and opening of the Iapetus Ocean at ca. 570 Ma followed by late-stage rifting of microcontinents from the margin around ca. 550 Ma and transition of eastern Laurentia to a passive margin by ~535 Ma (e.g., Cawood et al., 2001). In this model, the early pulse of synrift magmatism on the St. Lawrence promontory is implicitly related to first-stage break out of Laurentia. Synrift stratigraphy in the lower Labrador Group (Bateau and Lighthouse Cove Formations) may also reflect this early rift history. The uniform Early Cambrian age of the rift-to-passive-margin transition in the northern Appalachians implies that the second-stage rift event affected the entire northern margin. The result of this latter rift stage was the opening of a marginal seaway (the Humber Seaway) between the eastern Laurentian margin and a strand of ribbon continents outboard of the margin (Waldron and van Staal, 2001;

Cawood et al., 2001). The second-stage rift event was also responsible for the current configuration of promontories and embayments along the entire length of the eastern Laurentian margin.

To summarize, multiple data sets converge on a model for continental rifting in the northern Appalachians that was punctuated by a shift in the oceanic spreading center into the Laurentian craton, either by ridge jump or the development of new continental rift (Cawood et al., 2001). Multiple episodes of continental rifting in the northern Appalachians parallel the current tectonic model for the opening of the Iapetus Ocean in the southern Appalachians. In the Ouachita embayment, Early Cambrian synrift volcanics along the Southern Oklahoma fault system are unconformably overlain by a Late Cambrian passive-margin succession, whereas rift-parallel graben systems (i.e., Birmingham graben, Mississippi Valley graben) contain stratigraphic successions that indicate Early to early-Late Cambrian synsedimentary movement (Thomas, 1991). These observations are consistent with the break-out of a microcontinent from the Ouachita embayment during the Early Cambrian, which occurred well after the initiation of continental extension along the eastern Laurentian margin in Alabama, Tennessee, and Virginia (e.g., Thomas, 1991; Thomas and Astini, 1999).

The Argentine Precordillera of South America is the likely candidate for the continental block that rifted out of the Ouachita embayment (Thomas and Astini, 1996). In the northern Appalachians, however, it has been suggested that candidates for the string of rifted microcontinents include the Manhattan Prong, the Chester dome, the Chain Lakes massif, and the Dashwoods block (Thomas, 1977; Waldron and van Staal, 2001; Hibbard et al., 2007). It has also been suggested that internal basement massifs along the southern Appalachian margin (i.e., Baltimore Domes, Sauratown Mountains, Pine Mountain window) are also remnants of a microcontinental block(s) rifted from the eastern Laurentian margin (Thomas, 1977). To fit the available models for the eastern Laurentian rift, we speculate that a trans-Iapetus transform system aligned with the Alabama-Oklahoma transform separated a southern Iapetus Ocean (present coordinates) where microcontinents were transferred from Laurentia to Gondwana, from a northern Iapetus Ocean where rifted Laurentian blocks remained adjacent to and were later reaccreted to the eastern Laurentian margin.

2.4.2 Characteristics of a Low-Angle Detachment Rift

The 4-D architecture of a rifted continental margin can be inferred from lateral variations in the synrift and post-rift stratigraphy. Previous studies in the southern Appalachians indicate that the eastern Laurentia continental rift developed as a low-angle detachment rift system (Thomas, 1993; Thomas and Astini, 1999). In the northern Appalachians, the Laurentian margin succession also displays conspicuous along-strike variations in thickness, age, and depositional environment that strikingly match the modeled stratigraphic characteristics for low-angle detachment continental rift systems. Low-angle detachment continental rifts include distinctive structural configurations and thermal patterns for continental extension along a rifted margin (e.g., Wernicke, 1985; Lister et al., 1986; 1991; Buck et al., 1988; Thomas and Astini, 1999). Extension is facilitated by a shallow dipping (<30°) listric fault system that separates the crust into conjugate lower- and upper-plate domains, which are partitioned along strike by steep transform (transfer) faults. The structural configuration of low-angle detachment rifts imposes complementary asymmetry of the synrift and post-rift structure and stratigraphy on conjugate margins.

On the lower plate, rotated crustal blocks are bounded by listric faults that sole into an oceanward dipping detachment, beneath which continental crust thins gradually (>200 km) oceanward (Lister et al., 1986). Rotated half-graben form sediment traps that accumulate thick, fault-rotated, synrift deposits. In contrast, the upper plate is characterized by a relatively narrow, broadly arched zone of transition (≤100 km) from full thickness continental crust to oceanic crust and by a few steeply dipping normal faults antithetic to the main crustal detachment. The proximity of full-thickness continental crust on the upper plate to the active spreading center results in prolonged thermal uplift (Figure 2.6), which delays passive-margin thermal subsidence (Buck et al., 1988). Consequently, initial synrift and post-rift sedimentary deposits on the upper plate are younger than those on the conjugate lower plate, and are more limited in both thickness and distribution. On the conjugate lower plate, however, a wide zone of crustal attenuation separates full-thickness continental crust from the heat-flow maximum in the rift (i.e., the active spreading ridge), resulting in thermal subsidence on the lower plate that begins earlier and reaches greater magnitude than that on the upper plate (Buck et al.,

1988). Thus, simple-shear continental rifts span complementary, asymmetric, opposing conjugate continental margins with syn- and post-rift stratigraphic successions that contrast in age, distribution, and thickness. Transform margins are distinctive because of an abrupt transition (<25 km) from full-thickness continental crust to oceanic crust. Transform faults both offset individual rift segments and bound domains of oppositely dipping detachments (Lister et al., 1986). Thus, transform faults facilitate abrupt along-strike changes in synrift and passive-margin structure and stratigraphy in a low-angle detachment rift system.

An important prediction of the simple-shear detachment fault model is that conjugate margins should exhibit complementary structural and stratigraphic asymmetry on a variety of scales (Lister et al., 1986). The same asymmetry is also predicted across transform faults that bound domains of oppositely dipping detachments. Thus, in the absence of a known conjugate margin, low-angle detachment rift systems can be recognized from abrupt along-strike changes in age, composition, facies, and distribution of synrift and early post-rift stratigraphy (e.g., Lister et al., 1986). This is especially important for ancient mountain belts where conjugate margins have been either removed or obscured by later tectonic episodes.

2.4.3 Architecture of the Laurentian Margin in northeastern North America

Initial breakup of Laurentia from Gondwana was followed by systematic break out of microcontinets from the eastern Laurentian margin at the end of the Neoproterozoic. This second-pulse of continental rifting resulted in the current configuration of promontories and embayments along the entire length of the margin (e.g., Thomas, 1977; Cawood et al., 2001). Lateral variations in the stratigraphy, age, facies, and geophysical characteristics of this late Neoproterozoic-early Paleozoic synrift and post-rift succession indicate that the Laurentian margin developed from a low-angle detachment rift system, which facilitated the margin architecture upon which the passive margin was later established.

Along the New England rift zone, thick, Neoproterozoic alluvial-fan deposits of the Pinnacle Formation are overlain by a thick (~2000 m) passive-margin shelf succession. Middle and Late Cambrian shelf carbonates along the New England rift zone

commonly interfinger eastward with shelf-edge and slope facies deposits. These observations indicate rapid synrift subsidence followed by prolonged instability of the Cambrian passive margin, which is consistent with a lower-plate rift setting for the New England rift zone (Figure 2.7). Northward across the international border, there is a sharp contrast between Laurentian margin of the New England and Quebec rift zones. Felsic volcanic phases in the Tibbit Hill Formation suggest thick Laurentian crust beneath Paleozoic cover. Synrift deposits in the Quebec rift zone are an order of magnitude thinner, undergo an abrupt facies change to coastal and deltaic deposits, and are younger than rift deposits south of the international boarder. Rift-to-passive-margin and passive-margin successions also thin from New England into Quebec. All of these observations indicate an upper-plate rift setting for the Quebec rift zone (Figure 2.7). An upper-plate setting is further supported by seismic profiles that image small, east-dipping antithetic faults that offset basement, which thins eastward within a short distance. The abrupt along-strike variation in synrift and post-rift stratigraphy near the international border implies a major transform fault (the Missisquoi transform) between the lower-plate New England rift zone and the upper-plate Quebec rift zone (Figure 2.7) (Cherichetti et al. 1998).

Along the Gaspé rift zone, the stratigraphy is dominated by synrift and passive-margin slope sediments, which requires a broad attenuated margin to accommodate the volume of slope deposits. Cousineau and Longuépée (2003) originally suggested that the Gaspé rift zone developed in a lower-plate rift setting; and our model, using the data presented here, supports their interpretation (Figure 2.7). This interpretation is consistent with the geochemistry of rift volcanics that indicate the Gaspé rift zone is underlain by highly attenuated continental crust. Furthermore, on the basis of rift volcanics that are interlayered with synrift sedimentary successions, synrift deposition in Gaspé commenced earlier than synrift sedimentation in southern Quebec. In the context of a low-angle detachment rift, outboard carbonate platform deposits (Middle Cambrian Corner-of-the-Beach Formation) may represent localized shallow-marine carbonate deposition on the uplifted edge of a rotated half-graben within the rift. The Saguenay-Montmorency transform is the boundary between the upper-plate Quebec rift zone and the lower-plate Gaspé rift zone, and marks a fundamental along-strike change in the

composition and facies of synrift and passive-margin deposits in the Quebec embayment (Cousineau and Longuépée, 2003). The increase in abundance of coarse conglomerates northeast of the transform is attributed to Cambrian and Ordovician reactivation of the transform system (e.g., Lavoie et al., 2003).

On the St. Lawrence promontory, the Early Cambrian stratigraphy of the Long Range rift zone around Port au Port peninsula and west of the Long Range massif on the Northern Peninsula (Figure 2.5) includes a thin synrift clastic shelf succession overlain by a thin passive-margin succession and no observed Neoproterozoic-Early Cambrian synrift slope deposits. These observations are consistent with an upper-plate rift setting for these segments of the promontory (Figure 2.7). In this context, the lack of Early Cambrian synrift slope deposits is attributed to thermal uplift of the upper-plate margin, which would limit Neoproterozoic-Early Cambrian synrift deposition. In contrast, the regions of the promontory around the Bay of Islands and Hare Bay (Figure 2.5) contain a thick synrift slope succession that includes coarse conglomerates with basement-derived clasts, indicating rapid subsidence and erosion of the margin along these two segments. Furthermore, shelf deposits (Reluctant Head Formation) east of the Bay of Islands in southwestern Newfoundland indicate prolonged subsidence and instability of the shelf that lasted through late Middle Cambrian. These observations are consistent with a lower-plate setting for these segments of the Long Range rift zone (Figure 2.7).

The boundaries between the upper- and lower-plate segments on the St. Lawrence promontory are expressed as abrupt (<20 km) along-strike discontinuities in shelf and slope stratigraphy (Cawood and Botsford, 1991). These zones of along-strike transition are interpreted as transform faults that separate upper- and lower-plate domains (Figure 2.7). Cawood and Botsford (1991) originally recognized these transforms on the basis of along-strike discontinuity in the Ordovician passive-margin and foreland-basin stratigraphy of the Humber Arm allochthon, and we adopt their nomenclature for these transform faults (Figure 2.7).

2.5 CONCLUSIONS

The configurations of salients and recesses in the northern Appalachian orogen (Figure 2.1) reflect a profound structure in the underlying Laurentian basement. Lateral

variation in the stratigraphy, age, and geophysical attributes of late Neoproterozoic-Middle Ordovician margin successions reveal that the eastern Laurentian margin was outlined by promontories and embayments defined by northeast-striking rift zones offset by northwest-striking transforms (Figure 2.2). Multiple lines of evidence converge on a protracted and complex history for the northern Appalachian continental margin, which began with breakup of Rodinia, followed by rifting of ribbon continents from the Laurentian margin, and finally passive-margin thermal subsidence and establishment of a broad carbonate bank.

Isotopic ages from synrift igneous complexes indicate diachronous late Neoproterozoic continental rifting, reflecting multiple stages of continental extension. Rifting began in the late Precambrian along a continental rift system that must have formed well outboard of the present northern Appalachian margin (Figure 2.8A) because, with the exception of synrift clastic and volcanic deposits on Belle Isle, no synsedimentary record of the older rift exists in the northern Appalachians. Synrift magmatic activity and localized faulting along the St. Lawrence promontory likely reflect an aborted attempt at activation of the Long Range rift zone during the initial rift stage. Lack of a stratigraphic record for the older rift system across most of the northern Appalachian margin precludes any precise interpretation regarding the structural geometry and exact position of the older rift relative to the incipient eastern Laurentian margin. A growing body of work on the Rodinian, Laurentian, and Atlantic continental margins indicates that continental margin geometries (e.g., promontories, embayments, transforms, etc…) are tectonically inherited from previous orogenic systems (Thomas, 2006, and references therein). Therefore, we conclude that the trace of the older rift system likely followed a similar trace as the younger eastern Laurentian margin and was marked by promontories and embayments offset by transform faults.

Paleomagnetic data indicate that Laurentia began to drift away from Gondwana around 570 Ma (McCausland and Hodych, 1998); thus around this time, the older outboard rift system began to progress to a passive-margin stage bordered by an open ocean basin (Iapetus Ocean) with an active spreading ridge system (Mid-Iapetus Ridge) (Figure 2.8B). Onset of the second rift stage must have occurred on the heels of the first-stage because early synrift sedimentary successions in the Pinney Hollow Formation

(New York promontory) and the Lac Matapédia suite (Gaspe rift zone) are interlayered with synrift volcanic deposits that have been dated around 570-565 Ma (Walsh and Aleinikoff, 1999; Hodych and Cox, 2007). Continental extension within the New England, Quebec, Gaspè, and Long Range rift zones was recorded along a low-angle detachment rift system partitioned by transform faults. The initiation of this later rift stage is only preserved locally in the stratigraphic record because of the asymmetric structural geometry of the low-angle detachment rift system. The spreading-center shift and initiation of the younger rift system were accompanied by initiation of the Ottawa and Saguenay grabens as cratonward projections of transform faults.

The result of the shift in spreading centers inboard of the continental margin was successful rafting of a strand of ribbon continents from eastern Laurentia by Early Cambrian time (Figure 2.8C). This final stage of continental rifting also produced the New York and St. Lawrence promontories, and the Quebec embayment. A late-Early Cambrian clastic/carbonate transgressive sequence marks the end of active rifting along the entire length of the margin, which was flanked by a newly formed ocean basin (Humber Seaway) with an active spreading ridge (Mid-Humber Seaway Ridge). The strand of outboard ribbon continents separated Laurentia and the Humber Seaway from the Iapetus Ocean. It has been proposed that these microcontinents were reaccreted to the eastern Laurentian margin when the Humber Seaway closed during the Middle Ordovician Taconic orogeny (e.g., Waldron and van Staal, 2001). In this context, internal basement massifs are the exposed remnants of this chain of microcontinents (e.g., Hibbard et al., 2007).

Two internal basement massifs, however, are an exception in that they are part of the eastern Laurentian margin rather than isolated microcontinents. The Corner Brook Lake terrane is directly adjacent to Laurentian margin successions, and rocks within the terrane are nearly identical in both composition and facies to rocks exposed within the Humber Arm allochthon (e.g., Knight, 1996). Rocks of the Baie Verte terrane were deposited on an east-facing margin and are also nearly identical in facies and lithodemic stratigraphy to the Laurentian margin (Hibbard, 1988). Furthermore, oceanic debris in the Fleur de Lys Supergroup on Baie Verte Peninsula is dated at ca. 558 Ma (van Staal et al., 2009), which corresponds more closely to the ca. 560-550 Ma Humber Seaway rather

than the ca. 570 Ma Iapetus Ocean. Therefore, these two basement massifs likely represent marginal basins that formed as part of the younger eastern Laurentian rift, but that were later taken up in intense Paleozoic deformation.

Transgression of late-Early through early-Middle Cambrian shale and carbonate conglomerate facies in New England and southwestern Newfoundland suggests localized instability of the continental margin, possibly related to the lower-plate rift setting for these parts of the margin. By the end of the Middle Cambrian, the entire length of the Laurentian margin had developed into a carbonate bank, indicating onset of a full-fledged passive margin (Figure 2.8D).

In conclusion, lateral variations in synrift and post-rift stratigraphy reflect along-strike partitioning of the rift into segments that differ fundamentally in tectonic framework, subsidence history, and sediment dispersal. Specifically, these characteristics conform to a low-angle detachment model for rifting continental crust, and they constrain the range of acceptable models for continental rifting. Furthermore, continental extension appears to have been punctuated by a shift in spreading centers during the latest Neoproterozoic. The proposed model is consistent with the Iapetan rift along the entire length of the eastern Laurentian margin from Newfoundland to Mexico and provides a regional constraint on the breakup of Rodinia, as well as highlights stratigraphic constraints for models of continental rifting.

2.6 ACKNOWLEDGEMENTS

No review such as the one presented herein can be produced without first acknowledging the author's substantial debt to the many geoscientists that came before him. To all of the northern Appalachian geologists whose work was the basis for this chapter's narrative, I extend my humblest gratitude and thanks. Without your work, this manuscript would not have been possible. I would also like to thank Pierre Cousineau and Hughes Longuépée, along with the managing editors of the *Canadian Journal of Earth Science*, for permission to reproduce previously published figures in this manuscript (i.e., Figures 4A and 4B). Part of this research was supported by various grants from the Geological Survey of Canada, Geological Society of America, the University of Kentucky, and the University of Kentucky Department of Earth and

Environmental Sciences. A draft of this manuscript is currently under review for publication in a special Appalachian Volume as a *Geological Society of America Memoir* (Tollo, R., Bartholomew, J., Karabinos, P., and Hibbard, J., *Eds*). An earlier and more concise draft of this chapter was submitted and accepted for publication in the April 2009 issue of *Geology*. Dr. William A. Thomas and Dr. Denis Lavoie are co-authors of the manuscripts submitted for publication.

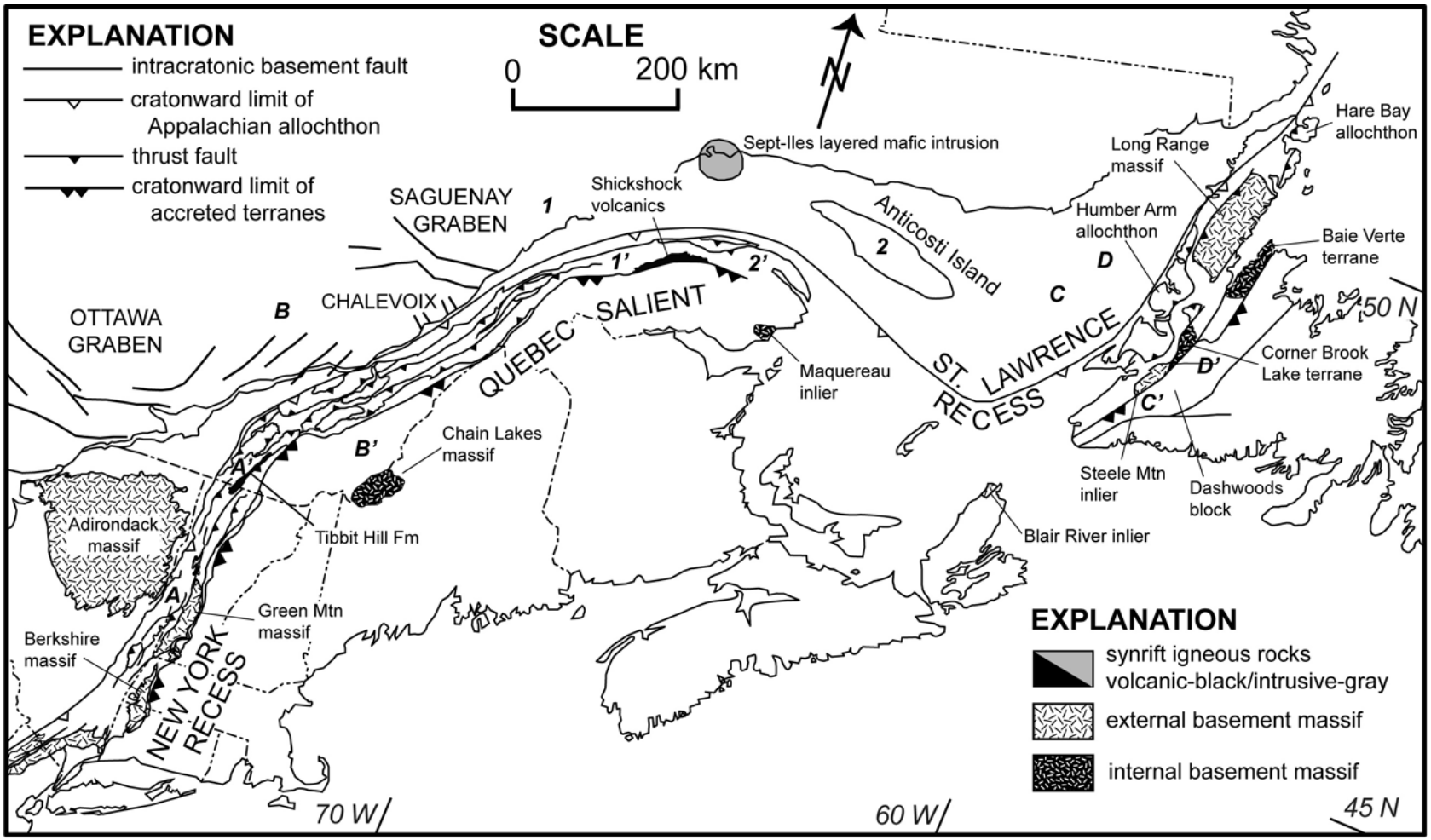

Figure 2.1. Outline map of the Appalachian orogenic belt highlighting structural salients and recesses, as well as intracratonic fault systems. Locations of continental margin rocks and basement massifs are shown in present structural position. Map and locations of structures and rocks compiled from references cited in text. End points of cross sections in Figures 3 and 4 indicated by letters and numbers.

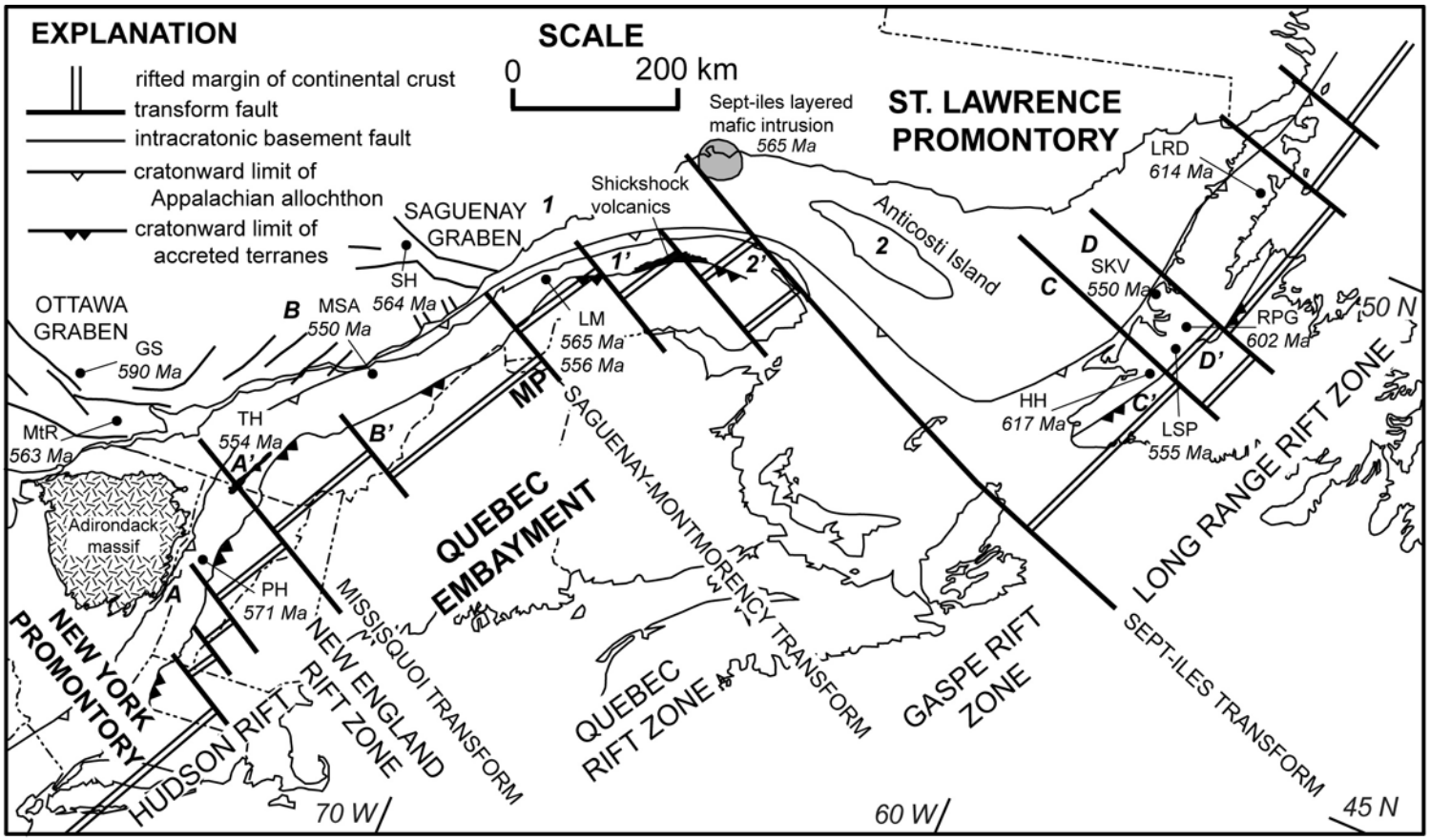

Figure 2.2. The interpreted Neoproterozoic-Early Cambrian continental margin defined by rift segments and transform faults (modified from Thomas, 1977). Map shows an outline of the Paleozoic Appalachian orogenic belt and intracratonic basement fault systems, as well as the current unrestored distribution and ages of synrift igneous rocks in the northern Appalachian orogen (compiled from references in text). Intersections between rift segments and transform faults are drawn orthogonally as a simplifying generalization. GS-Grenville dike swarm; HH-Hare Hill granite; LM-Lac Matapedia volcanics; LRD-Long Range dikes; LSP-Lady Slipper pluton; MP-Montmorency promontory; MSA-Mont de St-Anselme Formation; MtR-Mount Rigaud intrusion; PH-Pinney Hollow Formation; RPG-Round Pond granite; SKV-Skinner Cove volcanics; SH-St. Honeré complex; TH-Tibbit Hill Formation.

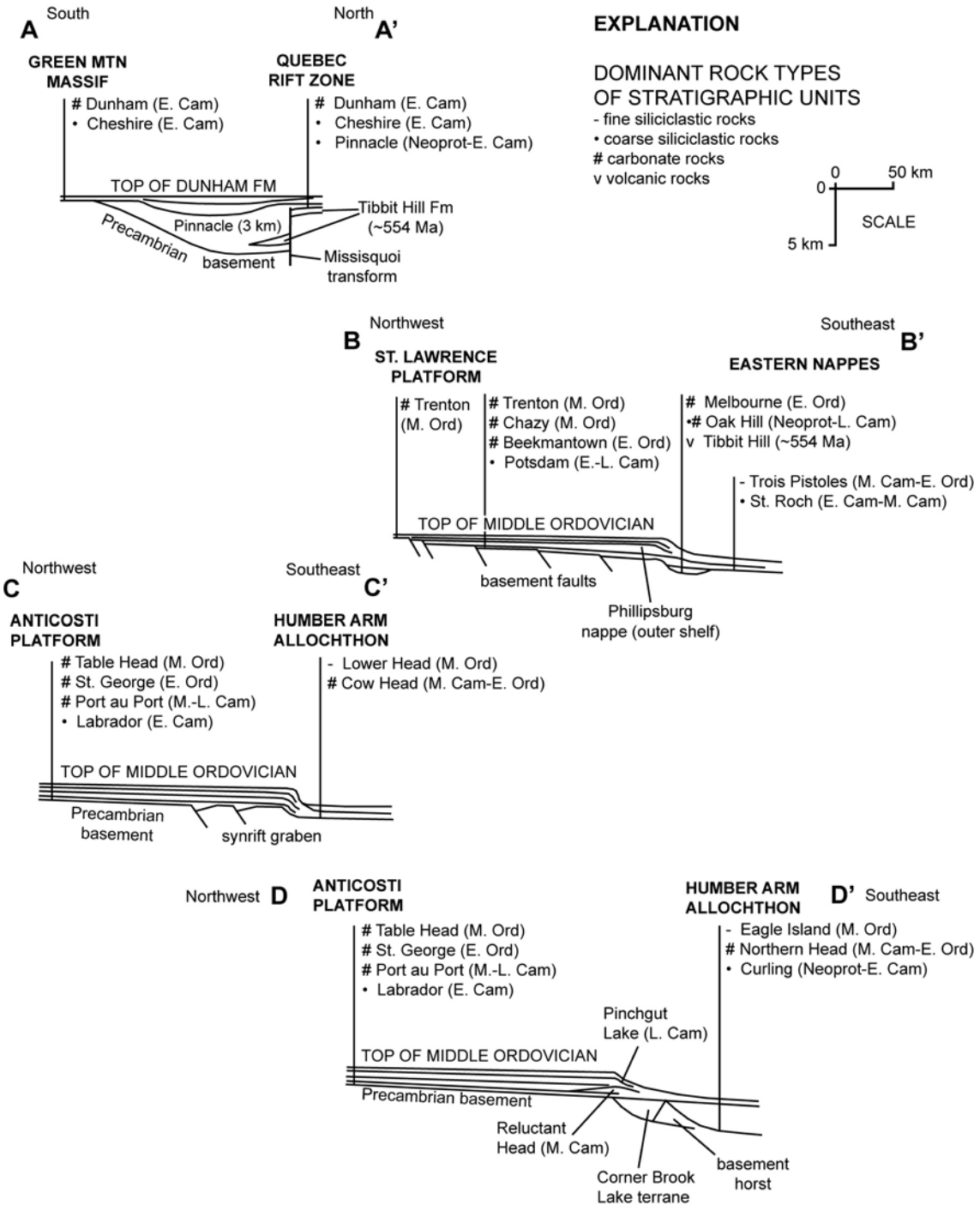

Figure 2.3. Schematic cross sections of the eastern Laurentian margin in New England, southern Quebec, and Newfoundland highlighting thickness contrasts in both the synrift and post-rift stratigraphy, as well as proposed basement structures. Cross section A-A' is parallel to strike; cross sections B-B', C-C', and D-D' are perpendicular to strike of the present northern Appalachian foreland structures. Data for cross sections compiled from references in text. End points of cross sections shown by letters in Figures 1 and 2.

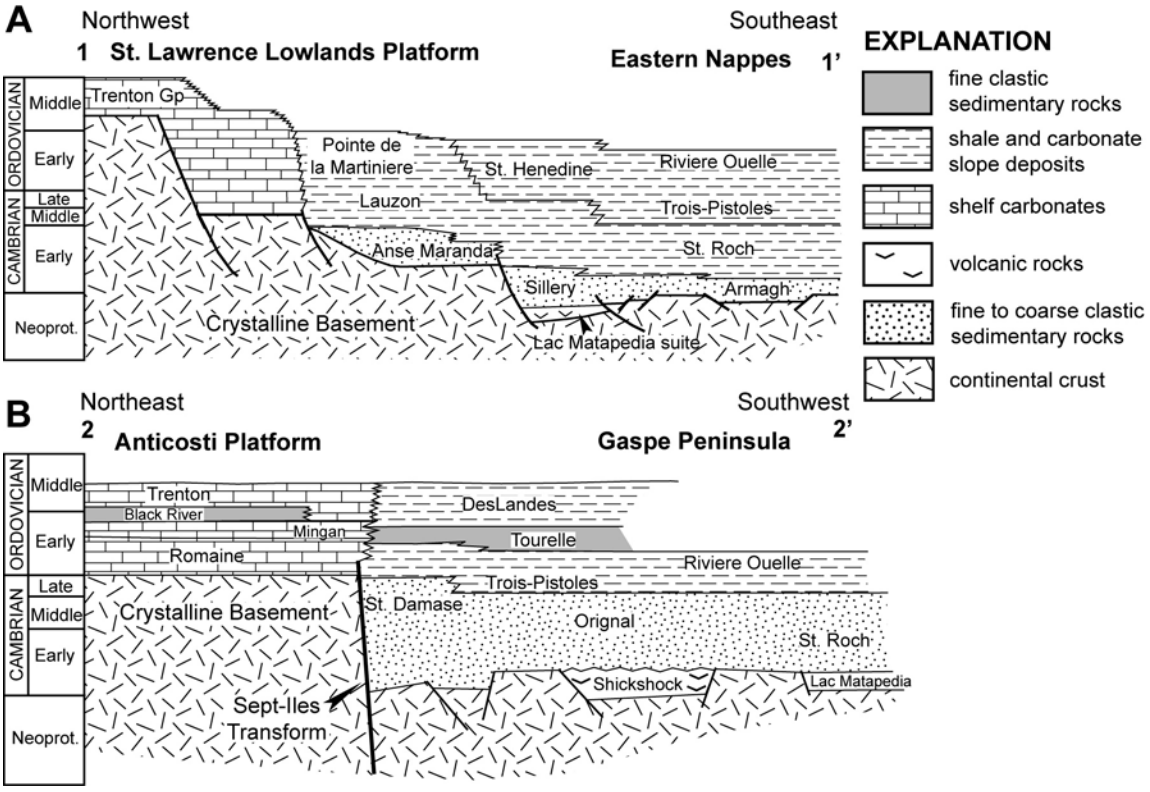

Figure 2.4. A) Schematic cross section perpendicular to the orogen through central Gaspé and the St. Lawrence lowlands depicting the across-strike structure and stratigraphy of the Gaspé rift zone. Stratigraphic units are depicted according to age and not unit thickness; B) schematic cross section across the Sept-Iles transform illustrating the variation in facies and age of Laurentian margin deposits on the Anticosti platform and the Gaspé rift zone. Stratigraphic units are depicted according to age and *not* unit thickness. End points of cross sections shown by numbers in Figures 1 and 2. Both cross sections from Cousineau and Longuépée (2003).

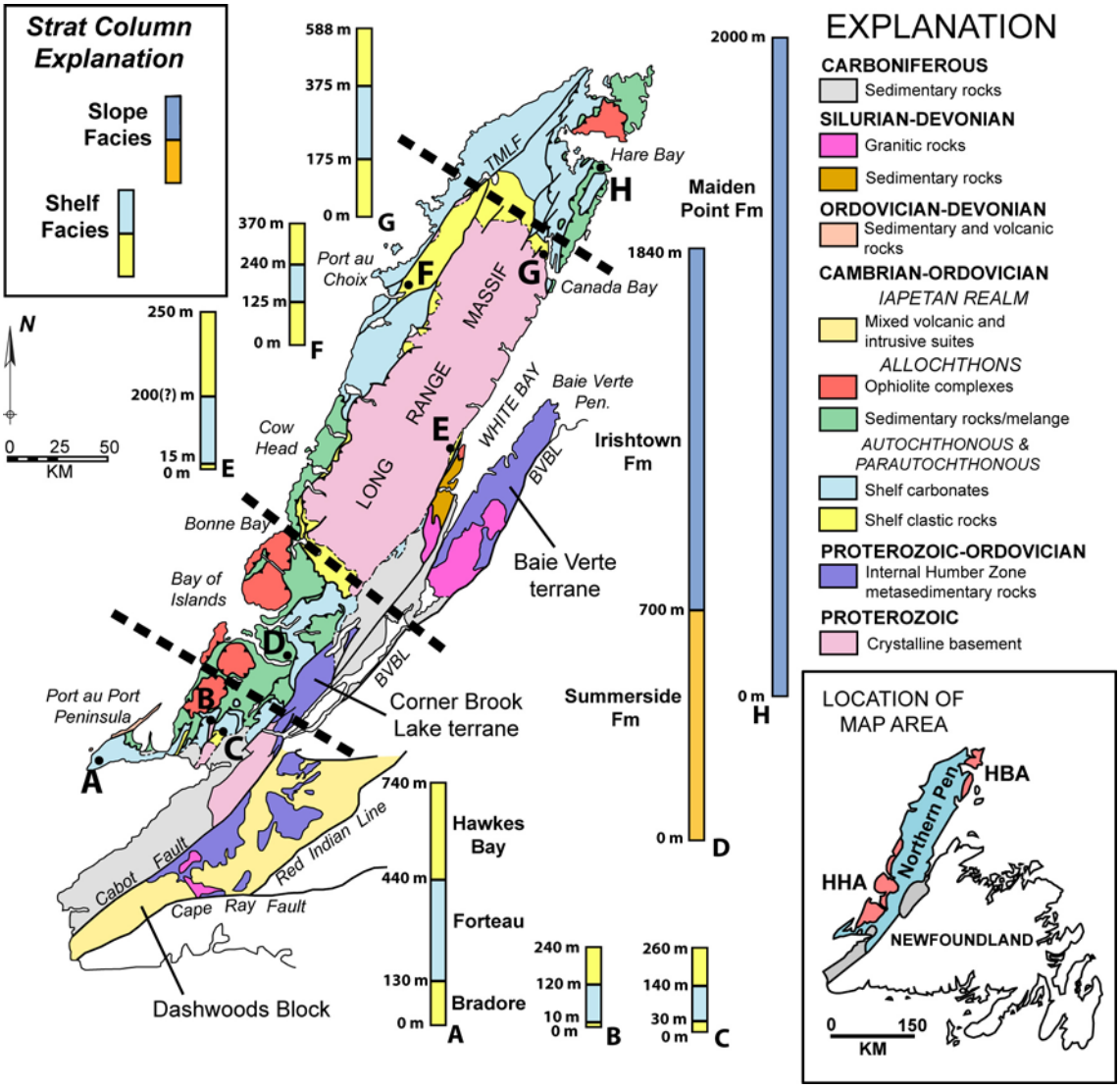

Figure 2.5. Geologic map of western Newfoundland showing the Laurentian margin geology, as well as the locations of the Humber Arm allochthon (HHA), Hare Bay allochthon (HBA), and important internal basement massifs. Stratigraphic columns represent the Neoproterozoic/Lower Cambrian stratigraphy of the Laurentian shelf and slope in western Newfoundland. Stratigraphic columns are to scale. Bold, dashed lines roughly correspond to locations of along-strike changes in the Laurentian shelf and slope stratigraphy. Geologic data compiled from references in text. Other abbreviations: BVBL-Baie Verte-Brompton Line; TMLF-Ten Mile Lake fault.

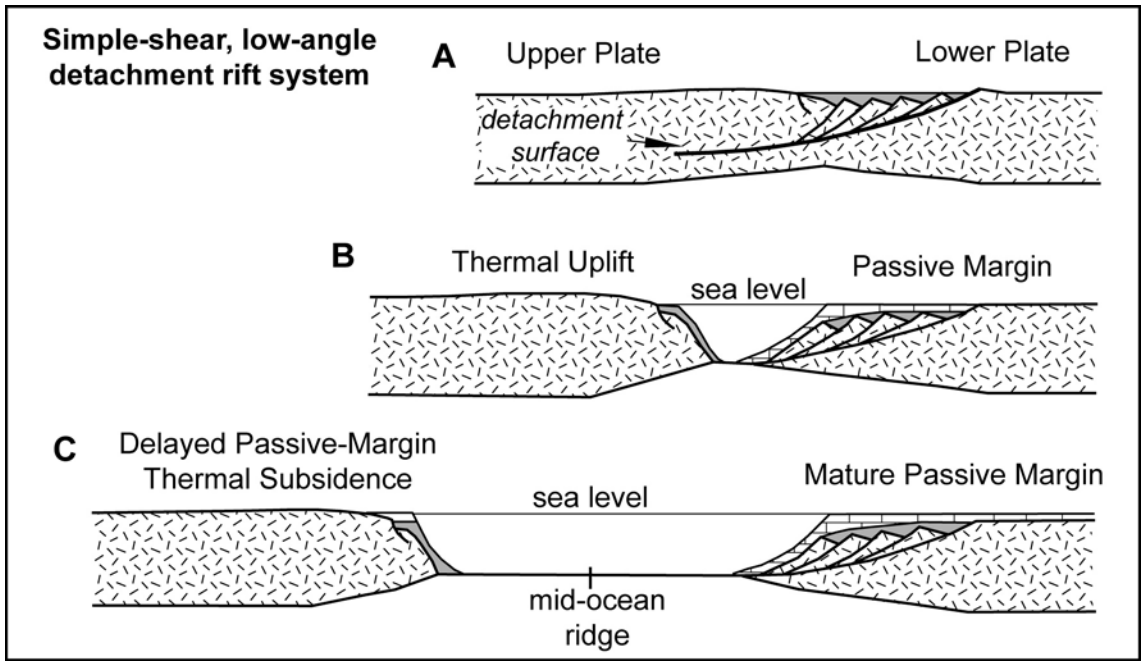

Figure 2.6. Schematic sequential cross sections depicting stages of continental break up by a simple-shear, low-angle detachment rift. Dark grey shows synrift sedimentary deposits; block pattern shows passive margin deposits. A) Extended crust prior to breakup. Maximum heat flow is at the intersection of the low-angle detachment and the surface. B) Directly following breakup, isostatic subsidence of thinned crust on the lower plate counteracts thermal uplift, resulting in the establishment of a passive margin. The upper plate undergoes a delay in thermal subsidence because of proximity of thick continental crust to the spreading ridge. C) During drift, the upper plate migrates away from the active ridge and undergoes passive-margin thermal subsidence. From Thomas and Astini, 1999.

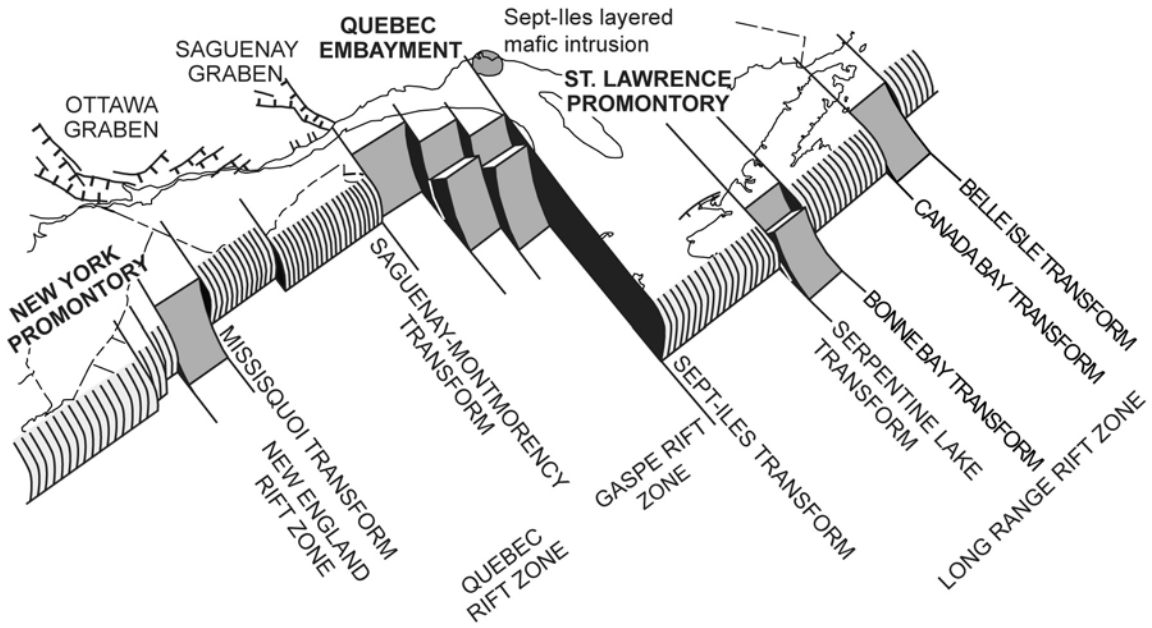

Figure 2.7. Schematic three dimensional block diagram of the eastern Laurentian rifted continental margin and intracratonic fault systems of northeastern North America (present coordinates) in the context of a low-angle detachment rift system.

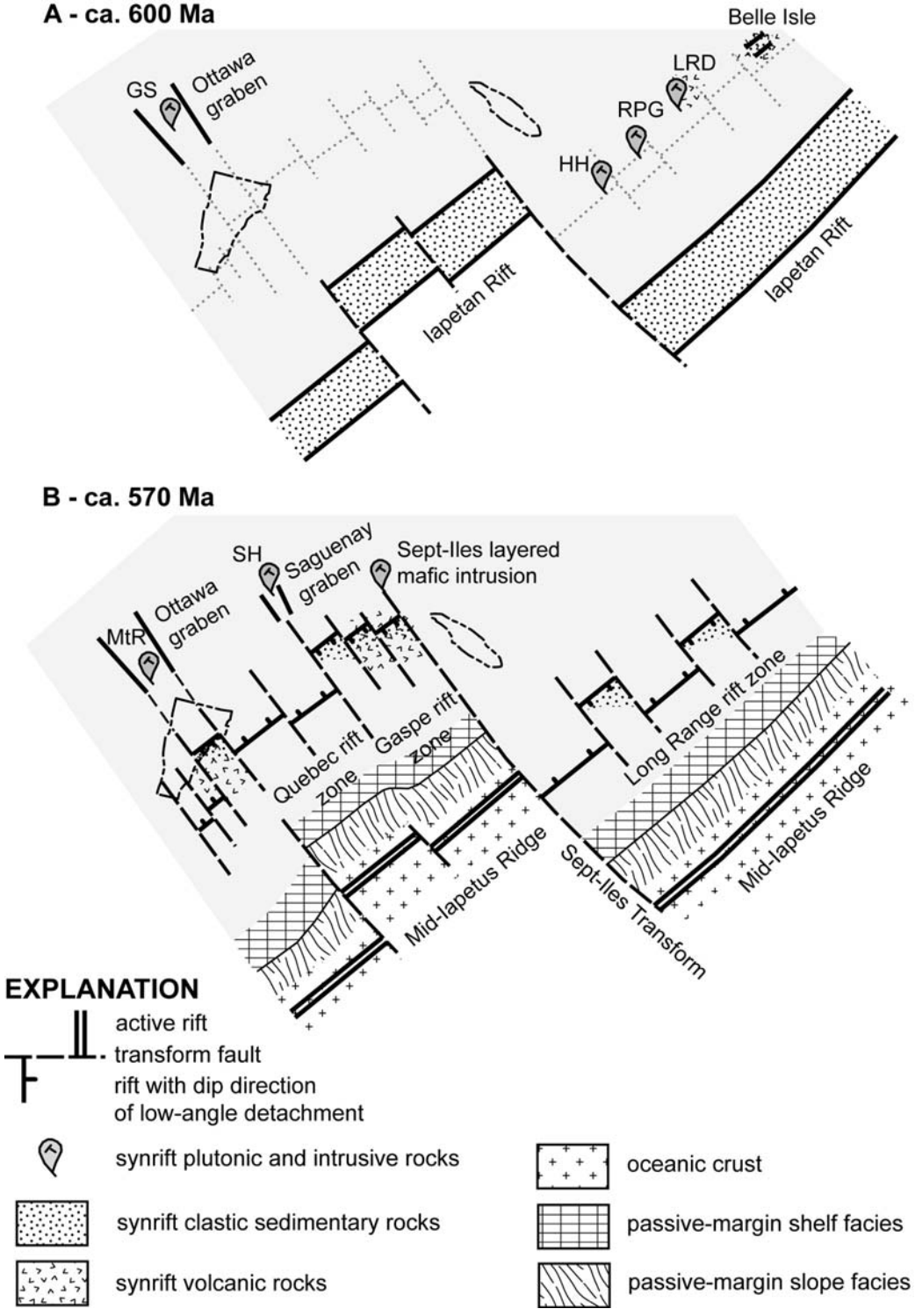

Figure 2.8. Sequential diagrammatic maps illustrating interpretation of the history of the Neoproterozoic-early Paleozoic eastern Laurentian rifted margin of northeastern North America. Outlines of the state of Vermont and Anticosti Island on each map for consistent locations. Abbreviations for synrift igneous complexes same as from Figure 2. Other Abbreviations: BVt-Baie Verte terrane; CBt-Corner Brook Lake terrane.

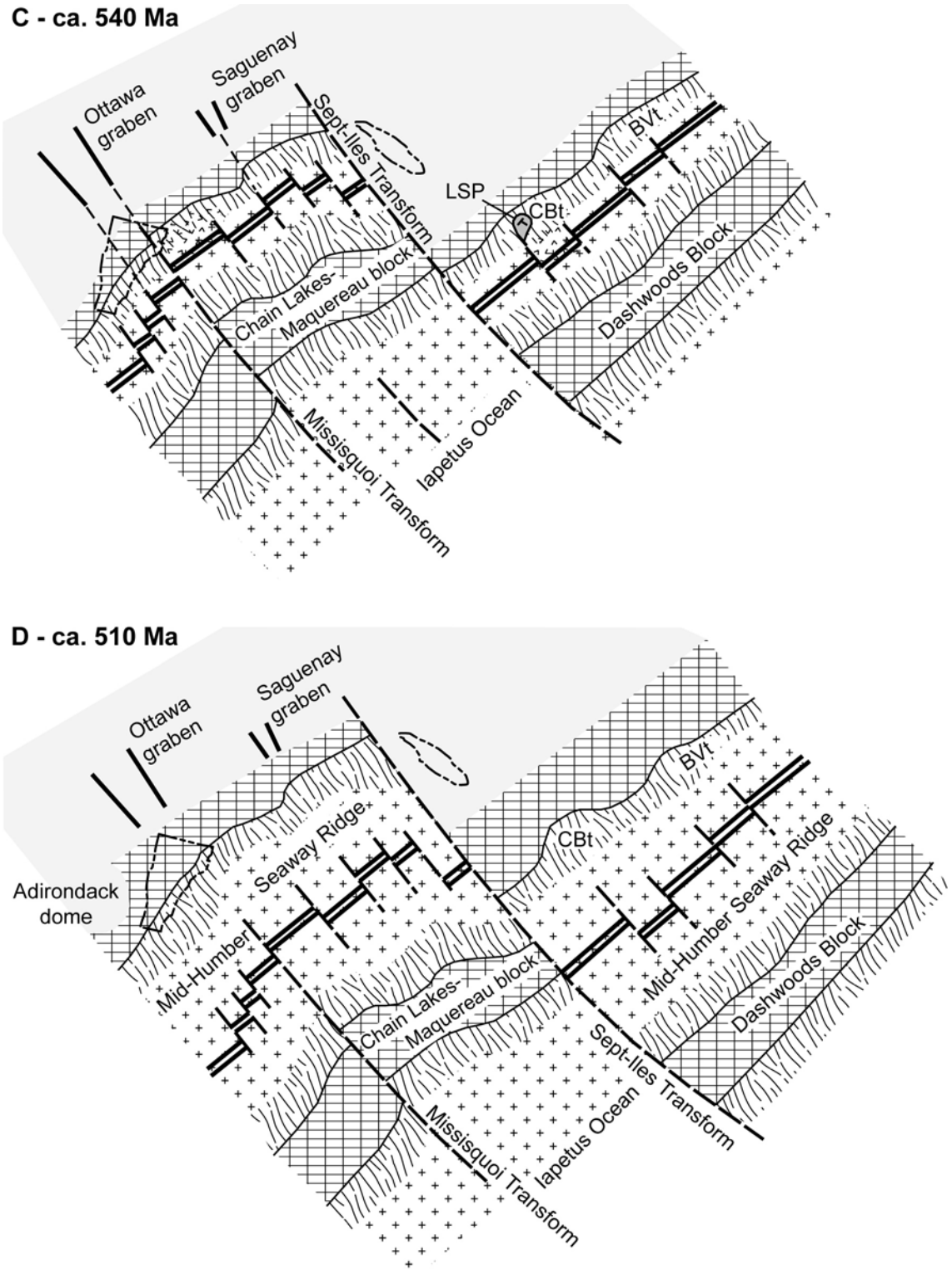

Figure 2.8 (continued)

CHAPTER 3 – PALINSPASTIC RESTORATION OF THE NEOPROTEROZOIC-PALEOZOIC EASTERN LAURENTIAN MARGIN ON THE ST. LAWRENCE PROMONTORY, WESTERN NEWFOUNDLAND

3.1 INTRODUCTION

The Appalachian Mountains along the St. Lawrence promontory in western Newfoundland (Figure 3.1) record a complete Wilson cycle punctuated by the opening and closing of the Iapetus Ocean (Wilson, 1966; Williams and Hatcher, 1983; van Staal et al., 1998). There, a dynamic stratigraphic succession indicates protracted Neoproterozoic-Early Cambrian continental rifting followed by the development of a stable Cambrian-Ordovician passive margin. This ancient rift and passive-margin succession has been subsequently deformed and obscured by a succession of overprinting Paleozoic orogenic cycles related to the accretion of outboard terranes to the Laurentian margin (Williams, 1979; Williams and Hatcher, 1983; Knight and Cawood, 1991; Williams, 1995; Waldron et al., 1998).

On the St. Lawrence promontory, abrupt along-strike variation in the distribution, thickness, facies, and age of synrift and post-rift successions suggest a profound three-dimensional basement architecture to the eastern Laurentian rifted margin that is broadly consistent with models proposed for continental rifting by a low-angle detachment system (e.g., Allen et al., 2009). This model is based primarily on broad field and literature observations of the regional stratigraphy, however, and has yet to be vigorously tested geometrically. The underlying architecture of the continental margin plays an important role in the subsequent development of compressional events that characterize the Appalachian orogen (e.g., Thomas, 1977; 2006; Bradley, 1989). Thus, understanding the basement geometry of the St. Lawrence promontory is critical to accurate analysis of the orogeny in the Newfoundland Appalachians.

The Appalachian orogen on the Island of Newfoundland is considered to be a two-sided symmetrical system in which vestiges of the early Paleozoic Iapetus Ocean (Dunnage zone) are bounded by the Laurentian craton to the west (Humber zone) and by elements of peri-Gondwanan origin to the east (Gander and Avalon zones) (Williams, 1964; 1979). In western Newfoundland, the Humber zone comprises basement and sedimentary deposits of the ancient Laurentian continental margin, which are divided into

a mildly deformed western external domain (James and Stevens, 1986; Williams and Hiscott, 1987; Williams, 1995) and an intensely deformed and metamorphosed eastern internal domain (Hibbard, 1983; 1988; Cawood et al., 1995). The Dunnage zone lies to the east of the Humber zone (Figure 3.2), and consists of a remnant peri-Laurentian arc (Notre Dame subdomain) and a peri-Gondwanan arc and back-arc basin (Exploits subdomain), which were sutured to the Laurentian margin during the Ordovician along the Baie Verte-Brompton Line (Dunning et al., 1990; van Staal et al., 1998; Waldron and van Staal, 2001; van Staal, 2005). East of the Dunnage zone, the Gander zone (Figure 3.2) comprises a distinct succession of Lower Cambrian to Early Ordovician clastic rocks deposited onto a complex basement that consists of late-Neoproterozoic to Early Cambrian magmatic arc successions (e.g. van Staal, 2005; Hibbard et al., 2007). The Avalon zone (Figure 3.2) is characterized by predominantly Neoproterozoic arc-related volcanic-sedimentary successions and an overlying early Paleozoic clastic platform succession (Williams, 1995; Hibbard et al., 2007). Both zones are considered to have formed near the margin of Gondwana (O'Brien et al., 1996; van Staal et al., 1996) and were accreted to the active Laurnetian margin during the Silurian (Gander zone) and the Devonian (Avalon zone) (van Staal, 2005).

Accretion of these zones to the eastern Laurentian margin has subsequently deformed the synrift and passive-margin strata deposited on the eastern Laurentian margin. Thus, in order to accurately study the margin on the St. Lawrence promontory, deformed rift and passive-margin successions must be palinspastically restored to the original depositional positions. The purpose of this Chapter is to test whether the palinspastic distribution and subsidence history of synrift and post-rift stratigraphy in the Humber zone on the St. Lawrence promontory fulfill the predicted parameters for an asymmetric, low-angle detachment continental rifted margin. To achieve this aim, a set of nine balanced cross sections has been constructed across the Humber zone in western Newfoundland (Plates 3.1 and 3.2). Cross sections were constructed using data gathered from geologic field mapping, deep wells, a wide array of seismic reflection profiles, and digitized potential field data, all of which provide depth control for interpretation of Appalachian structures mapped at the surface. Restored sections provide viable reconstructions of the eastern Laurentian rifted continental margin in western

Newfoundland, as well as highlight a complex, polyphase deformational history for the St. Lawrence promontory that spans the Paleozoic.

3.2 MODELS FOR CONTINENTAL RIFTING

Continental rifts consist of fault bounded basins produced by extension of continental crust, which results in thermally induced subsidence, deposition of locally thick immature clastic sedimentary accumulations, and emplacement of bimodal magmatic suites (e.g. Rosendahl, 1987; Condie, 2005). Current models for continental rifting can be grouped into two general end-member categories: a pure-shear, symmetric-rift model (e.g. McKenzie, 1978; Jarvis and McKenzie, 1980; Sclater and Christie, 1980); and a simple-shear, low-angle detachment, asymmetric-rift model (e.g. Wernicke, 1985; Lister et al., 1986; 1991). These alternative models predict distinctive heat-flow régimes, patterns of uplift and subsidence, and sedimentary accumulations that reflect the mechanical and structural geometry of the continental rift.

Pure-shear rift models imply symmetrical continental extension around an active rift axis, in which extension results in rapid breakup of the brittle upper crust by normal faulting, while thinning by ductile flow predominates in the lower crust and mantle lithosphere (e.g., McKenzie, 1978; Jarvis and McKenzie, 1980; Sclater and Christie, 1980). Crustal strains induced by pure-shear rifting are symmetrical in both direction and magnitude, and thus exhibit the characteristics of pure-shear deformation. The mechanical result is the development of symmetrical, oppositely dipping rotated fault blocks on opposite sides of the rift above symmetrically thinned lower crust. The symmetry of a pure-shear rift system is also reflected in symmetrical thermal regimes, which are reflected in post-rift thermal subsidence (e.g., Buck et al., 1988). The greatest heat flux (and thermal uplift) in a pure-shear system is focused at the active center of the rift. Heat generated by the rift dissipates symmetrically away from the rift. Models for pure-shear continental rifting predict similar patterns of synrift thermal uplift and post-rift subsidence on both margins of the opening rift (Buck et al., 1988). This implies a symmetrical distribution of 1) the age and distribution of synrift and post-rift stratigraphy on both rift shoulders, and 2) magnitude of synrift and post-rift thermal subsidence of the crust.

Models for simple-shear, low-angle detachment continental rifts imply asymmetrical rift structures (Figure 3.3) (e.g., Wernicke, 1985; Lister et al., 1986; 1991; Etheridge et al., 1989). Extension is facilitated by a shallow dipping listric fault system that separates the crust into conjugate lower- and upper-plate domains that are partitioned along strike by steep transform faults. On the lower plate, rotated crustal blocks are bounded by listric faults that sole into an oceanward dipping detachment, beneath which continental crust thins gradually (>200 km) (Lister et al., 1986). Rotated half-graben form sediment traps that accumulate thick, fault-rotated, synrift deposits. In contrast, the upper plate is characterized by a relatively narrow, broadly arched zone of transition (≤100 km) from full thickness continental crust to oceanic crust and by a few steeply dipping normal faults antithetic to the main crustal detachment. The proximity of full-thickness continental crust on the upper plate to the active spreading center results in prolonged thermal uplift that delays passive-margin thermal subsidence (Buck et al., 1988). On the conjugate lower plate, however, a wide zone of crustal attenuation separates full-thickness continental crust from the heat-flow maximum in the rift (i.e., the active spreading ridge), resulting in thermal subsidence on the lower plate that begins earlier and reaches greater magnitude than that on the upper plate (Buck et al., 1988). Consequently, initial synrift and post-rift sedimentary deposits on the upper plate are younger than those on the conjugate lower plate, and are more limited in both thickness and distribution.

Abrupt along-strike changes in the synrift and passive-margin structural geometry and stratigraphy are facilitated at transform faults, which both offset individual rift segments and bound domains of oppositely dipping low-angle detachments (Lister et al., 1986). Transform margins are distinctive because of an abrupt transition (<25 km) from full-thickness continental crust to oceanic crust (Keen, 1982, Scrutton, 1982, Keen et al., 1990). Steep faults parallel some transform systems (e.g., Mascle and Blarez, 1987; Sylvester, 1988; Keen et al., 1990), providing conduits for deep-source magmas (i.e., rift magmatism). An important prediction of the simple-shear low-angle detachment fault model is that conjugate margins should exhibit complementary structural and stratigraphic asymmetry on a variety of scales (Lister et al., 1986). Stratigraphic and structural asymmetry is also predicted across transform faults that bound domains of

oppositely dipping detachments. Thus, in the absence of a known conjugate margin, low-angle detachment rift systems can be recognized from abrupt along-strike changes in age, composition, facies, and distribution of synrift and early post-rift stratigraphy (e.g., Lister et al., 1986).

The subsidence history as determined from backstripping stratigraphic successions on rifted continental margins records the mechanical and thermal evolution of the rift (e.g., Bond et al., 1984). An exponential decay curve characterizes post-rift, passive-margin thermal subsidence of extended continental crust (McKenzie, 1978). Because the predicted heat flow and thermal subsidence patterns for pure-shear and simple-shear continental margins differ (e.g., Buck et al., 1988), analysis of the subsidence history for synrift and passive-margin successions on the St. Lawrence promontory should elucidate the mechanism through which the eastern Laurentian rift developed. Rates of subsidence along a pure-shear rifted margin should be symmetrical across the rift axis. On the other hand, subsidence of the crust along a simple-shear rifted margin will reflect the asymmetry of the thermal and mechanical régimes inherent in upper- and lower-plate domains in a low-angle detachment rift system (Thomas and Astini, 1999).

3.3 REGIONAL GEOLOGIC SETTING AND STRATIGRAPHY

The Humber zone on the St. Lawrence promontory includes the entire western coastal regions of the Island of Newfoundland (Figure 3.4). In western Newfoundland, the bedrock includes Mesoproterozoic crystalline basement and a dynamic Paleozoic sedimentary cover sequence (Figure 3.5). The structural and stratigraphic complexity of the promontory increases from the Anticosti basin in the west to the Long Range Mountains on the east (Figure 3.4). The Anticosti basin lies mostly in the subsurface of the Gulf of St. Lawrence and contains a nearly complete, undeformed Paleozoic sedimentary section (Sanford, 1993; Waldron et al., 1998). Farther east, rocks of the Laurentian margin include Neoproterozoic-Ordovician rift and platform successions that are tectonically overridden by coeval slope deposits and ophiolites incorporated into the Humber Arm and Hare Bay allochthons.

Post-Early Ordovician Paleozoic deformation has incorporated crystalline basement into the Appalachian orogen of western Newfoundland exemplified by the Long Range massif on the northern Peninsula, as well as produced sedimentary foreland and successor basins that overlie the early Paleozoic platform (Williams and Cawood, 1989; Waldron et al., 1998; Cooper et al., 2001). For the most part, westerly platform deposits have remained attached to the underlying crystalline basement; however, eastern inland carbonate platform deposits have been detached from underlying Precambrian basement and included into a narrow fold-and-thrust belt (Knight, 1994, 1996; 2006). The easternmost outcrops consist of a polydeformed and metamorphosed internal domain containing metaclastic and metacarbonate assemblages, which superficially resemble clastic-carbonate deposits in the more westerly allochthons and platform (Hibbard, 1983; 1988; Cawood et al., 1995; 1996).

Regional deformation along the promontory has long been recognized as reflecting the closure of the Iapetus and Rheic ocean basins during the Ordovician (Taconic), Silurian (Salinic), Devonian (Acadian), and Carboniferous (Alleghanian) (Rodgers, 1968; Williams, 1979; Williams and Hatcher, 1983; Dunning et al., 1990; Cawood et al., 1996; van Staal et al., 1998; Waldron et al., 1998; Nance and Linnemann, 2008). The following section outlines the prominent features of the regional stratigraphy on the St. Lawrence promontory from oldest to youngest, as well as addresses significant metamorphic rocks within the eastern internal domain.

3.3.1 Laurentian Margin Stratigraphy

The oldest rocks on the St. Lawrence promontory consist of middle and late Mesoproterozoic crystalline basement located in the Long Range massif and the smaller Indian Head massif of southwestern Newfoundland (Figure 3.4) (Williams, 1995). Lying unconformably over crystalline basement is a late Neoproterozoic-Early Cambrian clastic succession termed the Labrador Group. The Early Cambrian age, dominantly clastic-volcanic composition, and abrupt lateral changes in the thickness and facies of rocks in the Labrador group indicate they were deposited in a continental rift setting. The oldest units in the Labrador Group are located on Belle Isle at the very northern end of the Appalachian orogen (Figure 3.4). There, fault bounded arkoses and conglomerates of the

Bateau Formation are cross-cut by and interlayered with Neoproteorzoic basalts and dikes of the Long Range swarm (Kamo et al., 1989; Williams and Hiscott, 1987).

Outside the extent of sedimentary and volcanic accumulations on Belle Isle, Early Cambrian(?) sandstones of the Bradore Formation directly overlie Laurentian basement in western Newfoundland and eastern Labrador. The Bradore Formation grades upward into the late-Early Cambrian, archeocyathan-bearing shale and limestone of the Forteau Formation that is followed by mature sandstones of the Hawkes Bay Formation. The facies relations and succession within the late-Early Cambrian Forteau and Hawkes Bay Formations indicate the end of active continental rifting along the St. Lawrence promontory and the onset of passive-margin thermal subsidence for the eastern Laurentian continental margin (Williams and Hiscott, 1987).

The predominantly clastic Early Cambrian Labrador Group is overstepped by a Middle Cambrian to earliest Middle Ordovician carbonate-dominated shelf succession (Knight and Cawood, 1991). The Middle to Upper Cambrian Port au Port Group consists of thinly bedded limestones and dolostones deposited on a narrow, high-energy shelf (e.g., Williams, 1995). The overlying Lower Ordovician St. George Group is characterized by a wide, low-energy carbonate platform consisting of thickly bedded, massive limestones and dolostones. A regional unconformity marks the top of the St. George Group (Figure 3.6). It is interpreted to reflect erosion of the carbonate platform related to the migration of a foreland flexural bulge associated with the progressive advance of the Humber Arm and Hare Bay allochthons onto the margin during the Middle Orodovician Taconic orogeny (Jacobi, 1981; Knight et al., 1991). The unconformity marks the end of the passive margin on the St. Lawrence promontory and the initiation of an Ordovician foreland basin (e.g., Stockmal et al., 1995).

Foreland-basin deposits comprise a short-lived earliest Middle Ordovician carbonate bank manifest in the Table Head Group that is overlain by Middle Ordovician flysch of the Goose Tickle Group. In most reports, carbonates of the lower Table Head Group (Table Point Formation) are included as part of the Cambrian-Ordovician carbonate platform despite being interpreted as a foreland-basin deposit (e.g., Stockmal and Waldron, 1993; Waldron et al., 1998). Thus, the total thickness of the entire Cambrian-Ordovician platform section (Port au Port Group through Table Point

Formation) is typically quoted as between 1.0 and 1.2 km (James et al., 1989; Knight, 1991, 1996, 2003).

Within the Table Head Group, limestones of the Table Point Formation are overlain by differing formations depending on location, all of which indicate a progressive increase in subsidence and foundering of the carbonate platform (Stenzel et al., 1990). Along Port au Port peninsula and north of Stephenville, the Table Point Formation is abruptly overlain by coarse, massive limestone conglomerates of the Cape Cormorant Formation (Stockmal and Waldron, 1993). Where the Cape Cormorant Formation is absent, the Table Point Formation is overlain either by interbedded limestone and graptolitic shale of the Table Cove Formation, or by black shale of the Black Cove Formation (Figure 3.5) (Stenzel et al., 1990).

The Middle Ordovician Goose Tickle Group records a marked influx of turbiditic, clastic, foreland-basin sediments related to the advance of the Humber Arm and Hare Bay allochthons onto the continental margin (Stevens, 1970; Quinn, 1988; Stenzel et al., 1990). Outcrop and seismic data from most of western Newfoundland indicate that the Goose Tickle Group is relatively thin, between 150 and 500 m (Stenzel et al., 1990; Williams, 1995; Stockmal et al., 2004). On Port au Port peninsula, however, the Middle Ordovician flysch of the Goose Tickle Group is expressed as the Mainland Sandstone, which is as much as 1500 m thick (Waldron and Stockmal, 1991). The shale-sandstone succession in the Goose Tickle Group forms a regional weak layer, which hosts most of the basal faults in the Humber Arm allochthon.

The Humber Arm allochthon is a complex stack of structural slices, containing shelf-edge, slope, and marginal basin deposits coeval with rift and platform deposits on the promontory, as well as a diverse assemblage of Cambrian and Ordovician ophiolites (Williams, 1979; Cawood and Suhr, 1992; Waldron et al., 1998). The stratigraphy of individual, coherent thrust slices varies considerably with location. The oldest stratigraphic successions are preserved around the region of Humber Arm and Corner Brook (Figure 3.4). There, a thick succession of Neoproterozoic(?)-Early Cambrian synrift deposits in the Curling Group form the stratigraphic base of the Humber Arm allochthon (Waldron and Palmer, 2000; Palmer et al., 2001; Waldron et al., 2003). These rocks are overlain by a condensed section of Middle Cambrian-Early Ordovician

limestone and shale belonging to the Northern Head Group (Botsford, 1988; Waldron and Palmer, 2000). The youngest rocks in this part of the allochthon consist of early Middle Ordovicain flyschoid sandstone and shale of the Eagle Island Formation, which constitutes the oldest Ordovician flysch exposed in western Newfoundland (Waldron and van Staal, 2001).

North of Bonne Bay, the Humber Arm allochthon is expressed as a classic fold-and-thrust belt. Imbricate thrust slices contain late Middle Cambrian to Early Ordovician limestone conglomerate and shale of the Cow Head Group, indicating a proximal slope depositional environment (Figure 3.5) (Lavoie et al., 2003). Overlying passive-margin slope deposits of the Cow Head Group are Middle Ordovician foreland-basin sandstones of the Lower Head Formation (James and Stevens, 1986). Individual slices within the Humber Arm allochthon typically are bounded by chaotic mélange zones that are structurally complex and contain disaggregated blocks of slope and basin deposits derived from the allochthon, as well as tectonically severed blocks from the underlying shelf. The structural slices and mélange zones were assembled into the Humber Arm allochthon during the Middle Ordovician Taconic orogeny, when the closure of the Humber Seaway thrust marginal slope and basin successions onto the edge of the continental platform (Williams, 1979; Stockmal et al., 1995; Waldron and van Staal, 2001).

Outcrops of Late Ordovician to Devonian rocks are limited to Port au Port peninsula. Late Ordovician (Caradocian) shallow-marine limestones of the Long Point Group (Lourdes Limestone) lap onto Ordovician flysch of the Goose Tickle Group (Stockmal et al., 1995). The Lourdes Limestone is overlain by a thick, deepening-upward, Caradoc-Llandovery age, foreland-basin succession of turbiditic sandstone and shale in the upper part of the Long Point Group (Winterhouse and Misty Point Formations) (Figure 3.5). A major unconformity representing a time gap of approximately 20 m.y. separates the Long Point Group from the overlying Clam Bank Formation. On Port au Port peninsula, the Clam Bank Formation consists of a thick succession of latest Silurian to Early Devonian (Ludlovian-Pridolian) fluvial red beds that display abundant dewatering structures indicative of deposition into an active foreland-basin environment (Sanford, 1993; Cooper et al., 2001). Overlying the Clam Bank

Formation are Emsian red beds of the Red Island Road Formation. The youngest Paleozoic rocks exposed in western Newfoundland belong to Carboniferous strata of the Anguille, Codroy, and Barachois Groups (Knight, 1983). These rocks include fluvial and lacustrine sandstone, shale, and evaporites, which rest unconformably on exposed Mesoproterozoic crystalline basement in the Long Range massif and on deformed lower Paleozoic stratigraphic successions.

3.3.2 Eastern Internal Domain

Massifs of remobilized Precambrian basement and polydeforemd and metamorphosed Paleozoic cover rocks constitute an eastern internal domain embodied in the Corner Brook Lake and Baie Verte terranes (Figure 3.4). Both terranes are bounded on the east by the Baie Verte-Brompton Line, a major Paleozoic shear zone marked by ophiolitic material that separates the Humber zone from outboard Cambrian-Ordovician Iapetan oceanic terranes of the Dunnage zone (Williams and St. Julien, 1978). To the west, the Corner Brook Lake terrane is juxtaposed directly against Laurentian margin rocks along the Humber River fault system, whereas the Baie Verte terrane is tectonically severed from continental margin successions by the Carboniferous Cabot fault system.

In both terranes, Precambrian crystalline basement is overlain by a metaclastic assemblage with minor amphibolite (Hibbard, 1983; Cawood et al., 1995). Overlying the metaclastic rocks is a diverse succession of metacarbonate and schist that are identical to proximal slope deposits preserved in the Humber Arm allochthon (Hibbard, 1988; Knight, 1996; Cawood and van Gool, 1998). The upward change from metaclastic to metacarbonate slope successions is consistent with a transition from siliciclastic deposition on eroded basement to carbonate-dominated sedimentation corresponding to a rift-to-passive-margin transition (e.g. Cawood et al., 1996), suggesting these terranes represent intensely deformed blocks of the Laurentian proximal slope. Rocks in the metacover succession display metamorphic mineral assemblages indicative of upper greenschist to amphibolite facies (locally eclogite facies) (Jamesion, 1990; Cawood and van Gool, 1998). The metamorphic data indicate that rocks in the eastern internal domain were tectonically buried down to as much as 30 km beneath the Humber Arm allochthon and overlying ophiolites. Additional small blocks of polydeformed Laurentian margin

strata are recognized at Ming's Bight and within the Dashwoods block of the Dunnage zone (Figure 3.4) (Hibbard, 1983; Currie and can Berkel, 1992).

3.4 GEOPHYSICAL DATA

3.4.1 Correlation of seismic velocities to regional stratigraphic reflectors

During the 1980's and 1990's, numerous offshore and onshore seismic reflection profiles were acquired along western Newfoundland by both government and private entities. Since the late 1990's many of these seismic reflection surveys, in addition to data from deep wells, have been released to the public domain, providing a wide array of subsurface geophysical data for western Newfoundland. For this study, we have obtained access to more than 50 industry and government seismic reflection profiles shot both onshore and offshore around Port au Port peninsula and Cow Head, as well as 6 well reports from deep wells drilled either on or near traces of individual seismic reflection surveys (Figure 3.7). Raw data from these well log reports are provided in Appendix A.

Seismic reflection profiles were interpreted by comparing the stratigraphy recorded in well logs to seismic reflection profiles in close proximity to that particular well. Correlation of regional seismic reflectors with regional stratigraphic units in western Newfoundland can be seen in Figure 3.8. The overall along-strike consistency of stratigraphic reflector groups in seismic profiles from across western Newfoundland is remarkable. The broad, along- and across-strike similarity of reflector groups allows for the subdivision of the regional stratigraphy into individual lithotectonic units. The average velocity of each lithotectonic unit was calculated by comparing the known thickness of a given unit from well log information to the computed one-way travel time of that unit in the seismic profile.

Unit 1 in this study is the Labrador Group, which on most seismic reflection profiles consists of prominent layered reflectors at the base of the Paleozoic succession above crystalline basement (Figure 3.8). The contact between crystalline basement and the overlying Labrador Group is a profound Proterozoic-Paleozoic unconformity, and forms a strong, regional seismic reflector that is at a depth around 2.0 to 3.0 sec TWTT on most profiles. The average P-wave velocity calculated for the Labrador Group is 5.0 km/sec (16,404 ft/sec), whereas an assumed P-wave velocity of 6.5 km/sec (21,325

ft/sec) is used for crystalline basement, which is in accord with measured seismic velocities for common igneous and metamorphic rocks (i.e., granite, gneiss, etc…) (Lillie, 1999).

Unit 2 consists of the entire early Paleozoic carbonate shelf from the base of the Port au Port Group to the top of the Table Head Group (Figure 3.8). The brightest reflector in the unit is near the base of the carbonate-shelf succession. This strong reflector corresponds to a 50 m to 100 m thick shale bed in the Port au Port Group (Big Cove Member), the velocity of which contrasts sharply with the seismically fast carbonates above and below (Cooper et al., 2001). Because outcrop and well logs indicate that the Big Cover Member lies ~200 m stratigraphically above the Labrador-Port au Port Group contact, the base of Unit 2 is inferred to be the weak reflector beneath the prominent Big Cove Member reflector. The top of Unit 2 is marked by a strong seismic reflector that corresponds to the seismic contrast between limestone in the Table Point Formation and overlying shale in the foreland-basin succession (Unit 3). The interlayered limestone and dolostone of the carbonate shelf provide very little seismic contrast between individual beds, resulting in a relatively thick, seismically opaque zone between the upper and lower boundary reflectors in the unit. Comparison of the stratigraphic thickness of the carbonate shelf from well reports with seismic travel times indicates that Unit 2 has an average P-wave velocity of 6.645 km/sec (21,802 ft/sec).

In the Humber Arm allochthon north of Bonne Bay, slope deposits of the Cow Head Group are contemporaneous with carbonate-shelf deposits of Unit 2. Therefore, rocks in the Cow Head Group have been assigned to Unit 2a. Because rocks in the Cow Head Group consist of interbedded shale, ribbon limestone, and limestone conglomerate, Unit 2a typically makes bright, layered reflectors on seismic reflection profiles across the Humber Arm allochthon. A well report for Parsons Pond Well #1, which drilled through a substantial part of Unit 2a just to the south of Parsons Pond on the Northern Peninsula, includes an analytical seismic velocity study for rocks of the Cow Head Group. The well report gives an average P-wave velocity for rocks in the Cow Head Group of 5.103 km/sec (16,742 ft/sec) (Brooker, 2004), which we have adopted for this study.

Unit 3 includes the entire Middle Ordovician foreland-basin succession as it is mapped on the parautochthonous shelf (Goose Tickle Group). Shale and sandstone of the

Goose Tickle Group and the Mainland Sandstone form a seismically opaque zone that overlies the carbonate-platform succession of Unit 2. The average P-wave velocity for the Goose Tickle Group is 3.6 km/sec (11,811 ft/sec), which is a common velocity for shale-dominated strata (e.g., Lillie, 1999). Unit 3a encompasses Middle Ordovician foreland-basin deposits within the Humber Arm allochthon. Like the Goose Tickle Group, these beds also consist predominantly of seismically opaque zones. The Parsons Pond Well #1 report lists an average P-wave velocity of 3.778 km/sec (12,394 ft/sec) for the sandstone-shale dominated Lower Head Formation, which we apply to all rocks within Unit 3a.

Unit 4 consists of strata belonging to the Upper Ordovician Long Point Group and overlying Upper Silurian to Lower Devonian Clam Bank Formation. The base of Unit 4 is the Lourdes Limestone, which makes a very bright reflector above the seismically opaque Unit 3. Strata in the Long Point Group above the Lourdes Limestone consist mainly of turbiditic shale and sandstone, which produce a thick opaque zone above the Lourdes Limestone reflector. A set of moderately to strongly layered reflectors near the top of Unit 4 is interpreted to mark the Clam Bank Formation (Figure 3.8). Comparison of well log thicknesses for the Long Point Group and Clam Bank Formation with the seismic reflection profiles shows that Unit 4 has an average P-wave velocity of 3.962 km/sec (13,000 ft/sec). The top of the layered reflectors corresponding to the Clam Bank Formation is interpreted to be the top of Unit 4. Lying above Unit 4 only in the Port au Port peninsula region of western Newfoundland is Unit 5, which includes the Red Island Road Formation. Unit 5 is for the most part seismically opaque, and has an average P-wave velocity of 2.7 km/sec (8,858 ft/sec).

3.4.2 Significant Potential Field Data

A digitally reprocessed Bouguer gravity anomaly map (Figure 3.9A) (GSC website) for offshore western Newfoundland highlights several subsurface structures on the St. Lawrence promontory. Gravity lows along western Newfoundland and eastern Quebec and Labrador correspond to granitic/gneissic crust of the Grenville province. Broad positive anomalies in central Newfoundland reflect predominantly mafic, oceanic terranes related to the Dunnage and Gander zones (e.g., Williams, 1979; 1995). Analysis of regional Bouguer gravity map reveals several NW-trending linear anomalies defined

by sharp gravity contrasts off the western coast of Newfoundland (Figure 3.9B). These sharp NW-trending linear anomalies are coincident with along-strike changes in the regional Paleozoic stratigraphy exposed onshore in western Newfoundland (i.e., transform zones from Chapter 2), suggesting they may be related to basement structure at depth on the promontory.

Several along-strike industry seismic reflection profiles acquired just offshore of western Newfoundland come near to the southernmost linear gravity anomaly near Port au Port peninsula (Figure 3.9B). In Hunt Line 4 (Figure 3.10), an upper, southward dipping package of reflectors corresponds to Upper Ordovician through Devonian strata of the Long Point Group and Clam Bank Formation. Beneath this upper package of reflectors on the northeast part of Hunt Line 4 is a southward tapering wedge-shaped middle package interpreted to be the Humber Arm allochthon inserted into a tectonic wedge or triangle zone beneath the Upper Ordovician Long Point Group (e.g., Stockmal and Waldron, 1990; 1993; Waldron and Stockmal; 1994; Stockmal et al., 1998). Toward the southwest, the Humber Arm allochthon wedges out of the plane of the profile, and the Upper Ordovician through Lower Devonian sedimentary package lies directly on a lower seismic reflector package that corresponds to the Cambrian-Ordovician platform and rift succession (i.e., Units 1 and 2).

In the lower southwest part of the profile, the base of the Cambrian-Ordovician reflector package consists of a bright pair of layered reflectors at approximately 2.2 sec TWTT, which corresponds to the Proterozoic-Paleozoic basement unconformity. The basement unconformity reflector progressively dips northeastward on the profile from ~2.2 sec TWTT to at CDP 3095, to 3.0 sec TWTT at CDP 2500, to greater than 4.0 sec TWTT at CDP 2250 at the far northeastern end of the profile (Figure 3.10). Above the dipping basement unconformity reflector, a succession of reflectors below the Cambrian-Ordovician platform appears to onlap the basement unconformity, suggesting a sedimentary succession that post-dates Proterozoic crystalline basement yet predates the Cambrian-Ordovician rift and platform succession. Abrupt downward steps in the basement unconformity reflector at CDP 2700 and CDP 2400 likely correspond to steep, down-to-the-northeast normal faults that offset the top of basement (Figure 3.10).

Line CAH 92-2 is similar to Hunt Line 4 in that the Proterozoic-Paleozoic unconformity above crystalline basement appears to step abruptly downward in intervals to the northeast from 2.0 sec TWTT to 4.0 sec TWTT. As in Hunt Line 4, layered reflectors corresponding to the Early Cambrian Labrador Group and overlying Cambrian-Ordovician carbonate platform continue uninterrupted across line CAH 92-2 at 2.0 sec TWTT. The seismic data from these two independently gathered seismic reflection surveys strongly suggest that a steep, down-to-the-northeast, pre-Early Cambrian basement fault system exists beneath the platform northeast of Port au Port peninsula. The down-to-the-northeast basement faults that step downward towards the area of the northwest-trending linear gravity anomaly suggest that the linear anomalies in Figure 3.9 are an expression of basement structures. Location of the imaged basement faults in the seismic lines and the linear gravity anomaly along strike to the northwest of the proposed Serpentine Lake transform (see Chapter 2) suggest that these features are an expression of the Serpentine Lake transform.

Seismic lines located northeast of CAH 92-2 and Hunt Line 4 (Figure 3.7) demonstrate that Proterozoic crystalline basement lies directly beneath the Labrador Group (at ~2.0 sec TWTT). Line WN-3 is located approximately 20 km northeast from the ends of both line 92-2 and Hunt Line 4. Thus, the gap in the seismic data suggests that that a relatively deep basin roughly parallel to the Serpentine Lake transform offshore of southwestern Newfoundland is no wider than 20 km. The simplest explanation that takes into consideration all of the data is a pull-apart basin in a releasing bend section of the Serpentine Lake transform. In this model, sediments represented by the onlapping reflectors above basement (Figure 3.7) were deposited into the narrow pull-apart basin that developed along the transform while it was active during the Neoproterozoic. Such transtensional releasing bend structures are common in active strike slip tectonics (van der Pluijm and Marshak, 2004). A pull-apart basin also explains the relatively abrupt drop in basement from 2.0 sec TWTT to 4.0 sec TWTT (Figure 3.7).

Whether or not this transform fault is directly related to Iapetan rifting can only be a matter of speculation at this time. Clearly, sedimentation into the proposed pull-apart basin predates deposition of the Labrador Group, but what remains unclear is how much older is the basin with respect to the Cambrian-Ordovician platform. Regardless of the

exact age, both potential field and seismic reflection surveys indicate that vestiges of at least one, if not multiple, transform fault systems lie beneath the Paleozoic cover on the St. Lawrence promontory.

3.5 CROSS SECTIONS

Nine balanced cross sections have been constructed across deformed Laurentian continental-margin successions in western Newfoundland (Figure 3.11) in order to resolve the architecture and timing of tectonic events on the St. Lawrence promontory. The cross sections were constructed using data gathered from geologic field mapping, deep wells, numerous seismic reflection profiles, and digitized potential field data. All of the available seismic, geophysical, and deep well data provide depth control for interpretation of Appalachian structures mapped at the surface. The trace of each cross section through the deformed Paleozoic strata in western Newfoundland was carefully selected to answer specific questions concerning the structural architecture of that region of the promontory, and to maximize the utility of seismic and well data. Cross sections were balanced in two dimensions using line-length balancing where possible, and area balancing where a lack of coherent and traceable stratigraphic markers made line-length balancing impossible. Lines 1 through 4 are displayed in Plate 3.1, and Lines 5 through 9 are displayed in Plate 3.2.

Two important assumptions impact line-length balancing in two dimensions. First, the assumption that stratigraphic units represented in the cross section have not experienced significant volume change. Second, the assumption that no material has moved into or out of the plane of cross section (i.e., strike-slip faulting).

The first assumption has probably not been seriously violated by platform rocks exposed along the western coastal regions of Newfoundland, as cleavage is minimal in these rocks and strain markers (i.e., fossils) display very little evidence of significant strain. This assumption is more problematic with rocks in the Humber Arm allochthon, which display multiple cleavages and contain chaotic mélange zones. Mélange zones, in particular, provide a unique challenge to line-length balancing because they consist of material derived from both the overlying allochthon and underlying shelf, including some sediment that was deposited as the Humber Arm allochthon was being emplaced onto the

continental margin. Therefore, where a cross section crosses mélange zones and/or locations of potentially significant volume change, we have resorted to palinspastically restoring these rocks by area-balance rather than by line-length balancing techniques.

Violation of the second assumption was principally avoided by choosing lines of cross section that avoid fault systems with significant amounts of lateral displacement. Where lines are forced to cross strike-slip fault zones or thrust faults with significant oblique out-of-plane movement, we provide a "best estimate" fit for rock layers on opposing sides of the fault in question and note the caveat that the interpreted stratigraphic balance is conjectural. More complete studies would attempt to sequentially restore strike-slip and convergent/divergent deformation across major zones of out-of-plane motion; however, the lack of quantitative data regarding the magnitude of strike-slip displacement along major shear zones on the St. Lawrence promontory makes this task all but impossible. We stress that, where one or both assumptions appear to have been violated, our cross sections provide a feasible solution to the structure at depth and total shortening of the deformed strata, while recognizing that other solutions may also be viable.

Lines 2 through 7 depict the subsurface structural and stratigraphic geometry of the Humber Arm allochthon as it is interpreted from seismic reflection profiles, deep wells, and outcrop distribution and structure. The corresponding restored sections display the distance between the present position of the leading edge of the Humber Arm allochthon (i.e., Appalachian structural front of Stockmal and Waldron, 1993) and the restored leading edge of the allochthon. Because there are no piercing points between shelf rocks and slope rocks within the Humber Arm allochthon exposed in western Newfoundland, the leading edge of the Humber Arm allochthon is restored beyond the trailing edge of the restored shelf succession in each line of cross section. Therefore, each of the six restored cross sections presents only a minimum estimate for the total displacement of the Humber Arm allochthon during the Paleozoic Appalachian orogenies.

3.5.1 Southwest Newfoundland (Lines 1, 2, and 3).

The stratigraphic and structural relationships exposed in southwestern Newfoundland on Port au Port peninsula and around Stephenville are critical to understanding the tectonic evolution of the St. Lawrence promontory during the Paleozoic (e.g., Stockmal and Waldron, 1993). Geologic relationships in outcrop and in sub-crop in this region serve as a microcosm for the Paleozoic tectonic evolution of western Newfoundland. Port au Port peninsula is also an important geologic area because only there are Upper Ordovician and Late Silurian-Early Devonian sedimentary units exposed (Figure 3.12).

Stratigraphic Framework

Mesoproterozoic Laurentian crystalline basement rocks are exposed in the Indian Head massif, in the core of the Phillips Brook structure (Figure 3.12). Overlying crystalline basement are clastic deposits of the Labrador Group (Unit 1). Outcrop of the Labrador Group east of Stephenville in the Indian Head range is limited; measured sections indicate that it is between 240 m and 260 m thick above basement (Knight and Boyce, 2000; Knight, 2003). However, 50 km to the west on Port au Port peninsula, geophysical logs from the Port au Port No. 1 well demonstrate that the Labrador Group is as much as 750 m thick where it is in the hanging wall of the Round Head fault (Cooper et al., 2001). Seismic reflection profile line 93-5 also indicates that the Labrador Group increases in thickness toward the fault in the hanging wall of the Round Head fault (Figure 3.13); whereas in the footwall, reflectors that correspond to the Labrador Group show a relatively thin succession (< 300 m). These observations suggest that the Round Head fault is an Early Cambrian rift-related fault (Plate 3.1).

The passive-margin carbonate shelf succession (Unit 2) dominates much of the geology of southwestern Newfoundland. The broad uniformity of the carbonate platform in outcrop, as well as in seismic reflection profiles, suggests a more-or-less constant thickness for the Port au Port and St. George Groups across the region. North of Stephenville, however, measured sections at the top of the carbonate platform (e.g., Palmer et al., 2002) demonstrate that the thickness of the Table Head Group (upper part of Unit 2) increases in the hanging walls of the Western Boundary fault, the Romaines

Brook fault, and the West Blanche Brook fault in the Table Mountain and Phillips Brook structures (Line 3, Plate 3.1).

The Llanvirn Cape Cormorant Formation directly overlies the Table Point Formation (lower Table Head Group) on Port au Port peninsula and consists of clasts and olistoliths derived from the underlying upper 1000 m of the carbonate-platform succession (Stenzel et al., 1990). The unit lies in the immediate hanging wall of the Round Head fault on the Port au Port peninsula and in the hanging wall of the Piccadilly Bay fault beneath Port au Port Bay (Stockmal et al., 2004) (Lines 2 and 3, Plate 3.1). Overlying the Cape Cormorant Formation are Middle Ordovician foreland-basin flysch deposits of the Mainland Sandstone (Unit 3), which has a measured thickness of approximately 1.5 km on Port au Port peninsula in the hanging wall of the Round Head fault (Waldron and Stockmal, 1991). Both onshore and offshore seismic lines along the western edge of the peninsula, however, indicate the Mainland Sandstone is markedly thinner in the footwall of the Round Head fault (< 200 m) (Figure 3.14). These stratigraphic observations have led previous workers to suggest that the Round Head fault was a Middle Ordovician basement-involved normal fault, where limestone clasts in the Cape Cormorant Formation were derived from the exposed platform along the fault scarp (Waldron et al., 1993; Stockmal et al., 1998).

Mapping north of Stephenville has identified Middle Ordovician conglomerates that are similar to the Cape Cormorant Formation on Port au Port peninsula (located out of the line of cross section in Plate 3.1), which overlie the thickener sections of Table Head Group in the Table Mountain structure and the Phillips Brook structure (Palmer et al., 2002). These observations also indicate that the Table Mountain and Phillips Brook structures were active graben systems during the late-Early and Middle Ordovician.

Thermal maturation studies in southwestern Newfoundland elucidate the burial history of Cambrian-Ordovician shelf rocks in that region of the St. Lawrence promontory. Conodont alteration indices (CAIs) and acritarch alteration indices (AAI) demonstrate that the top of the carbonate platform along southwestern Port au Port peninsula reached burial temperatures between 65º and 80º C, which corresponds to between 2 and 3 km depth of burial (assuming a geothermal gradient of 25º C per 1 km) (Williams et al., 1998). Along the northeast coast of the peninsula and the eastern coast of

Port au Port Bay, CAIs and AAIs are higher, suggesting these areas were buried to greater depths, presumably beneath structural slices of the Humber Arm allochthon. The thermal maturity of carbonate and shale deposits in the upper platform increases eastward away from Port au Port peninsula, implying these rocks were buried at greater depth underneath thickened and complexly deformed thrust sheets in the allochthon. In the Phillips Brook structure north of Stephenville, AAIs and fluid inclusion studies indicate that shale and limestone in the Table Head and Goose Tickle Groups experienced burial temperatures around 100º and 120º C, corresponding to burial depths between 3 and 5 km (Williams et al., 1998).

Post-Middle Ordovician stratigraphic units (Units 4 and 5) are exposed along The Bar on Port au Port peninsula and on Red Island just off the northeast coast of the peninsula (Figure 3.12). Offshore seismic reflection surveys indicate the Late Ordovician-Early Devonian basin fill has an average thickness of 3 km. The lowest part of the Late Ordovician section is the Lourdes Limestone, which is locally overturned in the footwall the Round Head fault. The base of the Lourdes Limestone at Tea Cove and along The Bar is very sharp and exhibits strong slickenside and calcite fiber striations plunging downdip to the northwest with "steps" that indicate a top-to-the-southeast thrust sense (Stockmal and Waldron, 1993). The contact (termed the Tea Cove thrust; Line 3, Plate 3.1) separates the overlying Lourdes Limestone from a footwall that consists of brecciated green sandstone belonging to the Humber Arm allochthon, indicating that the allochthon has been wedged underneath the Late Ordovician-Devonian units. Along the northwest coast of The Bar, Late Silurian-Early Devonian strata of the Clam Bank Formation dip 20º to 40º to the northwest. On Red Island Road, late-Early Devonian (Emsian) strata of the Red Island Road Formation also dip gently to the northwest, indicating the Humber Arm allochthon was inserted beneath the Lourdes Limestone after deposition of the Clam Bank and Red Island Road Formations (Waldron et al., 1998; Stockmal et al., 1998; Cooper et al., 2001).

Undisturbed late-Early Mississippian (Visean) red beds of the Codroy Group overlie carbonate-platform deposits on Port au Port peninsula and onlap early Paleozoic stratigraphy and basement southeast of Stephenville (Figure 3.12). These deposits represent the northernmost edge of the Bay St. George basin (Knight, 1983), which

formed as a result of strike-slip wrench tectonics related to Carboniferous motion along the Cabot fault system (Thomas and Schenk, 1988).

Structural Framework

Structures in shelf rocks in southwestern Newfoundland, and around Port au Port peninsula in particular, include predominantly thick-skinned elements. The most prominent of these is the Round Head fault, which is spatially associated with the Cape Cormorant Formation and the Mainland Sandstone. The fault makes a very strong reflector in regional seismic profiles (Figures 3.13 and 3.14) and displays a maximum net reverse offset of 7 km on the southwestern end of the peninsula. Net reverse offset along the fault appears to decrease from southwest to northeast. Basement involvement of the Round Head fault is unequivocally demonstrated in the Port au Port No. 1 well, which penetrated more than 800 m of crystalline basement in the hangingwall and crossed the fault into Paleozoic strata in the footwall (Cooper et al., 2001).

Geophysical and stratigraphic data indicate that the Round Head fault originated as an Early Cambrian synrift normal fault and was later reactivated as part of a foreland-basin graben system during the Middle Ordovician. As it is currently exposed, the Round Head fault displays net reverse offset rather than normal offset, indicating that it has subsequently been inverted as a thrust fault. Reverse motion on the fault clearly deforms and overturns the Tea Cove thrust and strata in the Humber Arm allochthon tectonic wedge (Line 2, Plate 3.1), indicating that structural inversion must post-date Emsian time (Cooper et al., 2001). Flat lying rocks of the Visean age Codroy Group do not unconformably overlie the Round Head fault in outcrop; however, the undeformed state of the Codoy Group on Port au Port peninsula suggests that reverse motion along the Round Head fault likely pre-dates late-Early Mississippian time.

Seismic data indicate multiple thick-skinned blind thrusts in the footwall of the Round Head fault. The blind thrusts deform layered reflectors corresponding to Units 1, 2, and 3, as well as the tectonic triangle zone that contains the Humber Arm allochthon (Lines 1, 2, and 3, Plate 3.1). Several of these blind thrusts carry a greater thickness of Unit 1 reflectors in the hanging wall as compared to the footwall, suggesting these faults may be inverted synrift faults (Lines 1 and 3, Plate 3.1).

The Victors Brook, Red Brook, and Piccadilly Bay faults comprise a system of thick-skinned reverse faults in the hanging wall of the Round Head fault (Lines 1 and 2, Plate 3.1). Seismic reflection profiles, outcrop distributions, and well data indicate these major faults are antithetic to the Round Head fault, dipping moderately to steeply to the northwest. The Victors Brook and Red Brook faults cut obliquely up section from southeast to northwest across Port au Port peninsula. The Victors Brook fault appears to merge with the Round Head fault offshore beneath Port au Port Bay, whereas the Red Brook fault terminates against the Piccadilly Bay fault off the northeast shore of the peninsula (Figure 3.12).

Net reverse offset across each of the faults appears to be relatively minor (~200 to 600 m). No seismic data or geophysical well logs indicate that these faults were active during the Early Cambrian. Seismic reflection profiles beneath Port au Port Bay demonstrate a thick section of Mainland Sandstone (Unit 3) in the hanging wall of the Piccadilly Bay fault, overlying a set of layered reflectors that likely corresponds to the Cape Cormorant Formation (Figure 3.15) (Stockmal et al., 2004). The existence of Cape Cormorant Formation in the hanging wall of the Piccadilly Bay fault is confirmed by well cuttings and geophysical logs from well K-39 (Stockmal et al., 2004). On Port au Port peninsula along Victors Brook, a 500-m-thick section of Goose Tickle Group, which contains clasts of the underlying carbonate platform, overlies the Table Head Group in the hanging wall of the Victors Brook fault (Stockmal and Waldron, 1993). The observations suggest that, like the Round Head fault, the Victors Brook, Red Brook, and Piccadilly Bay faults were parts of a Middle Ordovician foreland basin graben system that were later inverted.

The geology north of Stephenville in the Indian Head range is dominated by a set of thick-skinned “pop-up” structures termed the Table Mountain, Whale Back, and Phillips Brook structures (Line 3, Plate 3.1), which emplace basement and overlying Cambrian-Ordovician shelf successions above the Humber Arm allochthon (Figure 3.12). Palmer et al. (2002) previously palinspastically restored the Table Mountain, Whale Back, and Phillips Brook structures (Palmer et al., 2002). The cross section in Line 3, therefore, incorporates many of the major structural and stratigraphic interpretations from that study.

The Table Mountain structure contains a nearly complete section of the Cambrian-Ordovician platform bounded by the informally named Western Boundary fault and the more formally defined Romaines Brook fault (Palmer et al., 2002). The Western Boundary fault is a moderately southeast dipping reverse fault that brings the Port au Port and St. George Groups up above the Table Head and Goose Tickle Groups, as well as the overlying Humber Arm allochthon, forming a west-facing monocline of platform strata in the hanging wall (Line 3, Plate 3.1). The eastern boundary of the Table Mountain structure is the Romaines Brook fault; a steep, west-dipping fault zone with shear-sense indicators that display primarily east-directed reverse motion with a minor component of dextral strike-slip (Palmer et al., 2002). The fault zone juxtaposes the Labrador Group and lower Port au Port Group on the west against the Humber Arm allochthon on the east (Line 3, Plate 3.1). South of Table Mountain, the Romains Brook fault plunges beneath relatively undeformed cover rocks of the Visean Codroy Group, indicating the last major movement along this fault was pre-Visean.

The Phillips Brook structure is a complex zone of anastomosing faults that uplifts basement and overlying Cambrian-Ordovician platform and foreland-basin deposits above the Humber Arm allochthon (Line 3, Plate 3.1) (Knight and Boyce, 2000; Palmer et al., 2002). To the southwest, early Paleozoic strata and structures preserved in the Phillips Brook structure are obscured by Carboniferous onlap of the Codroy Group. The southwestern boundary of the structure is defined by the West Blanche Brook fault, a moderately east-dipping thrust fault (Palmer et al., 2002). Along the axis of the Phillips Brook structure, the Cambrian-Ordovician platform succession has been folded into an open northeast-plunging antiform (Knight and Boyce, 2000). The Phillips Brook structure is divided by the Cold Brook fault, which strikes north-northeast and dips steeply to the northwest. Shear-sense indicators along the fault indicate a strong component of dextral strike-slip motion (Palmer et al., 2002). East of the fault, bedding dips moderately to steeply northwest, forming a tightly folded syncline against the Cold Brook fault that contains a preserved remnant of the Humber Arm allochthon in the core (Figure 3.12).

Whale Back ridge is a steep, prominent geographic feature west of the Phillips Brook structure (Line 3, Plate 3.1). It consists of the uppermost St. George and Table Head Groups, which dip and young to the east (Line 3, Plate 3.1) (Palmer et al., 2002).

The western edge of the ridge is defined by the inferred Kippens fault that juxtaposes the upper carbonate platform and foreland basin on the east against a narrow strip of the Humber Arm allochthon on the west (Figure 3.12). Palmer et al. (2002) interpreted the Kippens fault as a shallow, east-dipping thrust fault rooted in the Phillips Brook structure. In Line 3, the Kippens fault represents a thin-skinned footwall shortcut to the West Blanche Brook fault (Plate 3.1).

In the core of the Phillips Brook structure (Indian Head inlier), crystalline basement is thrust over the deformed Cambrian-Ordovician shelf by the Indian Head thrust, which is inferred to dip moderately to the southeast (Line 3, Plate 3.1). In the hanging wall of the Indian Head thrust, the Labrador Group rests unconformably on basement. At this location, the Bradore Formation is only 5 to 10 m thick, suggesting that the thick-skinned Indian Head thrust is not a reactivated Iapetan rift fault. To the north, the Indian Head fault is cut off by the Cold Brook fault (Palmer et al., 2002). South of the Phillips Brook structure, crystalline basement in the Indian Head massif plunges offshore beneath flat lying Carboniferous strata.

Stratigraphic data from the top of the platform in the Table Mountain and Phillips Brook structures suggest that these geologic features originated as Middle Ordovician foreland graben systems. The relatively thin Labrador Group in the core of the Phillips Brook structure, however, suggests that both of these structures are not related to Early Cambrian Iapetan rifting. After the Middle Ordovician, the Phillips Brook and Table Mountain structures were inverted into “pop-up” structures between Emsian and Visean time because fault zones in each structure deform the Humber Arm allochthon yet are unconformably overlain by Carboniferous strata.

Palinspastically restoring pop-up structures, such as the Round Head fault system and the Table Mountain structure, presents some unique challenges. Horsts and grabens in extensional fault systems are typified by conjugate sets of normal faults that converge downward into a master fault system. When such structures are subjected to inversion by compressional deformation, a variety of structures is produced, including pop-up structures that represent inverted graben (e.g., McClay and Buchanan, 1992). Palinspastic restoration of pop-up geometries by line-length balancing requires a significant amount of flexural slip along bedding planes. To palinspastically restore the pop-up structures in

these lines of cross section, as well as the other lines, we are forced to relax the common assumption that "pin lines" in thrust sheets remain perpendicular to bedding (see Elliot and Johnson, 1980).

Palinspastic restoration of the inverted thick-skinned structures in southwestern Newfoundland demonstrates that the Cambrian-Ordovician shelf succession experienced between 20% and 35% net shortening during the Paleozoic. In Line 3, the present deformed geometry of the Table Mountain structure is reproduced after Palmer et al. (2002). Palinspastic restoration across the Cold Brook fault produces conjectural results because of unquantifiable strike-slip (out-of-plane) motion al ong the fault, which post-dates contractional deformation in the Phillips Brook structure. The results presented in Line 3, however, represent a "best estimate" for both the deformed and restored geometry of Laurentian margin stratigraphy across the Cold Brook fault.

Humber Arm Allochthon

The Humber Arm allochthon in southwestern Newfoundland contains deep-water equivalents of the Cambrian-Ordovician passive-margin shelf succession and siliciclastic flysch of the Middle Ordovician foreland basin. The internal stratigraphy has been broken into variably deformed thrust slices separated by moderately to strongly deformed structural mélanges (Waldron, 1985; Waldron et al., 1988; 1998). Regional stratigraphic studies in this region of the allochthon indicate that passive-margin slope and basin deposits along the western shore of Port au Port Bay contain a stratigraphy that corresponds to that of the Humber Arm allochthon north of Bonne Bay at Cow Head (e.g., Cow Head Group, Lower Head Formation) (Schubert and Dunbar, 1934; Kindle and Whittington, 1958). The uppermost slices in the allochthon contain the Early Ordovician (ca. 485 Ma) Bay of Islands Ophiolite Suite (Jenner et al., 1991).

The Humber Arm allochthon in southwest Newfoundland is dominated by shale, which is conducive to mechanical weathering, producing low-lying, boggy landscapes with little to no outcrop except along the immediate shoreline of Port au Port Bay. The relative lack of continuous, unambiguous outcrop of the Humber Arm allochthon in southwestern Newfoundland has made division of discrete stratigraphic units within deformed thrust sheets exceedingly difficult. Seismic reflection profiles of the allochthon

beneath Port au Port Bay do not produce conclusive results, either. In nearly all reflection surveys, the Humber Arm allochthon is characterized by seismically opaque to chaotic zones; individual seismic reflectors within the allochthon can not be traced to any surface outcrop. Therefore, for Lines 2 and 3, the Humber Arm allochthon has been palinspastically restored using area balance because of the inadequate structural and stratigraphic data from surface mapping and seismic reflection profiles. Dilation and apparent ductile deformation of the Humber Arm allochthon in these lines of cross section is inferred to be the result of brittle deformation along imbricate thrusts and duplexes within the allochthon, which are neither visible in seismic profiles nor mappable because of insufficient outcrop.

Regional relationships between the Humber Arm allochthon and the Cambrian-Ordovician platform succession demonstrate that the allochthon was emplaced onto the margin in a thin-skinned manner along a complex, regional basal detachment (Humber Arm allochthon basal detachment or HAABD) (Waldron et al., 1998). In southwestern Newfoundland, the HAABD is exposed in outcrop (Figure 3.16), and is visible in regional seismic lines. The footwall beneath the HAABD varies from place to place between the Goose Tickle Group, the Table Cove Formation, or the top of the Table Point Formation (Stockmal et al., 2004). Offshore seismic reflection data demonstrate that the Humber Arm allochthon was inserted into a thin-skinned triangle zone or tectonic wedge (Figure 3.15) (Stockmal and Waldron, 1990; 1993; Stockmal et al., 1998). Geophysical logs and well cuttings from well M-16 demonstrate that rocks from within the triangle zone imaged in offshore seismic profiles belong to the Humber Arm allochthon (Cooper et al., 2001). The upper detachment of the triangle zone is termed the Tea Cove thrust (Stockmal and Waldron, 1993), and appears to directly underlie the Lourdes Limestone. The Lourdes Limestone makes a very strong regional seismic reflector (e.g., Stockmal and Waldron, 1990) that can easily be linked to outcrop on Port au Port peninsula, making it relatively easy to trace the extent of the Tea Cove thrust in the subsurface.

The northwestern structural front of the Newfoundland Appalachians is defined by the intersection of the Tea Cove thrust and the basal detachment in the Humber Arm allochthon. These two intersecting faults make up the structural triangle zone that wedges

the Humber Arm allochthon between the underlying Cambrian-Ordovician shelf (Units 1 through 3) and the overlying Upper Ordovician through Lower Devonian foreland basin (Units 4 and 5), implying that the Humber Arm allochthon was not emplaced into its present position until after the late-Early Devonian (Emsian). On Port au Port peninsula, limestone beds of the Lourdes Limestone in the footwall of the Round Head fault are overturned, dipping steeply to the southeast, indicating the Tea Cove thrust is cut by the Round Head fault.

Line 3 displays the greatest extent of the Humber Arm allochthon in southwestern Newfoundland. Thermal maturity studies on shale and carbonates in the Phillips Brook structure suggest that the top of the Cambrian-Ordovician platform was buried beneath 3 to 5 km of cover (Williams et al., 1998), which corresponds to the inferred roof of the eroded Humber Arm allochthon displayed in Line 3 (Plate 3.1). In palinspastically restoring the Humber Arm allochthon by area balance, we assumed a restored thickness of approximately 1500 m, which is equivalent to the restored thickness of the Cow Head Group and Lower Head Formation of the Humber Arm allochthon in Lines 5 though 7 (see Section 3.5.3).

The Humber Arm allochthon in Line 3 was internally shortened approximately 50% during emplacement. The total restored length of the Humber Arm allochthon is around 140 km (assuming a consistent thickness of 1500 m). Total horizontal displacement of the Humber Arm allochthon by restoring the present leading edge of the allochthon beyond the trailing edge of the restored shelf indicates the allochthon was displaced a minimum of 92.5 km to the current position on the margin. By extrapolating the restored length of the Cambrian-Ordovician platform from Line 3 along strike to Line 2, we are able estimate a minimum amount of westward translation of approximately 60 km along that line of cross section. Line 2 indicates that total westward displacement of the Humber Arm allochthon decreases to the southwest of Line 3. This interpretation is consistent with thermal maturation studies, which indicate that the Cambrian-Ordovician platform succession on southwestern Port au Port peninsula experienced no more than 3 km of post-Middle Ordovician burial, suggesting burial only by sedimentation rather than tectonic burial by the allochthon (Williams et al., 1998).

Summary

The balanced cross sections across southwestern Newfoundland highlight a complex sequence of events that occurred during the Paleozoic on the St. Lawrence promontory. Neoproterozoic-Early Cambrian continental rifting related to the breakout of Laurentia from Rodinia produced a set of east-dipping normal faults and graben that accumulated variable amounts of synrift fill during the Early Cambrian (Unit 1). Following rifting, the margin experienced a prolonged period of post-rift thermal subsidence that resulted in the deposition of a Cambrian-Ordovician carbonate platform on the shelf (Unit 2), and associated off-shelf facies which are now exposed in the Humber Arm allochthon. Flexural subsidence of the margin during the Middle Ordovician resulted in the deposition of a foreland-basin succession (Unit 3) and local activation of foreland-basin graben systems (i.e., Round Head fault, Table Mountain structure), which produced very thick accumulations of conglomerate and sandstone (e.g., Cape Cormorant Formation, Mainland Sandstone) (Figure 3.17A). Middle Ordovician foreland-subsidence was followed by deposition of a Late Ordovician-Devonian foreland basin succession (Units 4 and 5); the succession is thicker than the fill in the Middle Ordovician foreland basin by an order of magnitude, implying that the Humber Arm allochthon was being thrust westward onto the continental margin during that time (Figure 3.17B).

Final emplacement of the Humber Arm allochthon into a tectonic wedge is constrained to post-Early Devonian time because Emsian red beds in the Red Island Road Formation near Port au Port peninsula are deformed by the roof thrust to the tectonic wedge (Figure 3.17C). During emplacement, the Humber Arm allochthon traveled minimum distances of 60 km and 92.5 km, and experienced around 50% internal shortening. The final major deformational event is manifest as thick-skinned reactivation and inversion of earlier basement faults (i.e., Round Head fault), which formed in several places as pop-up structures (e.g., Table Mountain structure, Phillips Brook structure) in the shelf succession (Figure 3.17D). Thick-skinned faults and pop-up structures deform Emsian deposits in the Late Ordovician-Devonian foreland basin and appear to be unconformably overlain by Early Mississippian (Visean) clastic deposits of the Codroy

Group, bracketing the age of thick-skinned deformation between the early-Middle Devonian and late-Early Mississippian.

3.5.2 Humber Arm (Line 4)

The geology exposed around Humber Arm is regarded as the "type area" for the major tectonic units that comprise the Humber zone in Newfoundland (Williams, 1979). On a first-order scale, the geology of Humber Arm comprises allochthonous rift, slope, and rise successions (Humber Arm Supergroup) with structurally overlying ophiolite successions that are thrust over a deformed succession of early Paleozoic platform carbonates. East of Humber Arm is an internal massif of intensely deformed and metamorphosed schist, marble, and gneiss (Corner Brook Lake terrane) that superficially resembles shelf and slope strata exposed along the shores of Humber Arm (Figure 3.18). The purpose of Line 4 is to palinspastically restore the Humber Arm allochthon as it is exposed along the Bay of Islands and Humber Arm. Stratigraphic and structural relationships exposed along this part of western Newfoundland contrast with exposure in the Humber zone of southwestern Newfoundland (Lines 1-3) and north of Bonne Bay (Lines 5-9). Comparison of this line of cross section with the other cross sections also highlights important along-strike contrasts in the structural geology and stratigraphy of the eastern Laurentian margin on the St. Lawrence promontory.

Stratigraphic Framework of Shelf Rocks

The eastern half of the external Humber zone is host to Cambrian-Ordovician shelf rocks, which are exposed in an uplifted block between the Humber Arm allochthon on the west and the metamorphosed internal domain rocks of the Corner Brook Lake terrane on the east (Figure 3.4). North and south of Humber Arm, early Paleozoic shelf successions are assembled into a west-verging stack of imbricate thrust slices (Knight, 1994; 1996; 2006). Directly east of Corner Brook, however, only a narrow corridor of tightly folded platform rocks is exposed; seismic reflection data indicate that multiple thrust slices of Cambrian-Ordovician platform rocks are present beneath the Humber Arm allochthon (see below). The lower part of the Cambrian-Ordovician carbonate

sequence around Humber Arm contrasts sharply with platform rocks in southwest Newfoundland and the Northern Peninsula.

The oldest rocks within the shelf succession along Line 4 belong to the Reluctant Head Formation (Lilly, 1963; Knight, 1996), which is in narrow strip of outcrop along the western side of the Humber River fault (Figure 3.18). The formation consists of dolomitic and argillaceous ribbon limestone, thinly bedded phyllite, and minor limestone conglomerate (Knight 1996; Cawood and van Gool, 1998). Knight and Boyce (1991) report a trilobite fauna of late-Middle Cambrian to early-Late Cambrian age from the upper part of the Reluctant Head Formation, indicating the formation is the lateral equivalent to the lower Port au Port Group farther west. The base of the Reluctant Head Formation is faulted in the area of cross section; but elsewhere in western Newfoundland, the Reluctant Head Formation is mapped conformably overlying distal shelf equivalents of the Hawkes Bay Formation (upper Labrador Group) (Knight 1992; 1994; 1996). The top of the formation is conformably overlain by thick-bedded carbonates of the upper Port au Port Group (Knight and Boyce, 1991; Cawood and van Gool, 1998). Facies relationships within the formation, as well as with the overlying Port au Port Group, indicate the Reluctant Head Formation represents a Middle Cambrian prograding carbonate ramp that grades upward into a Late Cambrian shallow-marine carbonate platform (Knight and Boyce, 1991). The vertical succession indicates prolonged subsidence during the Early and Middle Cambrian on the shelf along this segment of the margin, resulting in a deeper water depositional environment. The thickness of the Reluctant Head Formation is estimated to be 250 m (Gillespie, 1983).

Carbonate-platform rocks of the Port au Port, St. George, and Table Head Groups successively overlie the Reluctant Head Formation within the area of the cross section. Rocks within each of the carbonate-dominated successions are essentially identical to the carbonate platform exposed in southwestern Newfoundland and on the Northern Peninsula, with the exception that limestone beds of the lower Port au Port Group are replaced by ribbon limestone and phyllite of the Reluctant Head Formation. Overlying the Table Head Formation is shale and siltstone of the Middle Ordovician Goose Tickle Group. The thickness of the overlying carbonate and foreland-basin succession is

estimated to be 1300 m, on the basis of map pattern thicknesses and a seismic reflection profile.

Exposure of the Late Ordovician through Devonian Anticosti foreland-basin succession is limited to offshore seismic reflection profiles, which indicate a thick accumulation of sediment above the autochthonous Cambrian-Ordovician platform (Figure 3.19). Correlation along strike from Port au Port peninsula in southwestern Newfoundland suggests these deposits are the Long Point Group and Clam Bank Formation. Seismic Line 90-2 also indicates that the Humber Arm allochthon has been inserted as a tectonic wedge beneath the Upper Ordovician-Devonian basin, which is similar to structural geometry of the leading edge of the allochthon in southwestern Newfoundland.

Stratigraphic Framework of the Humber Arm Allochthon

Sedimentary rocks of the Humber Arm allochthon around Humber Arm and Corner Brook belong to the Humber Arm Supergroup (Williams, 1979). Along Line 4, the Humber Arm Supergroup can be divided into three distinct stratigraphic successions that span overlapping time intervals between the Neoproterozoic and Early Ordovician and represent a distinctive depositional environment on the distal continental margin of Laurentia (Waldron et al., 2002; 2003). Each of the three successions is contained within individual thrust sheets in the allochthon; contacts between major thrust sheets that carry distinct stratigraphic successions are marked by thrust faults sub-parallel to stratigraphy and by thick, chaotic mélange zones. Informal names (i.e., Watsons Brook succession, Corner Brook succession, Woods Island succession) have been assigned to each of the three stratigraphic successions, as well as the thrust sheets that carry them (Waldron et al., 2002).

The Watsons Brook succession (Figure 3.5) is exposed west of the allochthonous Cambrian-Ordovician platform and consists of rocks assigned to the Pinchgut Lake Group (Williams and Cawood, 1989; Knight 1996) and overlying Goose Tickle Group (Waldron et al., 2003). The Pinchgut Lake Group consists of dark-grey phyllite, ribbon limestone, oolitic limestone, and limestone conglomerate tentatively correlated with upper Port au Port Group and lower St. George Group, implying a Late Cambrian-Early

Ordovician age (Knight, 1996). The rock types and facies relationships within the Pinchgut Lake Group are indicative of depositional environments transitional between platform and slope (Waldron et al., 2003). Although the base of the group is unexposed, measured sections indicate a thickness of at least 350 m (Knight, 1996). Conformably above the Pinchgut Lake Group are gray-green, flyschoid sandstone and shale that are typical of the Goose Tickle Group (Waldron et al., 2002). The entire Watsons Brook succession is indicative of a Late Cambrian to Early Ordovician passive-margin shelf-edge and shelf-break depositional environment overlain by Middle Ordovician foreland-basin flysch.

The Corner Brook succession preserves the most complete sedimentary record of the distal Laurentian margin on the St. Lawrence promontory. Rocks of the Corner Brook succession are divided into the Neoproterozoic-Early Cambrian Curling Group, the Middle Cambrian-Early Ordovician Northern Head Group, and the Middle Ordovician Eagle Island Formation (Figure 3.5) (Waldron and Palmer, 2000; Waldron et al., 2002). The lowest unit in the Curling Group is the Summerside Formation, which consists of a late Neoproterozoic to Early Cambrian succession of red to grey-green shale interlayered with medium to very thick beds of red, coarse-grained arkosic sandstone (Palmer et al., 2001). The base of the Summerside Formation is tectonic, and nowhere is the stratigraphic base exposed. Measured sections along the north shore of Humber Arm indicate the Summerside Group has a minimum thickness of 700 m (Palmer et al., 2001). Conformably overlying the Summerside Formation is the late-Early Cambrian Irishtown Formation, which consists of black and dark grey, graphitic, pyrite-bearing sandstone and shale with minor conglomerate (Waldron and Palmer, 2000; Palmer et al., 2001). A measured section along the south shore of Humber Arm indicates a thickness of approximately 1200 m for the Irishtown Formation (Palmer et al., 2001). The Neoproterozoic-Early Cambrian age, abrupt vertical and lateral variation in rock type and facies, and the overall upward progression from coarse, red, arkosic sandstones (Summerside) to fine, black, shale (Irishtown) indicate that sediments in the Curling Group were deposited in a rift-related environment along the Laurentian margin (Williams and Hiscott, 1987).

Carbonate deposits of the Northern Head Group overlie the Curling Group and are divided into two separate formations. The Cooks Brook Formation overlies black shale of the Irishtown Formation with subtle unconformity (Palmer et al., 2001; Lavoie et al., 2003). The formation consists of Middle Cambrian-earliest Ordovician shale, ribbon limestone, calcarenite, and minor limestone conglomerate (Waldron and Palmer, 2000). Conformably above the Cooks Brook Formation is the Early Ordovician Middle Arm Point Formation, which consists primarily of gray-green shale with minor fine-grained ribbon limestone beds (Botsford, 1988). Shale and ribbon limestone of the Northern Head Group represent a condensed section of the distal passive-margin on the St. Lawrence promontory. The thickness of the Northern Head Group is measured around 500 m (Lavoie et al., 2003). Above the Northern Head Group is Middle Ordovician green sandstone and shale of the Eagle Island Formation, which represents the oldest foreland-basin flysch deposits preserved in the Appalachian orogen (Williams, 1995). The top of the Eagle Island Formation is tectonic; however, Botsford (1988) reports a maximum exposed thickness of 203 m for the formation.

The Woods Island succession (Waldron et al., 2002) consists predominantly of coarse, quartzose sandstone and red-black shale with intercalated flows and blocks of fine-crystalline basalt (Palmer et al., 2001; Calon et al., 2002). The base of the Woods Island succession is the Blow Me Down Brook Formation, which comprises a 400-m-thick section of shale and coarse sandstone that contain the trace fossil *Oldhamia* (Lindholm and Casey; 1990), indicating a late-Early Cambrian age for the formation (Palmer et al., 2001; Calon et al., 2002). Furthermore, the distribution of detrital zircon age populations in the Blow Me Down Brook Formation closely matches those in the late-Early Cambrian Hawkes Bay Formation and the upper part of the Irishtown Formation (see also Chapter 4) (Cawood and Nemchin, 2001), further substantiating a late-Early Cambrian age for the Blow Me Down Brook Formation.

The Bay of Islands ophiolite suite occupies the highest structural slice in the Humber Arm allochthon (Williams and Cawood, 1989). It consists of a complete section of ophiolite from ultramafic rocks at the base through gabbros and sheeted dikes to pillow basalts and hemipelagic sediments at the top (Williams, 1995). Originally, ophiolite and mantle lithosphere in the Bay of Islands suite was interpreted as slabs of Iapetus oceanic

crust obducted onto the eastern Laurentian margin as the Iapetus Ocean closed (Karson and Dewey, 1978; Williams, 1979; Karson, 1984). More recent geochronological and geochemical studies indicate that ophiloites in the Bay of Islands suite range in range from ca. 505 Ma to 485 Ma (Dunning and Krogh, 1985; Jenner et al., 1991; Kurth et al., 1998), and have a magmatic-arc geochemistry indicative of a supra-subduction zone setting (Jenner et al., 1991; Cawood and Suhr, 1992). The age and geochemical data indicate the ophiolites are younger than the Iapetus Ocean and were generated in a convergent environment after the Iapetus Ocean began to close (van Staal, 2005). ^{40}Ar-^{39}Ar analysis of on hornblendes from the metamorphic sole of the complex yield cooling ages of 469±5 Ma and 464± Ma (Dallmeyer and Williams, 1975; Dunning and Krogh, 1985), indicating the ophiolites where thrust onto sedimentary rocks in the Humber Arm allochthon during the Middle Ordovician.

Thermal maturation studies in the Humber Arm allochthon around Bonne Bay indicate that sediments in the Humber Arm Supergroup experienced deep tectonic burial (Nowlan and Barnes, 1987). CAIs and AAIs range between 4.0 and 5.0, indicating burial temperatures that exceeded 300º C (Nowland and Barnes, 1987; Williams et al., 1998). The thermal maturation data suggested to Williams et al. (1998) that, between Stephenville and Bonne Bay, most of the allochthonous sediments in the Humber Arm Supergroup were buried beneath warm, obducted ophiolites.

Structural Framework of Allochthonous Rocks

The Humber Arm allochthon around Corner Brook and Humber Arm demonstrates a complex, polyphase structural history (Waldron et al., 1998; 2003). The metamorphic grade of sedimentary rocks in the Humber Arm Supergroup is low and deformation is heterogeneous (Cawood and van Gool, 1998). The intensity of deformation, the frequency of overprinting structural fabrics, and the degree of metamorphism increase in the allochthon from west to east. Previous workers have classified structures into two main phases where clear overprinting relationships are readily identifiable (e.g., Cawood and van Gool, 1998; Waldron et al., 2003). D_1 structures are predominantly west-verging and most clearly recognizable along the western coastal outcrops in the Humber Arm allochthon. D_2 structures consist of east-

verging penetrative fabrics that overprint D_1 structures and are best developed in the eastern inland exposures of the allochthon (e.g., Cawood and van Gool, 1998).

D_1 structures are most recognizable at the macroscopic scale. They comprise major west-verging thrust zones that bound thrust sheets carrying each of the individual stratigraphic succession, zones of broken formation and structural mélange between thrust sheets, and west-verging folds and foliations that deform stratigraphy in the allochthon.

Mélange zones are the most characteristic deformational features of the Humber Arm allochthon south of Bonne Bay. They range from several meters to tens of kilometers in thickness, form the structural base to major thrust sheets within the allochthon, and consist predominantly of blocks of competent rocks (sandstone, limestone) immersed in a scaly matrix of deformed shale. Rocks characteristic of several different formations may be found together as blocks in a single outcrop of mélange, indicating significant mixing of rock types from most of the stratigraphic successions within the allochthon (Waldron and Palmer, 2000). Also, it is not uncommon to find blocks of shelf clastic and carbonate rocks in outcrops of mélange along the basal detachment of the Humber Arm allochthon. Fragmentation and mixing of stratigraphic blocks from the overlying thrust sheets into underlying structural mélange zone indicates that these zones where formed as a result of gravity sliding and mass wasting in front of the leading edge of the advancing thrust sheet as it was uplifted and thrust over the continental shelf (Figure 3.20A). Incorporation of underlying shelf rocks into basal mélange zones is likely the result of mechanical cataclasis of the shelf by the HAABD and entrainment of fragmented shelf blocks.

Most coherently bedded rocks in the Humber Arm allochthon display a strong bed-parallel cleavage that is axial planar to rare F_1 folds (Waldron et al., 2002; 2003). Folds related to F_1 are found a number of locations around the allochthon, but are not as pervasive as later F_2 folds (Waldron et al., 2003). West-verging F_1 folds are interpreted to be related to ramp anticlines and synclines, which formed during initial displacement of the Humber Arm allochthon.

Around the Bay of Islands and Humber Arm, all three of the stratigraphic successions are exposed within individual thrust sheets bounded by complex mélange

zones. In some locations, the stratigraphy within individual thrust sheets is duplicated by internal thrust faults sub-parallel to bedding, indicating further imbrication of major thrust sheets into tectonic slices as they were emplaced onto the continental margin. We follow the terminology of Waldron et al. (2003), who identify four major thrust sheets, three within the allochthon and one in the carbonate-platform sequence.

The Woods Island thrust sheet is the structurally highest sheet in the allochthon that carries sedimentary rocks of the Humber Arm Supergroup (Waldron et al., 2003). Thrust onto sedimentary rocks in the Woods Island thrust sheet are mafic and ultramafic igneous suites of the Bay of Islands ophiolites (Williams and Cawood, 1989). The Woods Island thrust sheet contains a section of the late-Early Cambrian Blow Me Down Brook Formation, the most continuous section of which is exposed on the coast of Woods Island (Palmer et al., 2001). The structural base of the sheet is exposed on the south coast of Woods Island where it sits above a west-dipping, highly deformed zone of mélange (Waldron and Palmer, 2000; Calon et al., 2002).

The Corner Brook thrust sheet structurally underlies the Woods Island sheet, from which it is separated by a wide zone of mélange. The thrust sheet is divided into several smaller thrust slices that duplicate stratigraphy within the thrust sheet. The Corner Brook thrust sheet is dominated by a single, continuous slice of deformed but essentially intact sedimentary deposits of the Curling Group through the Eagle Island Formation (termed the Crow Hill slice) (Waldron et al., 2003). The base of the Crow Hill slice is the Crow Hill thrust (Line 4, Plate 3.1), which is well exposed in Corner Brook and along the north shore of Humber Arm. Outcrops of the Crow Hill thrust demonstrate that it has both a hanging-wall ramp and flat geometry, with respect to stratigraphic bedding in the Curling and Northern Head Groups (Waldron et al., 1998; Cawood and van Gool, 1998). Below the Crow Hill thrust along the eastern shore of Humber Arm and in the city of Corner Brook is a structural slice that duplicates part of the upper stratigraphy in the Summerside Formation and approximately 700 m of overlying Irishtown Formation (Figure 3.18). This slice, termed the Corner Brook slice by Waldron et al. (2003), is here interpreted to be a deformed and translated slice of the footwall ramp to the Crow Hill thrust (Plate 3.1). Another structurally low slice is exposed in a window in the culmination of a doubly plunging anticline on the north shore of Humber Arm at Rattler Brook (Figure 3.18)

(Waldron, 1985). Within the window is a stratigraphic succession that spans the upper Irishtown through the Eagle Island Formation.

One possible interpretation of the Rattler Brook slice is that it represents a westward continuation of the lower Corner Brook slice (suggested by Waldron et al., 2003). In a palinspastic restoration, however, the leading edge of the overlying Crow Hill slice must palinspastically restore outboard of the trailing edge of the underlying Corner Brook slice because the Crow Hill thrust carries the lowest stratigraphic components of the Curling Group. For the Rattler Brook and Corner Brook slices to be a single continuous sheet underneath the main Crow Hill slice implies that at least 300 m of Summerside Formation must be present at the leading edge of the main Crow Hill slice in the hanging wall of the Crow Hill thrust. Where the Crow Hill thrust re-emerges at the Rattler Brook window, only the Irishtown Formation is observed in the immediate hanging wall of the thrust, indicating the Crow Hill thrust cuts up-section through the Summerside Formation somewhere in the subsurface between the Corner Brook and the Rattler Brook slices. Thus, the hanging wall cut-offs in the leading edge of the Crow Hill slice do not match the footwall cut-offs required to make a continuous Rattler Brook-Corner Brook slice. A more simple explanation is that the structural slice exposed in the Rattler Brook window was a part of the leading edge of the Corner Brook thrust sheet, which was subsequently beheaded by out-of-sequence thrusting along the Crow Hill thrust and structurally overridden by the main Corner Brook thrust sheet (Figure 3.20B).

East of the Corner Brook sheet, the Watsons Brook thrust sheet carries stratigraphy corresponding to the Late Cambrian-Early Ordovician Pinchgut Lake Group and the Middle Ordovician Goose Tickle Group (Waldron et al., 2002). The thrust sheet structurally underlies the Corner Brook thrust sheet and apparently contains at least two structural slices. Waldron et al. (2003) report an upper slice, which contains a structural window into the lower slice at the culmination of a doubly plunging fold to the south of the town of Corner Brook (Figure 3.18).

The structurally lowest rocks consist of allochthonous slices of the Cambrian-Ordovician carbonate platform. Although these rocks are allochthonous, the stratigraphy is part of the shallow-marine shelf succession. Therefore, these thrust slices are not considered to be part of the Humber Arm allochthon. Thrust slices of the carbonate

platform thrust sheet form a west-verging thrust stack, thrust into and over the lower structural slices of the Humber Arm allochthon (Knight, 1994; 1996). The basal decollement completely detaches carbonate platform thrust sheets exposed east of Humber Arm from underlying crystalline basement; the decollement apparently parallels shale and phyllite in the Middle Cambrian Reluctant Head Formation (Knight, 1996; 2006). In Line 4, outcrop of the carbonate thrust sheet is limited to a narrow strip between the Harry's Brook fault and the Humber River fault. Several sets of prominent layered reflectors along Lithoprobe East seismic lines 89-1 and 89-2 (Figure 3.21) show an apparent west-verging stack of imbricate thrust sheets beneath the Humber Arm allochthon. The geometry of these prominent reflectors mimics the structural geometry of the carbonate thrust sheet, where it is mapped at the surface both north and south of Humber Arm (Knight, 1994; 1996; Cawood and van Gool, 1998). The seismic data suggest that at least three allochthonous sheets of carbonate platform have been detached and inserted beneath the Humber Arm allochthon along Line 4.

D_2 structures comprise a later set of penetrative folds and fabrics that deform D_1 structures. The most prominent of these is an S_2 cleavage that deforms sedimentary rocks primarily along the eastern and central parts of the Humber Arm allochthon and that is axial planar to F_2 folds (Waldron and Palmer, 2000). Open to tight F_2 folds are conspicuous in many outcrops within the Humber Arm allochthon. F_2 consists of an east-verging set of upright to inclined, doubly plunging folds that dominate the map pattern of the allochthon. Notable map scale F_2 folds include the Rattler Brook window and the Cooks Brook syncline.

Corner Brook Lake Terrane

The Corner Brook Lake terrane is a high-grade internal domain in the Humber zone (Williams, 1995). The oldest rocks in the terrane consist of a crystalline core of granitic gneiss dated at ca. 1500 Ma, indicating these gneisses correlate with crystalline basement in the Long Range complex (Cawood and van Gool, 1998). In several locations, basement is intruded by rift-related, alkalic granites with late-Neoproterozoic crystallization ages (Williams et al., 1985; Cawood et al., 2001). Lying unconformably on Mesoproterozoic crystalline basement and synrift magmatic suites are

metasedimentary rocks of the Fluer de Lys Supergroup (Hibbard, 1988; Cawood and van Gool, 1998; Cawood et al., 2001), which in the Corner Brook Lake terrane consists of the South Brook and Breeches Pond Formations (Figure 3.5). The South Brook Formation consists of polydeformed paragneiss, quartzite, and metaconglomerate. Overlying the South Brook Formation, the Breeches Pond Formation comprises an extensive metacarbonate cover made up of calcareous metaconglomerate, marble, and marble breccia (Cawood and van Gool, 1998). The succession of rock types is consistent with a transition from siliciclastic deposition on eroded basement to carbonate-dominated sedimentation corresponding to a rift-to-passive-margin transition (e.g., Cawood et al., 1996). Metaconglomerates and metagreywackes in the South Brook Formation strongly resemble synrift deposits of the Curling Group in the Humber Arm allochthon, whereas marble breccias and conglomerates in the Breeches Pond Formation are nearly identical to the Pinchgut Lake Group in the Watsons Brook thrust sheet (Figure 3.22).

Basement and metasedimentary successions in the Corner Brook Lake terrane have subsequently been metamorphosed and thrust onto the continental margin. The map pattern of basement and metasedimentary rocks of the Fleur de Lys Supergroup outlines a large-scale flexural bend in the Corner Brook Lake terrane, herein termed the Corner Brook Lake flexure (Figure 3.23). The core of the flexure is marked by the most extensive outcrop of crystalline basement. Southwest of the flexure, the Fleur de Lys Supergroup mainly consists of metacarbonate deposits of the Breeches Pond Formation; metaconglomerate and metaclastic rocks of the South Brook Formation comprise a thin (5 m) layer separating the Breeches Pond Formation from underlying Mesoproterozoic basement. Northeastward from the flexure, the South Brook Formation thickens considerably where basement plunges beneath it (Figure 3.23).

Map-view curves and flexures in thrust belts typically form in response to several different contributing factors, including the pre-thrust geometry of the sedimentary basin and irregularities on colliding margins (Thomas, 1977; Bradley, 1989; Marshak, 2004). Basin-controlled curves can result from along-strike changes in the depth and slope of the sedimentary basin. Furthermore, basins with variable depths along a continental margin may result in differing along-strike geometries in the thrust belt. The distribution of remobilized basement and metasedimentary rocks around the hinge zone of the Corner

Brook Lake flexure suggests significant along-strike variations in the original basin geometry of the Corner Brook Lake terrane (Figure 3.24). Thick across-strike sections of South Brook Formation northeast of the flexure likely correspond to a deep rift basin near the continental margin. Southwest of the flexure, thin metaclastic rocks lying between basement and a thick section of metacarbonate rocks indicates a part of the margin that was relatively stable and shallow during Iapetan rifting. In this analysis, the hinge zone of the Corner Brook Lake flexure corresponds to a large-scale, Neoproterozoic-Early Cambrian continental-margin transform fault. The restored cross section presented in Line 4 (Plate 3.1) suggests the Corner Brook Lake terrane palinspastically restores ~90 km southeast of the current exposed position. In the palinspastic restoration, the hinge zone to the Corner Brook Lake flexure roughly aligns with the proposed linear northwest trace of the Serpentine Lake transform, suggesting it is a physical expression of the transform fault.

Following deposition of the South Brook and Breeches Pond Formations, the Corner Brook Lake terrane experienced widespread greenschist and amphibolite facies metamorphism during mid-Silurian time. Metamorphic mineral assemblages in the Fleur de Lys Supergroup indicate P-T paths with an early high-pressure metamorphic event followed by decompression and an increase in temperature (Jamieson, 1990). Peak temperatures and pressures recorded in the Corner Brook Lake terrane are at 650º C and 0.7-0.9 GPa, indicating a maximum burial depth of between 30 and 40 km (Cawood and van Gool, 1998). U-Pb ages in monazite and ^{40}Ar-^{39}Ar ages in hornblende and muscovite constrain the timing of peak metamorphism in the Corner Brook Lake terrane to ca. 430-423 Ma (Dallmeyer, 1977; Cawood et al., 1994; 1996).

Regional metamorphic isograds within metasedimentary rocks of the Fleur de Lys Supergroup are deformed by west-verging thrust faults in the Corner Brook Lake terrane and the large Yellow Marsh antiform, which is exposed in the core of the thickest section of the South Brook Formation (Figures 3.18 and 3.23) (Cawood and van Gool, 1998). Seismic profile 89-2 clearly images broadly folded reflectors at depth along the eastern side of the profile, which corresponds to the Yellow Marsh antiform (Figure 3.21). The seismic data demonstrate that the Yellow Marsh antiform has a ramp anticline geometry related to westward thrusting of Corner Brook Lake rocks onto the margin. Both the

seismic and structural data indicate that westward emplacement of the Corner Brook Lake terrane post-dates Silurian metamorphism of the Fleur de Lys Supergroup. A single muscovite sample collected along one of the west-verging thrust faults yielded an ^{40}Ar-^{30}Ar cooling age of 413±3 Ma (Cawood and van Gool, 1998), which suggests that westward emplacement of the Corner Brook Lake terrane occurred during the Early Devonian.

Late Structures

Several significant late faults along Line 4 deform and juxtapose contrasting elements of the Humber zone. Analysis of seismic line 89-2 between CDP-1250 and CDP-1400 reveals a prominent set of steeply west-dipping reflectors that truncate continuous, gently east-dipping reflector groups corresponding to the strata in the Humber Arm allochthon and the underlying carbonate thrust sheet (Figure 3.21). These west-dipping reflectors project to surface outcrop of the Humber River fault and the Hughes Brook fault.

The Hughes Brook fault is a steep, west-dipping fault that juxtaposes rocks of the carbonate thrust belt on the east against rocks of the Humber Arm allochthon on the west (Figures 3.18). At the surface, the trace of the fault strikes roughly north-south. South of the town of Corner Brook, the Hughes Brook fault merges with the Humber River fault. The fault plane at the surface is slightly steeper than bedding in the carbonate platform footwall and dips between 75º and 80º southwest (Cawood and van Gool, 1998). Omission of stratigraphic units across the fault plane and the apparent westward dip in both outcrop and seismic reflection profiles indicates downward movement of the western hanging wall to the Hughes Brook fault. Downward displacement of the hanging wall appears to diminish south of Corner Brook.

The Humber River fault along Line 4 forms the boundary between low-grade platform carbonates on the west and polydeformed, high-grade rocks of the Corner Brook Lake terrane on the east (Figure 3.18). The structural nature of this lithotectonic boundary is largely enigmatic because the fault plane is not exposed along much of the inferred trace of the fault (Cawood and van Gool, 1998). Seismic reflection analysis, coupled with the dips of foliations along the fault trace, indicate the fault dips steeply to the northwest.

Interpretations of the Humber River fault range from an overturned thrust fault (Kennedy, 1981) to a late normal fault (Cawood and van Gool, 1998). In seismic line 89-2, folded reflectors corresponding to the Yellow Marsh anticline overlie and truncate continuous, east-dipping reflectors that correspond to stacked thrust sheets of the carbonate platform (Figure 3.21), indicating the Corner Brook Lake terrane is thrust over the carbonate imbricate thrust belt. The hanging wall of the Humber River fault, however, contains the deformed carbonate thrust sheet, suggesting the hanging wall has uplifted the Corner Brook Lake terrane and the underlying carbonate thrust belt. The uplift of the lower carbonate thrust sheet in the hanging wall, along with the position of cut-offs in the hanging wall and footwall of the Humber River fault in Line 4 (Plate 3.1) that are required to palinspastically restore the lithotectonic elements along the line of cross-section, indicate the Humber River fault displays net reverse motion.

Summary: Palinspastic Restoration of the Humber Arm Allochthon

Although the Humber Arm allochthon around the type area is clearly thrust onto the Laurentian continental margin of the St. Lawrence promontory, the structural characteristics displayed in this part of the allochthon contrast with those of a typical foreland thrust belt. For example, tectonic slices containing stratigraphy from the most distal reaches of the continental margin lie to the west beyond more proximal margin successions, indicating that entire thrust sheets have "leap-frogged" underlying thrust sheets. Also, thrust sheets are separated by wide, complex mélange zones, indicating erosion and mass wasting of the leading edges of individual thrust sheets as they were uplifted and transported westward. Finally, projection of thrust faults that separate major tectonic elements in the allochthon from outcrop and seismic data indicates they dip northwest at moderate to shallow angle (Figure 3.18 and 3.21). The overall structural geometry of the Humber Arm allochthon at Humber Arm mimics a foreland dipping duplex system (e.g., Boyer and Elliot, 1982).

Palinspastic restoration of tectonic mélange zones, which underlie major thrust sheets, produces some unique challenges. These mélange zones consist of material that slumped off of the leading edges of the overriding thrust sheets during westward thrusting. Material in the mélange zones was primarily derived from the individual thrust

sheets that structurally override them. Therefore, we have attempted to palinspastically restore each of the mélange zones using area-balancing techniques to the leading edge of the thrust sheet that structurally overlies it. Rocks in the Corner Brook Lake terrane, which have experienced high-grade metamorphism and polyphase deformation, have also been restored by area balance.

In Line 4, the Watsons Brook thrust sheet palinspastically restores outboard of the trailing edge of the carbonate platform. This interpretation fits the stratigraphic data, which indicates that phyllite and limestone conglomerate in the Pinchgut Lake Group form the transition from platform shelf to slope facies. During emplacement onto the margin, sediments in the Watsons Brook thrust sheet experienced 40% internal shortening and approximately 98 km of westward displacement. The overlying Corner Brook thrust sheet palinspastically restores outboard of the trailing edge of the Watsons Brook thrust sheet. The Corner Brook sheet experienced approximately 32% total shortening and 169 km of westward translation. The Woods Island thrust sheet is interpreted to palinspastically restore outboard of the Corner Brook thrust sheet. The only known cohesive stratigraphic unit in the Woods Island thrust sheet is the Blow Me Down Brook Formation, which only comprises a minor fraction of the sheet. Most of the Woods Island thrust sheet consists of mélange and undivided shale and sandstone (Calon et al., 2002). Therefore, although the Blow Me Down Brook Formation has been palinspastically restored by line-length balance, most of the sheet is restored by area balance. Palinspastic restoration of the Blow Me Down Brook Formation in the Woods Island sheet indicates approximately 255 km of westward displacement. The cumulative restored length of all the thrust sheets that comprise the Humber Arm allochthon from leading edge to trailing edge is 209 km. Total westward translation of the leading edge of the Humber Arm allochthon from the restored position to the current structural position in the tectonic triangle zone is 132 km. Cumulative internal shortening within the allochthon is approximately 63%.

Palinspastic restoration of the Corner Brook Lake terrane is constrained by rock-type and facies similarites between the Breeches Pond Formation in the Corner Brook Lake terrane and the Pinchgut Lake Group in the Watsons Brook thrust sheet. Both units display identical shelf-edge and shelf-break facies. Furthermore, Knight (1996; 2006) has

directly correlated unmetamorphosed Pinchgut Lake Group rocks across the Humber River fault with calcareous metaconglomerates and carbonates in the Breeches Pond Formation. Therefore, we choose to palinspastically restore the Corner Brook Lake terrane beneath the Watsons Brook thrust sheet. This restored location allows for a direct vertical correlation between from Breeches Pond to Pinchgut Lake Group rocks, and also places the Corner Brook Lake terrane in a location where it can be overridden by thick structural slices of the Humber Arm allochthon required to produce greenschist-amphibolite grade metamorphism throughout the terrane.

The timing of tectonic events along Line 4 is constrained by overprinting structural relationships. A thin, Middle Ordovician foreland-basin fill manifest by the Goose Tickle Group/Eagle Island Formation extends across most of the line of cross section, indicating that only the very leading edge of the continental margin was overridden and loaded by dense ophiolites during the Middle Ordovician Taconic orogeny (Stockmal et al., 1995). This observation is supported by Middle Ordovician cooling ages from sediments in the Humber Arm Supergroup that directly underlie the Bay of Islands Ophiolite suite. By the Middle Silurian, approximately 30 to 40 km of allochthonous material (either Humber Arm allochthon or ophiolites or both) had advanced as far as the Corner Brook Lake terrane, to explain metamorphic mineral assemblages in the Fleur de Lys Supergroup. During the Late Silurian and Early Devonian, the Humber Arm allochthon must have completely overridden the early Paleozoic shelf; Early Devonian thrusting in the Corner Brook Lake terrane propagated up through the slope succession and into the Reluctant Head Formation, forming an imbricate thrust stack of Cambrian-Ordovician platform rocks that in some places are thrust over structural slices in the Humber Arm allochthon (Knight, 1994; 1996). The final kinematic event is tectonic extrusion of the hanging wall block between the Hughes Brook fault and the Humber River fault, which occurred sometime after emplacement of the Humber Arm allochthon into a tectonic wedge beneath the Late Ordovician-Devonian foreland basin.

3.5.3 Northern Peninsula; Bonne Bay – Portland Creek Pond (Lines 5, 6, and 7)

Rocks north of Bonne Bay and south of Portland Creek Pond belong to three distinct tectonic elements: 1) Mesoproterozoic basement of the Long Range massif; 2) clastic and carbonate platform successions of the early Paleozoic Laurentian margin; and 3) early Paleozoic sedimentary rocks of the Humber Arm allochthon (Figure 3.25) (Williams and Cawood, 1989). Most of the exposed Laurentian margin geology lies to the west of the Long Range massif along the coastal lowlands and shorelines of the Gulf of St. Lawrence. A small sliver of parautochthonous lower Paleozoic shelf stratigraphy is exposed, however, on the eastern flank of the massif along White Bay (Figure 3.4). Lines of cross section 5, 6, and 7 were constructed across the geology of the Northern Peninsula between Bonne Bay and Portland Creek Pond for two principal reasons: *1)* to restore the deformed lower Paleozoic shelf strata on both the western and eastern limbs of the Long Range massif to establish the total width of the Cambrian-Ordovician shelf across the Northern Peninsula; and *2)* to palinspastically restore deformed Laurentian slope stratigraphy within the Humber Arm allochthon outboard of the restored shelf edge.

Stratigraphic Framework

South of Portland Creek Pond, outcrop of the lower Paleozoic shelf succession is primarily limited to a narrow strip of land between the Parsons Pond fault and the Long Range fault (Figure 3.25). Outcrops of Mesoproterozoic basement are restricted to the Long Range massif, which makes up the core of the Long Range Mountains on the Northern Peninsula. Unconformably overlying Precambrian basement are clastic deposits of the Labrador Group, which in this region of the Northern Peninsula, consists only of the Forteau and Hawkes Bay Formations (Williams, 1985; Williams et al., 1986; Cawood et al., 1987). The thickness of the Labrador Group is estimated between 350 and 450 m on the basis of seismic reflection profiles and map pattern width.

Overlying the Labrador Group is the Cambrian-Ordovician carbonate platform succession, which, like in other regions of western Newfoundland, consists of the Port au Port Group, the St. George Group, and Table Head Group. Along the western flank of the Long Range massif, carbonate beds are moderately to strongly deformed and thrust over the Humber Arm allochthon by the Parsons Pond fault (Line 7, Plate 3.2). At Portland

Creek Pond, however, the carbonate platform dips gently south beneath the northern edge of the allochthon. Seismic data gathered to the south of Portland Creek Pond indicate the carbonate platform is around 1,100 m thick.

Shale and sandstone of the Middle Ordovician Goose Tickle Group lie above the Table Head Group and are well exposed around Portland Creek Pond, as well as in some uplifted blocks of Cambrian-Ordovician platform east of the Parsons Pond fault (Williams and Cawood, 1989). Seismic reflection data from the Norcen Line 92-067 demonstrate that the Goose Tickle Group has a thickness of approximately 650 m in the hanging wall of the Parsons Pond fault (Figure 3.26). The same seismic profile also indicates the Goose Tickle Group is only 200 m thick in the footwall of the Parsons Pond fault. In the immediate hanging wall of the Parson Pond fault is the Daniel's Harbour Member of the Goose Tickle Group, which consists of massive and oligomictic limestone conglomerate with clasts from limestone beds in the underlying Table Head Group (Stenzel et al., 1990). The stratigraphic and seismic data indicate that the Parsons Pond fault is an inverted Middle Ordovician normal fault, similar to the Round Head fault (Stockmal et al., 1998).

The Humber Arm allochthon consists of northeast-trending thrust slices of Middle Cambrian to early Middle Ordovician rocks of the Cow Head Group and the overlying Middle Ordovician Lower Head Formation (James and Stevens, 1986). Offshore seismic reflection profiles (Figure 3.19) in the Gulf of St. Lawrence demonstrate, that as far north as Bonne Bay, the Humber Arm allochthon has been inserted as a structural triangle zone into Late Ordovician-Devonian strata (Unit 4 and 5?) of the Anticosti basin (Stockmal et al., 1998). Onshore to the east, strata in the imbricate thrust slices of the allochthon are truncated by the Parsons Pond fault.

The Late Ordovician through Devonian foreland-basin strata are not exposed onshore in this part of western Newfoundland. Offshore seismic reflection profiles, however, indicate a thick accumulation of post-Middle Ordovician sediments that overlie reflector groups corresponding to the autochthonous Cambrian-Ordovician platform (Figure 3.19). Correlation along strike from Port au Port peninsula in southwestern Newfoundland suggests these deposits are the Long Point Group and Clam Bank Formation. Interestingly, the strong seismic reflector at the base of the Late Ordovician

section, denoting the Lourdes Limestone, is absent north of the Bay of Islands, suggesting that the Lourdes Limestone was not deposited in this part of the Anticosti basin. Carboniferous strata are limited to the Deer Lake basin on the southeastern edge of Long Range massif (Figure 3.4). There, post-Touraisian to pre-Visean red beds of the lower Deer Lake Group unconformably overlie crystalline basement of the Long Range massif (Williams, 1995), suggesting uplift of the massif sometime during the Early Mississippian.

Structural Framework of the Parautochthonous Shelf

The structural geology of the Northern Peninsula between Bonne Bay and Portland Creek Pond is dominated by imbricate thrust slices within the Humber Arm allochthon. Exposures of structures that deform the underlying shelf are fairly limited because of the limited outcrop of the Cambrian-Ordovician platform rocks. Seismic reflection profiles across the western lowlands of the Northern Peninsula display thick-skinned pop-up structures and reverse faults that deform both autochthonous shelf and the structurally overlying allochthon (Figures 3.27 and 3.28). The dips of these reverse faults are steep; reverse faults dip both to the southeast and northwest. Reverse offset across these faults ranges from less than 100 m to more than 400 m.

The Parsons Pond fault marks the eastern boundary of the Humber Arm allochthon (Williams and Cawood, 1989; Waldron and Stockmal, 1994). To the east, in the hanging wall of the Parsons Pond fault are uplifted tectonic slices of west-facing, locally overturned, partial sections of the Cambrian-Ordovician rift, passive-margin, and foreland-basin strata (Cawood et al., 1987). Strata of the Humber Arm allochthon in the immediate footwall of the Parsons Pond fault are mostly overturned in a west-facing synform (Line 5, Plate 3.2). Approximately 15 km north of Parsons Pond, the Parsons Pond fault strikes north-northwest, diverging from the Long Range fault to separate parautochthonous Goose Tickle Group from the strata in the Humber Arm allochthon (Figure 3.25). Stockmal et al. (1998) indicates that the offshore trace of the Parson Pond fault swings abruptly to the northeast and trends parallel to the western coastline. Farther south, the Parsons Pond fault merges with the Long Range fault but can be traced as far as Western Brook Pond (Figure 3.25) (Williams and Cawood, 1989).

The Parsons Pond fault makes a strong seismic reflector in regional seismic profiles. Seismic data demonstrate that the Parsons Pond fault is a thick-skinned reverse fault that dips between 30º and 40º southeast and truncates regional seismic reflector groups that correspond to the Cambrian-Ordovician rift and shelf succession (Units 1 through 3) at depth (Figures 3.27 and 3.28). The Parsons Pond fault carries a much thicker section of the Goose Tickle Group in the hanging wall in comparison to the footwall, as well as massive Middle Ordovician conglomerates of the Daniels Harbour Member in the immediate hanging wall (Stenzel et al., 1990; Stockmal et al., 1998). These data indicate that the Parsons Pond fault is an inverted structure; an early component of Middle Ordovician normal motion was followed by later structural inversion by compressional tectonics, which resulted in a net reverse offset of approximately 5 km.

The Long Range fault is one of several of east-dipping, north-northeast trending faults that comprise the Long Range Boundary fault system. The eastern hanging wall of the fault is composed primarily of Precambrian granite and gneiss of the Long Range complex (Owen, 1991), with minor isolated outliers of the overlying Labrador Group (Williams and Cawood, 1989). Exposure of the fault indicates that it dips between 30º and 35º southeast; however, the sinuous trace of the fault near St. Paul's Inlet follows the local topography, suggesting a subhorizontal dip in that area. Thus, the Long Range fault appears to have an overall ramp-flat geometry in the southwestern corner of the Northern Peninsula.

Total displacement across the Long Range fault has been a matter of some controversy. Williams et al. (1986) noted that the presence of Labrador Group strata in both the hanging wall and footwall of the Long Range fault implies displacement of only a few kilometers. However, Waldron and Stockmal (1994) have suggested that the seemingly sinuous trace of the Long Range Boundary fault system indicates a regional, rather than local, subhorizontal orientation over much of the length of the fault system, implying westward displacement of many tens to hundreds of kilometers.

In seismic Line 96-069, the Long Range fault makes a weak, moderately southeast-dipping reflector in the hanging wall of the Parsons Pond fault (Figure 3.27). The seismic line indicates the Long Range fault has a consistent dip downward to where

it truncates the Parsons Pond fault at depth. There is no evidence that the Long Range fault flattens at depth in this seismic profile, which is required in the highly allochthonous model of Waldron and Stockmal (1994). Mapping east of Port Saunders (see Section 3.5.4) indicates that the faults in the Long Range Boundary fault system steepen to the north, making it difficult to envisage large magnitudes of horizontal displacement along the Long Range fault system in that region. Furthermore, many of the other faults that comprise the Long Range Boundary fault north of Portland Creek Pond are offset along strike by steep-dipping, west-striking transfer faults (Coleman-Sadd et al., 1990). Much of the trace of the fault system between Portland Creek and Port Saunders is poorly documented. Thus, the apparent sinuous trace of the Long Range Boundary fault system may be an artifact of insufficient mapping along the fault system on much of the Northern Peninsula.

Calculation of total uplift across the Long Range fault is problematic because in most places, hanging wall cut-offs have been completely removed by erosion. An apatite fission track study indicates that between 3 and 5 km of overburden have been eroded from the Long Range massif since the late Paleozoic (Hendricks et al., 1990), which places a maximum constraint on the structural elevation of the early Paleozoic platform in the hanging wall of the fault (Plate 3.2). By assuming the top of the carbonate platform (Unit 2) has an average structural elevation of 4 km above present topography in the Long Range Mountains, reconstructions across the Long Range fault yield an average throw of 6.5 km and a westward heave between 7 and 10 km.

Timing of motion on the Parson Pond fault and Long Range fault is constrained by relationships to the Humber Arm allochthon. Offshore seismic data show that the Humber Arm allochthon west of the Northern Peninsula was inserted as a structural triangle zone into the Late Ordovician-Devonian section of the Anticosti basin. This observation requires final emplacement of the Humber Arm allochthon on the Northern Peninsula to post-date the Early Devonian, which is in agreement with structural and stratigraphic observations in southwestern Newfoundland (see Section 3.5.1). The Parsons Pond fault and the Long Range fault truncate the Humber Arm allochthon; therefore, reverse motion along these two fault systems must follow after post-Early Devonian emplacement of the allochthon. Along the southeast limb of the Long Range

massif, middle-Early Mississippian deposits in the Deer Lake basin unconformably overlie crystalline rocks of the Long Range complex, indicating that rocks in the massif were uplifted and eroded no later than the Early Mississippian. The stratigraphic data suggest that reverse motion along the Parsons Pond and Long Range faults occurred between post-Early Devonian (Emsian) and Early Mississippian (Visean) time. The timing of kinematic events along the Northern Peninsula between Bonne Bay and Portland Creek Pond is similar to the tectonic evolution of southwestern Newfoundland highlighted in Lines 1, 2, and 3.

Coney Arm region

Cambrian-Ordovician carbonate and clastic successions are exposed along the eastern limb of the Long Range massif (Figure 3.4). Several previous studies along the eastern Humber zone demonstrate that Cambrian-Ordovician clastic and carbonate successions are nearly identical to the early Paleozoic platform rocks in the western external domain exposed along the Gulf of St. Lawrence (Knight, 1987; 1992; 1994; Kerr and Knight, 2004). On the western shore of White Bay, deformed Cambrian-Ordovician platform rocks form a narrow belt approximately 50 km long and 1 to 2 km wide (Figure 3.29) (Kerr and Knight, 2004). These rocks represent the easternmost exposed shallow-marine clastic and carbonate passive-margin deposits that autochthonously overlie Precambrian basement in the Long Range massif. The presence of this narrow belt of early Paleozoic rocks and other isolated outliers like it along the eastern flank of the Long Range massif (e.g., Coleman-Sadd et al., 1990) implies that the entire massif was previously covered by a broad Cambrian-Ordovician clastic and carbonate platform. Any regional palinspastic restoration of the early Paleozoic St. Lawrence promontory across the Northern Peninsula must take into account the fact that the entire across-strike width of the Long Range massif was previously overlain by rocks corresponding to the Labrador Group (Unit 1) and the carbonate platform (Unit 2).

The most complete section of early Paleozoic shelf rocks is along the Great Coney Arm of White Bay (Figure 3.29). There, Paleozoic rocks are divided into an autochthonous footwall succession and the structurally overlying Coney Arm allochthon (informal). The autochthonous succession consists of the Bradore Formation, which lies

unconformably on Mesoproterozoic crystalline basement in the Long Range massif, and the overlying Forteau Formation, which has been structurally thickened by deformation related to the emplacement of the Coney Arm allochthon (Kerr and Knight, 2004). The Coney Arm allochthon contains a nearly complete section of the early Paleozoic passive-margin from the upper Labrador Group (i.e., Hawkes Bay Formation) through the Table Head Group. The Goose Tickle Group and overlying Upper Ordovician-Devonian rocks (Units 3-5) are not preserved.

Paleozoic rocks in the Coney Arm allochthon were emplaced onto the autochthonous succession along a network of cross-cutting, west-verging thrust faults. The basal detachment to the shelf allochthon is the Cobbler Head fault, which follows the contact between the Forteau and Hawkes Bay Formations of the Labrador Group and along much of the trace of the fault (Figure 3.29, also Line 7, Plate 3.2). Approximately 1 km west of Aspy Cove, however, the Cobbler Head fault cuts abruptly up section southwestward through the Port au Port Group into the upper St. George Group, suggesting a lateral ramp geometry. Geologic mapping west of Aspy Cove also reveals that carbonates of the Port au Port Group and St. George Group have been thrust directly onto Precambrian granites in the Long Range massif (Kerr and Knight, 2004), implying the Cobbler Head fault cuts down section into the footwall at this location. Foliations in intensely sheared shale and phyllite of the Forteau Formation in the underlying autochthonous footwall succession indicate the Cobbler Head fault dips between 25º and 50º southeast; mineral lineations and asymmetric foliations display top-to-the-northwest directed sense-of-shear (Kerr and Knight, 2004).

The Aspy Cove fault truncates the Cobbler Head fault approximately 2.5 km southwest of Great Coney Arm (Figure 3.29) (Kerr and Knight, 2004). Geologic mapping and well cuttings indicate the Aspy Cove fault dips southeast at 45º and thrusts younger strata of the upper Port au Port Group and lower St. George Group over older, autochthonous strata in the Labrador Group (Kerr, 2004). The informally designated Beaver Dam fault located in the hanging wall of the Aspy Cove fault (e.g., Kerr, 2004; Kerr and Knight, 2004) is here interpreted as a structural duplication of the Cobbler Cove fault by the Aspy Cove fault (Line 7, Plate 3.2). Both the Cobbler Cove and Aspy Cove

faults are truncated by the steep dipping Doucers Valley fault system (Kerr and Knight, 2004).

Palinspastic restoration of the Coney Arm allochthon requires a conjectural stratigraphic and structural geometry for Paleozoic shelf rock that extends east of the present trace of the Doucers Valley fault zone (Plate 3.2). In palinspastic reconstructions, one of the kinematic requirements of a restored cross section is that thrust faults must cut upsection in the direction of fault propagation (e.g., Boyer and Elliot, 1982). The only situation in which a thrust fault can cut down section in the direction of transport is where the footwall stratigraphy has been previously deformed. Structural mapping along the Cobbler Head and Aspy Cove faults indicates that both faults thrust younger strata over older strata (Kerr and Knight, 2004), which requires that both thrust faults cut down section in the direction of transport. These observations indicate that the early Paleozoic stratigraphy and underlying crystalline basement at Coney Arm were deformed prior to thrusting of the Cobbler Head fault. Tilting the autochthonous early Paleozoic strata ~40º southeast prior to thrust faulting appears to fulfill the kinematic requirements for palinspastically restoring the Cobbler Head and Aspy Cove faults in the Coney Arm allochthon.

A sequence of kinematic events elucidates the timing of fault movement in the Coney Arm allochthon. The first deformational event is tilting of Paleozoic strata on the eastern flank of the Long Range massif, perhaps related to post-Emsian motion along the Long Range fault. The second kinematic event is thrusting along the Cobbler Cove fault, which cut down in the stratigraphic section in the footwall to emplace Cambrian-Ordovician carbonates over Precambrian basement in the Long Range massif. Following motion on the Cobbler Head fault, the Aspy Cove fault truncated and structurally duplicated the Cobbler Head fault. The final kinematic event is deformation along the Doucers Valley fault, which truncates both the Aspy Cove and Cobbler Head faults. If deformation along the Cobbler Head fault post-dates Emsian time, it is likely that the Cobbler Head, Aspy Cove, and Doucers Valley faults resulted from dextral transpression related to Carboniferous strike-slip tectonics along the Cabot fault system, which trends through White Bay approximately 10 km to the east of Great Coney Arm.

Humber Arm allochthon

The Humber Arm allochthon between Bonne Bay and Portland Creek Pond is restricted to the coastal zone west of the Long Range massif (Figure 3.25) (Williams and Cawood, 1989). In this region, strata of the Humber Arm allochthon include the Cow Head Group and overlying synorogenic flysch of the Lower Head Group (James and Stevens, 1986). These units are in an imbricated stack of west-verging thrust slices that do not contain any significant amounts of intervening mélange (Waldron and Stockmal, 1994).

The Cow Head Group (Schubert and Dunbar, 1934; James and Stevens, 1986; Lavoie et al., 2003) consists of limestone breccia interstratified with ribbon limestone, calcarenite, and shale (Figure 3.30). Limestone conglomerates are coarsest and thickest along the western shoreline of the Northern Peninsula (James and Stevens, 1986). To the east, conglomeratic facies are less prominent and individual limestone beds are thinner and contain clasts of smaller sizes. The easternmost outcrops of Cow Head Group are dominated by gray-green shale and thin, platy limestone. The entire sequence appears to indicate a west to east deepening of the margin. The sedimentary rocks exposed in the Cow Head Group range in age from late-Middle Cambrian to late-Early Ordovician; pre-late Middle Cambrian synrift and post-rift slope stratigraphy is absent in this part of the allochthon (James and Stevens, 1986). Measured sections indicate the thickness of the Cow Head Group ranges between 300 and 500 m with a maximum around 700 m (James and Stevens, 1986).

Stratigraphically overlying the Cow Head Group is the Lower Head Formation (James and Stevens, 1986), which consists of interbedded green sandstone and grey-green shale. Sandstone and shale in the Lower Head Formation represent westward influx of synorogenic sediments related to subsidence of the Laurentian margin during the Taconic orogeny (Bradley, 1989). Sparse graptolites from the formation in the map area suggest a latest Arenig to early Llandeilo age (Cawood and Williams, 1986). The top of the formation everywhere is tectonic; however, seismic reflection profiles through the Lower Head Formation, coupled with stratigraphic thicknesses from map pattern distributions in the Humber Arm allochthon, indicate a maximum thickness of 800 m for the Lower Head Formation.

Unlike the Humber Arm allochthon exposed in Corner Brook, the stratigraphy of the various thrust slices has remained largely intact with little to no internal deformation or broken formation. Mélange zones at the structural bases of individual slices are relatively thin. Many of the transported slices are traceable by virtue of the distinctly recognizable sequences in the Cow Head Group and Lower Head Formation (Williams et al., 1986; Cawood et al., 1987). Measured sections, a deep well report (Parsons Pond Well #1), and seismic reflection profiles indicate the stratigraphic thickness of individual thrust slices in the Humber Arm allochthon ranges between 1000 and 1500 m. Thermal maturation studies from rocks in the Cow Head Group yield CAIs of 1.0 to 1.5, which corresponds to burial temperatures around 80º to 100º C (Nowlan and Barnes, 1987). The thermal maturation of rocks exposed in the Humber Arm allochthon north of Bonne Bay indicates the allochthon in this region was neither deeply buried nor covered by obducted ophiolites (Nowland and Barnes, 1987; Williams et al., 1998).

Offshore seismic reflection profiles through Bonne Bay, as well as to the south of Bonne Bay, all image sets of seismic reflector groups that correspond to the autochthonous shelf (Units 1-3), the Humber Arm allochthon, and the Late Ordovician through Early Devonian foreland-basin successions (Units 4 and 5?) (Figure 3.19). In particular, seismic reflectors outline an opaque triangle zone wedged between the underlying Cambrian-Ordovician platform and overlying Anticosti basin deposits, indicating that at least as far north as Bonne Bay, the Humber Arm allochthon has been structurally inserted into a tectonic wedge between the platform and the Anticosti foreland basin (Stockmal et al., 1998). In Hunt Line 90-1, strong reflectors at the top of the Ordovician platform and foreland-basin succession are separated from reflectors corresponding to the HAABD by 100 to 200 ms TWTT (Figure 3.19), suggesting that the tip of the allochthonous wedge was inserted into the Anticosti basin strata above the Goose Tickle Group (Unit 3) – Long Point Group (Unit 4) contact. The very strong reflectors at the base of the Upper Ordovician section, which correlate to the Lourdes Limestone farther south around Port au Port peninsula, are absent in this seismic profile.

Onshore seismic lines traverse the width of the Humber Arm allochthon, as well as cross the Parsons Pond and Long Range faults (Figure 3.25). The profiles across the exposed allochthon, in general, contain two sets of seismic reflector groups. A lower

group of strong, continuous, subparallel and relatively flat reflectors is interpreted to represent the autochthonous Cambrian-Ordovician rift and platform succession (Units 1-3) (Figures 3.27 and 3.28). An upper group of transparent to strong reflectors demonstrates a system of discrete east-dipping fault surfaces that project to surface outcrop of thrust faults mapped in the allochthon (e.g., Williams et al., 1986; Cawood et al., 1987). The east-dipping seismic reflectors truncate continuous, layered reflectors in the subsurface, which have been folded into ramp anticlines (Figure 3.28). The upper group of seismic reflectors is here interpreted to represent imbricate thrust slices of the Humber Arm allochthon; folded and truncated layered reflectors correspond to interstratified limestone conglomerate and shale of the Cow Head Group. Zones of seismic opacity above strong layered reflectors in individuate slices are interpreted to correspond to the Lower Head Formation. The seismic data demonstrate that several imbricate thrust slices are buried at depth beneath overlying thrust slices mapped at the surface.

Previously, Stockmal et al. (1998) interpreted the very strong, imbricated layered reflectors in Line 92-072 just above the platform section (around 0.5 to 0.8 TWTT) to correspond to transported slices of the Lourdes Limestone, implying that the HAABD entrained part of the Upper Ordovician succession. Conversely, Parsons Pond Well #1, which was drilled vertically into the ramp antiform imaged at 0.5 TWTT at CDP-520 on Line 92-072 (Figure 3.28) intersected approximately 430 m of ribbon limestone, limestone conglomerate, and shale corresponding to the Cow Head Group (Brooker, 2004). The results from Parsons Pond Well #1 suggest that the HAABD only carries strata of the Cow Head Group and Lower Head Formation in the hanging wall.

The overall structural geometry of the Humber Arm allochthon north of Bonne Bay is that of a foreland propagating, hinterland-dipping, duplex system. The roof thrust of the allochthon (i.e., Tea Cove thrust) is interpreted to comprise the roof to the duplex, which has been subsequently eroded. Toward the foreland thrust slices, the roof thrust steps downward. Line-length balancing the Humber Arm allochthon produces an average net internal shortening of approximately 63%. Restoration of the Cambrian-Ordovician platform across the Long Range Mountains in Line 7 allows for the along-strike extrapolation of the restored shelf edge to Lines 5 and 6 (Plate 3.2). When the total width

of the shelf as presented in Line 7 is taken into consideration, the average westward translation of the Humber Arm allochthon from the restored shelf edge to the current position in Lines 5 through 7 is approximately 90 km.

Summary

North of Bonne Bay the Humber Arm allochthon is mapped as a classic foreland-directed imbricate thrust system that crops out west of uplifted Proterozoic basement in the prominent Long Range massif. Shelf rocks are exposed primarily as small west-facing slivers uplifted in the hanging wall of the Parsons Pond fault. Offshore seismic data suggest the Humber Arm allochthon tectonic wedge extends as far north as Parsons Pond on the Northern Peninsula and allows inference of the approximate offshore trace of the Tea Cove thrust and projection of the tip of the tectonic wedge. Onshore seismic lines display a set of continuous flat-lying reflectors beneath the allochthon, consistent with the lower Paleozoic shelf. These seismic reflectors are truncated at depth by moderately dipping, thick-skinned faults that can be traced to surface exposure of the Parsons Pond and Long Range faults. The Parsons Pond and Long Range faults also deform slope deposits in the Humber Arm allochthon. A thick succession of Goose Tickle shale in the hanging wall of the Parsons Pond fault north of Portland Creek Pond indicates that the Parsons Pond fault experienced an early episode of normal motion during the Middle Ordovician before becoming inverted as a late thick-skinned thrust.

Emplacement of the Humber Arm allochthon to the current structural position must have occurred after deposition of Early Devonian strata in the Anticosti foreland basin. From restored sections across the Long Range massif, total westward displacement of the allochthon has an estimated minimum transport distance of 90 km. Final emplacement of the allochthon west of the Long Range massif deformed strata in the Cow Head succession into a hinterland-dipping, imbricate duplex system. Total shortening in the allochthon averages around 63%. After post-Early Devonian emplacement of the allochthon, the Parsons Pond and Long Range faults were structurally inverted by a compressional tectonic event. Flat lying middle-Early Mississippian strata in the Deer Lake basin unconformably overlie up-thrown crystalline basement on the southeastern side of the Long Range massif, suggesting an upper limit to

the timing of motion along the Long Range fault. Palinspastic restoration of the Long Range fault suggests a maximum westward displacement of 10 km, which is agreement with the interpretation of Williams et al. (1986). A seismic reflection profile across the Long Range fault fails to demonstrate that the fault flattens at depth, indicating the "highly allochthonous" model of Waldron and Stockmal (1994) is untenable. The succession of kinematic events expressed in Lines 5 through 7 are a close match to the interpreted tectonic events in southwestern Newfoundland, implying along-strike continuity in the structural and tectonic evolution of the St. Lawrence promontory.

3.5.4 Northern Peninsula; Port Saunders (Lines 8 and 9)

Lines 8 and 9 trend from the Gulf of St. Lawrence southeast across parautochthonous Laurentian margin strata on the Northern Peninsula and into exposed crystalline basement of the Long Range massif (Figure 3.11). South of Portland Creek Pond, the Humber Arm allochthon pinches out against the Parsons Pond fault; nowhere on the Northern Peninsula north of Portland Creek Pond is there any evidence of the Humber Arm allochthon. South of Hawkes Bay, the Appalachian structural front, manifest as the Port Saunders fault, makes landfall and trends north-northeast across the Northern Peninsula where it extends off the north shore of the peninsula into the Strait of Belle Isle (Figure 3.4). The purpose of Lines 8 and 9 is to interpret the structural geology of parautochthonous shelf and basement on the Northern Peninsula and calculate the magnitude of displacement across the Long Range fault system and the exposed structural front.

Stratigraphic Framework

Rocks in the region of Lines 8 and 9 are part of a parautochthonous and autochthonous early Paleozoic platform succession that extends from the northern tip of the Northern Peninsula south to Portland Creek Pond along the western side of the Northern Peninsula (Figure 3.31). The variably deformed Cambrian-Ordovician platform succession lies west of the Long Range massif, an uplifted fault block of Mesoproterozoic crystalline basement (Williams, 1995). The region is characterized by

gently dipping, westward younging strata broken into lensoid northeast-trending blocks by a system of anstomosing, northeast-striking, high-angle faults.

Rocks along Lines 8 and 9 are limited to Mesoproterozoic basement, the Labrador Group (Unit 1), and the Cambrian-Ordovician carbonate passive-margin shelf (Unit 2). There is no preserved outcrop of the overlying Goose Tickle Group (Unit 3) or the Late Ordovician through Devonian section (Units 4 and 5) along the western coastal region of the Northern Peninsula in the area of the cross sections.

Mesoproterozoic crystalline basement is exposed chiefly in the Long Range massif. Several smaller, isolated slivers of uplifted crystalline basement are exposed west of the Long Range massif near Ten Mile Lake and the Highlands of St. John (Figure 3.31). Unconformably overlying the basement are clastic deposits of the Labrador Group, which in the lines of cross section, primarily underlies mountainous terrain of the Highlands of St. John. Several smaller outliers sit piggy-back on the Long Range massif east of the Lady Worchester Brook fault (Knight, 1991). The Labrador Group has a reported thickness of 420 m in this part of the Northern Peninsula (Knight, 1991).

Overlying the Labrador Group are Middle Cambrian through late-Early Ordovician carbonate shelf deposits of the Port au Port, St. George, and Table Head Groups. The Port au Port Group is exposed primarily east of Hawkes Bay, where it has a reported thickness of 510 m (Knight, 1991). The St. George Group comprises most of the western coastal exposures along the Northern Peninsula. Along Lines 8 and 9, it has a measured thickness of 372 m (Knight, 1991). The Table Head Group is the youngest exposed stratigraphic element of the St. Lawrence promontory west of the Long Range inlier. The reported thickness of the Table Head Group around Hawkes Bay is 250 m (Knight, 1991), which is considerably thicker than sections of the Table Head Group exposed farther south.

Structural Framework

Parautochthonous carbonate rocks are, generally, very shallowly dipping and gently folded except close to faults where they display very steep to overturned dips (Knight, 1991). Faults, which have very steep dips and trend predominantly northeast, break up the lateral continuity of the platform stratigraphy. In a broad sense, the region

can be divided into three parts: 1) an autochthonous zone that lies to the west of the Appalachian structural front manifest in the Port Saunders and Ten Mile Lake faults; 2) a parautochthonous zone bounded between the structural front on the west and the Lady Worchester Brook fault on the east; and 3) the Long Range massif which is separated on the east from downdropped Paleozoic strata on the west by the Lady Worchester Brook fault (Figure 3.31). To date, there are no available seismic surveys or deep wells available from this part of the Northern Peninsula. Therefore, depths to basement in the autochthonous and parautochthous zones of Lines 8 and 9 are inferred from measured formation thicknesses provided by Knight (1991).

The autochthonous zone is marked by flat-lying carbonates of the upper St. George and Table Head Groups that lie west of the Port Saunders and Ten Mile Lake faults. Most rocks of the autochthonous zone are located offshore beneath the Gulf of St. Lawrence or on small isolated islands; however, a large tract of autochthonous carbonates crops out on the mainland northeast of Port Saunders on Port au Choix peninsula (Knight, 1991). There, the Ordovician carbonate platform is broken in several places by steeply dipping to vertical faults; however, offsets across these faults are relatively minor, ranging between 10 and 50 m (Line 8, Plate 3.2).

The Port Saunders fault is the westernmost fault system that displays significant offset of platform stratigraphy (Line 8, Plate 3.2). The fault is very steeply dipping and trends northeast through the Town of Port Saunders along the western coastal region of the Northern Peninsula. South of Port Saunders, the fault extends offshore and is interpreted to strike roughly parallel to the western coastline of Newfoundland (Figure 3.31). A previous study has suggested that the Port Saunders fault extends as far south as Portland Creek Pond, where it re-emerges onshore as the Parsons Pond fault (Stockmal et al., 1998). Offset of stratigraphic markers across the Port Saunders fault is consistent with reverse displacement (Knight, 1991). While several minor faults are mapped to the west of the Port Saunders fault (Line 8, Plate 3.2), those faults display very minor offsets (< 50 m), whereas the Port Saunders fault displays a much greater magnitude of vertical throw (~200 m). Therefore, the Port Saunders fault is interpreted to represent the structural front of the Appalachian orogen in northwestern Newfoundland.

The Big East River fault, east of the Port Saunders fault, is a steep-dipping to vertical strike-slip fault that trends north-northeast (Line 8; Plate 3.2). The fault juxtaposes Early Cambrian strata of the Labrador Group on the east against Late Cambrian carbonates in the Port au Port Group on the west, indicating a throw of approximately 400 m on the fault. The Port Saunders and Big East River faults merge west of the Highlands of St. John to form the Ten Mile Lake fault.

The greatest vertical displacement across any fault in the region is along the Ten Mile Lake fault (Line 9, Plate 3.2), which forms the west facing scarp of the Highlands of St. John, an impressive upstanding plateau underlain by flat-lying rocks of the Labrador Group (Figure 3.32). The fault dips moderately to steeply southeast and uplifts Mesoproterozoic basement and the overlying Labrador Group, juxtaposing them against Ordovician carbonates of the St. George Group in the footwall (Knight, 1991). Total vertical throw across the Ten Mile Lake fault is approximately 1300 m, indicating that reverse offset along the Appalachian structural front increases northeast from Line 8 to Line 9.

The Torrent River fault is part of a major west-dipping fault system (Knight, 1991) that is interpreted here to merge with the Port Saunders fault at depth in the crust (Line 8, Plate 3.2). The fault trends northeast and dips moderately to steeply northwest (Knight, 1991). Outcrop of the Torrent River fault is marked by overturned and brecciated bedding in the hanging wall, which thrusts strata in upper Labrador Group onto the Port au Port Group, indicating a reverse offset of 350 m.

The Lady Worchester Brook fault is part of the Long Range Boundary fault system that uplifts Precambrian crystalline basement in the Long Range massif (Lines 8 and 9, Plate 3.2). It strikes north-northeast and dips steeply southeast (Knight, 1991). North of where it merges with the Torrent River fault, the Lady Worchester Brook fault is a complex system of anastomosing splays that bifurcate and remerge with the main fault at irregular distances (Knight, 1991). Similarities in rock type and facies between exposure of the Labrador Group east of the Lady Worchester Brook fault with exposures of the Labrador Group west of the fault suggests that total displacement along the Long Range Boundary fault system on the Northern Peninsula was minimal. East of Port Saunders, the Lady Worchester Brook fault emplaces strata in the lower Labrador Group

(i.e., Forteau and Bradore Formations), which conformably overlies crystalline basement in the Long Range massif, over strata in the upper Labrador Group (i.e., Hawkes Bay Formation), indicating vertical offset of approximately 150 m. Projection of the basement-Labrador Group contact northward along strike from Line 8 indicates that, along Line 9, the Lady Worchester Brook fault has around 400 m of reverse offset.

Summary

Rocks exposed along the western coastal lowlands and the Long Range Mountains of the Northern Peninsula around the area of Port Saunders comprise only Laurentian crystalline basement and the overlying Cambrian-Ordovician rift and carbonate platform. These rocks are broken by a set of steep, northeast-trending reverse faults and strike-slip faults (Knight, 1991). The Appalachian structural front (e.g., Stockmal and Waldron, 1993) in this area of the western Newfoundland is the Port Saunders-Ten Mile Lake fault system, consisting of west-verging thick-skinned reverse faults with offsets between 200 and 1300 m. The offshore strike of the Port Saunders fault suggests that it may continue to the Parsons Pond fault farther south around Portland Creek Pond. The Long Range Boundary fault system is expressed as the Lady Worchester Brook fault, which is a west-verging reverse fault system that displays between 150 and 400 m of total reverse offset. This contrasts sharply with the 10 km of reverse offset recorded along the Long Range fault to the south between Bonne Bay and Portland Creek Pond, indicating that net reverse offset along the Long Range Boundary fault system decreases by an order of magnitude from south to north.

The timing of motion along the system of steep, northeast-trending fault systems can only be a matter of speculation. If the Port Saunders-Ten Mile Lake fault is the northern extension of the Parsons Pond fault (as suggested by Stockmal et al., 1998), then reverse motion along these faults commenced between Middle Devonian and late-Early Mississippian time. The Lady Worchester Brook fault is the northern extension of the Long Range thrust, which also was activated between the Middle Devonian and late-Early Mississippian. On the basis of the inferred age of motion along these two major fault systems, it is tempting to speculate that motion and deformation along the Big East River fault and Torrent River fault occurred over the same time interval. Alternatively,

the Big East River fault, which is interpreted as a steep to vertical strike-slip fault, may be related to Carboniferous strike-slip tectonics, which affect most of the geology in western Newfoundland.

3.6 SUBSIDENCE HISTORY

A tectonic subsidence curve is a graph of the tectonic component of subsidence in a sedimentary basin as a function of time. Tectonic subsidence along a continental margin is controlled by cooling and contracting of heated crust and lithosphere, which when plotted against time displays a pattern of exponential decay (McKenzie, 1978; Bond et al., 1984). Tectonic subsidence curves for sedimentary basins are constructed by quantitatively back-stripping sedimentary layers of a measured thickness and age from the basin and by removing the effects of lithification (compaction and cementation) from the fully lithified sedimentary section (Sleep, 1971; Steckler and Watts, 1978). The parameters for the degree of compaction and lithificiation within different rock types (e.g., porosity, constant c (1/km), average sediment grain density) used in this exercise are from Schmoker and Halley (1982). The final result of back-stripping sedimentary layers and removing the effects of sedimentary compaction and lithification is the removal of basin subsidence caused by sedimentary loading. In this procedure, water depth corrections were ignored. A 3000 m section of sandstone was artificially added to the top of each stratigraphic section to ensure that corrections for complete compaction and lithification of all sedimentary rock layers in the basin were taken into account.

Comparison of the subsidence histories from important locations on the St. Lawrence promontory illustrates a range of responses to synrift and post-rift thermal subsidence along the eastern Laurentian rifted margin. Thicknesses of synrift, passive-margin, and foreland-basin stratigraphy provide the critical information for determining rates of subsidence along segments of the margin interpreted to have developed in upper- and lower-plate régimes. The subsidence history for the St. Lawrence promontory is presented here with the use of profiles of the depth to top of crystalline basement as a function of time (Figure 3.33).

Subsidence curves in Figure 3.33A and 3.33B represent the subsidence history of the Laurentian platform on the Northern Peninsula and in southwestern Newfoundland,

respectively. The exposed stratigraphic sections and unconformable contacts with basement in both places are well exposed and documented (Knight, 1991; 2003; Stockmal and Waldron, 1993; Knight and Boyce, 2000; Cooper et al., 2001). The two regions selected for comparison are at sites approximately equidistant (~65-75 km) from the palinspastically restored shelf edge. The subsidence curve for the platform on the Northern Peninsula (Figure 3.33A) indicates continental breakup and initiation of passive-margin thermal subsidence during the Early Cambrian, which is in close agreement with the stratigraphic transition from rift to passive margin (e.g., Williams and Hiscott, 1987).

The two curves represented in the southwestern Newfoundland profile (Figure 3.33B) represent a section measured in the Indian Head Range north of Stephenville (gray line, open symbols) (Knight and Boyce, 2000; Knight, 2003) and stratigraphic and well data from Port au Port peninsula (black line, closed symbols) (data from Cooper et al., 2001). The two curves are strikingly similar to the subsidence profile from the Northern Peninsula. Each displays an Early Cambrian transition from rift to passive margin, followed by post-rift thermal subsidence that was terminated during the Middle Ordovician by collision-induced subsidence during the emplacement of the Humber Arm allochthon onto the continental margin. Exponential decay related to passive-margin thermal subsidence during the Middle Cambrian to Middle Ordovician is nearly identical in all three curves (Figures 3.33A and 3.33B), indicating similar passive-margin thermal régimes in those two regions of the St. Lawrence promontory.

Backstripping of two stratigraphic sections from the Humber Arm allochthon produces basement subsidence curves that are unique with respect to one another (Figure 3.33C and 3.33D). Both sections are truncated at the base by the basal detachment in the Humber Arm allochthon. Thus, the thickness and rock type of the initial deposits above basement are unknown.

The section from the Humber Arm allochthon at Cow Head (Figure 3.33C) is based on stratigraphic data and measured sections by James and Stevens (1986). Stratigraphy exposed within the Humber Arm allochthon in the region of Cow Head includes a dynamic, passive-margin and foreland-basin, proximal slope succession that records an upward progression of sealevel megacyclic events during the early Paleozoic

(James et al., 1989; Lavoie et al., 2003). The subsidence curve produced from the available stratigraphic data is typical of passive-margin thermal subsidence. The stratigraphic sections at Cow Head are incomplete at the base; however, projection of the profile backward in time to zero subsidence produces a result that is compatible with continental breakup at ca. 530 Ma. This age of breakup is in agreement with other studies that indicate breakup and onset of a passive continental margin on the St. Lawrence promontory during the Early Cambrian (Bond et al., 1984; Williams and Hiscott, 1987; Cawood et al., 2001).

The Humber Arm allochthon around Corner Brook (Figure 3.33D) contains some of the oldest Laurentian margin stratigraphy exposed in western Newfoundland. Rocks in this part of the promontory consist of synrift and distal passive-margin slope facies (Waldron et al., 2003). The section for the Corner Brook profile is based on a combination of measured stratigraphic sections from the Humber Arm allochthon (Botsford, 1988; Palmer et al., 2001), as well as palinspastic thicknesses from the restored section generated in this study. Like at Cow Head, the stratigraphic base of the Corner Brook section is unexposed. Backward projection of the profile through a rift to drift transition at 530 Ma indicates initiation of continental rifting at ca. 560 Ma, which is substantially older than the time of initial continental rifting in the other profiles. The rate of synrift subsidence and the initial rate of post-rift passive-margin thermal subsidence are also substantially greater than the other profiles. The subsidence profiles for the Humber Arm allochthon around Corner Brook does display some similarities with the other profiles in that they all show a relative exponential decrease in post-breakup subsidence until the time of collision-induced subsidence related to the Taconic orogeny. Thus, following the more rapid synrift and initial post-rift subsidence in the Corner Brook region, the subsidence rates for the Middle Cambrian through Early Ordovician passive margin in the Humber Arm allochthon and the Laurentian platform are similar.

3.7 TECTONIC EVOLUTION OF THE ST. LAWRENCE PROMONTORY

3.7.1 Structure of the eastern Laurentian rift on the St. Lawrence promontory

Continental extension and rifting along the eastern Laurentian margin is punctuated by initial breakout of Laurentia from Rodinia and opening of the Iapetus

Ocean during the late Neoproterozoic (ca. 570 Ma), followed by rifting of a strand of microcontinents from the eastern margin during the latest Neoproterozoic (ca. 550 Ma) (Thomas and Astini, 1999; Cawood et al., 2001; Waldron and van Staal, 2001; see also Chapter 2). The final stage of continental rifting and break out of microcontinents produced a set of continental promontories and embayments along the eastern margin of Laurentia defined by northeast-striking rift-segments offset by northwest-striking transform faults (Thomas, 1977). Along the margin, Neoproterozoic-Cambrian synrift and early post-rift stratigraphy has been used as a proxy for interpreting the three- and four-dimensional architecture of the eastern Laurentian rift; several proposed hypotheses equate the rifted margin to a low-angle detachment rift system (Thomas, 1993; Cherichetti et al., 1998; Thomas and Astini, 1999; Allen et al., 2009).

The Humber zone of western Newfoundland offers one of the best locations in the northern Appalachians to test this hypothesis on the deformed Laurentian continental margin because, there, basement and overlying Neoproterozoic-Ordovician shelf and slope successions, although deformed, are well exposed and easily accessible. The Early Cambrian in southwestern Newfoundland around Port au Port peninsula and along the Northern Peninsula is marked by thin late-synrift and early post-rift clastic deposits (e.g., Labrador Group) (Figure 3.34). Locally thick, Early Cambrian sections are preserved in narrow, synrift graben, with master faults that dip towards the continental margin (e.g., Round Head fault). Subsidence profiles for the platform in southwestern Newfoundland (Figure 3.33B) and the Northern Peninsula (Figure 3.33A) indicate a delay in post-rift cooling until ~520 Ma. After this time, the rate of post-rift subsidence is consistent with exponential thermal decay along a passive continental margin (e.g., McKenzie, 1978; Bond et al., 1984).

Figure 3.33B shows a slight difference in the initial subsidence recorded in two places in southwestern Newfoundland. The Stephenville section (gray line) is located closer to the edge of continental crust (within ~65 km) and, thus, likely experienced greater thermal uplift during rifting, which resulted in a greater delay in the onset of passive-margin thermal subsidence. The section from Port au Port peninsula is farther inboard from the margin and overlies a synrift graben system (Round Head graben), which accounts for the greater degree of Early Cambrian syn- and post-rift subsidence.

Slope rocks in the Humber Arm allochthon north of Bonne Bay also appear to record a delay in the onset of passive-margin thermal subsidence (Figure 3.33C), relative to rocks exposed in the allochthon near Humber Arm. Although the stratigraphic base of the Cow Head Group is unexposed, linear projection of the subsidence curve back to zero subsidence results in an age of breakup around 530 Ma, which is consistent with breakup and passive-margin thermal subsidence recorded in the platform rocks on the Northern Peninsula (Figure 3.33A).

Palinspastic restoration of the Early Cambrian slope along the southwestern Newfoundland and Northern Peninsula segments of the margin is impossible because Early Cambrian sedimentary rocks are not exposed in the Humber Arm allochthon along those parts of the promontory (Figure 3.34). Palinspastically restored Middle Cambrian through Early Ordovician successions in the allochthon, however, may elucidate the extent of attenuated crust outboard of the platform edge in these two areas of the margin (Figure 3.35). North of Bonne Bay, Lines 5 and 6 (Plate 3.2) indicate that the Humber Arm allochthon has a restored across-strike width between 90 km and 100 km, which requires at least 90 to 100 km of attenuated continental crust to accommodate the Middle Cambrian-Early Ordovician slope deposits expressed in the Cow Head Group. Line 3 in southwestern Newfoundland indicates the width of transitional crust required to accommodate the restored sedimentary deposits in the Humber Arm allochthon, from the leading edge to the trailing edge of the allochthon, is approximately 140 km. The delay in passive-margin thermal subsidence, the thin Early Cambrian rift stratigraphy, the rift-graben faults that dip toward the margin, and the width of transitional crust between 90 and 140 km all indicate that the St. Lawrence promontory in southwestern Newfoundland and along the Northern Peninsula was an upper-plate margin in a low-angle detachment system.

In the Humber Arm allochthon around Humber Arm, the basal, coarse, red sandstones of the Summerside Formation represent synrift accumulations, which were probably deposited into rift basins associated with large-scale basement faults. Metaclastic and metaconglomerate assemblages in the Corner Brook Lake terrane also correspond to synrift deposition on eroded crystalline basement. The overlying Irishtown Formation and Northern Head Group in the allochthon, along with the Breeches Pond

Formation in the Corner Brook Lake terrane, comprise a transition from rift to passive margin along this segment of the St. Lawrence promontory. The Curling (Summerside and Irishtown Formations) and Northern Head Groups document significantly greater subsidence and sediment accumulation than anywhere else along the St. Lawrence promontory, including in southwestern Newfoundland and along the Northern Peninsula as far north as Port au Choix. Initiation of continental rifting from the subsidence curve for strata in the Humber Arm allochthon has a projected age of 560 Ma, which is in agreement with microfossil assemblages in the Summerside Formation (Palmer et al., 2001). This age is between 20 and 30 m.y. older than the initiation of continental rifting indicated by subsidence curves from Port au Port peninsula and along the Northern Peninsula (Figure 3.33).

Synrift sedimentary accumulations in the Humber Arm allochthon and the Corner Brook Lake terrane palinspastically restore well outboard from the trailing edge of the restored continental shelf. Thick accumulations of Neoproterozoic-Early Cambrian deposits highlight two separate sub-basins on the slope; the inboard Corner Brook Lake basin (after the Corner Brook Lake terrane) and the more outboard Curling basin (after deposits in the Curling Group) (Figure 3.34). The thickness of Neoproterozoic-Early Cambrian deposits varies across strike; the deepest parts of the two basins (i.e., ~2000 m) are separated by a narrow zone of thinner (~700 m) synrift sedimentary accumulation (Figure 3.34). These relationships are consistent with synrift deposition on a faulted surface in which thick sedimentary accumulations represent deposition on a downthrown basement block, whereas thinner accumulations indicate synrift deposition on uplifted basement. In the palinspastic restoration presented in Line 4, the total width of transitional crust required to accommodate the restored sedimentary deposits in the Humber Arm allochthon, from the leading edge to the trailing edge of the allochthon, is >200 km (Plate 3.1).

The subsidence history, thickness, and the palinspastically restored length of synrift strata along the segment of the margin around Humber Arm are consistent with a lower-plate margin. The contrast between the subsidence history of the Humber Arm allochthon at Humber Arm to the rest of the Humber zone in Figure 3.33 is consistent with the predicted contrasts in basin subsidence history between lower- and upper-plate

segments in a low-angle detachment system. Furthermore, palinspastic restoration of the St. Lawrence promontory highlights an asymmetric distribution of Neoproterozoic and Early Cambrian sedimentary rocks (Figure 3.34), which is best explained by contrasting synrift and post-rift sediment dispersal into upper- and lower-plate margins (i.e., greater sedimentary accumulation on a lower-plate margin, less accumulation on an upper-plate margin). In the context of a low-angle detachment system, the Corner Brook Lake and Curling basins likely represent synrift sedimentary accumulations into two separate rotated half-graben on the lower plate.

One of the more curious aspects of the early Paleozoic sedimentary system preserved in the St. Lawrence promontory is the absence of Early Cambrian slope deposits in the Humber Arm allochthon north of Bonne Bay and on Port au Port peninsula in southwestern Newfoundland. It is unrealistic to assume that the Laurentian slope in southwestern Newfoundland and along the Northern Peninsula experienced no Early Cambrian synrift and early post-rift sedimentary deposition. Nevertheless, the extent, thickness, and facies of Early Cambrian deposits along the slope in these areas must have been such that they precluded structural inclusion into the Humber Arm allochthon as it was thrust onto the margin. We suggest that absence of Early Cambrian slope deposits in these two parts of the Humber zone is the result of limited deposition on thermally expanded crust at the edge of an upper-plate margin. Several workers have suggested that the Blow Me Down Brook Formation, which is currently exposed in the Woods Island thrust sheet, may comprise the stratigraphic base of the succession in the allochthon beneath Port au Port Bay (Ian Knight and Denis Lavoie, pers comm. 2008). If so, it strengthens the argument for an asymmetrically rifted margin in southwestern Newfoundland because the Blow Me Down Brook Formation and equivalents (i.e., Green Sandstone Unit in Quebec) have a maximum thickness of 600 m (e.g., Lavoie et al., 2003), have a late-Early Cambrian age, and are the lateral equivalents of the Hawkes Bay Formation, which is part of the early passive-margin succession.

The boundaries between the upper- and lower-plate segments on the St. Lawrence promontory are expressed as abrupt (<20 km) along-strike discontinuities in shelf and slope stratigraphy, and in lithostratigraphic elements in the internal domain (Figure 3.36). These zones of along-strike transition are here interpreted as transform faults that

separate upper- and lower-plate margins (Figure 3.37). Stratigraphic discontinuities in shelf and slope rocks roughly correspond to sharp, linear, northwest-trending, gradients in Bouguer gravity anomaly maps of western Newfoundland (Figure 3.9). These linear gravity anomalies are interpreted to reflect transform faults at depth in the crust. The two transform faults pertinent to this study are the Serpentine Lake transform and the Bonne Bay transform, which were originally identified by Cawood and Botsford (1991) on the basis of along-strike discontinuity in the passive-margin slope and foreland-basin stratigraphy in western Newfoundland.

The Serpentine Lake transform separates the upper-plate margin in southwestern Newfoundland from the lower-plate margin at Humber Arm to the northeast. The transform is perhaps best expressed as the Corner Brook Lake flexure, where metaclastic rocks of the South Brook Formation thicken abruptly from southwest to northeast (Figure 3.36). Seismic data off the northeast shore of Port au Port peninsula also indicate a deep, narrow, pre-Early Cambrian basin that parallels the inferred trace of the transform. This basin is interpreted to be a result of transtension along the transform while it was active during the Neoproterozoic. In shelf successions, the Serpentine Lake transform is indicated by the northward appearance of the Reluctant Head Formation in the lower Port au Port Group (Figure 3.36).

The Bonne Bay transform was first described by Cawood and Botsford (1991), who noted a contrast in the late Tremadoc (earliest Ordovician) depositional history between the Cow Head and Northern Head Groups in the Humber Arm allochthon across the transform and that the Eagle Island Formation on the south is at least one graptolite zone older than the Lower Head Formation on the north. The Humber Arm allochthon south of Bonne Bay also contains a very thick section of Neoproterozoic-Early Cambrian rift stratigraphy (Curling Group), which is absent in the allochthon north of Bonne Bay (Figure 3.36). The Bonne Bay transform also corresponds to a dramatic change in the structural architecture of the Humber Arm allochthon. South of the Bonne Bay transform, the Humber Arm allochthon has a complex, foreland-dipping duplex geometry with wide zones of chaotic mélange and broken formation (Waldron et al., 2003). North of the Bonne Bay transform, the Humber Arm allochthon is expressed as a simple hinterland-dipping duplex system with little to no structural mélange. The data and observations

indicate that the Bonne Bay transform separates the lower-plate segment of the margin at Humber Arm from an upper-plate segment along the Northern Peninsula.

3.7.2 Paleozoic evolution of the St. Lawrence promontory

The balanced cross sections across the deformed Laurentian margin highlight a complex Paleozoic stratigraphic and structural environment on the St. Lawrence promontory. Diachronous early Paleozoic continental rifting along a low-angle detachment rift system (Figure 3.37) provided the continental framework around which the Cambrian-Ordovician passive-margin shelf and slope were deposited and later deformed. The overall structural regime responsible for deforming rocks in the Humber zone is divided into an early thin-skinned tectonic event involving emplacement of slope deposits in the Humber Arm allochthon onto the margin, followed by a later thick-skinned event that truncated and tectonically shuffled many of the thin-skinned structures. As a result, many previous tectonic interpretations of the Paleozoic evolution of the St. Lawrence promontory accredit the early thin-skinned event to the Middle Ordovician "Taconian" orogeny, whereas later thick-skinned deformation is attributed chiefly to the Devonian "Acadian" orogeny (Hibbard, 1988; Williams and Cawood, 1988; Cawood and Botsford, 1991; Williams, 1995). In contrast, Late Ordovician through Silurian foreland deposits in the Anticosti basin (Sanford, 1993), as well as Silurian magmatism and metamorphism in the eastern internal domain (Dunning et al., 1990; Cawood et al., 1994), suggest a protracted and complex Paleozoic evolution for the St. Lawrence promontory.

The earliest record of tectonism relating to the closure of Iapetus is in the Dunnage zone, east of the Humber zone. There, rocks of the Fleur de Lys Supergroup in the Dashwoods block (Figure 3.4) indicate that elements of Laurentian continental crust interacted with Cambrian oceanic island arcs as early as 490 Ma (Dube et al., 1996; Swinden et al., 1997). Although the Dashwoods block in the Dunnage zone appears to record Late Cambrian arc-continent collision, the most distally derived flysch deposits (Eagle Island Formation) in the Humber Arm allochthon do not indicate collision-induced subsidence of the margin until the middle-Arenigian (ca. 475 Ma). Therefore, several workers have proposed that tectonic relationships in the Dunnage zone reflect

Late Cambrian subduction of an outboard microcontinent into an east-dipping Benioff zone within the closing Iapetus Ocean (Waldron et al., 1998; Waldron and van Staal, 2001; van Staal, 2005). This microcontinent, now manifest as the Dashwoods block in the Dunnage zone, is likely part of the same strand of microcontinents that rifted off the Laurentian margin during the latest Neoproterozoic to open the Humber Seaway (e.g., Cawood et al., 2001).

After end-Cambrian subduction of the Dashwoods microcontinent, the east-dipping Iapetan subduction zone must have stepped back into the Humber Seaway to form a new east-dipping subduction zone (Figure 3.38A). This scenario explains the generation of Early Ordovician oceanic arc terranes and tonalites in the adjacent Dunnage zone, and also the generation of Early Ordovician ophiolites, such as the Bay of Islands ophiolite suite (van Staal, 2005). Thermal maturation studies indicate that only sedimentary rocks in the Humber Arm allochthon between Port au Port and Bonne Bay were covered by obducted ophiolites (e.g., Williams et al., 1998), suggesting a systematic explanation for generation and obduction of ophiolite onto the margin. After subduction stepped back into the Humber Seaway, the rate of slab rollback along the subduction zone axis increased locally on the highly attenuated continental crust along the lower-plate segment of the margin, as opposed to the upper-plate segments of the margin. As a result of enhanced slab rollback along the lower-plate margin, a supra-subduction zone spreading axis would have to form to accommodate extension in the upper plate of the subduction zone as the slab hinge migrated westward toward the continental margin (Figure 3.38A). This explanation also satisfies the geochemistry of the Bay of Islands ophiolites, which indicates they formed in a supra-subduction zone setting (Jenner et al., 1991).

The earliest tectonic event to affect the continental margin on the St. Lawrence promontory was the obduction of the Bay of Islands ophiolites and thin-skinned emplacement of the Humber Arm allochthon onto the edge of continental crust during the Middle Ordovician “Taconic” orogeny (Figure 3.38B). Collision-induced subsidence of the margin generated a Middle Ordovician foreland basin filled by the Goose Tickle Group, the Lower Head Formation, and the Eagle Island Formation. Flexural subsidence of the margin as it was subducted into the Humber Seaway subduction zone also

reactivated older rift graben (i.e., Round Head fault), which produced locally thick carbonate conglomerates (i.e., Cape Cormorant Formation) and Middle Ordovician foreland basin deposits (i.e., Mainland Sandstone). Obduction of ophiolites onto the sediments in the Humber Arm allochthon is constrained to ca. 469 Ma, which is the age of the metamorphic aureole in the Humber Arm Supergroup at the base of the ophiolite suite (Dallmeyer and Williams, 1975). Ophiolites in the Bay of Islands suite were only obducted and incorporated into the Humber Arm allochthon where they were generated along the lower-plate segment of the margin; north of the Bonne Bay transform and south of the Serpentine Lake transform, sedimentary rocks in the Humber Arm allochthon were emplaced onto the margin without overlying ophiolites. Directly beneath the ophiolites, the highest slices of the Humber Arm allochthon were metamorphosed to amphibolite faceis (Fergusson and Cawood, 1995); however, most of the rocks in the Humber Arm Supergroup were incorporated into the advancing allochthon at shallow depth (Waldron, 1985; Waldron et al., 1988).

North of Bonne Bay, sedimentary rocks in the Humber Arm allochthon were broken into imbricate thrust sheets in a hinterland-dipping duplex system. South of Bonne Bay, the Humber Arm allochthon is characterized by chaotic mélange zones and less coherent thrust slices that contain abundant broken formation. In general, older strata in the allochthon south of Bonne Bay occupy the highest structural slices, whereas lower slices predominantly contain the youngest stratigraphy. The overall configuration mimics a foreland-dipping duplex system with a basal detachment that climbs upsection from east to west in the direction of transport. Rift and early slope deposits predominate in the metamorphic terranes of the eastern internal domain (Fleur de Lys Supergroup) (Hibbard, 1988; Cawood et al., 1995). Whereas slope rocks in the Curling basin were incorporated into the Humber Arm allochthon, rocks of the Fleur de Lys Supergroup in the Corner Brook Lake basin were overridden in the Middle Ordovician by the allochthon.

The relatively thin succession in the Middle Ordovician foreland basin (~200 m thick) indicates that the Humber Arm allochthon and overlying ophiolites were emplaced only onto the very leading edge of continental crust on the St. Lawrence promontory. The Late Ordovician Lourdes Limestone, which conformably overlies the Goose Tickle Group in the Anticosti basin, indicates a brief lull in tectonic activity along the St.

Lawrence promontory. Rapid subsidence resumed during the latest Ordovician (Caradoc; ca. 450 Ma) and continued into the Early Silurian (Llandovery; ca. 430 Ma), manifest in the Winterhouse and Misty Point Formations. Late Ordovician-Early Silurian subsidence was great enough to produce a foreland-basin stratigraphic succession that is an order of magnitude thicker than the underlying Middle Ordovician Goose Tickle Group (Cooper et al., 2001). Coeval with the deposition of the uppermost successions in the Long Point Group, rift and passive-margin successions of the Fleur de Lys Supergroup in the Corner Brook Lake basin experienced peak metamorphic conditions between ca. 430 and 425 Ma (Cawood et al., 1994; Cawood and van Gool, 1998). P-T paths from metamorphic mineral assemblages in the Corner Brook Lake terrane indicate that rocks of the Fleur de Lys Supergroup were buried to depths of 30 to 40 km during the Early and Middle Silurian (Cawood and van Gool, 1998). The thickness of the Late Ordovician-Early Silurian foreland-basin succession and the tectonic burial of the Corner Brook Lake basin indicate the Humber Arm allochthon was thrust farther westward onto the continental margin during the Late Ordovician and Early Silurian (Figure 3.38C). Continued westward displacement of the allochthon during the latest Ordovician and Early Silurian can be attributed to compressional deformation related to final closure of the Iapetus Ocean along the Red Indian Line (Figure 3.2) in the Dunnage zone followed by accretion of the Gander zone to the Laurentian margin during the Silurian "Salinic" orogeny (van Staal et al., 1998).

Renewed tectonism along the St. Lawrence promontory during Late Silurian-Early Devonian is recorded by deposition of the Clam Bank and Red Island Road Formations in the Anticosti basin (Cooper et al., 2001). Early Devonian shortening also resulted in westward thrusting of the Corner Brook Lake terrane onto the continental margin, as indicated by post-metamorphic, west-verging thrust faults, one of which yielded an Early Devonian $^{40}Ar/^{39}Ar$ cooling age (e.g., Cawood and van Gool, 1998). Westward displacement of the Corner Brook Lake terrane onto the margin beneath the Humber Arm allochthon also resulted in the incorporation of part of the Cambrian-Ordovician carbonate platform into an imbricate fold-and-thrust belt. As the Early Devonian basal detachment to the Corner Brook Lake terrane propagated onto the platform, it utilized the shale-dominated Reluctant Head Formation as a primary

detachment surface for the carbonate thrust belt. Early Devonian subsidence of the Anticosti basin and compressional deformation related to westward displacement of the eastern internal domain and carbonate thrust belt are here interpreted to result from Early Devonian "Acadian" accretion of the Avalon zone to Laurentia (Williams and Hatcher, 1983; Williams, 1995; van Staal, 2005).

Final emplacement of the Humber Arm allochthon into a tectonic wedge is constrained to post-Early Devonian because Emsian red beds in the Red Island Road Formation near Port au Port peninsula appear slightly deformed by the roof thrust to the tectonic wedge (Tea Cove thrust) (Figure 3.38D). The final major deformational event to affect rocks on the St. Lawrence promontory is manifest as a wholesale thick-skinned reactivation of earlier basement faults, generating several inverted pop-up structures in the shelf succession (Figure 3.38F). The timing of this thick-skinned event is relatively vague; thick-skinned faults and pop-up structures deform both the Humber Arm allochthon and Emsian deposits in the Anticosti basin. Basement massifs and inverted graben uplifted by late thick-skinned faults appear to be unconformably overlain by flat lying Lower Mississippian (Visean) clastic deposits of the Bay St. George and Deer Lake basins. Therefore, thick-skinned deformation is bracketed between post-Early Devonian (Emsian) and Early Mississippian (Visean). As a result, this final event may be related either to late-stage "Acadian" compression as the Avalonian microcontinent was being accreted to the eastern Laurentian margin, or to early "Alleghanian" transpression along the promontory as major Carboniferious strike-slip faults were being activated in the northern Appalachian orogen during the final assembly of Pangaea.

3.8 CONCLUSIONS

Previous interpretations of the three-dimensional architecture of the eastern Laurentian rifted margin along the St. Lawrence promontory are supported by palinspastic restoration of synrift and post-rift stratigraphic successions and compatible subsidence histories. Distinct differences in the palinspastically restored stratigraphy along strike, the structural geometry of deformed marginal successions, and synrift and post-rift subsidence demonstrate an asymmetry to the eastern Laurentian rift that is fully compatible with models for simple-shear, low-angle detachment rift systems. A lower-

plate configuration is demonstrated by the geology and subsidence history for rocks in the area around Humber Arm. This lower-plate margin is bounded along strike by upper-plate margins to the southwest in the Port au Port peninsula/Stephenville area and northeast along the Northern Peninsula as far north as Port au Choix. Upper-plate and lower-plate configurations are separated by abrupt along-strike transitions in palinspastically restored shelf and slope stratigraphy, which are here interpreted to be transform faults.

The results of this investigation also highlight a complex and protracted Paleozoic tectonic evolution for the Appalachian orogen on the St. Lawrence promontory. Palinspastic restoration of deformed stratigraphic successions in the Humber zone resolves the timing and structure of Ordovician, Silurian, Devonian, and Carboniferous deformation that affected the eastern Laurentian margin. Furthermore, the asymmetrical geometry of the rifted continental margin played an important role in the early Paleozoic tectonic evolution of the Appalachian orogen.

Verification of the asymmetrically rifted margin geometry for the St. Lawrence promontory has important implications for the interpreted structural geometry of the eastern Laurentian margin the New York promontory and Quebec embayment. Previous observations suggest that the eastern Laurentian rift along these two segments of the margin reflect a low-angle detachment rift (Allen et al., 2009; see also Chapter 2). Demonstration that the St. Lawrence promontory developed as a result of low-angle detachment continental rifting strongly suggests a consistent structural style along the entire northern Appalachian Laurentian margin. The results of this investigation are also consistent with interpretations of the rifted margin in the southern Appalachian and Ouachita orogen (Thomas, 1993; Thomas and Astini, 1999). Recognition of the low-angle detachment geometry for the entire eastern Laurentian margin provides an orogen-scale logic for the Neoproterozoic-early Paleozoic evolution of eastern Laurentia, which can now be applied to regional models for the tectonic development of the Appalachian orogen.

3.9 ACKNOWLEDGEMENTS

The author acknowledges the Geological Survey of Canada, Geological Society of America, the University of Kentucky, and the University of Kentucky Department of Earth and Environmental Sciences, all of whom funded this research through generous grants. I would like to extend my thanks to Denis Lavoie and Cees van Staal at the Geological Survey of Canada, who initially approached the author with the idea for this investigation and provided constructive ideas and criticism regarding the geology of the Laurentian margin in western Newfoundland. I would also like to thank John W. Waldron, Ian Knight, and Doug Boyce for critical discussions and input regarding the structural geology of western Newfoundland. Finally, the author would like to extend his sincerest thanks to all of the individuals that he had the privilege of meeting during his time spent in the field in western Newfoundland, with special reference to the GCSU Backlot crew. Without your friendship and support, I would not have made it through the summer of 2007.

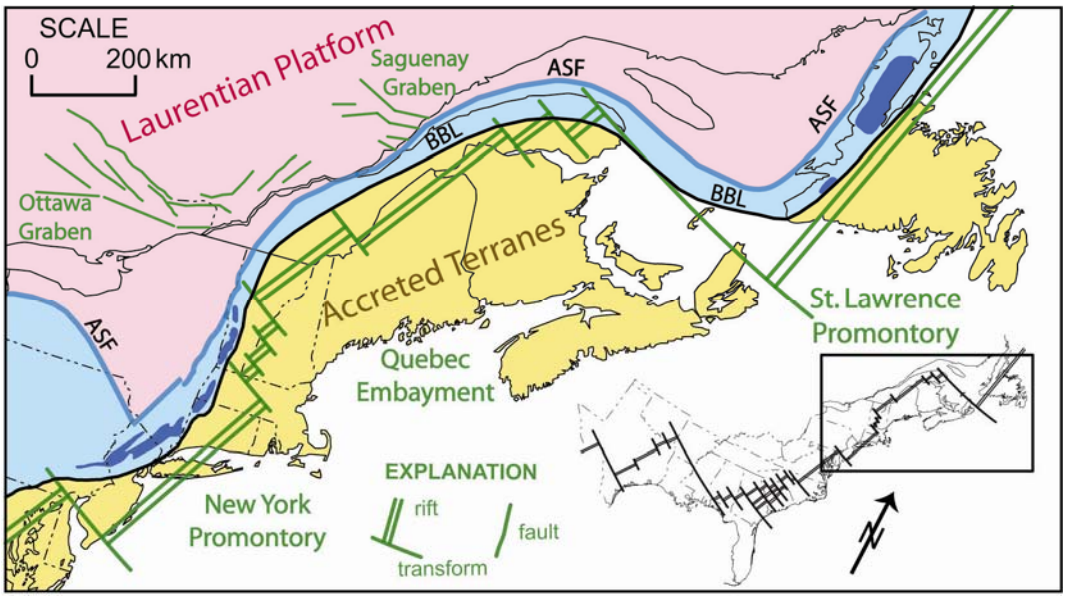

Figure 3.1. Outline map of the Laurentian rifted margin in the northern Appalachians; inset shows southward extent of the rifted margin of Laurentia (Thomas, 1977; 1991). Green lines show rift-related structures. Synrift and post-rift strata (light blue) and external basement massifs (dark blue) are incorporated into the Humber zone between the Appalachian structural front (ASF) and the Baie Verte-Brompton line (BBL).

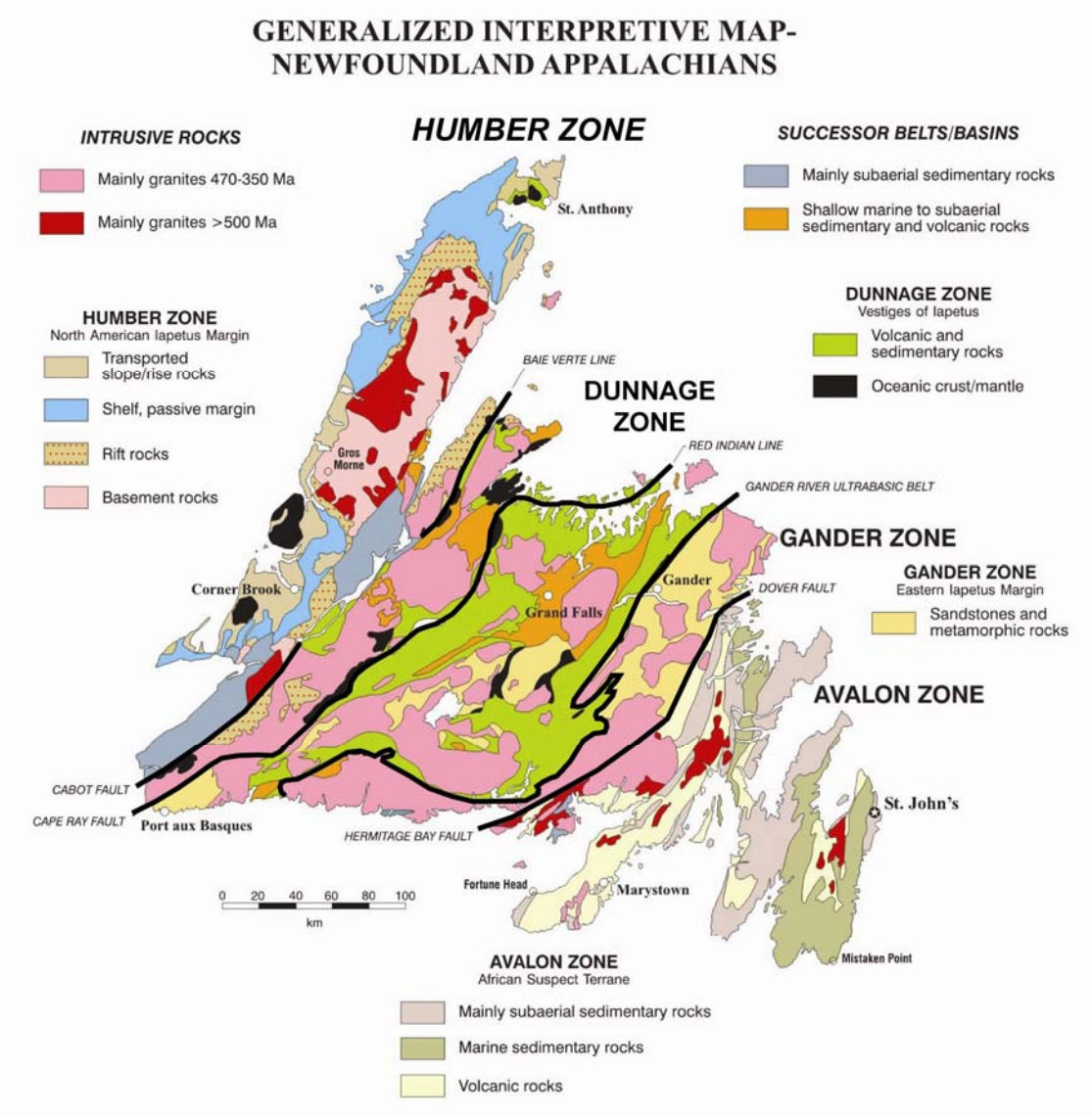

Figure 3.2. Simplified geologic map of the Island of Newfoundland (map from Geological Survey of Canada website); subdivided by early Paleozoic lithotectonic elements (see text).

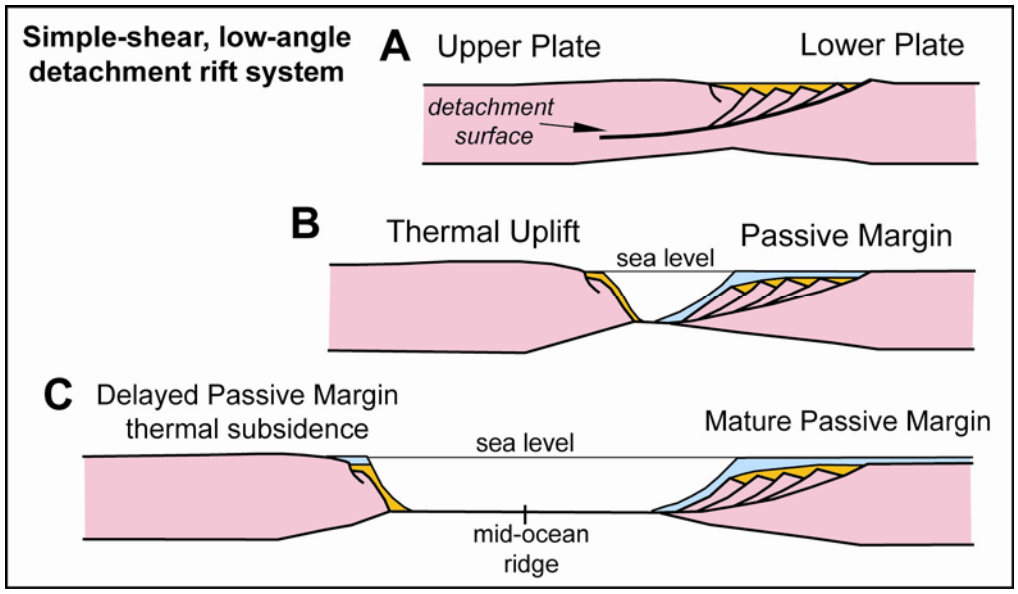

Figure 3.3. Schematic sequential cross sections depicting the interaction of thermal uplift and isostatic subsidence during extension on opposing plates in a simple-shear rift. Orange shows synrift sedimentary accumulations; light blue shows passive margin deposits. (A) Extended crust prior to breakup. Maximum heat flow is at the intersection of the low-angle detachment and the surface. (B) Directly following breakup, isostatic subsidence of thinned crust on the lower plate counteracts thermal uplift, resulting in the establishment of a passive margin (Buck et al., 1988). The upper plate undergoes a delay in thermal subsidence because of proximity of thick continental crust to the spreading ridge. (C) During drift, the upper plate migrates away from the active ridge and undergoes passive-margin thermal subsidence; a passive margin is well developed on the lower plate. Modified after Lister et al. (1986; 1991); Thomas and Astini (1999).

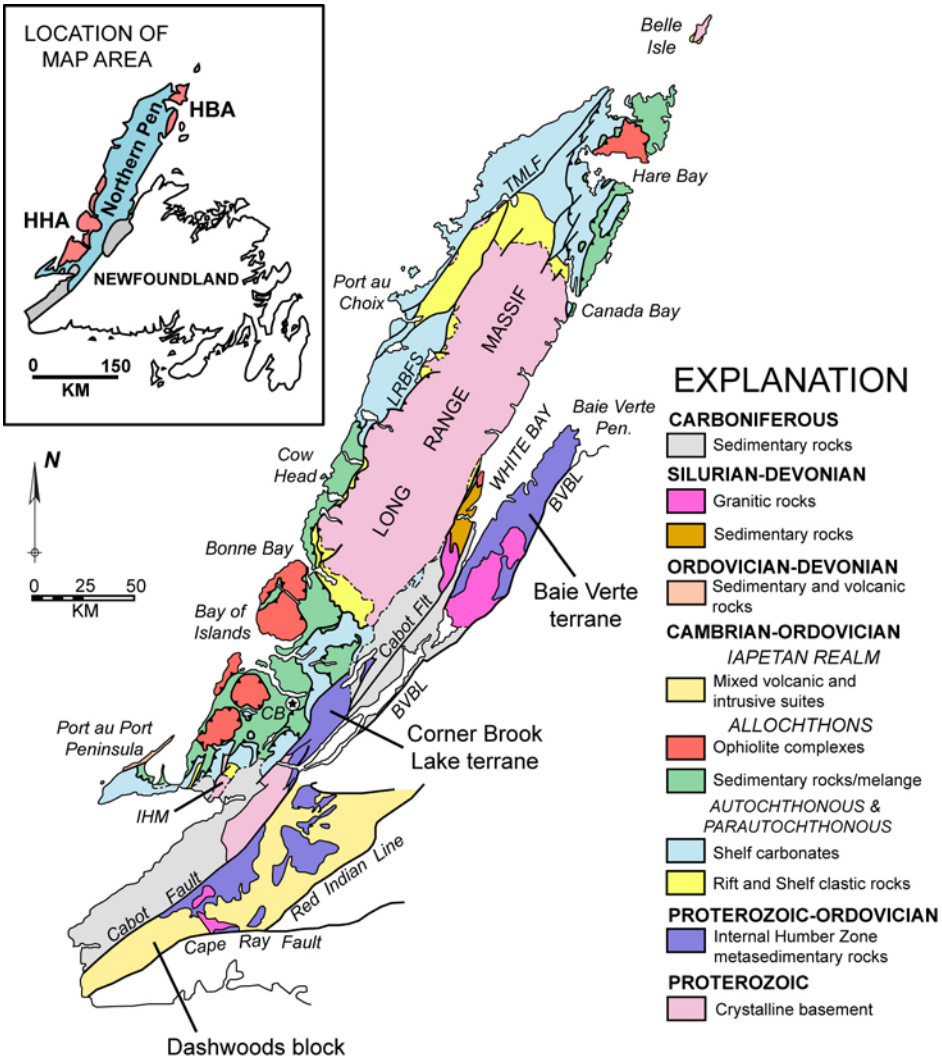

Figure 3.4. Geologic map of western Newfoundland showing the Paleozoic Laurentian margin geology, as well as the locations of the Humber Arm allochthon (HAA), Hare Bay allochthon (HBA), and important internal basement massifs. Geologic data compiled from references in text. Other abbreviations: BVBL = Baie Verte-Brompton Line; CB = Corner Brook; IHM = Indian Head Massif; LRBFS = Long Range boundary fault system; TMLF = Ten Mile Lake fault.

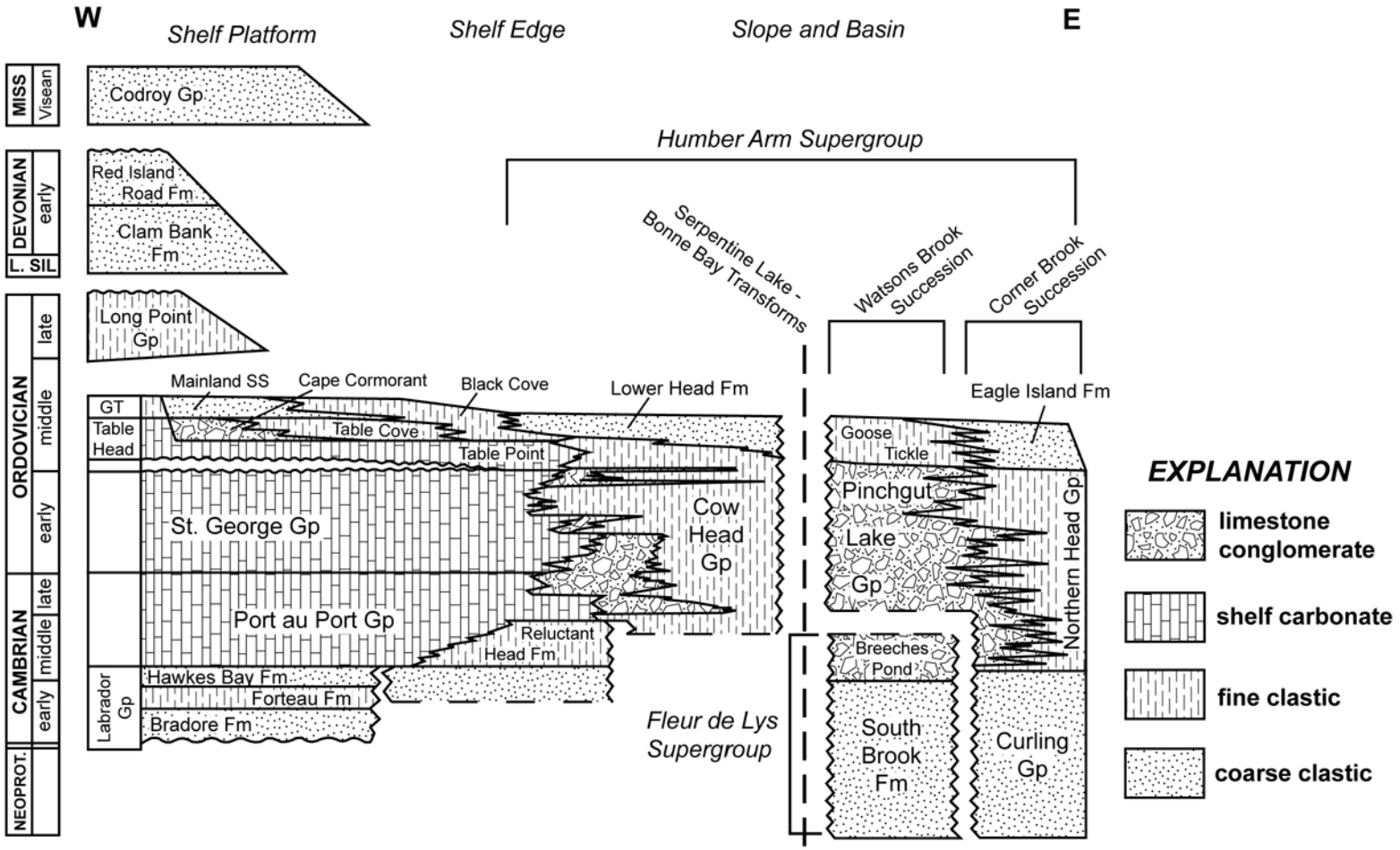

Figure 3.5. Stratigraphic summary diagram of the Humber zone Paleozoic strata. Slope stratigraphy is broken into two subdivisions based on location relative to the Serpentine Lake and Bonne Bay transforms. GT = Goose Tickle Group. Modified after Cooper et al. (2001).

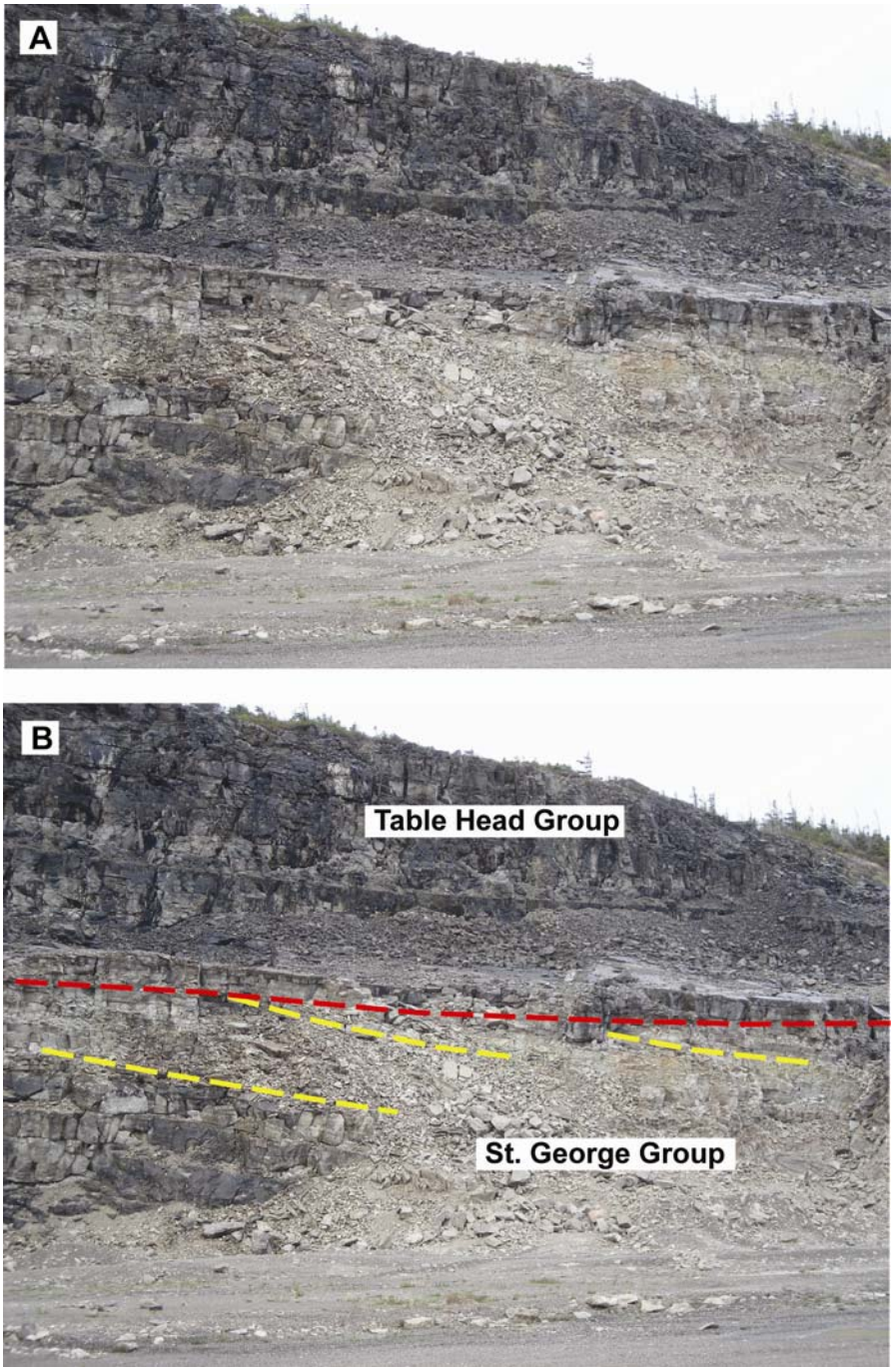

Figure 3.6. Uninterpreted (A) and interpreted (B) photographs of the St. George unconformity at the Aguathuna quarry, Port au Port peninsula. Dark beds in the upper part of the outcrop are limestones in the Table Head Group. Underlying the Table Head Group are cream-colored dolostones of the St. George Group. Note that gently dipping beds in the St. George Group (yellow lines) are truncated by the unconformity (red line).

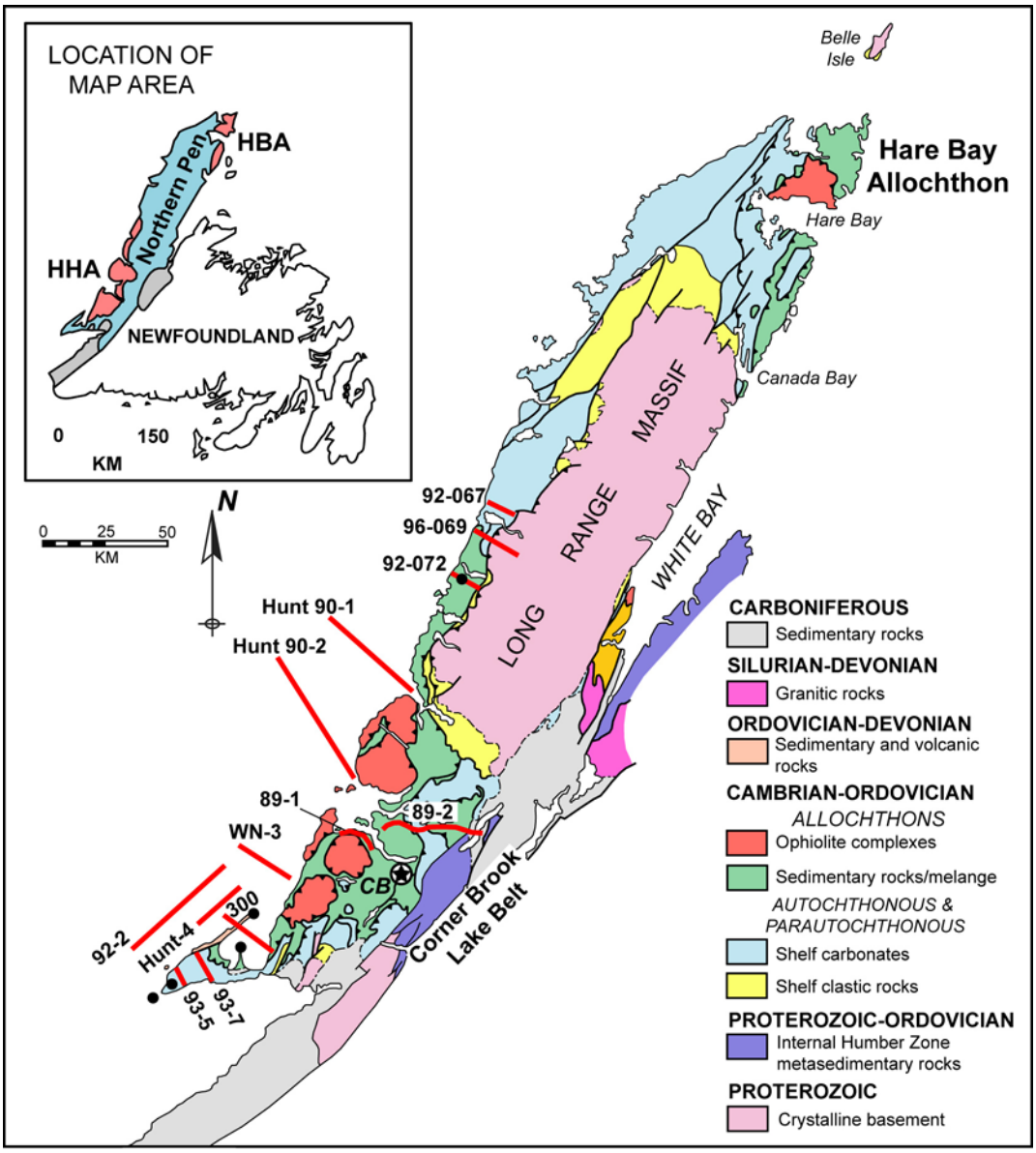

Figure 3.7. General geologic map of western Newfoundland and part of the Gulf of St. Lawrence displaying the locations of selected seismic lines (red lines) and deep wells (black dots) discussed in the text.

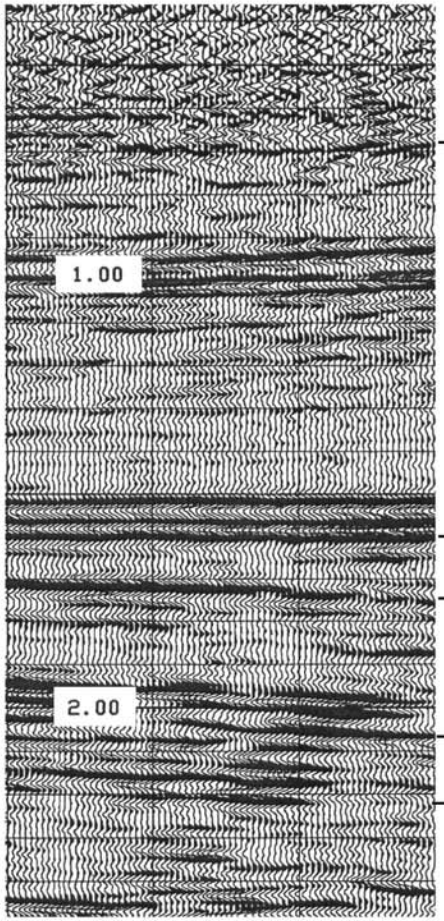

Lithotectonic Unit	Lithostratigraphy	Average Seismic Velocity -- Thickness
5	LOWER DEVONIAN Red Island Road Formation	2.7 km/sec
4	*post-Middle Ordovician foreland basin and shallow-marine facies* UPPER SILIURIAN-LOWER DEVONAN Clam Bank Formation UPPER ORDOVICIAN Long Point Group	3.962 km/sec average thickness of 3000 m
3	*Taconic foreland basin* MIDDLE ORDOVICIAN Goose Tickle Group Mainland Sandstone	3.6 km/sec or 3.778 km/sec maximum thickness of 1500 m average thickness of 200 m
2	*passive margin carbonate shelf* LOWER ORDOVICIAN Table Head Group St. Geroge Group MIDDLE AND UPPER CAMBRIAN Port au Port Group	6.645 km/sec average thickness between 1000 m and 1200 m
1	*synrift and early post-rift facies* LOWER CAMBRIAN Labrador Group	5.0 km/sec maximum thickness of 800 m average thickness of 350 m
	crystalline basement rocks	6.5 km/sec

Figure 3.8. Seismic column through part of the Paleozoic stratigraphic section in the Anticosti basin showing the correlation of stratigraphy and lithotectonic units to reflector stratigraphy typical of seismic reflection profiles used to construct balanced cross sections in Plates 3.1 and 3.2.

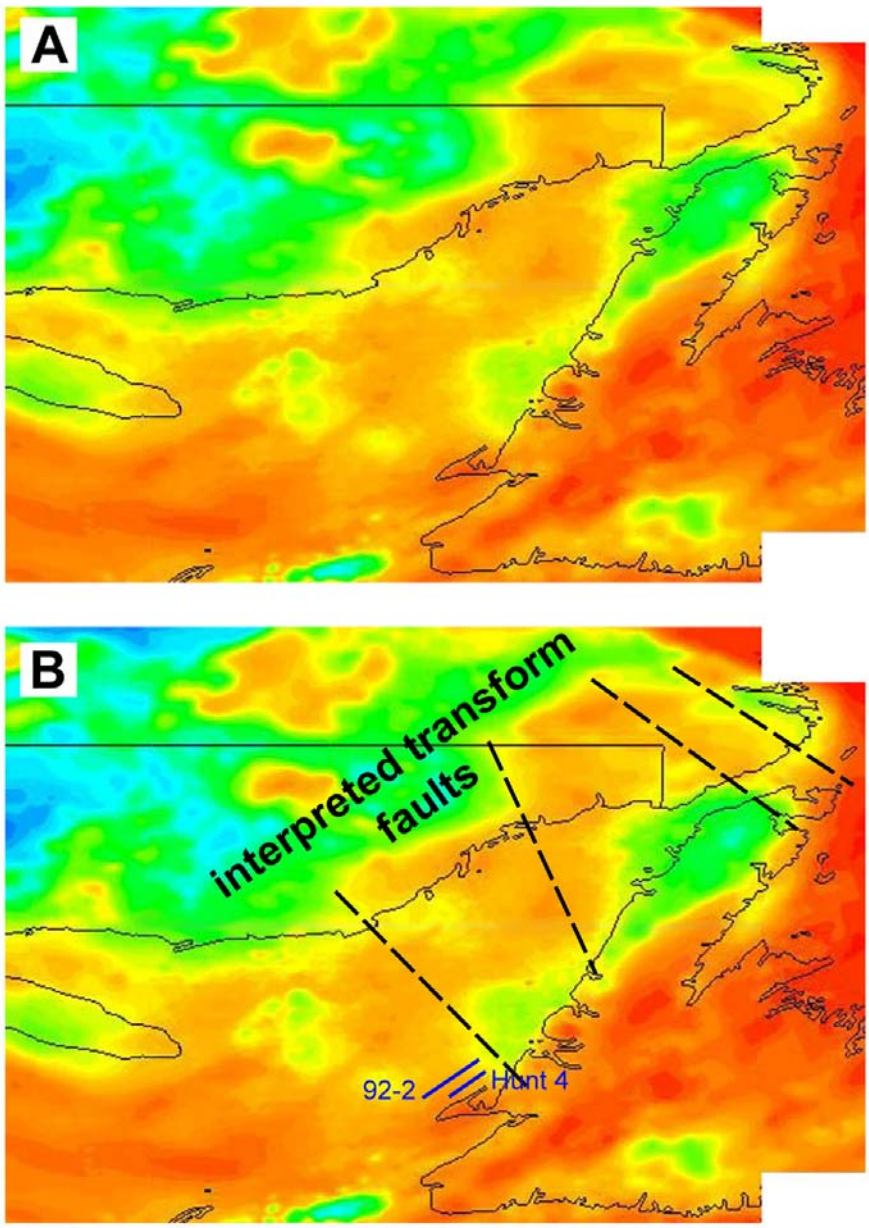

Figure 3.9. Uninterpreted (A) and interpreted (B) Bouguer gravity anomaly map for Newfoundland, the Gulf of St. Lawrence, eastern Quebec, and eastern Labrador. Warm colors (red, yellow) indicate high values for observed gravity (+mGal), whereas cold colors (blue, green) indicate low values of observed gravity (-mGal). Traces for seismic profiles Hunt Line 4 and 92-2 are displayed in gravity map *B*. Data from the Geological Survey of Canada website.

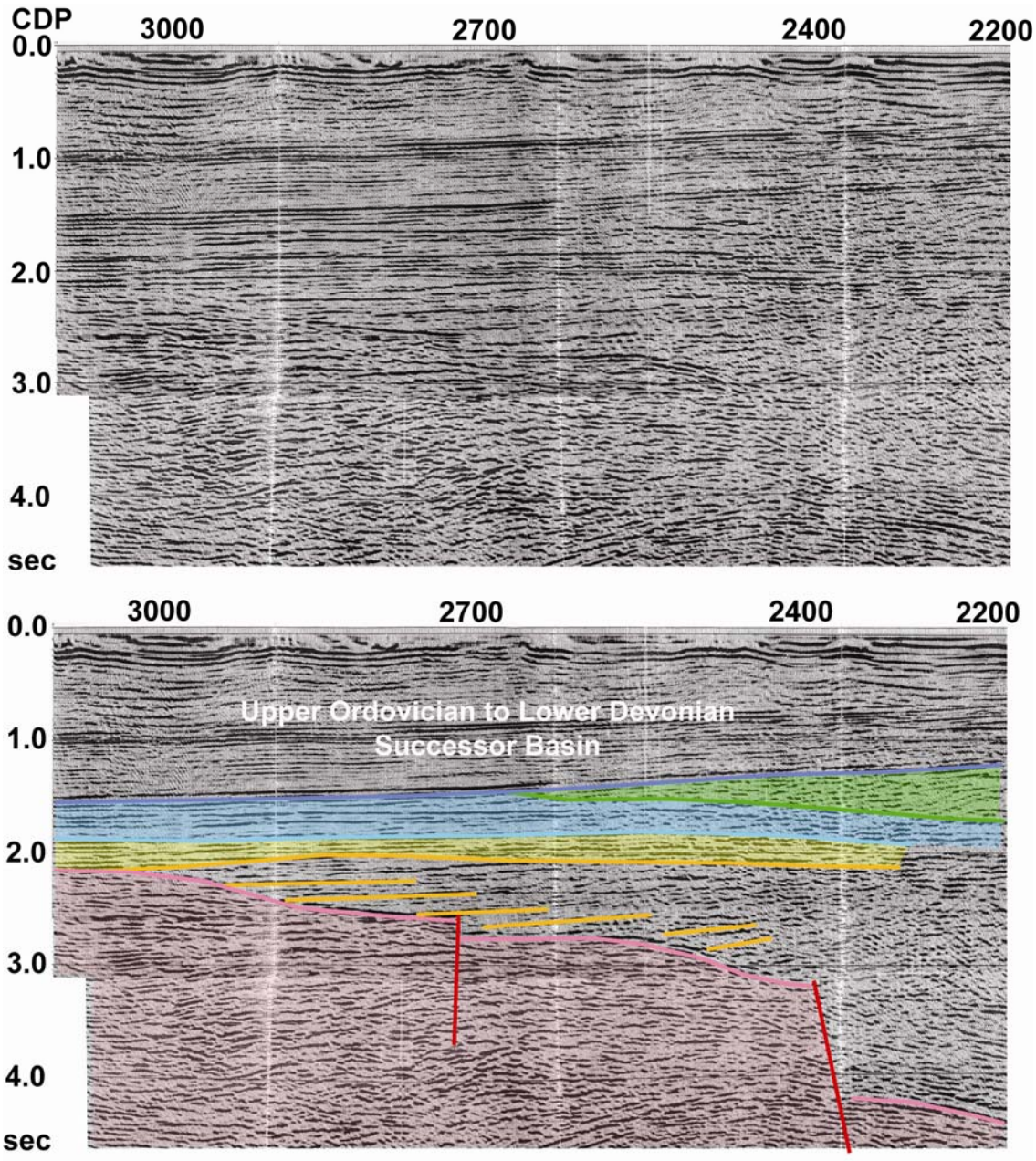

Figure 3.10. Uninterpreted and interpreted seismic data, Hunt Oil Co. Line 4. Pink shaded region is interpreted as Mesoproterozoic crystalline basement whereas solid pink line is the interpreted top of basement; orange shaded region is the Labrador Group while orange lines mark the base of the Labrador Group and outline onlapping reflectors in underlying stratigraphic section; light blue region is the Cambrian-Ordovician carbonate platform; dark blue line is the interpreted position of the Lourdes Limestone; green is the interpreted position of the Humber Arm allochthon; sub-vertical red lines are interpreted positions of basement faults.

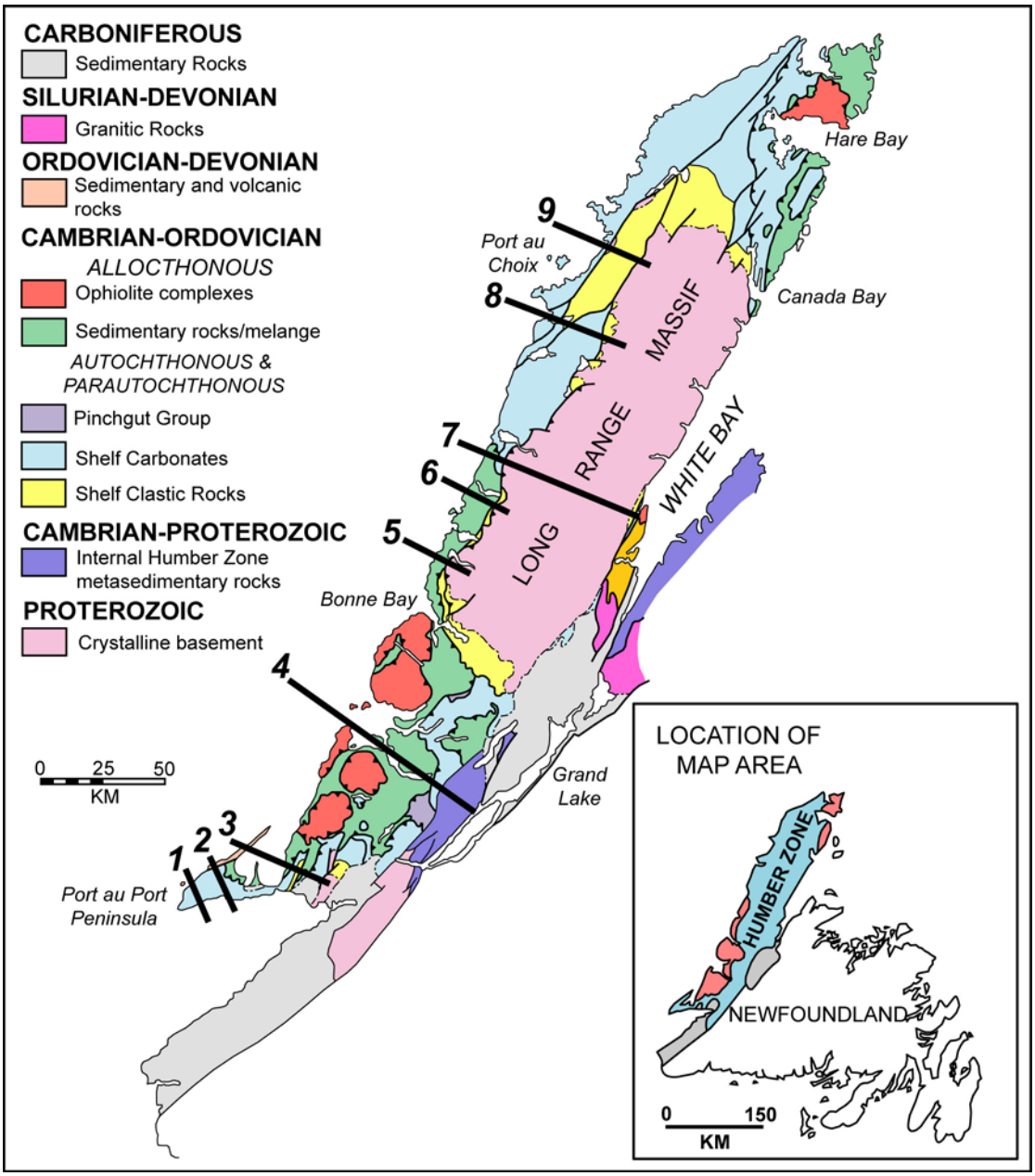

Figure 3.11. Generalized geologic map showing the trace of each line of cross section. Geologic color symbols from Figure 3.3.

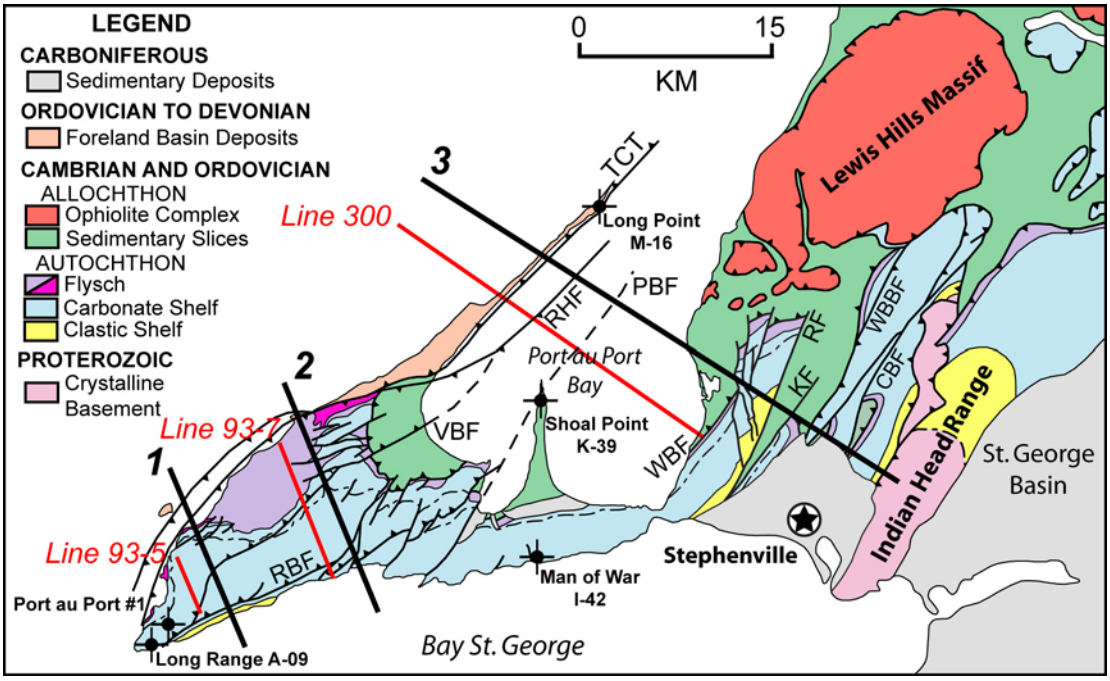

Figure 3.12. General geologic map of southwestern Newfoundland illustrating the early Paleozoic geology of Port au Port peninsula and the Indian Head Range north of Stephenville. Cross-section Lines 1, 2, and 3 are displayed (black lines), as well as pertinent seismic lines (red lines) and locations of deep wells. CBF = Cold Brook fault; KF = Kippens fault; PBF = Piccadilly Bay fault; RBF = Red Brook fault; RF = Romaines Brook fault; RHF = Round Head fault; TCT = Tea Cove Fault; VBF = Victors Brook fault; WBBF = West Blanche Brook fault; WBF = Western Boundary fault.

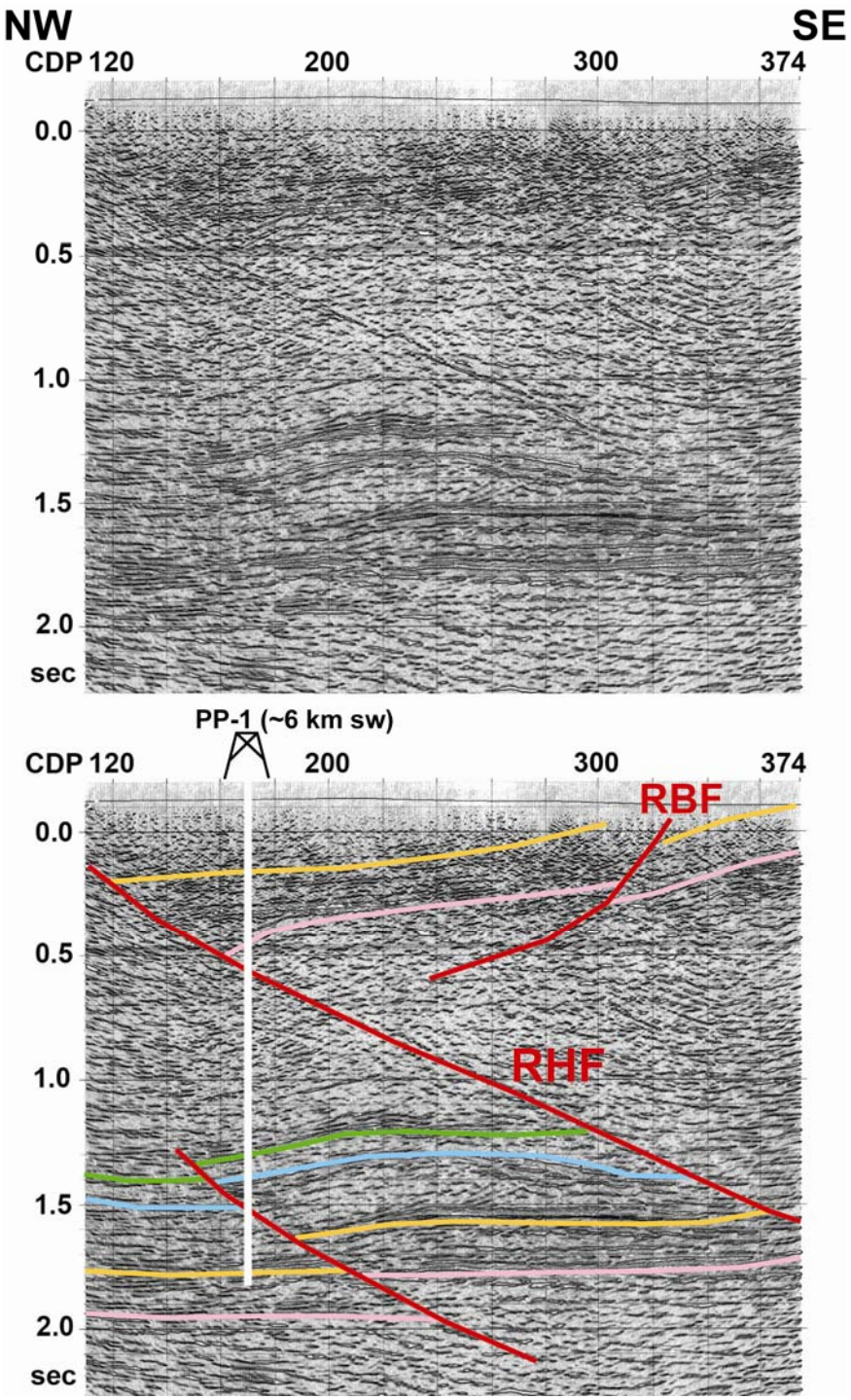

Figure 3.13. Uninterpreted and interpreted seismic data, Hunt Oil Co. line 93-5. Interpreted line also shows the approximate trace of the Port au Port #1 well. Pink line corresponds to top of Mesoproterozoic crystalline basement; orange line marks the top of early Paleozoic Labrador Group; light blue line is interpreted top of Cambrian-Ordovician carbonate platform; green line is the interpreted position of the Lourdes Limestone; red lines indicate significant faults that break regional stratigraphy. PP-1 = Port au Port #1 well; RBF = Red Brook fault; RHF = Round Head fault.

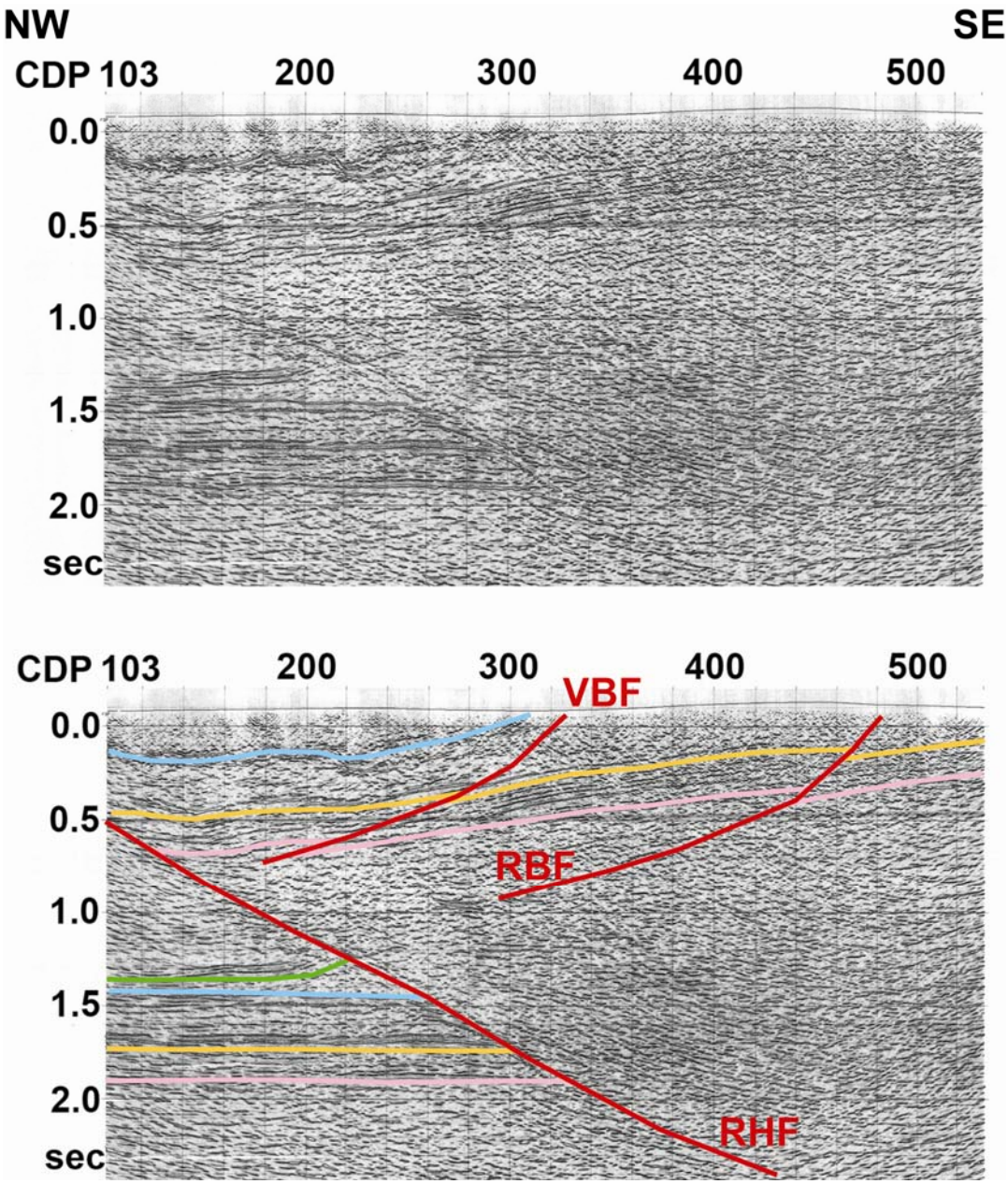

Figure 3.14. Uninterpreted and interpreted seismic data, Hunt Oil Co. line 93-7. Significance of individual line colors same as in Figure 3.13. The Mainland Sandstone occupies the region between the light blue and dark green seismic reflectors. Note that in this seismic profile the thickness of reflectors correlated to the Mainland Sandstone is greater in the hanging wall of the Round Head fault than in the footwall. RBF = Red Brook fault; RHF = Round Head fault; VBF = Victors Brook fault.

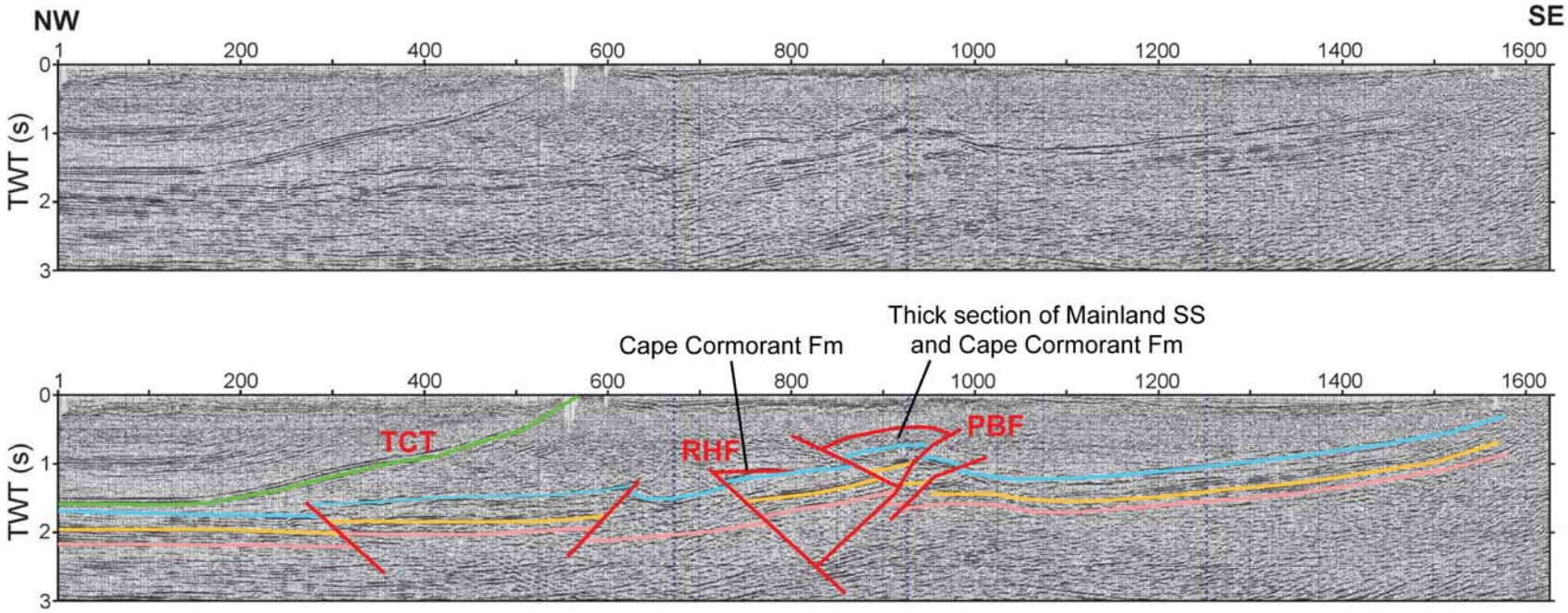

Figure 3.15. Uninterpreted and interpreted seismic data in line 300 through Port au Port Bay. Significance of individual line colors same as in Figure 3.13. PBF = Piccadilly Bay fault; RHF = Round Head fault; TCT = Tea Cove thrust.

Figure 3.16. Photograph of the structural contact between the Humber Arm allochthon (above) and the Table Cove Formation (below). The gentleman in this picture is Dr. John Waldron, who is standing on the bedded limestone of Table Cove Formation and has his finger on tectonic mélange in the overlying allochthon.

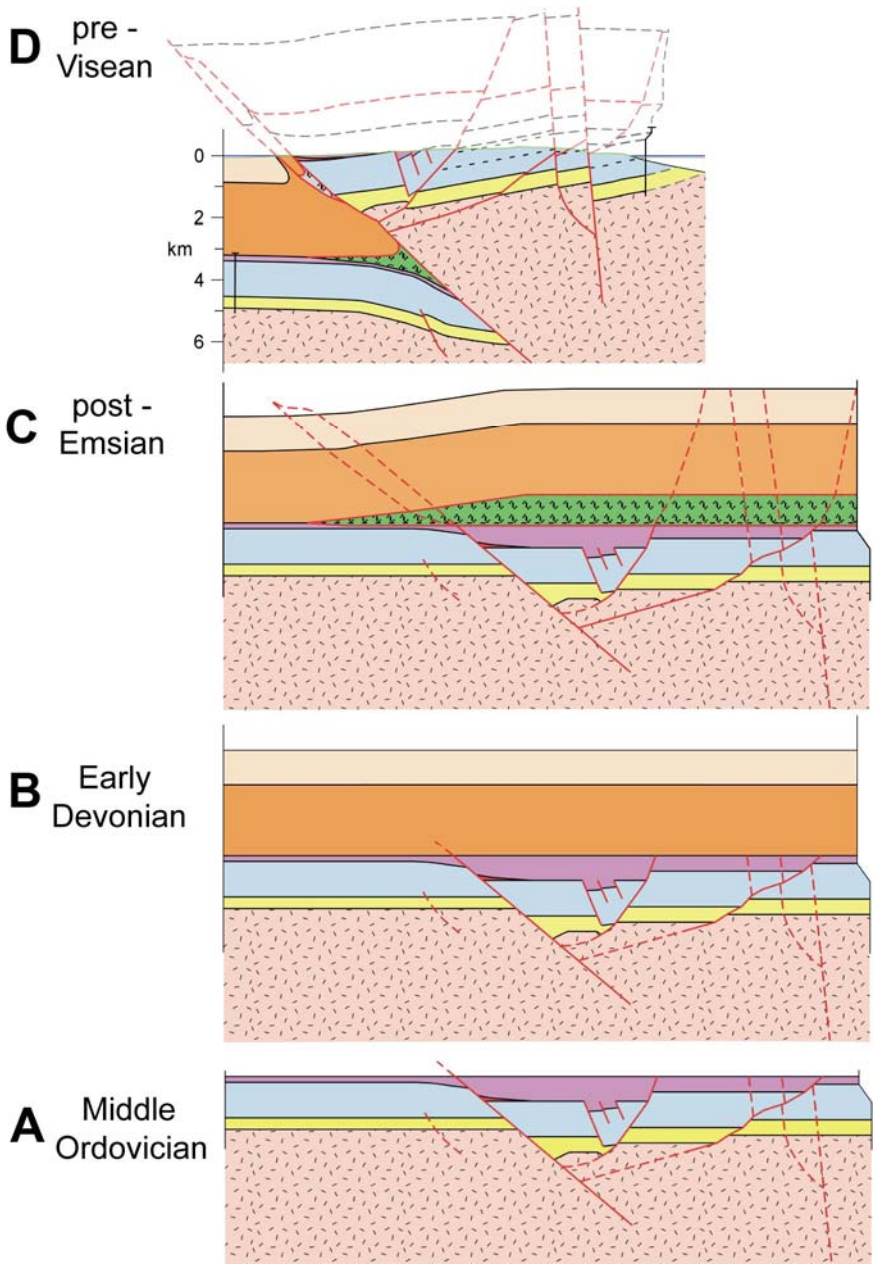

Figure 3.17. Kinematic model for the Paleozoic tectonic evolution of the geology on Port au Port peninsula in sequential cross sections along Line 2 (Figure 3.11). All panels are kinematically balanced. Panel A shows a palinspastic restoration of Line 2 for the Middle Ordovician; Panel B shows the Late Ordovician-Early Devonian foreland basin (Units 4 and 5) deposited over Port au Port peninsula; Panel C shows insertion of the Humber Arm allochthon beneath Units 4 and 5; Panel D shows the present structural and erosional configuration for Line 2. A discussion of each stage appears in the text.

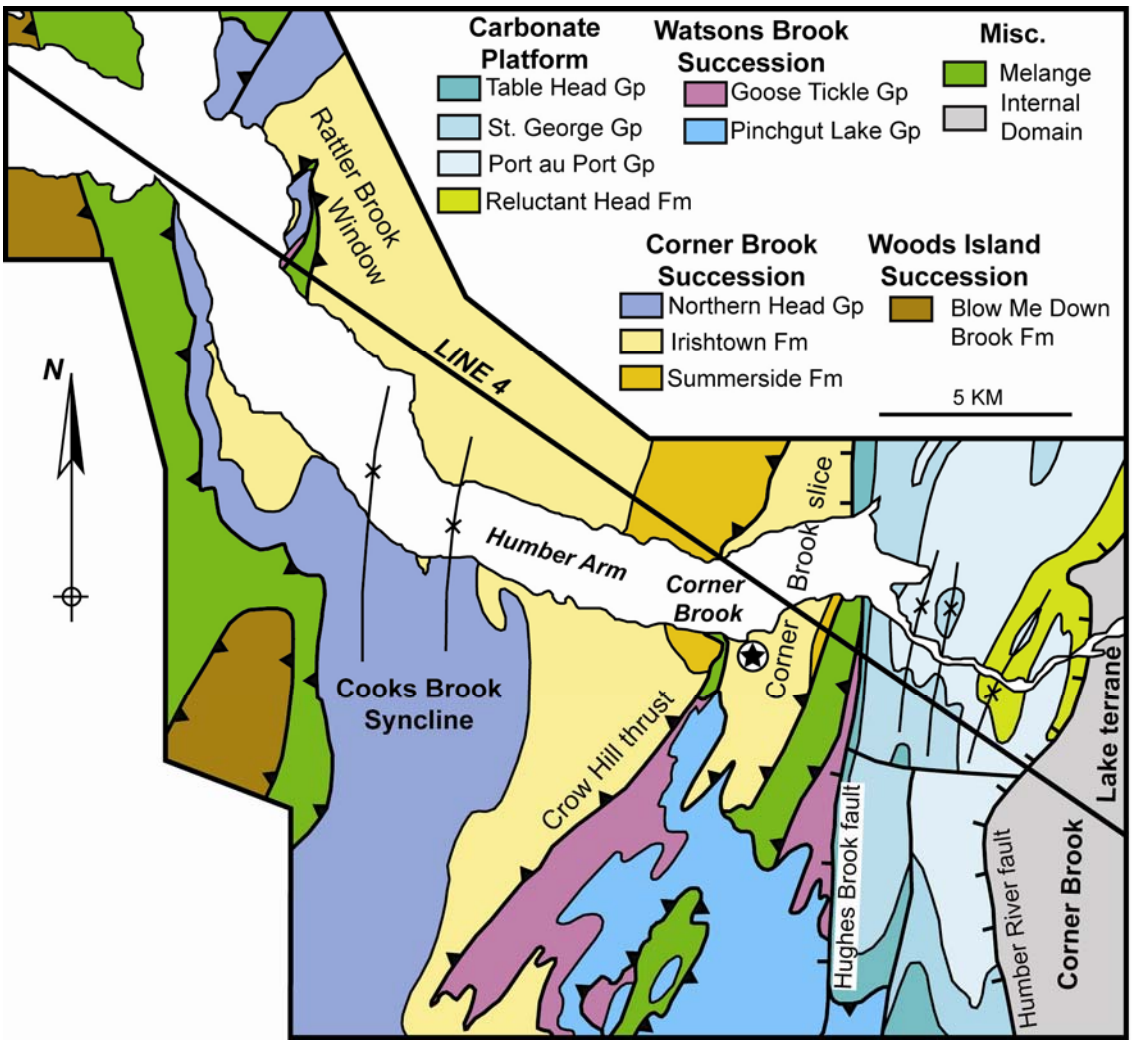

Figure 3.18. General geologic map of the Humber Arm allochthon and underlying platform rocks in the area of Corner Brook and Humber Arm. Figure displays significant structural slices within the allochthon in region, significant map scale structure, and part of cross-section Line 4. Geologic map based on previously published maps by Knight (1996), Waldron et al (2003), and geologic mapping by the author.

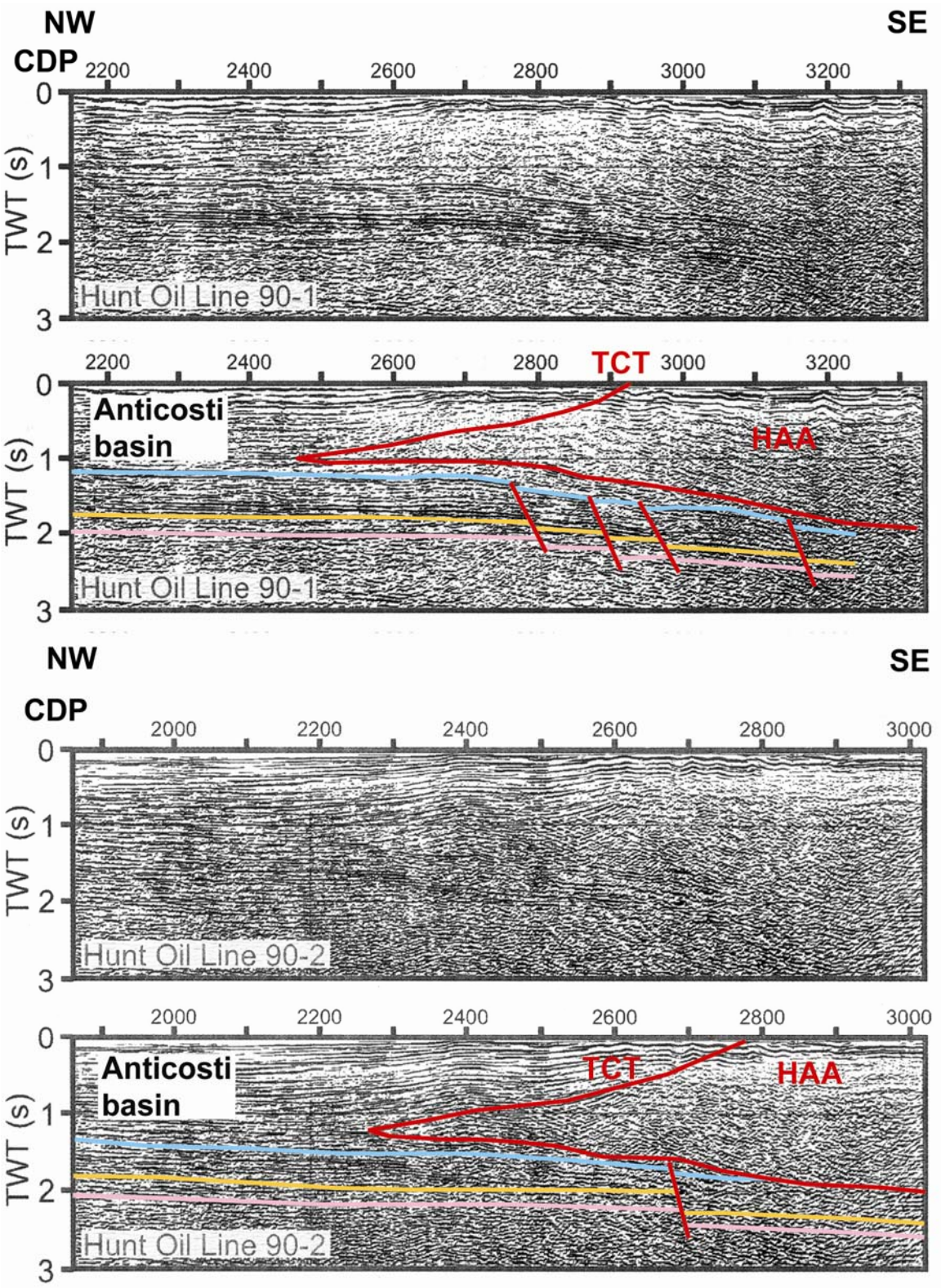

Figure 3.19. Uninterpreted and interpreted seismic data, Hunt Oil Co., lines 90-1 and 90-2. See Figure 3.7 for location. Color for interpreted stratigraphic and structural contacts same as Figure 3.13. Lines modified after Stockmal et al., (1998).

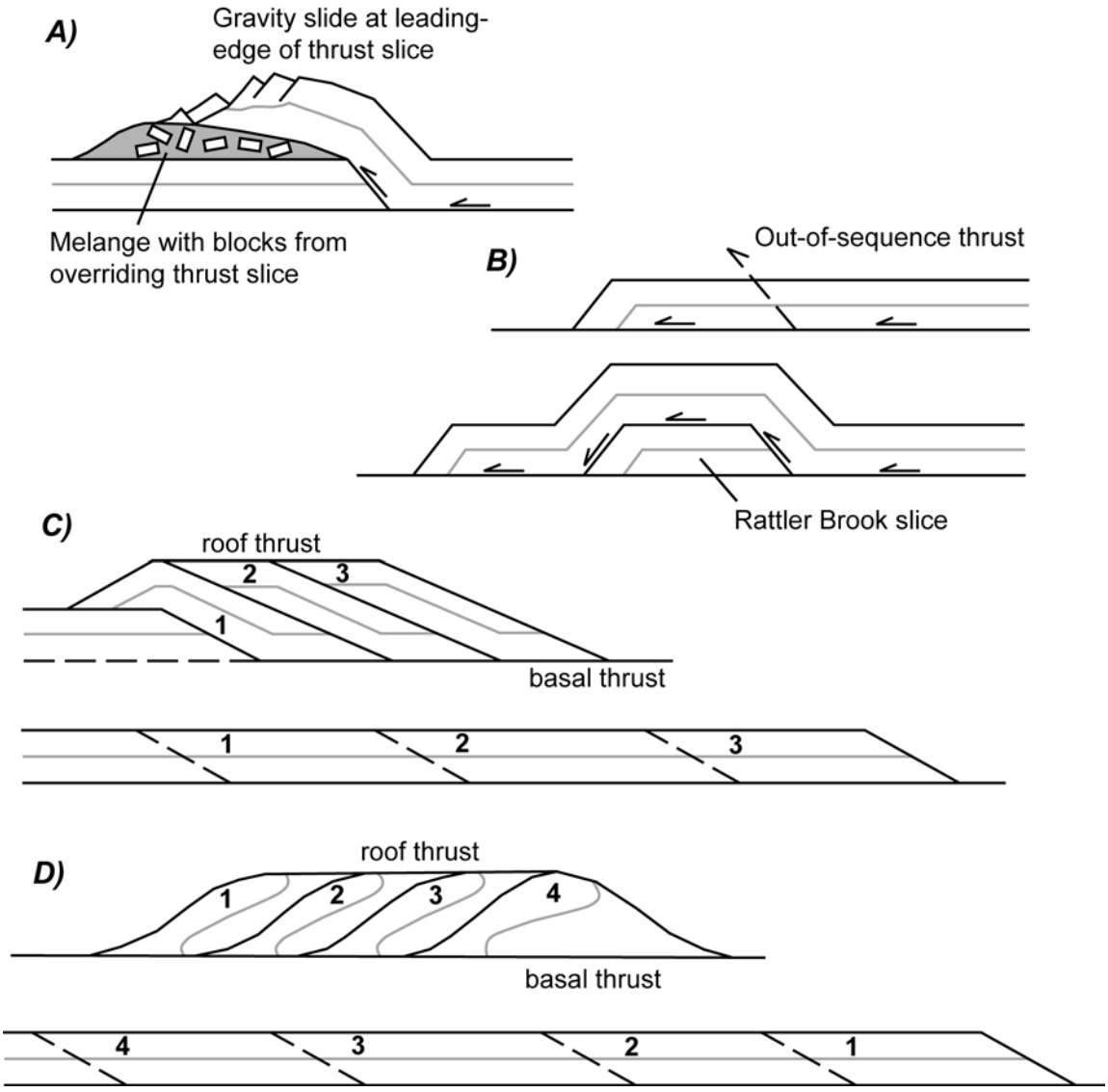

Figure 3.20. Schematic representations of structures within the Humber Arm allochthon. *A)* Illustration of the formation of a structural mélange zone at the base of a thrust sheet. Sediments and blocks are eroded from the leading edge of the sheet and then structurally overridden by the advancing thrust sheet. *B)* Structural illustration demonstrating the formation of the Rattler Brook slice. *C)* A deformed and palinspastically restored hinterland dipping duplex system; the Humber Arm allochthon north of Bonne Bay displays this structural geometry; *D)* A deformed and palinspastically restored foreland dipping duplex system where each thrust sheet must "leap frog" the sheet in front of it; the Humber Arm allochthon at Humber Arm displays this structural geometry.

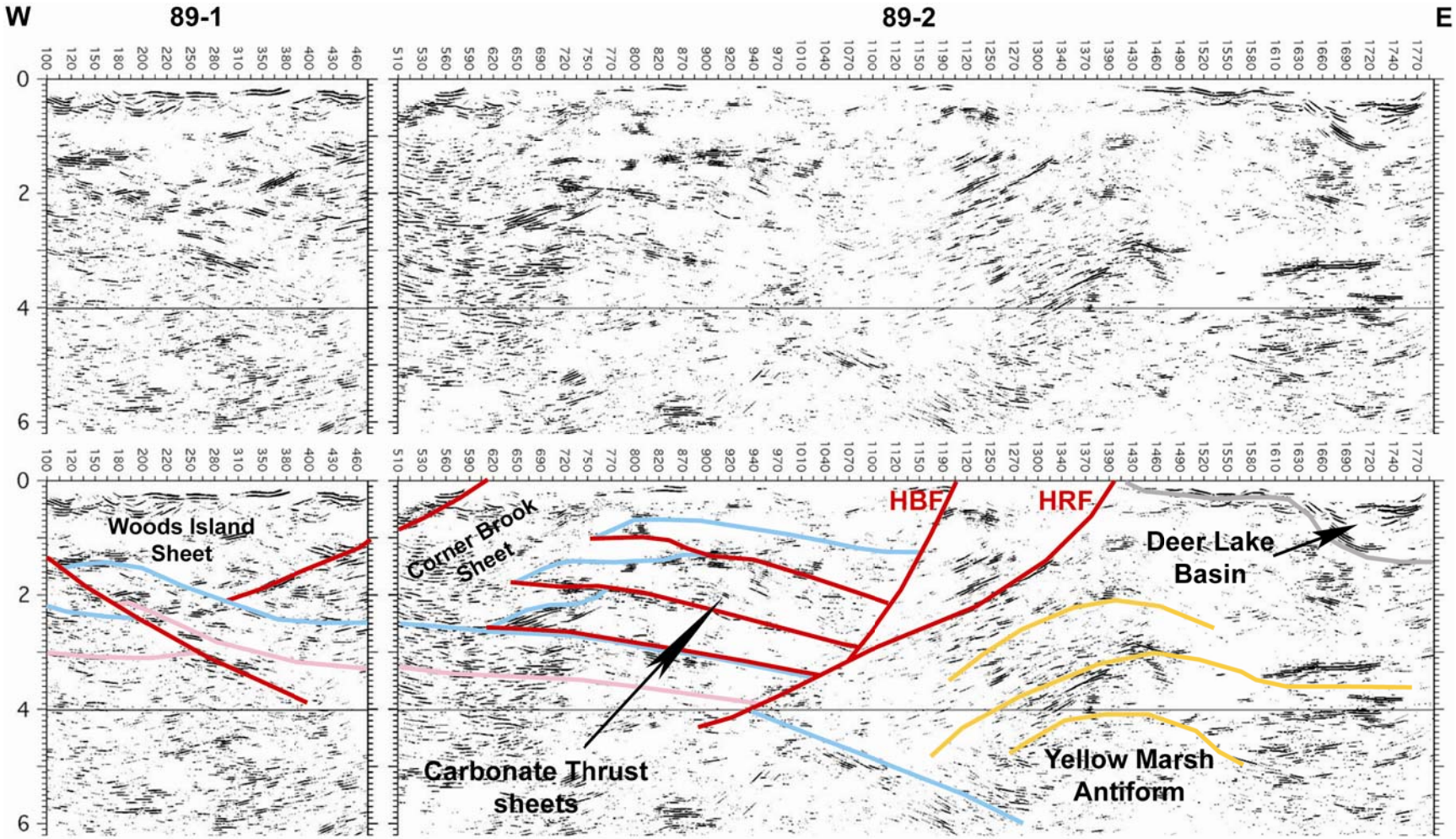

Figure 3.21. Uninterpreted and interpreted seismic data, Lithoprobe East lines 89-1 and 89-2. Location displayed in Figure 3.7. Pink, blue, and red colored lines indicate same structure and stratigraphy as in Figure 3.13. Orange lines display folded metamorphic fabric in the Corner Brook Lake terrane; gray line indicates base of the Carboniferous Deer Lake basin fill. HBF = Hughes Brook fault; HRF = Humber River fault.

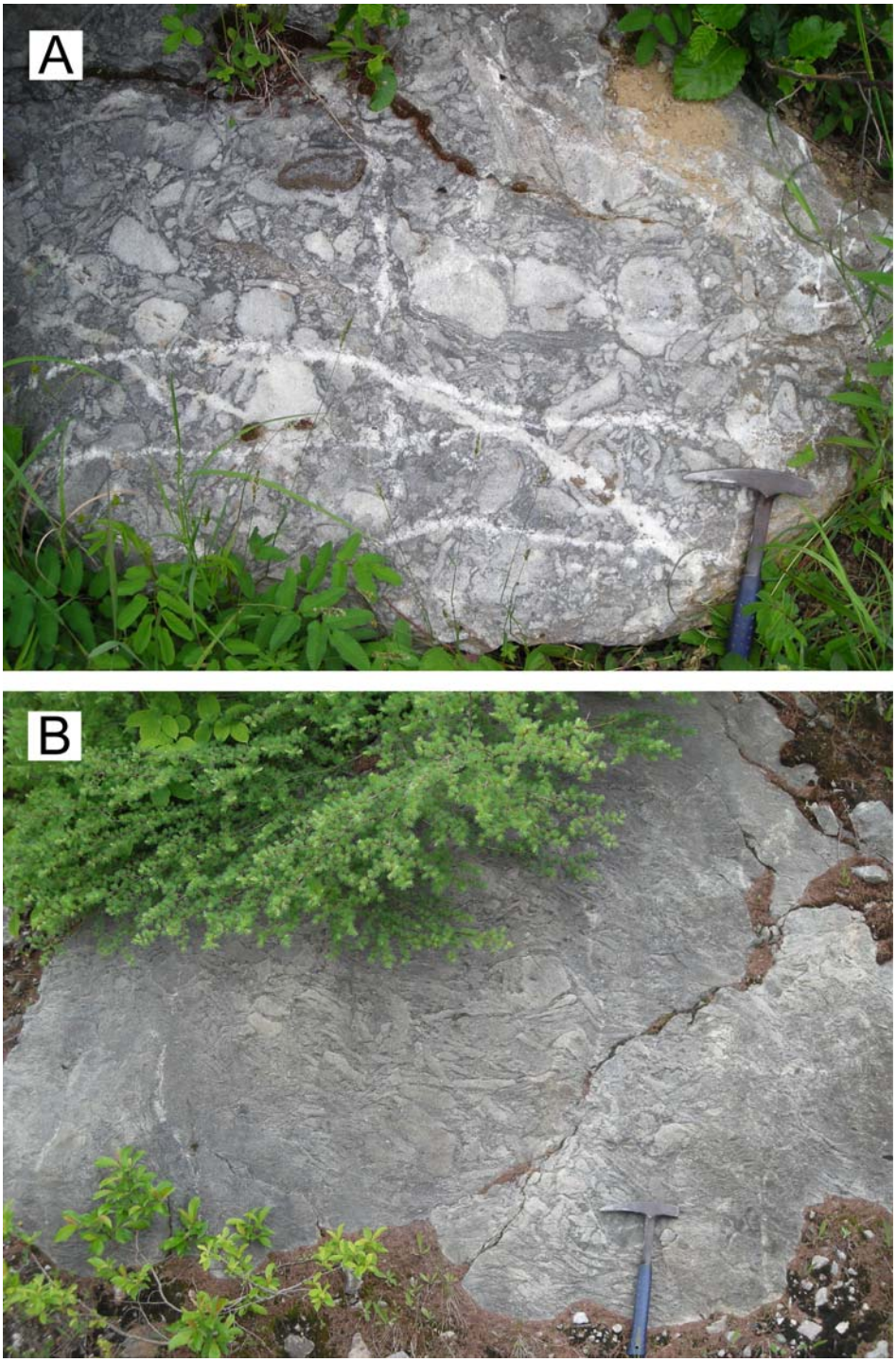

Figure 3.22. Photographs of limestone conglomerate in the Pinchgut Lake Group (A) and the Breeches Pond Formation (B). Note that despite a higher grade of metamorphism, the conglomerate in the Breeches Pond Formation is nearly identical to the Pinchgut Lake conglomerate.

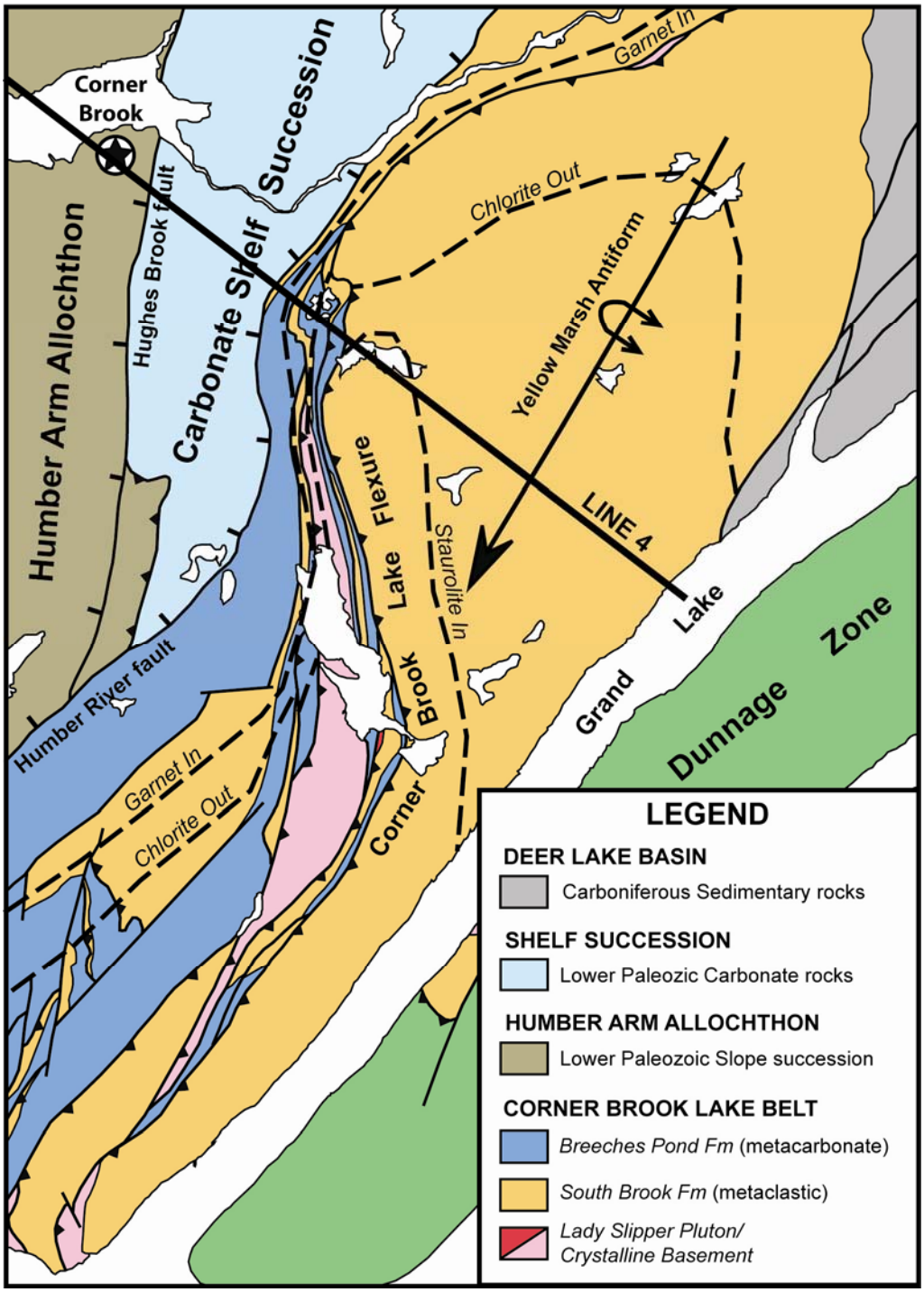

Figure 3.23. Generalized geologic map of the Corner Brook Lake terrane and surrounding geology. Map illustrates the distribution of rock types in the terrane, along with significant structures and metamorphic isograds (dashed lines). Note the contrasting geology around the Corner Brook Lake flexure. Modified after Cawood and van Gool (1998).

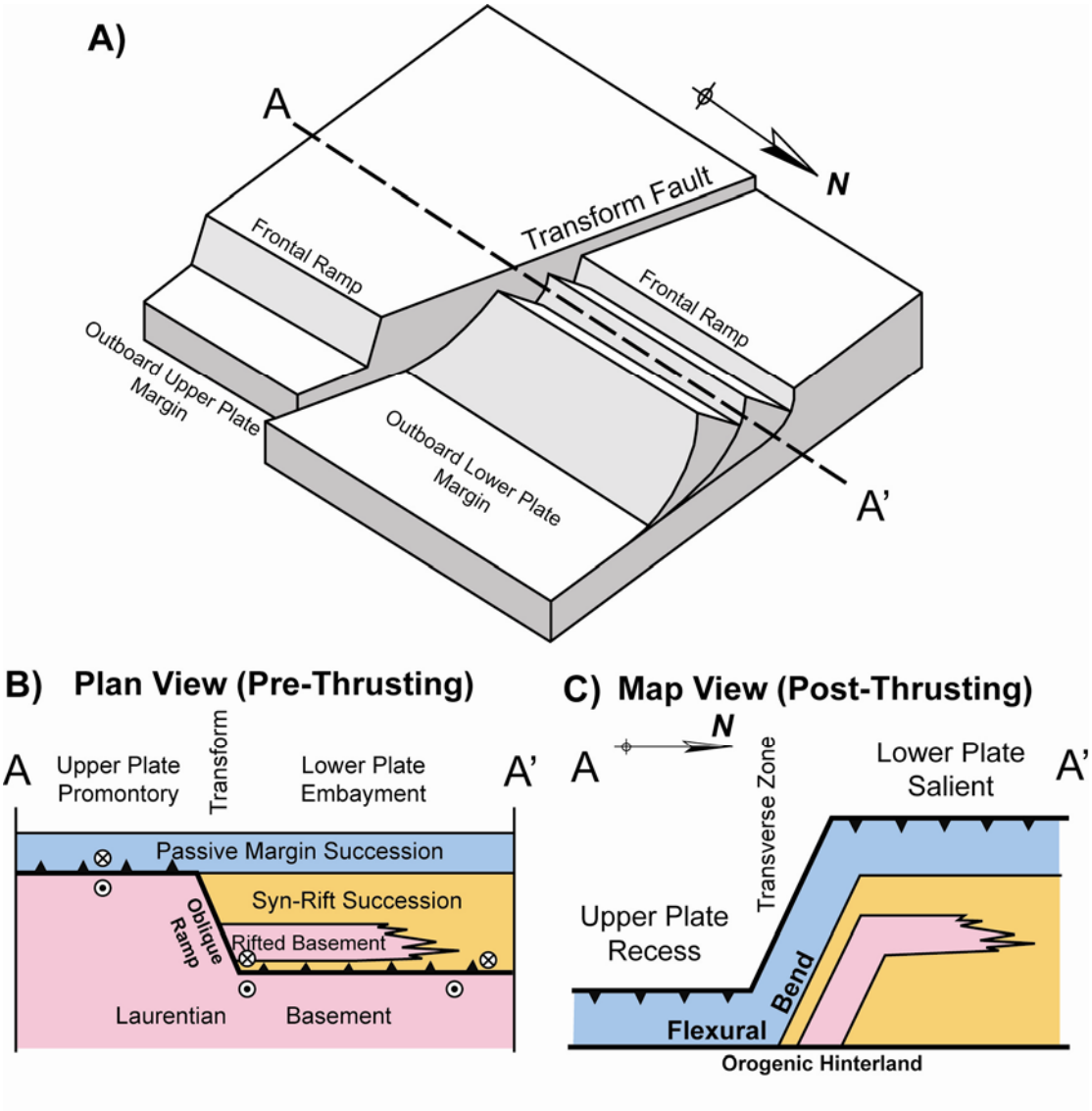

Figure 3.24. Schematic block diagrams illustrating the origin of the Corner Brook Lake flexure in relation to the Serpentine Lake transform. *A)* A schematic block diagram of an upper- and lower-plate domains bounded by a transform fault. *B)* Schematic cross section through a transform fault system that separates an upper-plate margin from a lower-plate margin prior to thrust faulting, showing the configuration of stratigraphic sequences, rifted basement graben, and trajectories of future (Devonian?) thrust faults. *C)* Map view of the configuration from C following (Devonian?) thrusting. Rift and passive-margin strata in the lower-plate basin are thrust up a frontal ramp comprised of the rotated half graben and thus display a curved, southward plunging ramp anticline geometry.

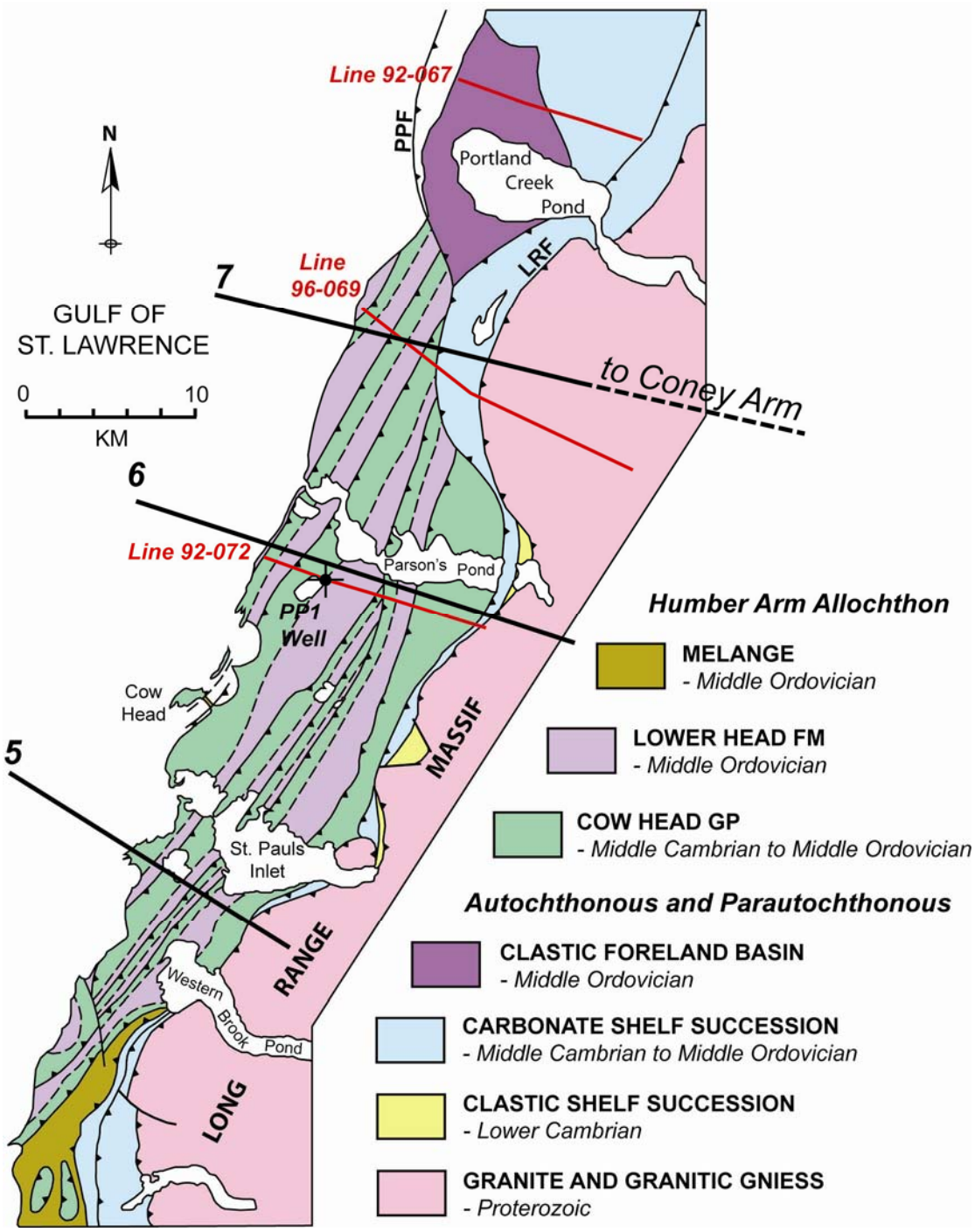

Figure 3.25. Generalized geologic map illustrating the geology of the Humber Arm allochthon and the lower Paleozoic shelf stratigraphy between Bonne Bay and Portland Creek Pond, west of the Long Range massif. Lines of cross sections 5, 6, and part of 7 are displayed (black lines), as well as pertinent seismic reflection lines (red lines) and locations of Parson's Pond Well #1. LRF = Long Range fault; PPF = Parson's Pond fault.

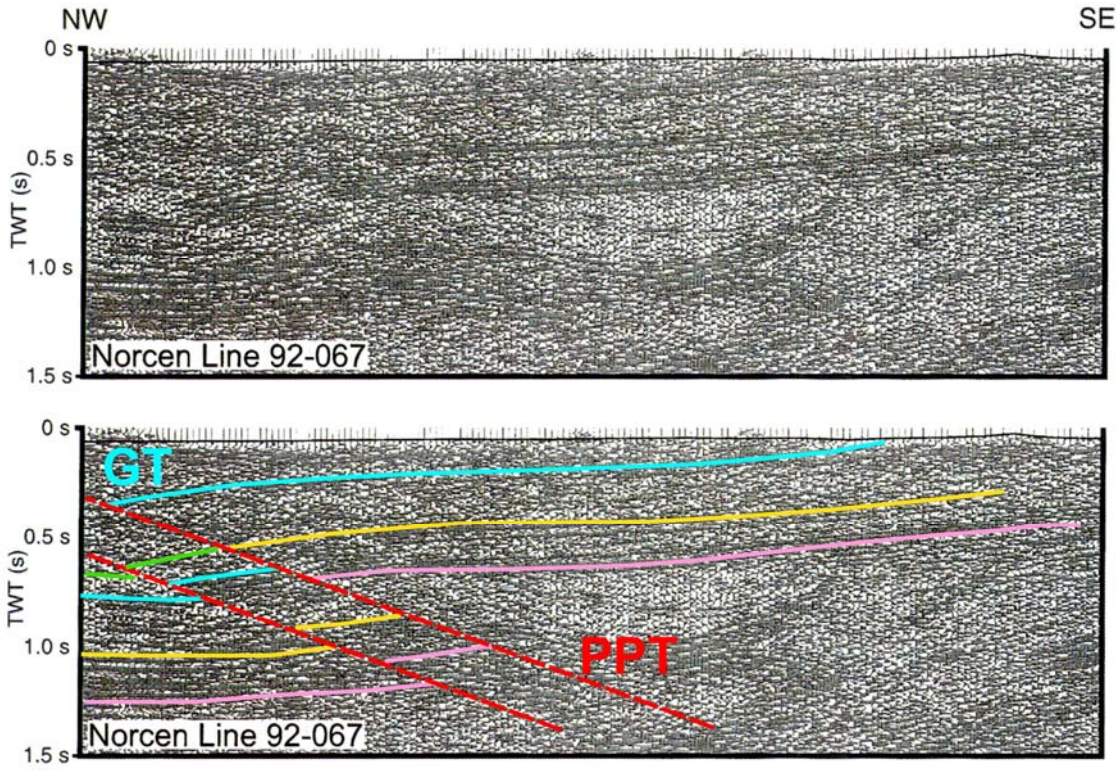

Figure 3.26. Uninterpreted and interpreted seismic data, Norcen line 92-067. See Figures 3.7 and 3.25 for location. Color for interpreted stratigraphic and structural contacts same as Figure 3.13. GT = thick section of Goose Tickle Group; PPT = Parson's Pond fault.

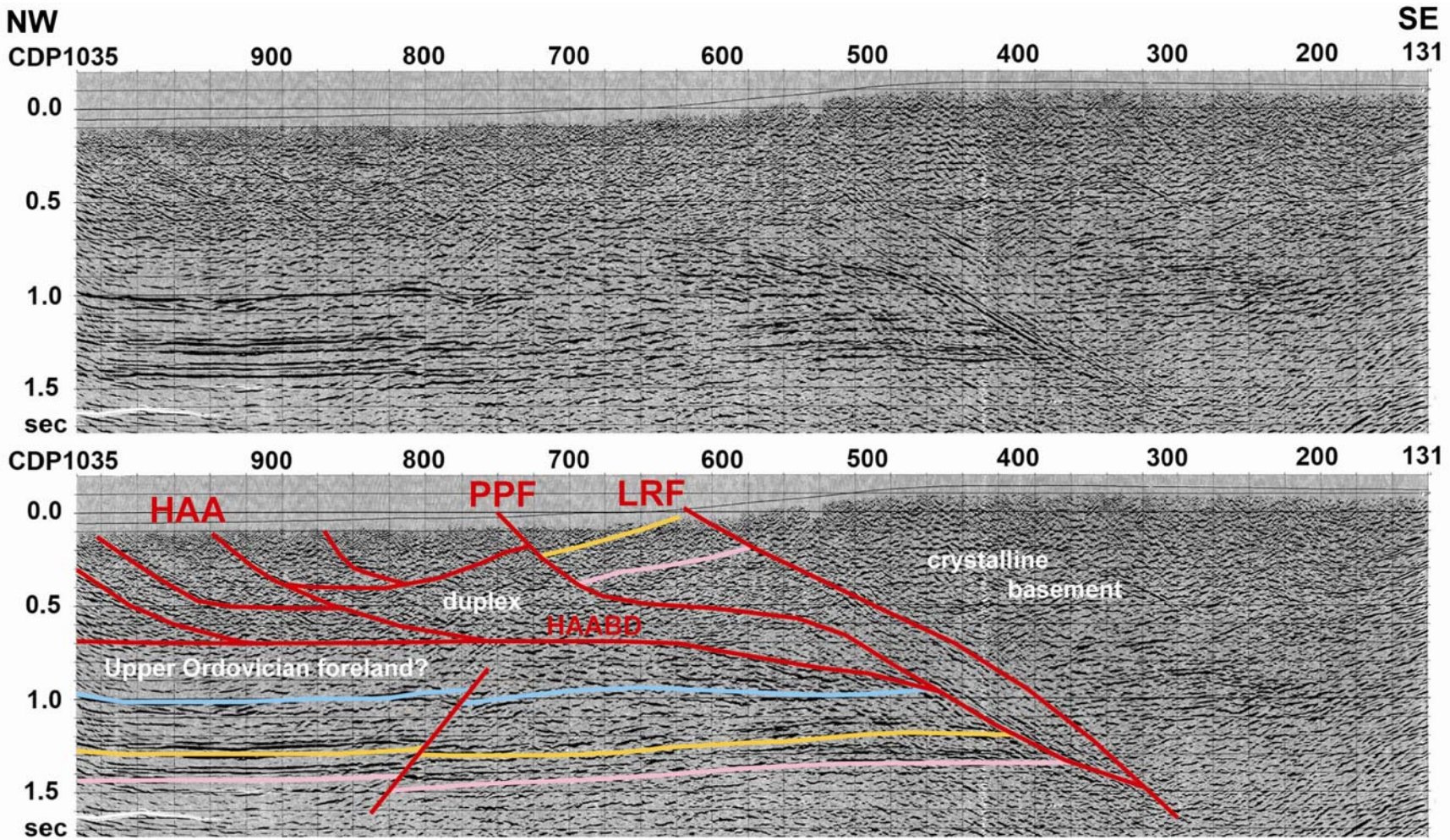

Figure 3.27. Uninterpreted and interpreted seismic data, Talisman Energy line 96-069. See Figures 3.7 and 3.25 for location. Color for interpreted stratigraphic and structural contacts same as Figure 3.13. HAA = Humber Arm allochthon; HAABD = Humber Arm allochthon basal detachment; LRF = Long Range fault; PPF = Parson's Pond fault.

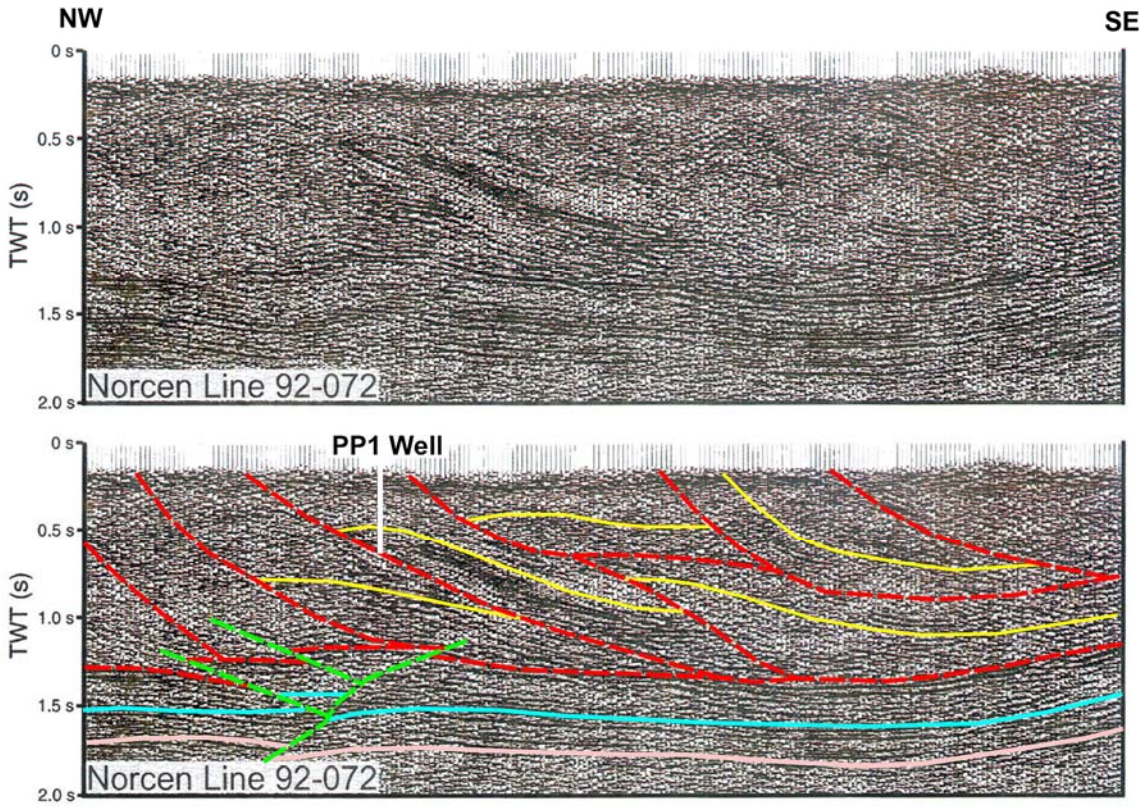

Figure 3.28. Uninterpreted and interpreted seismic data, Norcen line 92-072. See Figures 3.7 and 3.25 for location. Color for red, pink, and light blue lines same as Figure 3.13. Yellow lines indicate stratigraphic contact between the Cow Head Group and the Lower Head Formation in the Humber Arm allochthon. Green lines illustrate a late "pop-up" structure that deforms the shelf succession and overlying Humber Arm allochthon. PP1 = Parsons Pond Well #1.

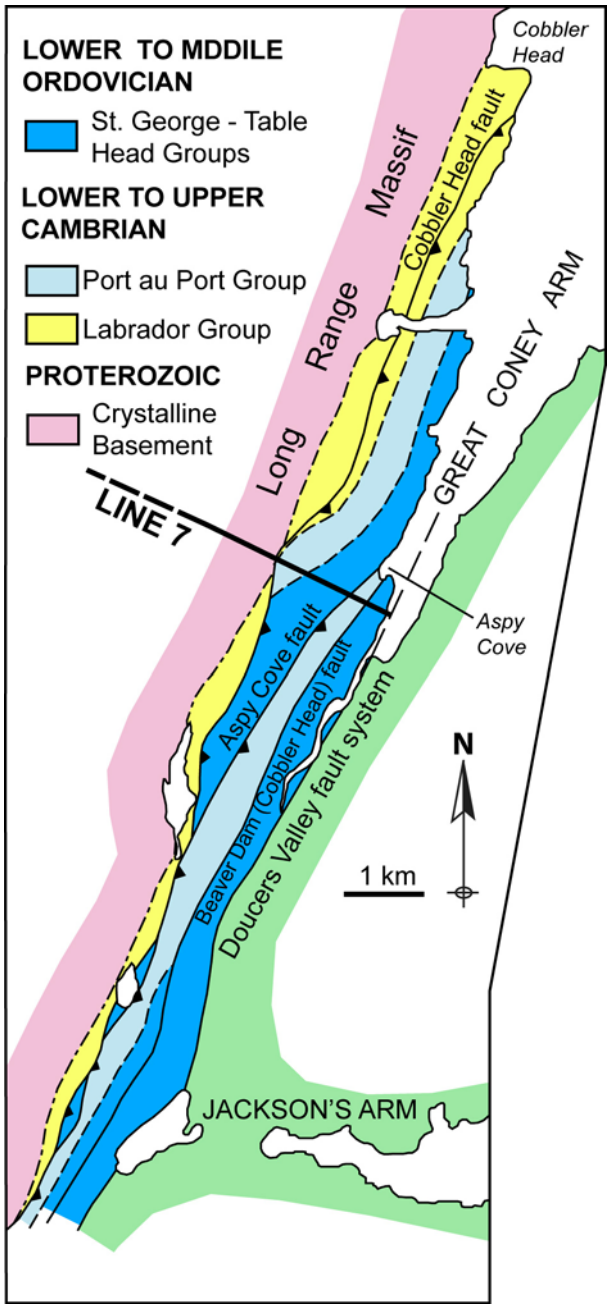

Figure 3.29. General geologic map displaying the lower Paleozoic Laurentian shelf stratigraphy along the western coast of Coney Arm. Black line marks the trace of cross section Line 7. Modified after Kerr and Knight (2004).

Figure 3.30. Photograph of an outcrop of interbedded ribbon limestone and shale, which is overlain by a thick bed of limestone conglomerate. The succession is part of the Shallow Bay Formation in the Cow Head Group. Photograph taken along the western shore of Cow Head.

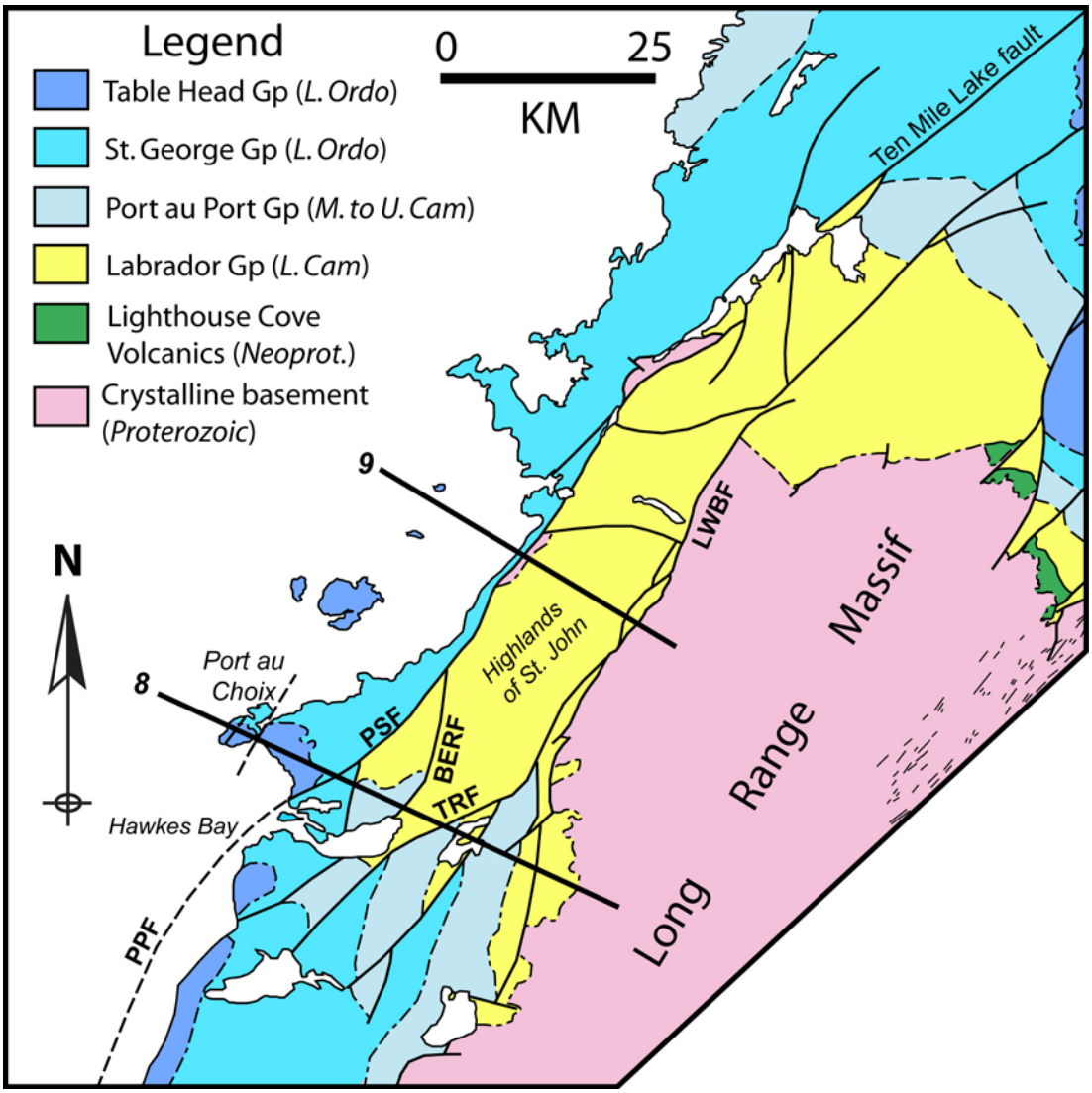

Figure 3.31. Generalized geologic map of lower Paleozoic stratigraphy on the Northern Peninsula west of the Long Range massif around Hawkes Bay and Port au Choix. The trace of Lines 8 and 9 are displayed. BERF = Big East River fault; LWBF = Lady Worchester Brook fault; PPF = Parsons Pond fault; PSF = Port Saunders fault; TRF = Torrent River fault.

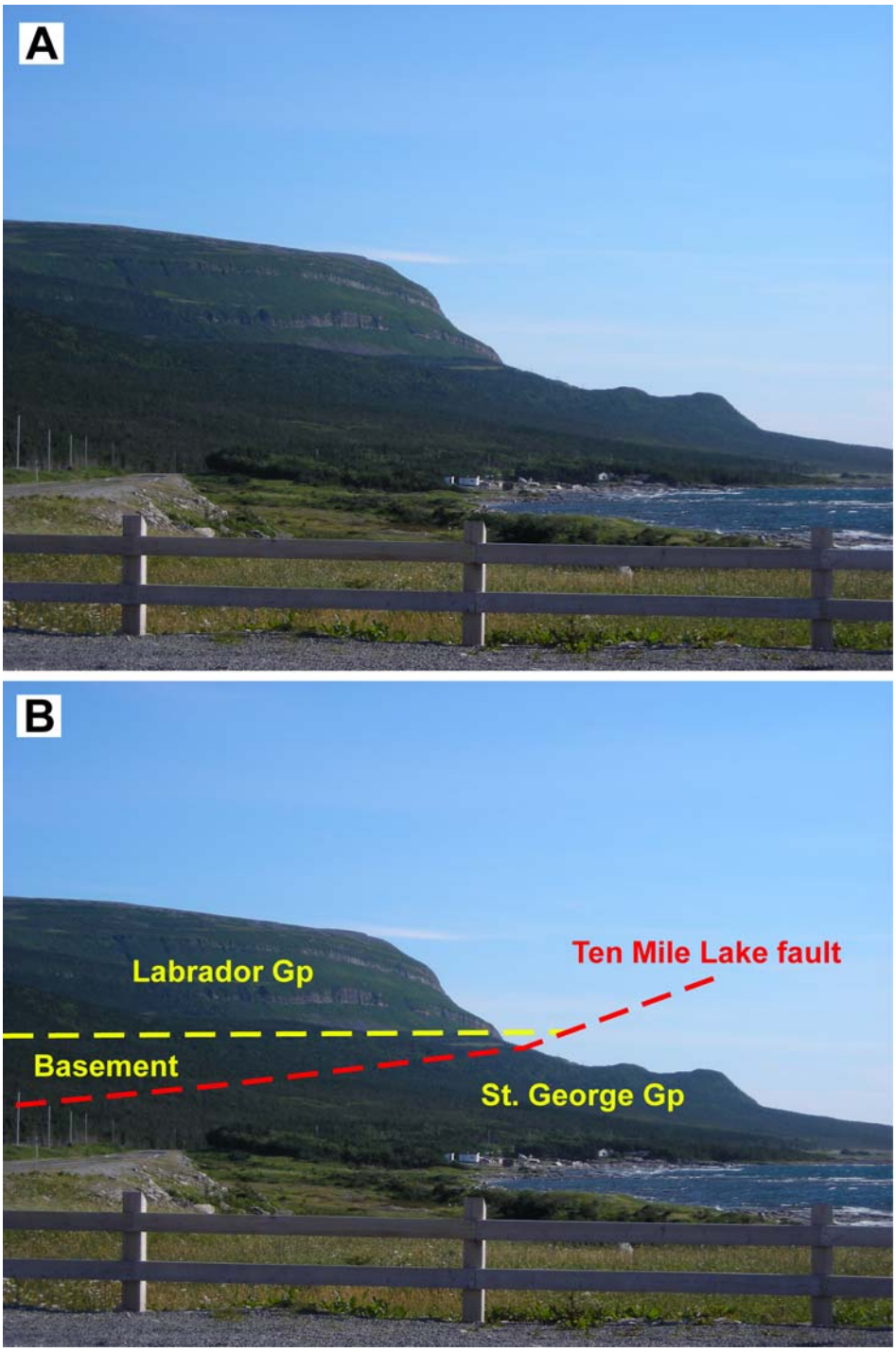

Figure 3.32. Uninterpreted (A) and interpreted (B) photographs looking south toward the Highlands of St. John on the Northern Peninsula. Layered rocks that comprise the mountainous highlands consist of clastic strata in the Labrador Group, which have been uplifted along with basement by the Ten Mile Lake fault.

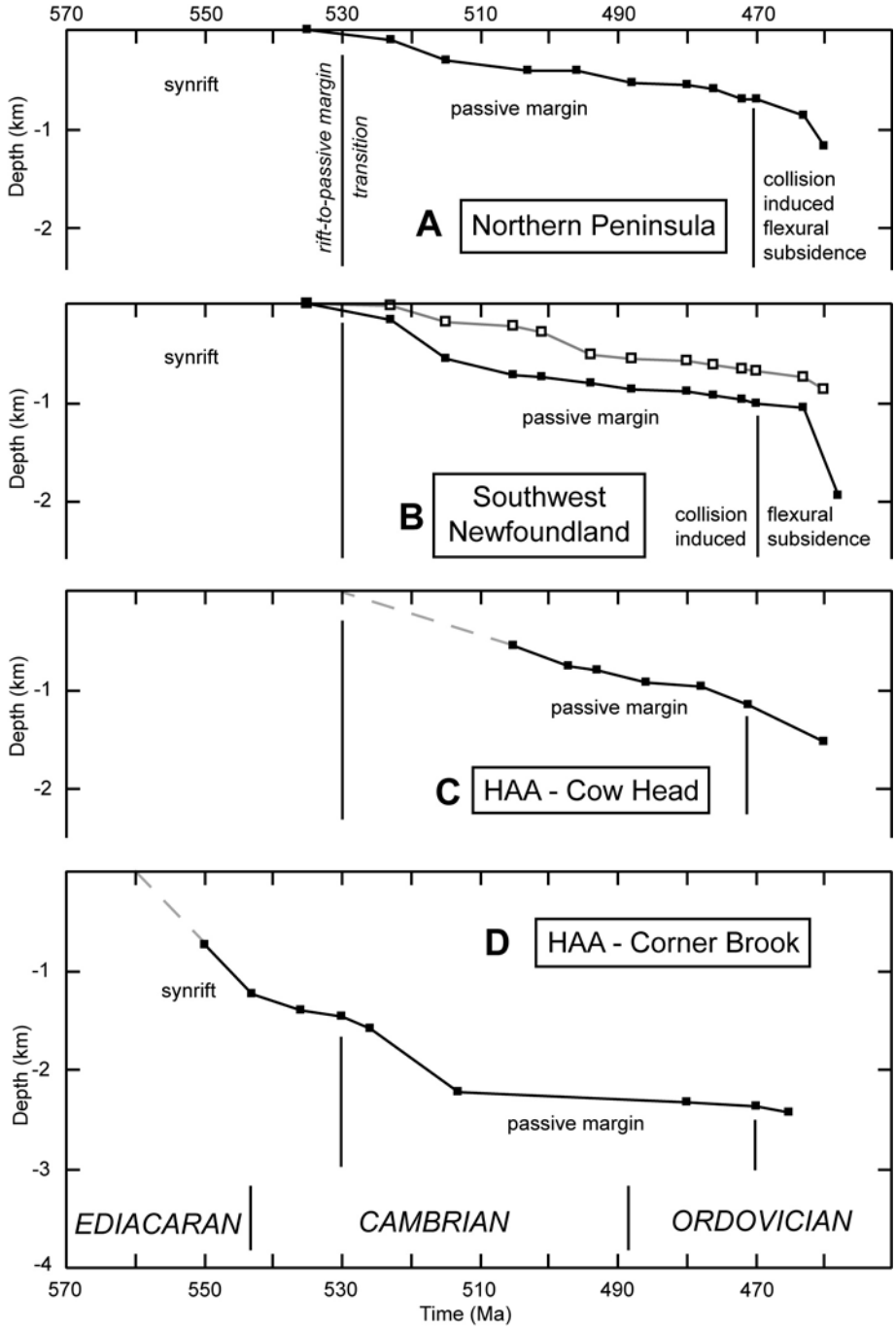

Figure 3.33. Tectonic subsidence profiles for top of basement rocks derived from rocktype-dependent decompaction and backstripping calculations (program by Wilkerson and Hsui, 1989; using porosity/depth data from Sclater and Christie, 1980, and Schmoker and Halley, 1982). A) Passive-margin shelf successions at locations along the Northern Peninsula; B) Passive-margin shelf successions from Port au Port peninsula (black line) and north of Stephenville (gray line) in southwestern Newfoundland; C) Passive-margin slope successions from the Humber Arm allochthon at Cow Head; D) Rift and passive-margin slope succession from the Humber Arm allochthon at Humber Arm. See discussion in text for references.

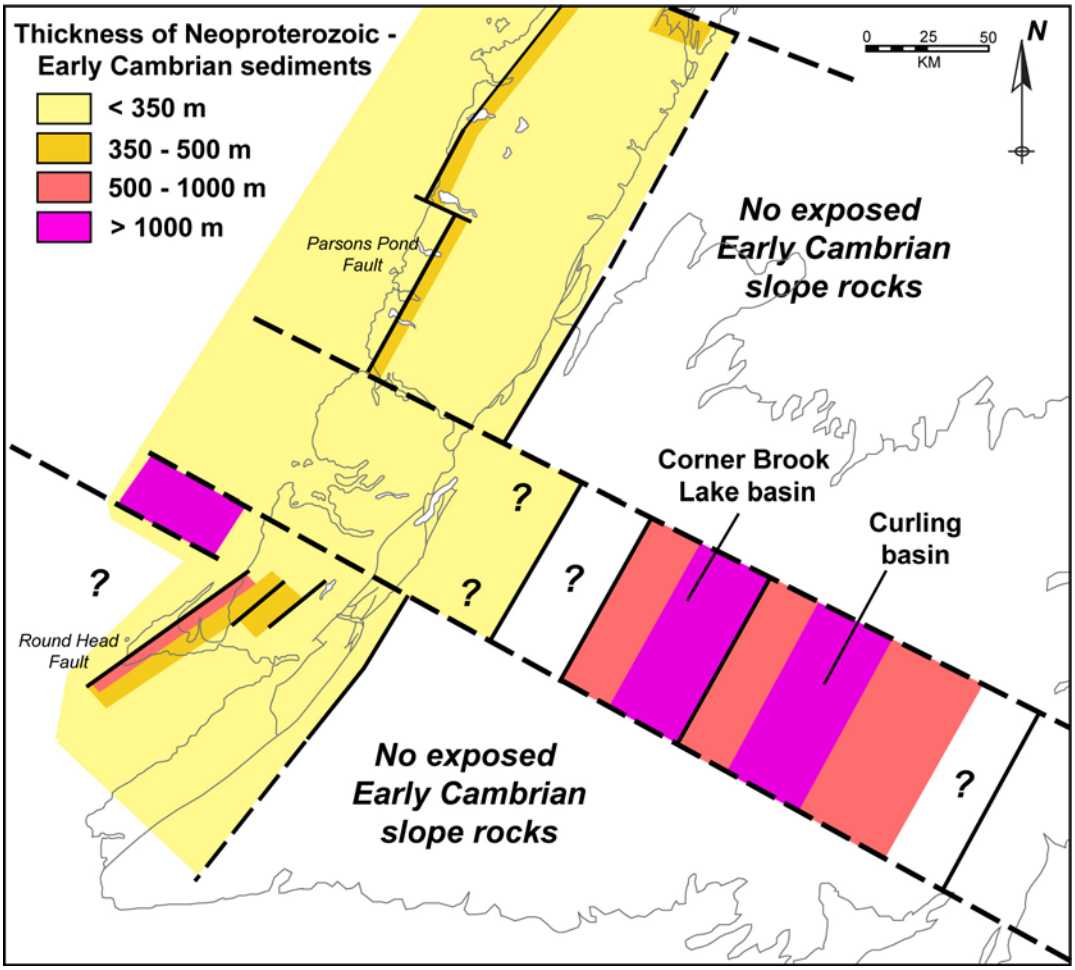

Figure 3.34. Palinspastic map of shelf and slope stratigraphy on the St. Lawrence promontory in western Newfoundland at the top of the Lower Cambrian.

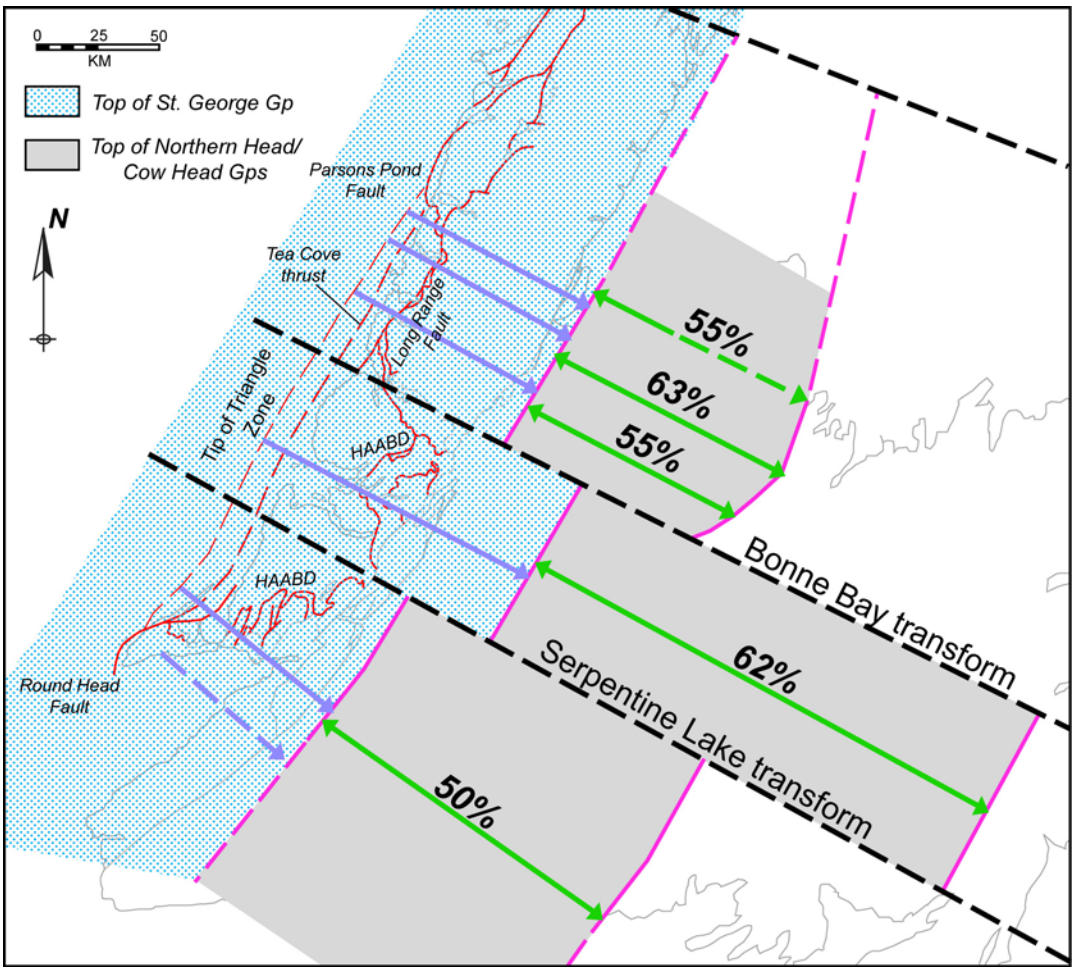

Figure 3.35. Palinspastic map of shelf and slope stratigraphy on the St. Lawrence promontory in western Newfoundland at the top of the Lower Ordovician. Numbers indicate amount of total shortening in the allochthon.

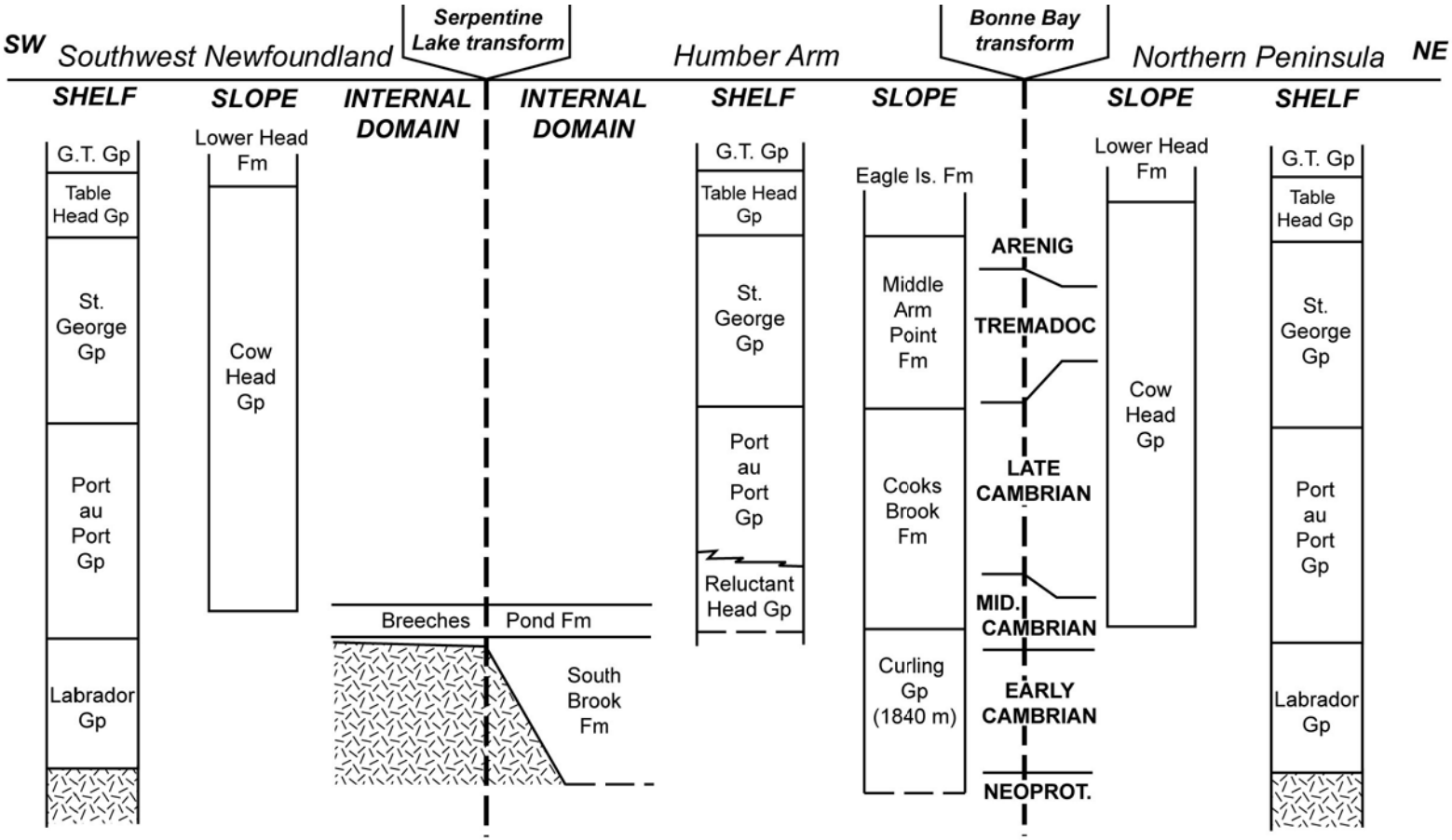

Figure 3.36. Chart illustrating the along-strike contrasts in the shelf, slope, and internal domain stratigraphy across the Serpentine Lake and Bonne Bay transforms. Shelf and slope stratigraphic units are depicted according to age.

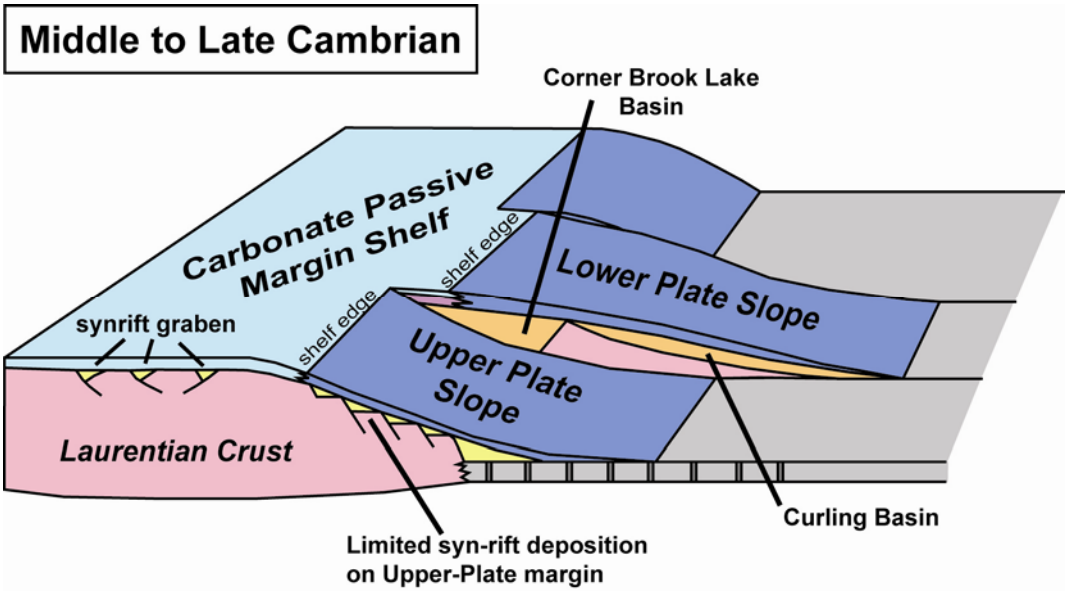

Figure 3.37. Three-dimensional block diagram illustrating the upper-plate and lower-plate structural configuration of the St. Lawrence promontory with corresponding rift and passive-margin successions.

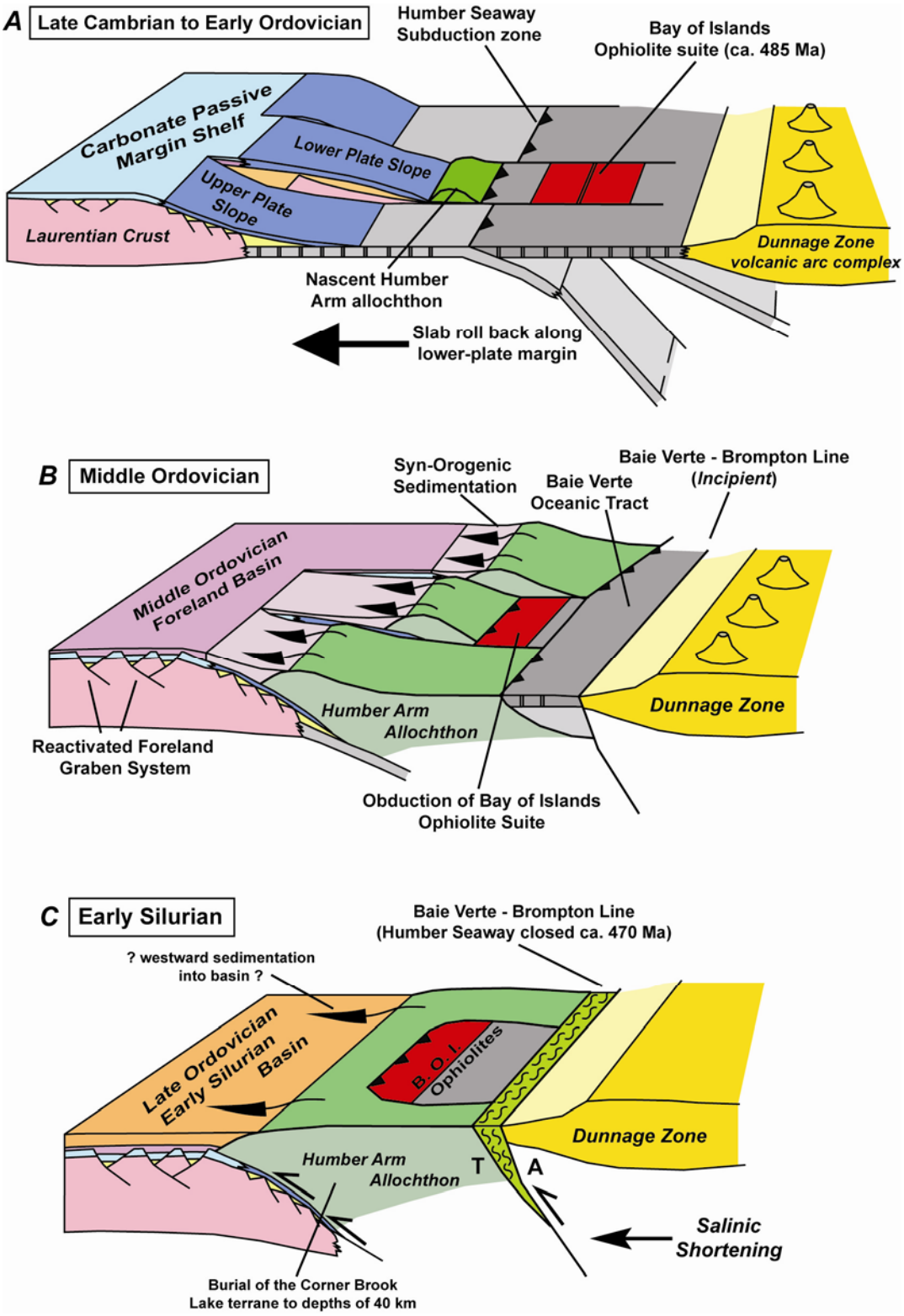

Figure 3.38. Diagrams A, B, and C. Full caption on the following page.

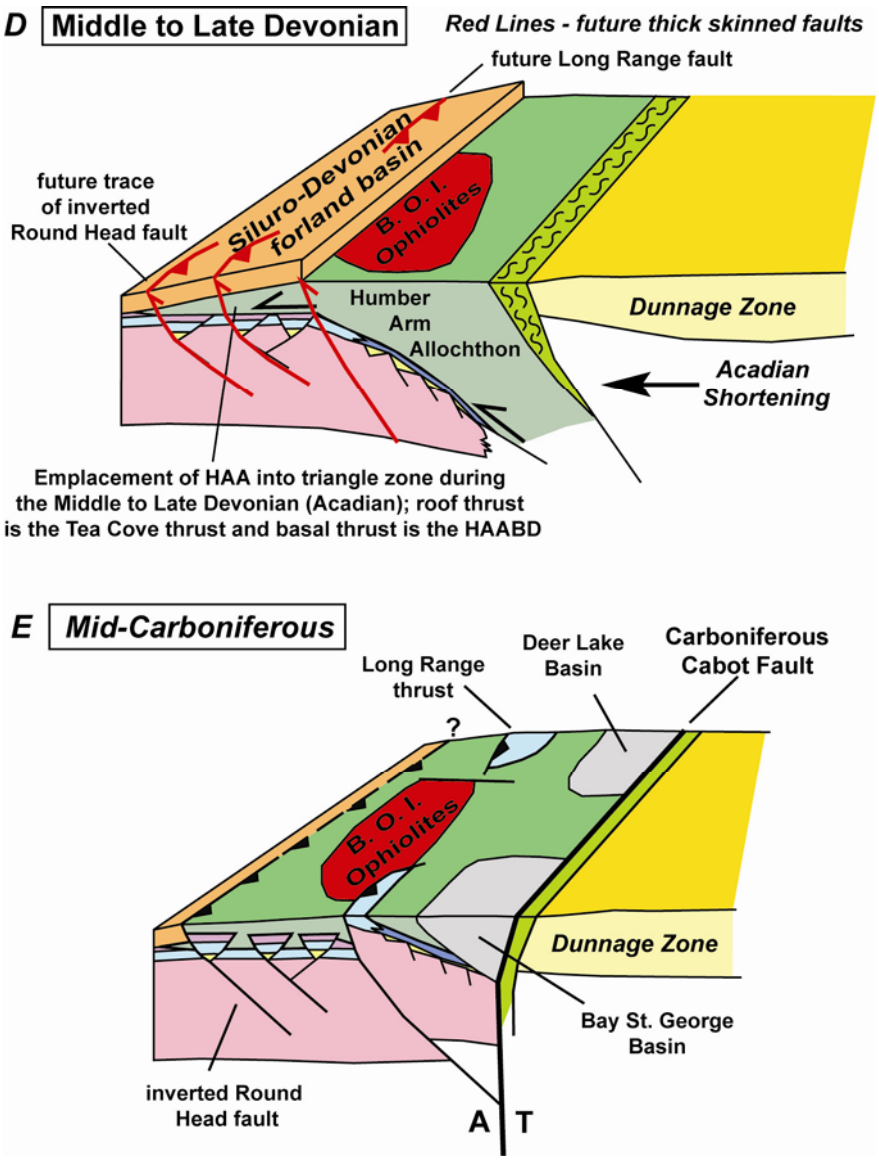

Figure 3.38 (continued). A sequence of three-dimensional interpretative block diagrams illustrating the Paleozoic tectonic evolution of the St. Lawrence promontory. A) Late Cambrian-Early Ordovician tectonic environment within the Humber Seaway just prior to collision of the St. Lawrence promontory with oceanic elements in the Dunnage zone; B) Middle Ordovician Taconic orogen; C) Early Silurian Salinic orogeny; D) Middle to Late Devonian Acadian orogeny; E) St. Lawrence promontory during Middle Carboniferous Alleghanian strike-slip tectonics. A detailed discussion of each stage appears in the text. Abbreviations: HAA = Humber Arm allochthon; HAABD = Humber Arm allochthon basal detachment.

CHAPTER 4 - PROVENANCE OF IAPETAN SYNRIFT SEDIMENTARY ACCUMULATIONS ON THE ST. LAWRENCE PROMONTORY, WESTERN NEWFOUNDLAND: PALEOGEOGRAPHIC CONSTRAINTS FROM U-PB AGE DATING AND LU-HF ISOTOPES FROM DETRITAL ZIRCON

4.1 INTRODUCTION

Latest Neoproterozoic to Early Cambrian continental rifting and breakup of the supercontinent Rodinia framed the continental margins of eastern Laurentia and the departing conjugate cratons around the opening Iapetus Ocean (Hoffman, 1991; Cawood et al., 2001). Along the eastern Laurentian margin, continental extension by a low-angle detachment system produced a zig-zag set of promontories and embayments that accumulated variable amounts of sedimentary detritus, presumably from Laurentia and its neighboring cratons (Thomas, 1977; 1993; Allen et al., 2009). In the Appalachians of western Newfoundland, the eastern Laurentian rifted margin is manifest as the St. Lawrence promontory (Figure 4.1). Although much is now known concerning the subsequent structure, stratigraphy, and tectonic history of the eastern Laurentian margin, the identity of conjugate cratons in the reconstruction of Rodinia to specific segments of the Laurentian margin (i.e., St. Lawrence promontory) remains largely unresolved. Previous studies have narrowed the potential conjugates to the St. Lawrence promontory to either Baltica or Amazonia (e.g., Dalziel, 1997; Cawood and Pisarevsky, 2006). Either of these cratons may have left a geochemical fingerprint on the St. Lawrence promontory preserved in the form of U-Pb ages and Lu-Hf isotopes in detrital zircon deposited as part of the synrift sedimentary record.

Detrital zircons are one of the most effective means for recognizing terrane/cratonic signals in the sedimentary record (e.g., Mueller et al., 1994, Cawood and Nemchin, 2001; Mueller et al., 2007a). The most significant issue, however, with any Appalachian detrital-zircon study is the dominance of Mesoproterozoic zircons in a vast majority of Paleozoic Laurentian sedimentary samples (e.g., Stewart et al., 2001; Eriksson et al., 2003). This overabundance of ca. 1.0 Ga detrital zircons has been attributed to an overabundance of zircon in 1.0 Ga igneous rocks (e.g., Moecher and Samson, 2006), which, along with their metamorphic derivatives, formed as a result of accretion of cratonic and oceanic elements to Laurentia during the Grenville orogeny

from 1350-1000 Ma (e.g., McClelland et al., 1996; 2001; Rivers, 1997; Whitmeyer and Karlstrom, 2007). Although detrital-zircon U-Pb age populations of post-Grenville age sedimentary rocks in Laurentia commonly are dominated by 1.0 Ga grains, detrital zircons still offer one of the best tools available to determine the provenance of sedimentary rocks for two principal reasons: 1) the cratons proposed as conjugates have distinctive age distributions compared to Laurentia; and 2) zircons provide the opportunity to measure Lu-Hf isotopes, which can allow for distinctions between zircons of similar age that were derived from cratons with distinct crustal histories (e.g., Mueller et al., 2007). Analysis of detrital zircon by in-situ laser ablation microprobe inductively coupled plasma-mass spectrometry (LAM-ICP-MS) allows for rapid acquisition of large sets of isotopic data which can be useful to determine the relative distribution of detrital age populations within a clastic sample, identify paleogeographic terranes, and interpret changes in provenance due to tectonics.

This paper presents detrital-zircon U-Pb geochronologic and Lu-Hf isotopic data from rift-related sediments collected from the late Neoproterozoic-Early Cambrian margin of eastern Laurentia along the St. Lawrence promontory, western Newfoundland. The aim of this paper is to determine the identity of cratons that were conjugate to the St. Lawrence promontory in the Rodinia assembly by characterizing the provenance of detrital zircon in synrift sedimentary deposits. Synrift sediments with a provenance exotic to the Laurentian craton must have been derived from one or more cratons that bordered the Iapetan rift as Rodinia broke apart during the Neoproterozoic. Our results highlight a broad similarity between the crustal histories of eastern Laurentia and Baltica during the Mesoproterozoic, implying that the two cratons share a similar tectonic history over this time period. Furthermore, when combined with other tectonic and paleomagnetic data from Laurentia, Baltica, and Amazonia, the detrital zircon data presented herein provide important constraints on the paleogeographic evolution of the St. Lawrence promontory during the Proterozoic.

4.2 REGIONAL TECTONIC SETTING

The deformed eastern continental margin of Laurentia is represented by the Humber zone, which extends continuously along strike from northern Mexico to

Newfoundland (e.g. Thomas, 1977; Williams, 1979; Williams and Hatcher, 1983; Williams, 1995). On the St. Lawrence promontory in western Newfoundland, the Humber zone consists of Proterozoic crystalline basement unconformably overlain by stratigraphic successions that record a nearly continuous record of continental-margin initiation and destruction associated with the opening and closing of the Iapetus Ocean (e.g., Waldron et al., 1998). A western external domain consists of parautochthonous, late Neoproterozoic to Middle Ordovician, clastic and shelf-carbonate succession that are in places structurally overlain by a transported succession of coeval continental slope and basin deposits (Humber Arm and Hare Bay allochthons). An eastern internal domain contains rocks that have been complexly deformed and metamorphosed to upper greenschist and amphibolite (locally eclogite) facies, yet lithodemically resemble shelf and slope deposits in the western external domain (Williams et al., 1995; Cawood et al., 1996).

On the St. Lawrence promontory, a dynamic succession of Neoproterozoic through Middle Ordovician clastic and carbonate deposits record protracted continental rifting followed by the onset of passive-margin thermal subsidence. Rift-related sequences consist predominantly of siliciclastic strata that display abrupt along-strike changes in facies and thickness, are interlayered with and intruded by Neoproterozoic-Early Cambrian alkalic volcanic-plutonic suites, and commonly overlie Laurentian basement unconformably. Systematic lateral variations in the character of Iapetan synrift successions imply a complex and profound basement structure that mimics proposed models for continental extension by a low-angle detachment system. The distribution of thin, Early Cambrian shallow-marine rift clastic deposits along some parts of the Humber zone (e.g., Port au Port peninsula, west of Long Range massif), along with the relatively narrow implied transition from continental crust to oceanic crust as indicated from palinspastic restorations (see Chapter 3), suggest that these are upper-plate rift segments (Figure 4.2). Elsewhere, rift deposits are an order of magnitude thicker, palinspastically restore over a more attenuated continental margin, and are as old as the Neoproteorzoic, indicating rapid subsidence related to the evolution of a lower-plate rift segment (Figure 4.2). Zones of along-strike stratigraphic transition between each of the rift segments on the St. Lawrence promontory are abrupt and coincide with northwest-trending linear

gravity anomalies, which is consistent with transform faults offsetting upper- and lower-plate rift domains in a complex low-angle detachment rift system (e.g., Lister et al., 1986).

Subsequent Paleozoic deformation related to the Appalachian orogenic cycle has obscured the eastern Laurentian rift and, in some places, displaced synrift strata as much as 100 km. Closure of the Iapetus Ocean between the Ordovician and Devonian produced a dynamic foreland basin in the Humber zone, generated ophiolites that are now structurally emplaced on the Humber Arm allochthon, metamorphosed parts of the Laurentian margin, and uplifted large massifs of crystalline Laurentian basement (e.g., Williams, 1995; Waldron et al., 1998; van Staal et al., 1998). While deformation of the Laurentian margin by later Paleozoic orogenic cycles may seem an obstacle to investigation of the early Iapetan rift, Appalachian Paleozoic deformation works to our advantage in allowing for direct observation of vestiges of the eastern Laurentian Iapetan rift stratigraphy.

4.2.1 Local Synrift Stratigraphy

Synrift stratigraphy in the Humber zone is characterized by a mixed clastic-volcanic succession that displays abrupt lateral changes in both thickness and facies, contrasting sharply with the uniform thickness and broad lateral continuity of overlying passive-margin formations (Thomas, 1977; Williams and Hiscott, 1987). Abrupt lateral variations in the thickness, age, facies, and composition of rift sediments suggests that the eastern Laurentian rift developed as a low-angle detachment rift system partitioned by northwest-trending transform faults (Allen et al., 2009). The synrift succession in western Newfoundland is broadly expressed in the Labrador Group, the Curling Group, and the Mount Musgrave Group, which are distributed across the Humber zone.

The Labrador Group consists of a Neoproterozoic to Early Cambrian clastic-volcanic succession with minor carbonate that unconformably overlies ≥1.0 Ga crystalline basement. Local geologic evidence indicates that parts of the Labrador Group were deposited in extensional graben related to the opening of Iapetus Ocean (see Chapters 2 and 3). Outside the extent of local synrift accumulations on Belle Isle, immature, fluvial and shallow-marine, red sandstones of the Bradore Formation lie

unconformably on Laurentian basement across eastern Labrador and western Newfoundland (Williams and Hiscott, 1987). Sparse biostratigraphic data from the formation in southern Labrador suggest an Early Cambrian age; limestone and shale in the overlying Forteau Formation contain abundant trilobite and archeocyathan fauna of late-Early Cambrian age (Williams and Hiscott, 1987). Stratigraphic sections and deep well data indicate that the Bradore Formation ranges in thickness from ≤5 m to 175 m and that it is commonly thickest in the hanging wall of steep basement faults (Bostock, 1983; Williams and Hiscott, 1987; Knight, 1991; 2003; Copper et al., 2001), suggesting that parts of the Bardore Formation were deposited in an Iapetan synrift environment (see Chapter 3).

Rift-related rocks of the Curling Group are the more distal time-equivalents of clastic deposits in the Labrador Group (e.g., Botsford, 1988; Palmer et al., 2001). These rocks are exposed only within the Humber Arm allochthon, which has experienced at least 130 km of westward displacement during the Paleozoic Appalachian orogenic cycle (see Chapter 3). Synrift deposits of the Curling Group are distributed between various thrust sheets that are aerially extensive and best exposed along the shore of Humber Arm in the Bay of Islands region (Figure 4.1). The base of the Curling Group lies along a thin-skinned thrust fault system that emplaced the Humber Arm allochthon onto the continental margin without incorporating underlying Laurentian basement. Thus, nowhere are sedimentary deposits of the Curling Group observed overlying crystalline basement.

The stratigraphically lowest unit in the Curling Group is the Summerside Formation (Figure 4.3), which is a 700-m-thick succession of red to grey-green shale interlayered with medium to very thick beds of coarse-grained arkosic sandstone (Palmer et al., 2001). Thicker beds of sandstone tend to be massive and contain isolated elongate plates of red and green shale; whereas finer sandstone beds are typically graded and cross-laminated, and display abundant dewatering structures. The base of the Summerside Formation is tectonic; the stratigraphic base of the formation is unexposed. No body fossils have been reported from the Summerside Formation; however, a late Neoproterozoic to Early Cambrian age has been estimated for the formation on the basis of palynomorphic assemblages and trace fossils in the uppermost shale beds (Waldron

and Palmer, 2000; Palmer et al., 2001). Conformably overlying Summerside Formation is the Irishtown Formation, which is consists of black and dark grey, graphitic, pyrite-bearing sandstone and shale with a measured thickness of 1140 m and a palinspastic thickness of 1400 m (Palmer et al., 2001, Chapter 3). The most abundant rock type is black shale. Sandstones in the Irishtown Formation are dark gray to black, quartz-rich, and have a glossy, sugary texture that distinguishes them from sandstone in the underlying Summerside Formation. Typical bedding structures include flute clasts on basal surfaces, groves, and load casts. Lenticular beds of polymictic conglomerate are locally present but pinchout laterally. The age of the Irishtown is constrained by late-Early Cambrian fossils in limestone clasts within conglomerates near the top of the formation (Stevens, 1970; James et al., 1989); however, the base of the Irishtown Formation may extend lower into the Early Cambrian (Waldron and Palmer, 2000).

Rocks of the Mount Musgrave Group (Cawood and van Gool, 1998) in the Corner Brook Lake terrane (Figure 4.1) are interpreted to represent the polydeformed and metamorphosed equivalents of the synrift and passive-margin succession exposed in the external domain of the Humber zone (Hibbard, 1983; 1988; Cawood et al., 1995). The Corner Brook Lake terrane is juxtaposed against both parautochthonous shelf successions and slope deposits in the Humber Arm allochthon in different places along the Humber River fault system (Cawood and van Gool, 1998; Waldron et al., 2003). Metaclastic assemblages of the Mount Musgrave Group in the basal South Brook Formation consist of a quartz-rich metasedimentary package of metagreywacke, schist, paragneiss, and metaconglomerate with minor amphibolite (Cawood et al., 1995) (Figure 4.3). Rocks in the South Brook Formation unconformably overlie Precambrian crystalline basement, as well as several peralkaline intrusive suites with Iapetan synrift ages (Cawood and van Gool, 1998; Cawood et al., 2001). The thickness of the South Brook Formation varies considerably, from 5 m to several thousands of meters (Cawood and van Gool, 1998), although a maximum thickness is not currently known because of deformation and metamorphism. Overlying the metaclastic South Brook Formation is an extensive metacarbonate cover succession termed the Breeches Pond Formation (Figure 4.3) (Cawood and van Gool, 1998).

The degree of deformation and metamorphism makes assigning the South Brook Formation an age by fossil assemblage essentially impossible. The gross similarity between rock types in the South Brook Formation and known synrift stratigraphic successions in the Curling and Labrador Groups suggests that metaclastic rocks in the South Brook Formation were deposited in an Iapetan rift setting. The age of the South Brook Formation can be constrained by underlying late Neoproterozoic synrift plutons (555 +3/-5 Ma, Lady Slipper pluton; 602±10 Ma, Round Pond granite; e.g., Cawood et al., 2001) and deposits in the overlying metacarbonate Breeches Pond Formation, which are identical to Middle Cambrian passive-margin slope deposits (e.g., Cow Head Group; Pinchgut Lake Group) (e.g. Waldron et al., 2003). Thus, the available data suggest that the South Brook Formation was deposited between the late Neoproterozoic and Middle Cambrian.

4.3 METHODOLOGY.

4.3.1 Sampling Strategy.

U-Pb ages and Lu-Hf isotopic concentrations from a total of 524 zircon grains were analyzed from seven samples of Neoproterozoic-Early Cambrian rift-related (meta)clastic rocks and two samples of Precambrian crystalline basement (Figures 4.1 and 4.3). Sample selection from individual rock units was based on solving specific geologic problems. Three samples of rift-related clastic rocks were collected from a vertical stratigraphic section through the Curling Group (CB-219, CB-259, CB-260, Figure 4.3) to test for temporal variations in the isotopic composition and provenance of synrift detritus. Two samples of metaclastic rocks were collected from the South Brook Formation (CB-212, CB-230, Figure 4.3) to test whether synrift detritus shed into the Corner Brook Lake terrane shares a genetic relationship with synrift rocks in the Curling Group. To aid in distinguishing Laurentian detrital input into rift basins on the St. Lawrence promontory from other potential exotic sedimentary detritus, two samples of Laurentian crystalline basement were collected (STV-30A, NP-10A, Figure 4.3), as well as two sandstones from the Bradore Formation (STV-30, NP-10, Figure 4.3) within 2 m of the Proterozoic-Paleozoic unconformity. These basement-cover samples represent the exposed and eroded eastern Laurentian continental margin upon which the rift and

passive margin was developed, thus, they are the best candidates for direct contribution of Laurentian sedimentary detritus into the opening Iapetan rift.

4.3.2 U-Pb and Lu-Hf Analytical Techniques.

Zircons were separated from 5 to 10 kg of sample at the Department of Geological Sciences, University of Florida (UF), using conventional methods (i.e., crushing, water table, heavy liquids, and magnetic separation). Individual grains were hand-picked under a binocular microscope from the least magnetic separates obtained from the Frantz^{TM} isodynamic separator (typically 4˚ non-magnetic split). Between 100 and 160 zircons were selected from each sample and then mounted in a 2.5 cm diameter epoxy filled mount. The dried mounts were then polished to expose even surfaces at the cores of the zircon grains for analysis. No cathodeluminesence or back-scatter images were obtained for these zircons; however, prior to mounting, zircons of different color and morphology were intentionally included into each mount in order to obtain a diverse range of zircon populations and to minimize possible omission of zircons from rare age groups.

In-situ U-Pb and Hf isotopic analyses were conducted at UF on a Nu Plasma multicollector plasma source mass spectrometer (MC-ICP-MS), which is equipped with three ion counters and 12 Faraday detectors. Mounted zircon grains were ablated in a He atmosphere using a New Wave 213-nm ultraviolet laser. During ablation, the sample was mounted on a computer-driven motorized stage underneath the microscope and moved beneath the stationary laser for each analysis. For U-Pb isotopic analyses, the specially designed collector block equipped to the MC-ICP-MS was set for simultaneous acquisition of ^{204}Pb (^{204}Hg), ^{206}Pb, and ^{207}Pb signals on the ion-counters and ^{235}U and ^{238}U signals on Faraday detectors. The sample was decrepitated in a He stream and then mixed with Ar gas (gas flows optimized daily) for sample transport into the mass spectrometer. Actual ablation during U-Pb analyses proceeded for 30 s with the laser set to a diameter of 30 um at 50% intensity at 5-6 Hz to minimize ablation pit depth and elemental fractionation. The isotopic data were acquired using the Nu-Instruments Time Resolved Analysis software, which allowed isotopic ratios to be calculated from data acquired at specific time intervals.

Data calibration and drift corrections for the U-Pb analyses at the UF laboratory were routinely checked against the FC-1 zircon standard (Duluth Gabbro), which has been previously described by Paces and Miller (1993) and Black et al. (2003). To monitor the accuracy, reproducibility, and efficiency of each analysis, the FC-1 standard was analyzed twice at the beginning of each session and then once before and after every ten unknowns. Age calculations were made using the ^{238}U (1.55125×10^{-10} yr^{-1}) and ^{235}U (9.8485×10^{-10} yr^{-1}) decay constants and the present day ^{238}U /^{235}U ratio of 137.88 (Jaffey et al., 1971). Age data generated from the U-Pb zircon isotopic analyses were reduced with in-house software; zircon ages with greater than 10% discordance were discarded from the data set. No common Pb correction was applied to the data. Final ages and Concordia diagrams were calculated using Isoplot (Ludwig, 2003). Analyzed ages range in age from Archean to latest Neoproterozoic. Ages older than 1000 Ma were calculated from the $^{206}Pb/^{207}Pb$ ratios, which have a much smaller error at ages of 1.0 Ga and older. For ages younger than 1000 Ma, $^{206}Pb/^{235}U$ ratios are reported, except for those with a calculated error for $^{206}Pb/^{207}Pb$ ratios less than the calculated error for $^{206}Pb/^{235}U$ ratios (which is typical for ages that are slightly less than 1.0 Ga).

For Hf isotopic analyses, ^{180}Hf, ^{178}Hf, ^{177}Hf, ^{176}Hf, ^{175}Lu, ^{174}Hf, and ^{172}Yb measurements were made simultaneously in static mode on the Faraday detectors. Ablation during Hf analyses proceeded for 60 s with the laser diameter set to 50-60 um for maximum surface area sampling to ensure that enough material was ablated for a precise analysis. The analyses were preformed with on-line Lu and Yb isobaric interference corrections, using $^{176}Lu/^{175}Lu = 0.02653$ and $^{176}Yb/^{172}Yb = 0.5870$, which are within the range of published values (Vervoort et al., 2004). All isotopic ratios were corrected for mass bias using $^{178}Hf/^{177}Hf = 1.46718$. Measured and mass-bais-corrected $^{176}Lu/^{175}Lu$ ratios were used to calculate initial $^{176}Hf/^{177}Hf$ ratios, after Griffin et al. (2000; 2002). Because of the very low Lu/Hf ratios in zircon, the difference between the present-day measured and calculated initial $^{176}Hf/^{177}Hf$ ratios is typically <1 ε unit. To ensure accuracy of the measurement, FC-1 standards were analyzed once before and after every 15 unknowns. Multiple analyses of FC-1 yielded a mean $^{176}Hf/^{177}Hf = 0.282182$ (± 0.000013, 2σ, $n = 36$), which is statistically indistinguishable from previous analyses of the FC-1 standard dissolved and aspirated into a dry plasma ($^{176}Hf/^{177}Hf = 0.282174 \pm$

0.000013, 2σ; data from Mueller et al., 2008), as well as from a previous report published by Woodhead and Hergt (2005; $^{176}Hf/^{177}Hf = 0.282172 \pm 0.000042$, 2σ). For the calculation of ε_{Hf} values, we have adopted the recently reported chondritic values of Bouvier et al. (2008). Depleted-mantle values are based on a linear model ($\varepsilon_{Hf} = 0$ at 4.56 Ga and 15.6 at 0 Ga); whereas Lu/Hf CHUR parameters are $^{176}Lu/^{177}Hf = 0.0336$ (±0.0001, 2σ) and $^{176}Hf/^{177}Hf = 0.282785$ (±0.000011, 2σ), which are higher than previously reported estimates (Bouvier et al., 2008). The ^{176}Lu decay constant (1.867×10^{-11} yr^{-1}) is after Soderlund et al. (2004).

4.4 SAMPLE DESCRIPTIONS AND DATA.

Results from the U-Pb analyses are listed in Table 4.1, and the results of Lu/Hf analyses are displayed in Table 4.2. The U-Pb ages of zircons from all samples of Neoproterozoic-Cambrian Laurentian synrift sedimentary deposits range from Archean to late Neoproterozoic. Zircons from two samples of underlying Laurentian crystalline basement have Mesoproterozoic ages. Calculated initial $^{176}Hf/^{177}Hf$ ratios from individual zircon grains range from 0.282546 to 0.280403 (ε_{Hf} between +10.2 and -17.7). Analysis of the U-Pb data set allows for zircons to be categorized into common age groups that differ in the total percentage of zircon represented within each group. Analysis of the Hf data set reveals variation in the Hf composition within each age group, implying contribution of zircon from source rocks of similar age but varying magmatic/tectonic background. The following sections are divided into basement-cover samples, synrift samples, and metaclastic samples.

4.4.1 Basement-Cover Samples.

Laurentian Basement #1 (NP-10A)

Laurentian crystalline basement rocks throughout the Humber zone are in discrete fault bounded massifs, the most prominent being the ~8500 km^2 Long Range massif on the Northern Peninsula (Figure 4.1). These basement massifs typically consist of gneiss, schist, granitoids, and local metabasic rocks that are commonly correlated with the amphibolite-granulite gneissic terranes in nearby Labrador and Quebec (e.g., Williams, 1995; Heaman et al., 2002).

A sample of Laurentian crystalline basement (NP-10A) was collected from the eastern flank of the Long Range inlier along Cat Arm Road near White Bay approximately 1 km north of Apsy Cove Pond (E 0512691/N 5529368). This sample of basement, along with the overlying sandstone (NP-10, see below), was chosen because it represents the easternmost exposed example of autochthonous basement and sedimentary cover. A previous study reported that basement in this region consists of reworked, medium crystalline granite and granitic gneiss of probable Labradorian age (two zircon fractions with upper intercept ages of 1631±1 Ma and 1533±1 Ma) that is intruded by a complex granitic and granodioritic sills and dikes that fall into an age range between ~1032 Ma and 990 Ma (Heaman et al., 2002). The sample collected for this study consists of a dark, medium- to medium-coarse crystalline granite with conspicuous, coarse (>5 mm), pink K-feldspar idioblasts surrounded in an igneous matrix of quartz, epidote, biotite, and plagioclase.

A total of 38 zircons was analyzed with an overwhelming dominance of late Mesoproterozoic ages (n = 34; 89%) that cluster around a sharp peak of ca. 1043 Ma on the cumulative probability plot, with four slightly older peaks between 1120 Ma and 1220 Ma (Figure 4.4). All of the zircons analyzed for U-Pb isotopes plot on or near Concordia (Figure 4.5). Excluding the 4 older crystals, U-Pb zircon ages from the analyzed sample have a weighted average of 1045±5.7 Ma (95% confidence, MSWD = 5.5). Zircon crystals from the ca. 1043 Ma age group show a narrow range of ε_{Hf} values that fall between +0.1 and +3.5 ($^{176}Hf/^{177}Hf$ = 0.282222 – 0.282134) (Figure 4.6). The older zircons, range in ε_{Hf} between +2.0 and +4.0 ($^{176}Hf/^{177}Hf$ = 0.282129-0.282155).

Bradore Formation #1 – Labrador Group (NP-10)

Sample NP-10 was collected from the Bradore Formation approximately 1.5 m above the sample location for the basement granite sample NP-10A. Here, the Bradore Formation is approximately 15 m thick. The sample consists of a dark, medium- to coarse-grained, thin-bedded to massive, partially recrystallized sandstone. Sedimentary grains consist of sub-angular to rounded quartz; the percentage of detrital feldspar and mica increases toward the nonconformable contact with underlying basement. The contact between the Bradore Formation at NP-10 and crystalline basement is well

exposed, sharp, and parallel to bedding in the overlying sandstone (Figure 4.7A); a 10 cm thick bed of very coarse, massive arkose lies just above the contact.

Analyzed detrital zircon grains (n = 60) within the sample lie near or on Condordia (Figure 4.5). Analyzed zircons are almost exclusively Mesoproterozoic in age; the oldest grain is dated at 1523±4.2 Ma and the youngest at 988±3.9 Ma. Age groups define a strong bimodal distribution on the cumulative probability plot (Figure 4.4) with 29 analyses (48%) in an age cluster around ca. 1030 Ma and second cluster of 24 analyses (40%) around ca. 1135 Ma. Another 5 grains yield ages between 1266±7.2 Ma and 1506±4.1 Ma, defining a series of smaller peaks on the cumulative probability diagram (Figure 4.4). Because of the consistency of U-Pb ages recovered from detrital zircons analyzed in sample NP-10, only 50 out of the 60 total grains were analyzed for Lu/Hf concentrations. Hf analyses reveal that zircon grains in the younger age group have a slightly lower range of ε_{Hf} values (-0.8 to +3.8; $^{176}Hf/^{177}Hf = 0.282233\text{-}0.282134$) than zircons that in the ca. 1135 Ma age group, which have ε_{Hf} values between +0.3 and +5.2 ($^{176}Hf/^{177}Hf = 0.282217\text{-}0.282140$) (Figure 4.6). The six older grains have ε_{Hf} values that range between +5.0 and +10.2, which places them near the calculated Hf value for depleted mantle.

Laurentian Basement #2 (STV-30A)

The other sample of crystalline Laurentian basement (STV-30A) was collected from a logging road outcrop in the Indian Head range of southwest Newfoundland approximately 28 km north-northeast of Stephenville (Figure 4.1) (E 0393708/N 5394102). Crystalline basement within the Indian Head range has been exhumed along steep dipping basement faults that outline a set of late Paleozoic pop-up structures, which are likely reactivated synrift- and foreland-basin graben systems (Palmer et al., 2002; Chapter 3). The outcrop location for STV-30A constitutes the eroded core of the Phillips Brook structure, which displays evidence of both normal and reverse faulting (see Chapter 3). The sample consists of a pink, phaneritic granitic gneiss that is intruded in places by red, fine- to medium- crystalline granite veins and dikes. Common mineral phases in both the gneiss and granitic intrusions are K-feldspar, plagioclase, quartz, biotite, and epidote with foliation defined by aligned biotite and feldspar.

The vast majority of zircon crystals from STV-30A (n = 39) plot on or near Concordia (Figure 4.5) within a single early Mesoproterozioc age group between 1470 Ma and 1520 Ma. U-Pb ages make a unimodal peak centered around 1495 Ma on a cumulative probability plot (Figure 4.4) and have a weighted mean age of 1491±3.3 Ma (95% confidence, MSWD = 3.4). One zircon plots slightly off Concordia at 1371±17 Ma. Because of the overall consistency of U-Pb analyses, only 30 zircons were analyzed for Lu/Hf concentrations. Crystals in the unimodal 1470-1520 Ma age group display a tight range of ε_{Hf} values that fall between +3.9 and +7.4 ($^{176}Hf/^{177}Hf$ = 0.282053-0.281971) (Figure 4.6).

Bradore Formation #2 – Labrador Group (STV-30)

The sample of Bradore Formation (STV-30) was collected approximately two meters above the sample location of basement sample STV-30A. At this location, the Bradore Formation is moderately well exposed, 5 to 10 m thick, and consists of a light pink, medium- to coarse-grained, medium-bedded sandstone. Bedding displays cross-beds and trough cross-beds (Figure 4.7B). The unconformity with the underlying granitic gneiss is not well exposed; however, within one meter of the basement contact the Bradore Formation is a reddish purple, poorly sorted, massive, conglomerate with angular to sub-rounded clasts of feldspar and vein quartz. The conglomeratic facies grades upward into a poorly sorted sandstone, which in turn passes upward into shale of the Forteau Formation.

Nearly all of the analyzed zircon grains (n = 59) plot around Concordia within the late Mesoproterozoic (Figure 4.5). The dominant age group defines a sharp, unimodal peak on a cumulative probability plot around ca. 1135 Ma (Figure 4.4); 49 grains (83%) define an age group between 1080 Ma and 1165 Ma. Of the remaining analyses, 10 grains (17%) have younger ages that range between 990 Ma and 1070 Ma, whereas a single grain has an older age of 1219±22 Ma. Of the 59 total U-Pb detrital zircon analyses, only 40 grains were analyzed for Lu/Hf concentrations because of the consistency of the analyzed U-Pb isotopic ages. Zircons in the older, dominant age group (1080-1165 Ma) have ε_{Hf} values between +0.8 and +6.1 ($^{176}Hf/^{177}Hf$ = 0.282101-

0.282250) (Figure 4.6). Younger zircon grains on the other hand have slightly more evolved ε_{Hf} values (between -1.7 and +2.2; $^{176}Hf/^{177}Hf$ = 0.282120-0.282190).

4.4.2 Synrift Samples.

Summerside Formation – Curling Group (CB-219)

Sample CB-219 was collected from a 20 m thick sandstone bed in the Summerside Formation at a road side outcrop along Highway 440, which follows the northern shore of Humber Arm (E 0429615/N 5425259) (Figure 4.1). This particular bed is the stratigraphically lowest sandstone bed mapped within the Summerside Formation, lying approximately ~30 m from the inferred base of the Curling Group (Figure 4.3). The sample is a light gray, coarse- to very coarse-grained, massive, arkosic sandstone consisting predominantly of rounded to sub-angular quartz and feldspar (Figure 4.7C).

The analyzed grains (n = 64) within the sample lie on or near Concordia (Figure 4.8). The oldest analyzed grain has an age of 1521±5.5 Ma, whereas the youngest grain has an age of 582±9 Ma. The other analyses are separated into several age groups that span the Mesoproterozoic. The dominant group consists of 58 analyses (91%) that range from 980 to 1250 Ma and produce a sharp, bimodal peak on cumulative probability plots that are centered around 1040 Ma and 1140 Ma (Figure 4.9). A minor group consists of 4 analyses (6%) that range in age between 1400 and 1500 Ma, and an accessory group consists of the youngest zircon and one other grain with an age of 612±10 Ma. Of the 64 zircons analyzed for U-Pb, only 45 were selected for Hf analysis because of the consistency of U-Pb ages in the sample. Within the dominant age group, zircons with U-Pb ages that cluster around 1040 Ma have a range of ε_{Hf} values that fall between -1.1 and +3.4 ($^{176}Hf/^{177}Hf$ = 0.282106-0.282228) with one outlier at -7.5 (Figure 4.10). Grains in the ca. 1140 Ma age cluster have slightly more juvenile ε_{Hf} values that range between +2.0 and +6.0 ($^{176}Hf/^{177}Hf$ = 0.282111-0.282221). The older zircons are also predominantly juvenile (ε_{Hf} = +6.0 to +8.7), with one slightly negative outlier (ε_{Hf} = -1.3).

Summerside Formation – Curling Group (CB-259)

The analyzed sample CB-259 was collected along the north shore of Humber Arm 300 m west of Pettipas Point (E 0427575/N 5425635) (Figure 4.1). The sample was collected from the stratigraphically highest bed of Summerside sandstone beneath the Irishtown-Summerside contact (Figure 4.3). Sandstone beds at the top of the Summerside are medium bedded, are normally graded, have weakly developed cross laminations, and are interlayered with thin beds of black shale. The sample consists of a green, medium- to fine-grained sandstone composed predominantly of rounded quartz with a minor component of pyrite crystals. The sample location with respect to a vertical measured section of the Curling Group (e.g., Palmer et al., 2001) places it near the middle of the synrift succession at the transition from a shallow-marine, high-energy, active rift environment to a deep-marine, distal rift setting.

Analyzed U-Pb ages (n = 64) for detrital zircons from CB-259 range between 2932±4 Ma and 972±7 Ma, and individual analyses fall on or near Concordia (Figure 4.8). A large percentage of analyzed zircons (n = 37; 58%) fall into a late Mesoproterozoic age group that ranges between 970 and 1200 Ma. The distribution of these ages on a cumulative probability plot produces a polymodal distribution of peaks with the most dominant around 1078 Ma (Figure 4.9). Middle and early Mesoproterozoic ages (n = 17; 27%) fall into more constricted ranges of age clusters at 1300-1400 Ma and 1450-1600 Ma. The remaining analyses form smaller groups of late Paleoproterozoic and Archean ages with U-Pb analyses that range from 1600-1830 Ma and 2450-2930 Ma, respectively; producing smaller peaks on the cumulative probability diagram.

Because of the greater distribution of Archean, Paleoproterozoic, and Mesoproterozoic ages in sample CB-259, a greater percentage of detrital zircons in the sample was analyzed for Lu-Hf isotopes (n = 58). Analyzed detrital zircons that fall into the late Mesoproterozoic group (i.e., 970-1200 Ma) have a range of ε_{Hf} values that spans between -4.0 and +5.1 ($^{176}Hf/^{177}Hf$ = 0.282032-0.282280) (Figure 4.10), which is a greater range of ε_{Hf} than is observed in late Mesoproterozoic zircons from synrift sample CB-219. Older Mesoproterozoic zircons display an even greater range of ε_{Hf} (between -3.8 and +8.9; $^{176}Hf/^{177}Hf$ = 0.281845-0.282201). Late Paleoproterozoic zircons have a

range of ε_{Hf} values from -2.7 to +3.7 ($^{176}Hf/^{177}Hf$ = 0.281569-0.281825), whereas Archean zircons range from -5.4 to +3.6 ($^{176}Hf/^{177}Hf$ = 0.280876-0.281218).

Irishtown Formation – Curling Group (CB-260)

Sample CB-260 was collected from an outcrop of polymictic conglomerate in the Irishtown Formation near downtown Corner Brook (E 0431325/N 5423257) (Figure 4.1). This particular outcrop of conglomerate is inferred to lie near the top of the Irishtown Formation (Figure 4.3), thus placing it close to the stratigraphic transition from rift to passive margin. The outcrop was chosen for this reason, and because the diversity of polymitic clasts allows for the possibility of a sampling a diverse array of detrital zircon groups. Conglomeratic beds are thick (1-2 m) and contain poorly sorted, rounded clasts of shale, quartzite, limestone, and granitic gneiss (Figure 4.7D). Clast sizes range from <1 cm to >1 m in diameter. The analyzed sample was collected from a bed of matrix-supported conglomerate. Clast sizes in the sample range from ≤1 cm to 5 cm and consist primarily of shelf limestone fragments; however, some red and dark gray sandstone clasts were observed. Matrix consists of a light grey, well lithofied, clastic-calcareous mud.

U-Pb analyses (n = 69) plot on or near Concordia (Figure 4.8) with the oldest age at 3605±5 Ma and the youngest age at 544±8 Ma. The wide range in U-Pb isotopic ages appears as a diverse array of age groups on a cumulative probability density plot (Figure 4.9). A large proportion (n = 35; 51%) of analyses fall into a middle- and late-Mesoproterozoic age range. Another 26 analyses (38%) range between 1000 Ma and 1200 Ma, and produce a prominent late Mesoproterozoic peak on the probability diagram. Yet another 9 analyses (13%) fall into a 1260-1340 Ma age group. A smaller group of early Mesoproterozoic ages (n = 5; 7%) produces a set of smaller peaks on the cumulative probability plot between 1440 Ma and 1570 Ma (Figure 4.9). Paleoproterozoic analyses make up approximately 23% of the total population (n = 16) and, with the exception of one analysis with an age of 2118±5 Ma, fall into a late-Paleoproterozoic age range between ca. 1640 and 1900 Ma. The most prominent peak is centered around 1870 Ma on the probability density diagram. Archean zircons (n = 12; 17%) fall into a tight cluster of ages that range between ca. 2650 and 2840 Ma with a dominant peak at 2740 Ma. Two older outliers yield ages greater than 3000 Ma.

For the Lu/Hf isotopic analysis, 68 out 69 zircon grains were analyzed because of the great diversity in age groupings. Late Mesoprotoerozoic zircon grains in sample CB-260 show the greatest range of ε_{Hf} values (between -6.4 and +6.0; $^{176}Hf/^{177}Hf$ = 0.281967-0.282284), in contrast to zircons of the same vintage from the other two synrift samples (Figure 4.10). Older Mesoproterozoic grains (ca. 1200-1600 Ma) also show a wide distribution of ε_{Hf}, ranging between -8.3 and +8.6 ($^{176}Hf/^{177}Hf$ = 0.281712-0.282194). Paleoproterozoic aged zircons can be broken into two separate groups on the basis of both age and ε_{Hf} values: *i)* a late Paleoproterozoic group of zircons between 1600 and 1730 Ma (n = 5) with ε_{Hf} values between -0.6 and 6.8 ($^{176}Hf/^{177}Hf$ = 0.281716-0.281914); and *ii)* a middle Paleoproterozoic group between 1790 and 1900 Ma with one tight cluster of analyses (n = 5) between -1.1 and -1.9 ε_{Hf} ($^{176}Hf/^{177}Hf$ = 0.281540-0.281581) and a dispersed cluster (n = 5) of highly evolved ε_{Hf} values ranging between -17.7 and -8.5 ($^{176}Hf/^{177}Hf$ = 0.281102-0.281407) (Figure 4.10). Zircon grains with Archean U-Pb isotopic ages have ε_{Hf} values between of -0.3 to +3.9 ($^{176}Hf/^{177}Hf$ = 0.281022-0.281169), with the exception of two outliers that display highly evolved ε_{Hf} values of -8.5 and -11.3.

4.4.3 Metaclastic Samples.

South Brook Formation – Mount Musgrave Group (CB-212)

Sample CB-212 from the South Brook Formation was collected from an outcrop along Steady Brook near an access road on Marble Mountain (E 0441358/N 5421416) (Figure 4.1). The sample location is along the northwestern limb of the Yellow Marsh anticlinorium and has experienced Biotite grade metamorphism (Cawood and van Gool, 1998). This location was selected because of the relatively low metamorphic grade and high structural position in the Yellow Marsh anticlinorium, which likely corresponds to a high stratigraphic position in the South Brook Formation (Figure 4.3). The analyzed sample consists of a light grey to pinkish quartzite that displays compositional zoning from a medium-grained, impure quartzite to a coarse, feldspar-quartz gneiss. The sample has a planar foliation defined by aligned feldspar and phyllosilicates with no evidence of original bedding.

A total of 57 U-Pb analyses lie on or near Concordia (Figure 4.8) with the oldest age at 1499±8 Ma and the youngest at 999±9 Ma. The total population of analyzed grains is overwhelmingly dominated by zircons of late Mesoproterozoic age (n = 52; 91%). The range and density of late Mesoproterozoic ages produces a polymodal peak on a cumulative probability diagram with three prominent peaks around ca. 1010 Ma, 1040 Ma, and 1144 Ma (Figure 4.9). An older group of middle Mesoproterozoic zircons (n = 5; 9%) ranges from ca. 1330 Ma to 1500 Ma, producing smaller peaks on the probability density plot. Of the 57 U-Pb analyses, only 44 zircons were selected for Hf analysis because of the consistency of U-Pb ages. Analysis of the Hf data reveals that late Mesoproterozoic zircons can be split into two separate groups on the basis of both age and ε_{Hf} values. One group consists of zircons that range in age from 1000 Ma to 1080 Ma and have ε_{Hf} values between -0.4 and +4.7 ($^{176}Hf/^{177}Hf$ = 0.282140-0.282286), whereas another group consists of older zircons that range in age from 1140 Ma to 1210 Ma and have slightly higher ε_{Hf} values between +1.5 and +6.5 ($^{176}Hf/^{177}Hf$ = 0.282110-0.282245) (Figure 4.10). Middle Mesoproterozoic grains have even higher ε_{Hf} values between +5.1 and +10.0 ($^{176}Hf/^{177}Hf$ = 0.281981-0.282136).

South Brook Formation – Mount Musgrave Group (CB-230)

Analyzed sample CB-230 from the South Brook Formation was collected near the core of the Yellow Marsh anticlinorium along an unnamed logging road in Yellow Marsh (E 0447610/N 5416535) (Figure 4.1). Previous metamorphic analyses indicate that this part of the Corner Brook Lake terrane experienced garnet grade metamorphism and lies inside the chlorite-out isograd (Cawood and van Gool, 1998). The sample location was chosen primarily on the basis of a low structural position in the Yellow Marsh anticlinorium, implying a low stratigraphic position in the South Brook Formation (Figure 4.3). In this area, metaclastic rocks consist of paragneiss and psammitic schist. Individual compositional layers are around 0.5 m thick and grade upward from medium-grained, white, quartz-biotite gneiss to dark brown, garnet-biotite schist and schistose gneiss. Contacts between compositional layers are sharp, suggesting that individual compositional layers represent metamorphosed graded beds, likely consisting of a coarse,

sandy base grading upward into finer grained shale rich tops. Sample CB-230 consists of a medium- to fine-grained, leucocratic, foliated, quartz-feldspar gneiss (Figure 4.7E). Foliation is defined by aligned phyllosilicates. No evidence of original bedding structures were observed in the sample.

Analyzed grains (n = 54) fall on or near Concordia (Figure 4.8) and almost exclusively yield late Mesoproterozoic ages (n = 53, 89%). One U-Pb analyses produced a Neoproterozoic age of 664±9 Ma. The range of late Mesoproterozoic ages falls between 1000 Ma and 1300 Ma. The density and range of late Mesoproterozoic ages produces a bimodal peak on the cumulative probability plot with prominent peaks centered around ca. 1030 Ma and 1133 Ma (Figure 4.9). Only 40 zircons out of the 54 total U-Pb analyses were selected for Lu-Hf analysis because of the consistency of the U-Pb ages. Analysis of the Hf data reveals that late Mesoproterozoic zircons in sample CB-230 can also be split into two groups on the basis of age and ε_{Hf} values. A younger late Mesoproterozoic group with ages between 980 Ma and 1080 Ma has ε_{Hf} values between +0.3 and +5.6 ($^{176}Hf/^{177}Hf$ = 0.282136-0.282279), whereas a slightly older group with ages between 1110 Ma and 1320 Ma yields ε_{Hf} values between +0.9 and +6.3 ($^{176}Hf/^{177}Hf$ = 0.282059-0.282230).

4.5 DISSCUSION

4.5.1 Age Populations

In detrital-zircon studies, an age population consists of a group of zircons with U-Pb ages that lie between arbitrarily defined age limits. A common assumption in most studies is that the relative proportion of U-Pb ages analyzed in a given sample correlates directly with the true abundance of age populations within the sample. It has been demonstrated, however, that such an assumption is questionable, particularly when an inadequate number of detrital zircons is analyzed (i.e., typically less than 40 grains per sample) (Vermeesch, 2004; Andersen, 2005). In order to report meaningful detrital zircon age populations, it is important to include a summary of the detection limits for each analyzed sample, that is, the probability of finding an age population within each sample vs. overlooking an age population. A sedimentary rock is essentially an infinite reservoir of detrital zircons, thus there is always a level of uncertainty involved in classifying the

relative proportion of age populations in a sample from a finite number of zircon analyses. Noting the relative uncertainty for each age population is also important when reporting meaningful detrital-zircon populations.

In this study, we follow the statistical procedure of Andersen (2005). The population size, detection limits, and relative uncertainty for each detrital sample are displayed in Table 4.3. Detection limits are given at 50% and 95% confidence level. At $p_L = 0.5$, there is an equal probability of either detecting or overlooking zircons in a specified age population, whereas at $p_L = 0.95$, there is a 95% chance of finding at least one zircon that belongs to the same specified age population. Thus, the $p_L = 0.95$ limit represents a fairly safe indication that an age population of the corresponding true abundance will be detected. However, the $p_L = 0.5$ limit represents an upper abundance limit for age populations that more than likely have been overlooked rather than observed during a given analysis.

Analysis of the U-Pb zircon age data for the seven detrital samples indicates the following grouping into five principal age populations (Table 4.3): 1) late Archean grains (n = 16) with ages between 2930 to 2650 Ma and a principal peak at 2740 Ma; 2) late Paleoproterozoic grains (n = 19) with ages between 1900 and 1600 Ma and principal peaks at 1630 Ma and 1870 Ma; 3) early Mesoproterozoic grains (n = 23) with ages between 1450 and 1600 Ma; 4) middle Mesoproterozoic grains (n = 28) with ages between 1380 and 1265 Ma with a principal peak at 1330 Ma; and 5) late Mesoproterozoic grains (n = 333) with ages between 1200 and 980 Ma and principal peaks around 1135 Ma and 1040 Ma. The relative proportion of these age populations varies between samples; zircons of late Mesoproterozoic age are present in all analyzed samples. Detrital zircons of late Neoproterozoic, early Paleoproterozoic, and middle Archean age are also present in the analyzed detrital samples but not in sufficient number to include as a principal age population.

In most of the data sets, the 95% confidence detection limit is around 5%. Thus, there is a possibility that minor age populations (ca. <5%) have been overlooked in this study. However, it is important to bear in mind that at the $p_L = 0.5$ level, populations greater than ca 1% are more likely to have been detected than overlooked. Of the 28 total population abundances reported in Table 4.3, only six have a relative uncertainty less

than 15%. Most populations have a relative uncertainty that ranges between 29% and 70%. The smallest populations reported consist of a single zircon age, which makes up between 1% and 2% of the total data set for those samples and produces a relative uncertainty for the abundance of these populations that is ≥99%. The true abundance of zircons in these smaller age populations is likely to have been underestimated. One of the analyzed samples (STV-30) has an indeterminate relative uncertainty because 100% of the zircons analyzed fall into a single age population.

The proportion of detrital zircons within each age population varies throughout the vertical stratigraphic section. Within the Curling Group, detrital zircons are dominated by a late Mesoproterozoic age population; however, the range and proportion of other age populations increases up the vertical section (Figure 4.9). The absolute range of detrital zircon ages at the base of Summerside Formation in CB-219 is approximately 900 m.y.; the youngest zircon has an age of 612±10 Ma and the oldest of 1521±6 Ma. With the exception of the older Mesoproterozoic grains, the distribution of U-Pb ages in CB-219 is similar to previously reported detrital zircon ages from the Summerside Formation (Cawood and Nemchim, 2001). U-Pb ages in sample CB-260 near the top of the Irishtown Formation, however, have a range greater than 3000 m.y. with a minimum at 544±8 Ma and a maximum at 3605±5 Ma. Comparison of the distribution of age populations in the two metaclastic samples reveals that both samples CB-212 and CB-230 have a detrital record similar to that in synrift deposits within the Summerside Formation. The data further substantiate the interpretation that metaclastic deposits of the South Brook Formation are metamorphosed Laurentian synrift deposits.

The increase in the range and abundance of zircon populations upward through the vertical stratigraphic record reflects the evolution of the Laurentian margin during the early Paleozoic. At the initiation of continental rifting, sediment is derived locally from uplifted rift shoulders that bound rift basins, while axial flow between individual rift basins generally is limited, resulting in separate isolated basins within the early rift system (Leeder, 1995). As a rift develops into a full-fledged passive margin, thermal subsidence along the continental margin results in the development of major river systems that transport sediment from the craton into mature-rift and passive-margin basins (e.g., Bond et al., 1995). Thus, an increase in potential source terranes, and

therefore age populations, of detrital zircon is predicted as the edge of the continent evolves from active rift to passive margin. Furthermore, rift systems unroof and expose previously buried terranes to erosion, allowing them to contribute sediment into the rift.

4.5.2 U-Pb age and Hf isotopic characteristics of the basement-cover samples

Two samples of crystalline basement (i.e., STV-30A and NP-10A) were collected from the Humber zone, along with two samples of overlying Bradore sandstone (i.e., STV-30 and NP-10) that were collected stratigraphically above the two basement samples within 2 meters of the Proterozoic-Paleozoic unconformity. The geographic locations of the two basement-cover samples are separated by ~180 km (Figure 4.1). Basement samples STV-30A and NP-10A, along with the respective sedimentary cover samples (i.e., STV-30 and NP-10), represent unequivocal Laurentian basement (e.g., Dickin, 2004) and Early Cambrian sedimentary detritus. Therefore, the Lu-Hf geochemistry of zircon from these four samples represents a blueprint for Laurentian basement on the St. Lawrence promontory, against which the synrift and metaclastic detrital zircons can be compared for provenance.

U-Pb isotopic ages for the basement-cover samples are displayed in Table 4.1. Comparison of U-Pb age populations reveal some interesting relationships between the crystalline basement and overlying sedimentary cover samples. Detrital zircon grains from NP-10 are primarily late Mesoproterozoic in age with a distribution of zircon ages on a probability density diagram (Figure 4.4) that corresponds closely to the age of the underlying granite NP-10A. The distribution of ages in NP-10 implies that most of the sedimentary detritus at this location was derived directly from underlying basement, with some input from outside sources to account for the older grains. In contrast to sample NP-10, detrital ages from STV-30 do not match ages of crystalline zircon recovered from the underlying basement gneiss STV-30A. In fact, the oldest grain recovered from Bradore sandstone STV-30 yielded a $^{206}Pb/^{207}Pb$ age of 1219 Ma, which is nearly 150 m.y. younger than the youngest grain analyzed in the underlying basement sample. The overall age population of STV-30 is similar to detrital sample NP-10; 100% of analyzed zircons are of a late Mesoproterozoic age.

The relationship between detrital-zircon age populations observed in the two Bradore samples to the underlying basement likely reflects the sedimentary environment in which the two sandstones where deposited. Bradore sample NP-10 was collected from a dark, massive to poorly bedded, very immature sandstone with a detrital mineral assemblage that was a close match to the underlying granitic basement. Thus, it follows that detrtial zircon ages are a close match to the age of the basement sample because the underlying basement was the most obvious contributor of sedimentary detritus. Sample STV-30, on the other hand, was collected from a bed of red, medium-grained, moderately sorted, sandstone with a high density of ripple marks and cross-beds, indicating a highly energetic depositional environment. Thus, detrital minerals (including zircon) weathered from the underlying basement STV-30A were likely transported away by sediment dispersal processes and replaced by detritus from more distant sources.

Initial $^{176}Hf/^{177}Hf$ ratios, epsilon values, and model ages are listed in Table 4.2. The Lu-Hf isotopes from the basement samples NP-10A and STV-30A, along with Lu-Hf isotopes from the overlying detrital-zircon samples NP-10 and STV-30, provide a general geochemical blueprint for Laurentian sedimentary detritus in the Iapetan synrift system. The Lu-Hf isotopic system evolves in concert with the Sm-Nd system (Veervort and Blichert-Toft, 1999); and, therefore, the interpretation of epsilon notation for Hf data is similar to that of epsilon Nd (see Appendix A for explanation of epsilon calculation). Zircons with a negative ε_{Hf} value and a Hf model age that is significantly older than the U-Pb crystallization age indicate derivation from an evolved, continental crustal source. Conversely, where ε_{Hf} values are positive and U-Pb isotopic ages are a close match to calculated model ages, the likely proto-source for the zircon is crustal material derived directly from the depleted mantle reservoir.

The depleted mantle model age (T_{DM}) of a mineral reflects the time since the Hf contained by the mineral was last in isotopic equilibrium with the depleted mantle reservoir (e.g., Andersen et al., 2002) (Appendix A). Model ages are typically inferred as reflecting the time when the Hf contained in a particular rock system was separated as a melt from a depleted mantle source, and thus is commonly interpreted as a maximum crustal formation age for the protolith of the mineral analyzed. The significance of interpreting zircon Hf model ages does not come without caveats. Because of the very

low Lu/Hf ratio in zircon, a model age calculated from the $^{176}Hf/^{177}Hf$ and $^{176}Lu/^{177}Hf$ ratios measured directly from a zircon only represents a minimum estimate for the age of melt extraction from the depleted mantle reservoir. Furthermore, mixing of magmas from one or more differing sources can significantly alter the Hf composition and Lu/Hf ratio of a rock system, thereby generating hybrid model ages that are essentially meaningless geologically.

Figure 4.7 shows initial $^{176}Hf/^{177}Hf$ ratios for the four basement-cover samples expressed as epsilon values vs. U-Pb age. Zircons from the two basement samples NP-10A and STV-30A have $^{176}Lu/^{177}Hf$ ratios that range from 0.0025 to 0.0004 with no systematic difference in Lu/Hf ratios between the two samples. Because the zircons in each analyzed sample have relatively low $^{176}Lu/^{177}Hf$ ratios, the effect on initial $^{176}Hf/^{177}Hf$ from the contribution of in situ production of ^{176}Hf by decay of ^{176}Lu is minor. The two basement samples do not have overlapping U-Pb ages or Hf isotopic compositions. The total range in ε_{Hf} for the two basement samples individually is 3.5-5 units. The Bradore Formation detrital samples show a greater range in ε_{Hf} (7-10 units) suggesting input of detrital zircons from multiple Mesoproterozoic Laurentian basement sources, which is consistent with the distribution of detrital-zircon age populations in relation to the age of underlying basement. Analysis of the data presented in Figure 4.7 indicates that basement-cover zircons fall into three principle clusters based on U-Pb age and initial Hf composition: 1) a middle Mesoproterozoic cluster with juvenile ε_{Hf} values, 2) a late Mesoproterozoic cluster centered around ca. 1135 Ma with intermediate ε_{Hf}, and 3) a latest Mesoproterozoic cluster with the most evolved Hf composition.

Initial ε_{Hf} isotopic compositions for the middle Mesoproterozoic (ca. 1350-1500 Ma) zircon cluster, including basement sample STV-30A and detrital grains from NP-10, are moderately to strongly positive (+4 to +10 units). Model ages for middle Mesoproterozoic zircon form a unimodal distribution with a maximum peak centered over ca. 1700 Ma (Figure 4.11), suggesting an average crustal residence time of around 200 m.y. for the protolith of these zircons. The moderately positive epsilon values in the basement gneiss sample STV-30A and 200 m.y. gap between mantle extraction ages and the crystallization age suggests that the basement gneiss was derived from remelting of

older, late Paleoproterozoic juvenile crust. Alternatively, the model ages and moderately positive ε_{Hf} values from STV-30A may have resulted from mixing of older Archean Laurentian crustal sources (i.e., Nain province) with juvenile mantle material during the middle Mesoproterozoic. The most juvenile grains in the middle Mesoproterozoic cluster are detrital zircons from Bradore sandstone sample NP-10 (Figure 4.7), which have the highest ε_{Hf} values and model ages that are a close match to U-Pb crystallization ages indicating that these zircons were derived from crust that was extracted directly from the depleted mantle reservoir.

The subsequent generations of Laurentian zircon grains display a systematic decrease in ε_{Hf} over time (Figure 4.7). The late Mesoproterozoic cluster consists primarily of detrital grains with an age range between 1090 Ma and 1220 Ma, and that have ε_{Hf} values ranging between +2.2 and +5.2 units with a few positive and negative outliers. A latest Mesoproterozoic cluster consists of both igneous and detrital zircon that range in age from 990 Ma to 1080 Ma, and yield slightly more evolved initial Hf ratios between +0.1 and +3.8 epsilon Hf units. The three youngest zircons (~980 Ma) have negative ε_{Hf} values, which are the lowest in the entire basement-cover dataset. There is no significant variation in the distribution of model ages between the two zircon clusters. Zircons from the late Mesoproterozoic cluster (i.e., 1220-1090 Ma cluster) form a sharply unimodal distribution focused around 1450 Ma (Figure 4.11). The latest Mesoproterozoic cluster (i.e., 1080-990 Ma) produces depleted mantle model ages that are broadly unimodal on a histogram (Figure 4.11), with the greatest concentration at ca. 1460 Ma. This implies a crustal residence time of approximately 315 m.y. and 400 m.y. for zircons in the late Mesoproterozoic and latest Mesoproterozoic clusters, respectively (assuming average ages of 1135 Ma and 1060 Ma).

The decrease in the initial $^{176}Hf/^{177}Hf$ composition of the late Mesoproterozoic zircon populations, along with the increase in the gaps between model ages and U-Pb crystallization ages, has two alternate explanations. One is remelting of older, middle Mesoproterozoic crust (closed system process), in which the decrease in initial Hf ratios is the result of in situ Lu-decay in the crust from which the younger generations of zircon were derived. The other is contamination/mixing of juvenile late Mesoproterozoic melts

with older, more evolved crustal material (open system process). If the observed reduction of initial $^{176}Hf/^{177}Hf$ is the result of closed system Lu-decay in Laurentian crust, both the middle and late Mesoproterozoic zircon data points should fall along a linear Hf-growth curve with a slope that corresponds to acceptable Lu/Hf ratios for crustal rocks from which the zircons were derived (e.g., Lu/Hf = 0.023 for mafic rocks; Lu/Hf = 0.0093 for felsic rocks; Rudnick and Fountain, 1995; Vervoort and Patchet, 1996; Andersen et al., 2007) (Appendix A). If, on the other hand, the younger Laurentian zircons were derived from mixing of crustal melts during the late Mesoproterozoic, then the younger zircons should not fall on linear Hf-growth curves that plot back through the more juvenile middle Mesoproterozoic population.

In Figure 4.7, several Hf-growth curves have been calculated and plotted through zircon data points taken to represent average ages and epsilon values for the late Mesoproterozoic Laurentian dataset. These Hf-growth curves were calculated using $^{176}Lu/^{177}Hf = 0.015$, which corresponds to the average Lu/Hf ratio of continental crust (Rudnick and Gao, 2003). The linear growth curves plot through both late Mesoprotorozoic zircons and middle Mesoproterozoic zircons implying that the younger zircons were derived by remelting middle Mesoproterozoic crust with little or no mixing with an outside source(s). Thus, the U-Pb and Hf isotopic dataset for Laurentian crust in Newfoundland indicates that crustal material generated along the St. Lawrence promontory during the late Mesoproterozoic was produced almost exclusively by remelting of older, more juvenile crust. From the Lu/Hf dataset, it is possible to generate a model that predicts the evolution of initial $^{176}Hf/^{177}Hf$ compositions vs. time for Laurentian crust in the northern Appalachians (Figure 4.7). The observed range of the initial Hf ratios in the Laurentian zircon Lu/Hf model reflects variation in the Lu/Hf ratios of the rocks in which the zircons originally crystallized. Such a range is not surprising considering the heterogeneity of Laurentian crustal terranes preserved in Labrador and Quebec (e.g., Dicken, 2000; 2004).

4.5.3 Provenance of Synrift Detrital Zircon

Establishing the provenance of detrital zircons in a sedimentary system has significant implications for the tectonic and paleogeographic evolution of ancient

continental margins and basins (e.g., Cawood et al., 2007). In most studies, a provenance component is established through identification of U-Pb age populations that are interpreted as unique to a single protosource or group of protosources that make up a provenance terrain. However, in most circumstances, zircons in a single "age population" may be derived from multiple unrelated protosources, making identification of provenance terrains by age population alone essentially impossible. The advantage of measuring Lu-Hf systematics in detrital zircons, in addition to U-Pb ages, is that the initial $^{176}Hf/^{177}Hf$ isotopic composition of an individual zircon provides information on the crustal history of the terrane from which the zircon was derived. Thus, the Lu-Hf system, in conjunction with U-Pb isotopic ages, provides a means to identify zircons of similar age but differing provenance. Nonetheless, identification of zircon age populations that are unique to a particular craton or terrane can provide useful information so long as the limitations of this method are considered.

The range and distribution of U-Pb isotopic age populations in the analyzed samples increases upward through the vertical section, which is consistent with a transition in sedimentary dispersal processes in an active-rift to a passive-margin environment. The ages of detrital zircons presented in Table 4.1 allow for some observations concerning the provenance of synrift strata. Chiefly that as the eastern Laurentian rifted margin matured, sources for detrital zircons evolved from predominantly late Mesoproterozoic terranes to more complex late Archean, late Paleoproterozoic, early Mesoproterozoic, and late Mesoproterozoic sources, indicating a transition in provenance through time. A maximum age of deposition in three of the synrift samples is constrained by late Neoproterozoic zircons recovered from those samples.

A comparison between the U-Pb detrital zircon ages from all 7 detrital samples and the age of tectonothermal and magmatic events for the Laurentian craton and two proposed eastern conjugates (i.e., Baltica and Amazonia) are displayed in Figure 4.12. Approximately 85% of Newfoundland synrift detrital zircons fall into a middle and late Mesoproterozoic age population, which corresponds to tectonothermal events documented on all three cratons. Detrital zircons from two of the synrift samples with ages between 1.65 and 1.5 Ga form a small (n = 11; 3%) but significant population that

corresponds to a time of tectonic quiescence in eastern Laurentia. This age range, however, corresponds to a time of major tectonic and magmatic events on both the Baltican craton (Gothian) and the Amazonian craton (Rio Negro-Jurunea), suggesting potential detrital input from one (or both) of these cratons. Of the 427 total detrital zircons analyzed, a single grain yielded an age of 2118±5 Ma, which corresponds to the 2.2-2.0 Ga Trans-Amazonian orogen on the Amazon craton.

The dominance of late Mesoproterozoic detrital zircons in synrift sediment from western Newfoundland highlights the problem of interpreting a provenance component solely from age population. The Lu-Hf composition of individual zircons offers supplementary information concerning the origin of the rocks from which those zircons were derived. To further constrain the provenance of detrital zircon, initial Hf ratios for the 3 synrift samples and 2 metaclastic samples have been calculated and plotted in epsilon units vs. time in Figure 4.10. The chart shows the modeled range of crustal reservoirs corresponding to Laurentian crust from the St. Lawrence promontory based on the initial Hf isotope ratios from zircons in the basement-cover samples, as well as fields for Archean terranes in the Laurentian hinterland for which $^{176}Hf/^{177}Hf$ zircon data are available. Comparison of initial Hf ratios of zircon within each principle age population assists in determining the provenance of sedimentary detritus in the Newfoundland synrift succession.

Archean zircons – Detrital zircons with Archean ages were found only within synrift samples CB-259 and CB-260, which stratigraphically correspond to a time of rapid thermal subsidence that occurred as the Laurentian rift on the St. Lawrence promontory matured into a passive margin. The oldest detrital zircon yields a $^{206}Pb/^{207}Pb$ age of 3605±5 Ma; most Archean grains range between 2700 Ma and 3000 Ma. Initial Hf ratios for Archean detrital zircons range between -11.0 and +3.9 epsilon units. The oldest grain has an ε_{Hf} value of -1.7, indicating that continental crust was being tectonically recycled early in the Earth's history. The core of the Laurentian craton consists of multiple Archean shields that were welded together during the late Paleoproterozoic (Hoffman, 1988; Cawood et al., 2007). The main population of Archean detrital zircons has U-Pb ages and initial Hf ratios that closely correspond to values for the Superior province of central Canada (Corfu and Davis, 1992; Isnard and Gariepy, 2003; Davis et

al., 2005), whereas the older outlier is a close match to Itsaq gneisses from the Nain province of northern Labrador and southwest Greenland (Figures 4.10 and 4.13) (Nutman et al., 1996; Amelin et al., 2000; Hartlaub et al., 2006; Krogh and Kamo, 2006). The three highly evolved zircons ($\varepsilon_{Hf} < -5$) can be correlated back to the field for the Nain province using Hf-growth curves with Lu/Hf ratios between 0.017 and 0.023, which are acceptable values for average and mafic crust. The data indicate that Archean detritus in the synrift system on the St. Lawrence promontory was derived directly from Archean terranes in Laurentia.

Late Paleoproterozoic, early and middle Mesoproterozoic zircons – Detrital zircons with ages between 1900 Ma and 1250 Ma were recovered from all five synrift samples, however, late Paleoproterozoic (i.e., 1900-1600 Ma) grains were found only in CB-259 and CB-260. These Proterozoic zircon clusters closely correspond to episodes of arc accretion and continental-arc magmatism on the Laurentian craton related to Makkovikian, Labradorian, Pinwarian, and Elzevirian orogenic events (Figure 4.12) (Gower and Krogh, 2002). The Hf data reveal that late Paleoproterozoic detrital zircons are derived from evolved crustal sources with ε_{Hf} values between -18.0 and +3.6, whereas younger, early and middle Mesoproterozoic zircons were derived from more juvenile sources with an average range of -2.0 to +9.0 epsilon units (Figure 4.10).

Latest Paleoproterozoic grains (i.e., 1700-1650 Ma) have slightly negative to moderately positive initial Hf ratios (ca. -0.6 to +7.0 units), indicating derivation from continental crust heterogeneously mixed with juvenile melts. The chemistry and age of these zircons is highly consistent with the Labradorian orogeny in northern Labrador, which involved arc accretion followed by melting of Laurentian crust (Gower and Krogh, 2002). Older grains (ca. 1800-1900 Ma) have much more negative ε_{Hf} values indicating that they were derived from reworked Archean(?) continental crust. The most likely source region for these zircons is the Torngat province in northern Labrador (Figure 4.13), which records the collision between the Nain and Rae cratons between 1.90 and 1.80 Ga (Hoffman, 1988; Theriault and Ermanovics, 1997).

Of the 50 early and middle Mesoproterozoic grains, approximately 58% plot (n = 29) within the modeled range of initial Hf ratios for Laurentian crust on the St. Lawrence promontory (Figure 4.10), indicating a Laurentian provenance for these zircons. Detrital

zircons that fall just below the modeled field for Newfoundland Laurentian crust correlate back to late Paleoproterozoic zircon interpreted to be derived from Labradorian crust along a Hf-growth curve, suggesting that these younger middle Mesoproterozoic zircons were generated by remelting of older Labradorian crust. All of the available data suggest that early and middle Mesoproterozoic detrital zircon has a Laurentian provenance. Furthermore, the more juvenile initial $^{176}Hf/^{177}Hf$ ratios for early Mesoproterozoic detrital zircons is consistent with derivation from oceanic and continental arc terranes, which is consistent with models for the tectonic growth of eastern Laurentia during the early Mesoproterozoic (e.g., Gower and Krogh, 2002).

A single cluster of zircons falls into the North American magmatic gap (ca. 1650-1520 Ma), for which relatively few magmatic, metamorphic, or deformational events are recorded in eastern Laurentia (Rivers, 1997). Although rocks of this age are found on both Baltica and Amazonia, the nearly complete lack of 2.2-2.0 Ga detrital zircon in the Newfoundland synrift sediment (Table 4.1) (see also Cawood and Nemchin, 2001) suggests that Amazonia did not contribute sediment to the Laurentian rift on the St. Lawrence promontory. Interestingly, a prominent cluster early Mesoproterozoic zircon has initial $^{176}Hf/^{177}Hf$ ratios that correspond to the Trans-Scandinavian Igneous Belt on the Baltican craton (Figure 4.13) (Andersen et al., 2007), supporting Baltica as a potential source for zircon in the 1.63-1.52 Ga population.

Neoproterozoic-late Mesoproterozoic zircons – The largest age population (n = 224; 72%) common to all analyzed synrift samples spans the Neoproterozoic and late Mesoproterozoic (ca. 544-1200 Ma). The greatest concentrations of ages are constrained between 1040 Ma and 1175 Ma. Initial Hf ratios range between -7.5 and +6.5 epsilon units, and most zircons fall in a range of -1.7 and +6.0 ε_{Hf}. Of the 224 total synrift and metaclastic zircons in this population, nearly 73% (n = 213) plot within the model range determined for Mesoproterozoic Laurentian basement in Newfoundland (Figure 4.10), indicating that Neoproterozoic-late Mesoproterozoic aged zircons are overwhelmingly derived locally from Laurentian basement on the St. Lawrence promontory.

Previous whole-rock and mineral isotopic analyses from igneous and metamorphic rocks on the Baltican craton has produced a large repository of Lu-Hf and U-Pb data for comparison (e.g., Andersen et al., 2002; Andersen and Griffin, 2004;

Andersen et al., 2004; Soderlund et al., 2005; Andersen et al., 2007). Figure 4.13 plots the initial $^{176}Hf/^{177}Hf$ ratios of detrital zircon from this study against zircon from Proterozoic igneous suites from Baltica. Late Paleoproterozoic and Mesoproterozoic (i.e., 1600-1000 Ma) detrital zircon from western Newfoundland plot within the range of initial Hf ratios determined for Baltican crust of the same vintage.

Simple comparison of the Hf data (Figure 4.13) suggests that Proterozoic detrital zircons from western Newfoundland were derived from the Baltican craton; however, Baltica is unlikely to have been a primary contributor of synrift sediment on St. Lawrence promontory for several reasons. First, the presence of 1400-1250 Ma zircons in the analyzed samples is inconsistent with a Baltican source (Figure 4.12). Although 1400-1250 Ma magmatism and orogensis are common within Laurentia, rocks of this age are uncommon in the Mesoproterozoic orogens of Baltica (Andersen, 2005). Second, middle and late Mesoproterozoic zircons in the Newfoundland synrift samples show a much more constricted range of initial Hf ratios than Baltican zircons. The Fennoscandian orogen in Baltica consists of magmatic suites that formed along the western Baltican margin in a supra-subduction zone setting that was followed by back-arc rifting and related magmatism (Andersen et al., 2002; Andersen and Griffin, 2004; Andersen, 2005), which explains the more extensive range of Hf ratios for 1.20 Ga zircons. The ca. 1.25 Ga Elzeverian orogen on the Laurentian craton consisted of rejuvenated arc magmatism along the eastern Laurentian margin (Gower and Krogh, 2002), which better fits the more restricted range of Hf values for detrital zircon in the synrift samples. Third, there is an absence of 950-900 Ma detrital zircon in the synrift samples, which corresponds to a time of magmatism and high-grade metamorphism related to post-orogenic collapse of the Sveconorwegian orogen (Gorbatschev and Bogdanova, 1993; Soderlund et al., 2005). Fourth, there is an absence of late Mesoproterozoic zircons with initial $^{176}Hf/^{177}Hf$ ratios coinciding with the range of late Mesoproterozoic Hf ratios for the Trans-Scandinavian Igneous Belt (e.g., 0.28218-0.28220 between 1.2-1.0 Ga) (Figure 4.14).

On the basis of initial Hf composition and U-Pb age populations of detrital zircons, we interpret the primary source of synrift detrital zircon on the St. Lawrence promontory to be eastern Laurentia. Early rift deposits (i.e., CB-212, CB-219, CB-230) were derived from Grenville-aged Laurentian crust, which bounded opening rift basins

and formed the uplifted shoulders from which local sedimentary detritus was shed. As rifting progressed, extension of Laurentian crust may have unroofed tectonically buried terranes that could contribute subsequent synrift sediment into the evolving continental margin (i.e., CB-259). At the onset of passive-margin thermal subsidence by the end of the late Early Cambrian (i.e., CB-260), expanding drainage systems tapped older Laurentian terranes. Lu-Hf data from individual detrital zircons in the synrift succession establish that Archean and Proterozoic detritus on the St. Lawrence promontory was derived from older Laurentian cratonic terranes inboard of the margin in northern and central Canada, which is in agreement with the results of Cawood and Nemchin (2001)

Detritus from a potentially exotic source to Laurentia can not be ruled out. A small group of detrital zircons makes up an age population (i.e., 1.63-1.52 Ga) that is noticeably absent in the rocks of eastern Laurentia. The two probable candidates for zircon of this age range are Baltica and Amazonia. Although rocks of this age are common within the Amazon craton, the lack of detritus in the 2.2-2.0 Ga range, which makes up dominant age populations for detrital zircon collected from known Amazonian terranes, suggests that Amazonia was not a supplier of the late Paleproterozoic-early Mesoproterozoic detritus. In this context, Baltica is the more likely candidate for the source region of these zircons. Rocks of the 1.65-1.5 Ga Gothian orogenic belt (Figure 4.12) are fairly widespread on the Baltican craton, and initial $^{176}Hf/^{177}Hf$ ratios for 1.65-1.52 Ga zircon from the Newfoundland samples are a match to zircon of the same vintage from Baltican igneous terranes. Furthermore, Baltica can not be completely ruled out as a source craton for some of the late Mesoproterozoic detrital zircon recovered from the synrift samples.

4.5.4 Paleogeographic Tectonic Implications

Although there is general agreement that Baltica and Amazonia were juxtaposed against the eastern Laurentian margin in the late Mesoproterozoic Rodinian configuration, the location of these cratonic elements with respect to specific segments of the Laurentian margin remains unclear. Two end member models have arisen. One model proposes a fit between northeastern Laurentia (Greenland-Scotland-Labrador) and the proto-Andean margin of Amazonia (Dalziel 1994; Dalziel et al., 2000; Sadowski, 2002).

The other model places Amazonia along the southern Laurentian margin and has Baltica as the conjugate to northeastern Laurentia (Tohver et al., 2002; 2004; Cawood and Pisarevsky, 2006). The U-Pb and Lu-Hf isotopic data from detrital zircons in synrift sediment presented herein provide important constraints on the paleogeographic development of the St. Lawrence promontory when combined with previously reported paleomagnetic and tectonic data for Mesoproterozoic assembly of Rodinia.

Lu-Hf data from zircons in both Baltica and the St. Lawrence promontory are strikingly similar. If detrital zircons from the Newfoundland synrift sample were derived primarily from a Laurentian source, it implies that northern Laurentian and Baltican crust experienced similar magmatic/tectonic events during the Mesoproterozoic. The eastern parts of the Laurentian craton exposed in Labrador and eastern Quebec experienced arc accretion and continental-arc magmatism during the times of 1.90-1.71 Ga (Makkovikian), 1.65-1.60 Ga (Labradorian), 1.52-1.45 Ga (Pinwarian), and 1.25-1.19 Ga (Elzevirian) (Wardle et al., 1990; Tucker and Gower, 1994; Rivers, 1997; Dickin, 2000; Gower and Krogh, 2002; Ketchum et al., 2002). Late Mesoproterozoic orogenesis culminated in a continent-continent collisional event dated between 1.08 and 1.00 Ga (Grenvillian) that generated granulite-amphibolite grade metamorphism in eastern Laurentian basement rocks (Gower and Krogh, 2002), as well as produced synorogenic sedimentary basins and a complex thrust belt in the Laurentian foreland (e.g., Cawood et al., 2007; Rivers, 2008).

The Baltican craton consists of an Archean core surrounded by progressively westward younging Proterozoic orogenic belts (Figure 4.14) (Gorbatschev and Bogdanova, 1993; Bogdanova et al., 2008). Western Mesoproterozoic terranes are separated from eastern Archean and early Paleoproterozoic belts by a large suite of late Paleoproterozoic alkali-calcic granitic intrusions (i.e., Trans-Scandinavia Igenous Belt) (Hogdahl et al., 2004). Prior to major late Mesoproterozoic orogenesis, Baltica experienced arc magmatism and basin formation between 1.20 Ga and 1.14 Ga related to continental-arc accretion and back-arc spreading (Brewer et al., 2002; Andersen et al., 2004; 2007). The 1.05-0.90 Ga Sveconorwegian orogeny records continent-continent collision between western Baltica and eastern Laurentia that culminated around ca. 1.00

Ga and was followed by rapid gravitational collapse and crustal exhumation between 0.96 and 0.90 Ga (Bogdanova et al., 2008).

Paleomagnetic data from the late Mesoproterozoic substantiates collision between Baltica and northern Laurentia. Between 1100 Ma and 1050 Ma, Baltica appears to have drifted independently towards Laurentia across a large Pacific-style ocean basin (Figure 4.15) (Li et al., 2008). Closure of an ocean basin between Baltica and Laurentia between 1.20 and 1.10 Ga would generate juvenile-arc, back-arc, and continental-arc magmatism on both cratonic margins, consistent with the tectonic interpretations for both cratons, as well as U-Pb and Lu-Hf isotopic data. Paleomagetic poles indicate continent-continent collision between Baltica and northern Laurentia around 1050 and 1000 Ma (Pisarevsky et al., 2003). In this model, Laurentia is on the down-going plate to explain the synorogenic foreland basin and thrust belt within the Grenville orogen. Recent paleomagnetic and SHRIMP studies refute earlier configurations that place west Scandinavia against East Greenland in the Rodinian configuration at ca. 1.0 Ga (Dalziel, 1997; Kalsbeek et al., 2000; Cawood and Pisarevsky, 2006). The best fit between apparent polar wander paths places Baltica farther south adjacent to the Rockall platform and eastern Labrador, which is near to the St. Lawrence promontory (Cawood and Pisarevsky, 2006) (Figure 4.15).

Like Laurentia and Baltica, the Amazonian craton consists of an Archean core surrounded by Proterozoic accretionary and collisional belts (e.g., Cordani and Teixeira, 2007) (Figure 4.13). Paleoproterozoic and Mesoproterozoic orogenic belts on the Amazon craton define a time of nearly continuous crustal growth by arc accretion and continental-arc magmatism, along with associated deformation and metamorphism between 2.20 and 1.00 Ga (Sadwoski and Bettencourt, 1996, Bettencourt et al., 1999; Geraldes et al., 2001; Cordani and Teixeria, 2007). Magmatism and deformation related to the 1.25-1.00 Ga Sunsas orogen are interpreted to have resulted from late Mesoproterozoic collision between eastern Laurentia and Amazonia (Sadwoski and Bettencourt, 1996; Dalziel, 1997; Restrepo-Pace et al., 1997; Coridani and Teixeira, 2007); however, ca. 1.0 Ga magmatism related to the Sunsas orogen is not nearly as widespread on the Amazonian craton as Grenvillian deformation is on the Laurentian

craton, leading some to question the degree to which Amazonia was involved in eastern Laurentian orogenesis (Santos et al., 2008).

Paleomagnetic and geochronologic studies from the Amazonian craton and Laurentia indicate that Amazonia collided with southernmost Laurentia (Llano region, Texas) between 1.24 and 1.14 Ga (Tohver et al., 2002) (Figure 4.15). Pb and Nd isotopic studies in the southern Appalachians indicate that Mesoproterozoic basement massifs in the Blue Ridge represent a fragment of Amazonia that was transferred to Laurentia during break-up of Rodinia (Tohver et al., 2004; Berquist et al., 2005), suggesting Amazonia was at a similar latitude with the central Appalachians in the assembly of Rodinia. Interestingly, Tohver et al. (2002) report a late Mesoproterozoic sinistral strike-slip shear zone within the Amazonia craton termed the Ji-Parana shear zone. The timing and kinematics of this shear zone are consistent with migration of the Amazonian craton from the Llano region of Laurentia to the central Appalachians between 1.25 Ga and 1.0 Ga (Figures 4.14 and 4.15). Furthermore, U-Pb geochronologic and whole-rock Pb isotopic investigations fail to provide a direct correlation between Proterozoic basement rocks in Greenland, Scotland, and Labrador with Amazonian basement along the proto-Andean margin (Loewy et al., 2003). Thus, the available isotopic, geochronologic, and paleomagnetic data place Amazonia farther south along the eastern Laurentian margin with respect to the St. Lawrence promontory.

Detritus shed into rift basins on the St. Lawrence promontory was derived primarily from reworked Mesoproterozoic juvenile crust. Such crust is found on both the eastern Laurentian margin and within the Baltican craton. The provenance of synrift detrital zircons from the St. Lawrence promontory is dominantly Laurentian (e.g., Cawood and Nemchim, 2001); however, minor populations of late Paleoproterozoic and Mesoproterozoic Baltican zircons may have also been deposited into Iapten rift basins in western Newfoundland. The broad isotopic similarity between Baltican and northern Laurentian crust implies that the two cratons were tectonically linked during the late Mesoproterozoic. This interpretation is further supported by paleomagnetic data, which place the Baltican craton near to the St. Lawrence promontory by the late Mesoproterozoic. Furthermore, detrital zircons from western Newfoundland do not

support Amazonia as a conjugate to the St. Lawrence promontory, and neither does previous paleomagnetic, isotopic, and geochronologic data summarized herein.

4.6 CONCLUSIONS

The stratigraphy along the St. Lawrence promontory in western Newfoundland records the breakup of a supercontinent and transition of a low-angle detachment rift system into a broad, long-lived passive continental margin. U-Pb and Lu-Hf analyses of detrital zircon from the synrift succession on the St. Lawrence promontory show an overall age range from Archean to latest Neoproterozoic. Initial $^{176}Hf/^{177}Hf$ ratios are consistent with derivation from the Nain and Superior cratons, as well as Paleoproterozoic and Mesoproterozoic orogenic belts in the Laurentian hinterland. The distribution of age populations and Lu-Hf isotopes in detrital zircon from the synrift system indicate that sediment deposited into the opening Iapetan rift initially was supplied locally from Grenville-aged crust, which constituted the rift shoulders to the fledgling promontory. As continental extension progressed, thermal subsidence allowed for larger drainage systems to develop along the promontory, bringing sediment from the Laurentian hinterland to the rifted continental margin.

The age and geochemistry of a small but significant population of detrital zircons in the synrift stratigraphic system on the St. Lawrence promontory hint at the configuration of cratonic elements around the opening Iapetus Ocean. A small population of ca. 1630-1520 Ma zircons, along with several zircons in the main late Mesoproterozoic age population, has initial Hf ratios that are consistent with a Baltican source. Furthermore, the overall similarity observed in the Lu-Hf isotopic system between northern Laurentia and Baltica implies that the two cratons interacted tectonically during the Mesoproterozoic.

Involvement of northern Laurentia in the formation of the late Mesoproterozoic supercontinent Rodinia encompassed a complex and protracted collisional history of numerous continental arcs, volcanic arcs, and back-arc basins culminating in continent-continent collision (e.g., Rivers, 1997; 2008; Dickin, 2000; Gower and Krogh, 2002). Paleomagnetic data from multiple independent sources indicate that Grenvillian orogensis along the St. Lawrence promontory and northern Laurentia was the result of

collision with the Baltican craton around 1080-1000 Ma (e.g., Li et al., 2008, and references therein). The similarity in the age of Sveconorwegian and Grenville orogens, along with the broad similarity in the Lu-Hf geochemistry of Luarentian crust on the St. Lawrence promontory to that of Baltica further substantiates late Mesoproterozoic collision. The presence of Baltican detrital zircons in synrift sediment on the promontory, however small the population, suggests that Baltica (or Baltican crust) remained adjacent to the St. Lawrence promontory until final break out of eastern Laurentia from Rodinia.

Our study illustrates the depositional history of the late Neoproterozoic-Early Cambrian Laurentian synrift strata, as well as characterizes the Lu-Hf isotopic signature of northern Laurentian Mesoproterozoic crust. The Lu-Hf evolution of detrital zircon in the eastern Laurentian synrift system provides clues to identifying cratons that were conjugate to the St. Lawrence promontory during the Late Proterozoic. The recognition that zircon from Laurentian crust on the St. Lawrence promontory has Lu-Hf signatures that match Baltican zircons of the same age, along with detrital zircons with an interpreted Baltican provenance, indicate that Baltica, and not Amazonia, was adjacent to the St. Lawrence promontory in the Rodinia configuration. This interpretation is further substantiated by previous studies from the southern Appalachian orogen, which indicate that Amazonia was conjugate to the southern Laurentian margin (Tohver et al., 2002; 2004; Loewy et al., 2003).

4.7 ACKNOWLEDGMENTS

Funding for this project was provided by generous grants from the Geological Survey of Canada, the American Association of Petroleum Geologists, the University of Kentucky Dissertation Enhancement Award, the University of Kentucky Graduate School, and the University of Kentucky Department of Earth and Environmental Sciences. The author extends his personal thanks Dr. Paul Mueller and Dr. George Kamenov at the Department of Geological Sciences at the University of Florida. Without your help, this project would not have been possible. The author would also like to extend his thanks to Jennifer Gifford and Leeanna Hyacinth for all the help they offered during the author's trips to the LA-ICP-MS lab at the University of Florida in the spring and summer of 2008.

Table 4.1. U-Pb isotopic data of LAM-ICP-MS analysis of detrital and igneous zircons

	CONCORDIA COLUMNS							±2σ			*AGES and 1 σ error (Ma)*					
analysis	**$^{207}Pb/^{235}U$**	**1σ**	**$^{206}Pb/^{238}U$**	**1σ**	**$^{207}Pb/^{206}Pb$**	**1σ**	**RHO**	**$^{207}Pb/^{235}U$**	**$^{206}Pb/^{238}U$**	**$^{207}Pb/^{206}Pb$**	**$^{207}Pb/^{235}U$**	**1σ**	**$^{206}Pb/^{238}U$**	**1σ**	**$^{207}Pb/^{206}Pb$**	**1σ**
Mount Musgrave Group - South Brook Formation (CB-212) (E 0441358/N 5421416)																
1	1.6318	0.0667	0.1596	0.0064	0.0741	0.0006	0.98	8.17	8.02	1.55	982	25	955	36	1045	16
2	1.7797	0.0785	0.1725	0.0075	0.0748	0.0006	0.98	8.83	8.68	1.59	1038	28	1026	41	1064	16
3	1.7043	0.0710	0.1658	0.0068	0.0746	0.0006	0.98	8.33	8.19	1.49	1010	26	990	37	1057	15
4	1.3500	0.0531	0.1317	0.0051	0.0744	0.0006	0.98	7.86	7.72	1.51	867	23	798	29	1052	15
5	1.7208	0.0676	0.1676	0.0065	0.0745	0.0005	0.98	7.86	7.73	1.41	1016	25	1000	36	1054	14
6	1.5399	0.0623	0.1541	0.0061	0.0725	0.0005	0.98	8.10	7.97	1.42	946	25	924	34	1000	14
7	1.6232	0.0678	0.1571	0.0064	0.0749	0.0006	0.98	8.35	8.20	1.56	979	26	942	36	1066	16
8	1.6796	0.0686	0.1636	0.0066	0.0745	0.0005	0.98	8.16	8.04	1.41	1001	26	978	36	1054	14
9	1.5920	0.0643	0.1538	0.0061	0.0751	0.0006	0.98	8.08	7.94	1.52	967	25	923	34	1070	15
10	2.1250	0.0690	0.1975	0.0064	0.0780	0.0003	0.99	6.50	6.45	0.75	1157	22	1163	34	1148	7
11	1.7517	0.0572	0.1747	0.0057	0.0727	0.0003	0.99	6.53	6.48	0.81	1028	21	1039	31	1006	8
12	2.1320	0.0734	0.1922	0.0065	0.0805	0.0004	0.99	6.88	6.81	1.01	1159	24	1134	35	1208	10
13	1.7620	0.0537	0.1758	0.0053	0.0727	0.0003	0.99	6.10	6.06	0.69	1031	20	1045	29	1006	7
14	2.0754	0.0702	0.1932	0.0065	0.0779	0.0004	0.99	6.77	6.69	1.05	1141	23	1140	35	1145	10
15	1.6643	0.0588	0.1675	0.0058	0.0721	0.0005	0.98	7.06	6.91	1.45	995	22	999	32	988	15
16	3.5565	0.1124	0.2858	0.0089	0.0903	0.0004	0.99	6.32	6.26	0.87	1540	25	1622	45	1431	8
17	2.1771	0.0656	0.2019	0.0060	0.0782	0.0003	0.99	6.03	5.98	0.76	1174	21	1186	32	1153	8
18	1.7780	0.0601	0.1751	0.0059	0.0737	0.0003	0.99	6.76	6.70	0.93	1037	22	1041	32	1032	9
19	2.0993	0.0698	0.1958	0.0065	0.0777	0.0003	0.99	6.65	6.61	0.69	1148	23	1154	35	1140	7
20	1.7669	0.0608	0.1717	0.0058	0.0746	0.0004	0.99	6.89	6.80	1.10	1033	22	1022	32	1059	11
21	2.2585	0.0746	0.2084	0.0068	0.0786	0.0003	0.99	6.61	6.56	0.78	1199	23	1221	36	1162	8
22	1.8803	0.0562	0.1872	0.0055	0.0729	0.0003	0.99	5.98	5.93	0.75	1074	20	1107	30	1010	8
23	1.7556	0.0551	0.1748	0.0054	0.0728	0.0003	0.99	6.28	6.23	0.76	1029	20	1039	30	1010	8
24	1.7041	0.0550	0.1695	0.0054	0.0729	0.0003	0.99	6.46	6.41	0.78	1010	20	1010	30	1012	8
25	2.8152	0.0883	0.2381	0.0074	0.0858	0.0003	0.99	6.27	6.23	0.70	1359	23	1378	39	1333	7
26	2.1655	0.0686	0.2015	0.0063	0.0779	0.0003	0.99	6.34	6.30	0.73	1170	22	1184	34	1145	7
27	2.1545	0.0747	0.2003	0.0069	0.0780	0.0003	0.99	6.94	6.89	0.83	1166	24	1178	37	1147	8
28	2.0132	0.0653	0.1858	0.0060	0.0786	0.0003	0.99	6.49	6.44	0.76	1120	22	1100	32	1162	8
29	2.1422	0.0684	0.1998	0.0063	0.0778	0.0003	0.99	6.39	6.35	0.70	1162	22	1175	34	1141	7

Table 4.1. (continued)

30	1.8531	0.0597	0.1779	0.0057	0.0756	0.0003	0.99	6.44	6.40	0.74	1064	21	1056	31	1083	7
31	2.0389	0.0684	0.1895	0.0063	0.0780	0.0003	0.99	6.71	6.67	0.77	1128	23	1119	34	1148	8
32	1.8488	0.0588	0.1818	0.0057	0.0738	0.0003	0.99	6.36	6.33	0.68	1063	21	1078	31	1035	7
33	1.8535	0.0582	0.1814	0.0057	0.0741	0.0003	0.99	6.28	6.24	0.72	1065	20	1075	31	1044	7
34	1.7179	0.0568	0.1703	0.0056	0.0732	0.0003	0.99	6.61	6.57	0.75	1015	21	1014	31	1019	8
35	2.3440	0.0747	0.2125	0.0067	0.0800	0.0004	0.98	6.37	6.28	1.10	1226	22	1243	35	1197	11
36	2.0490	0.0648	0.1898	0.0060	0.0783	0.0003	0.99	6.32	6.28	0.76	1132	21	1121	32	1154	8
37	1.8591	0.0598	0.1812	0.0058	0.0744	0.0003	0.99	6.43	6.38	0.81	1067	21	1074	31	1053	8
38	1.5733	0.0534	0.1503	0.0051	0.0759	0.0004	0.99	6.79	6.72	0.94	960	21	904	28	1092	9
39	1.8098	0.0602	0.1776	0.0059	0.0739	0.0003	0.99	6.65	6.62	0.69	1049	22	1055	32	1039	7
40	2.1562	0.0656	0.2016	0.0061	0.0776	0.0003	0.99	6.08	6.04	0.73	1167	21	1185	33	1136	7
41	3.5033	0.1064	0.2756	0.0083	0.0922	0.0003	0.99	6.08	6.03	0.73	1528	24	1570	42	1472	7
42	3.2315	0.0999	0.2505	0.0077	0.0936	0.0004	0.99	6.18	6.12	0.85	1465	24	1442	39	1499	8
43	1.7824	0.0598	0.1747	0.0058	0.0740	0.0003	0.99	6.71	6.64	0.93	1039	22	1039	32	1041	9
44	3.3940	0.1074	0.2634	0.0083	0.0934	0.0003	0.99	6.33	6.29	0.74	1503	25	1509	42	1497	7
45	2.1911	0.0678	0.2008	0.0062	0.0791	0.0003	0.99	6.19	6.14	0.74	1178	21	1181	33	1176	7
46	2.0442	0.0652	0.1907	0.0060	0.0777	0.0003	0.99	6.37	6.32	0.87	1130	22	1126	33	1140	9
47	1.6223	0.0599	0.1579	0.0058	0.0745	0.0003	0.99	7.39	7.35	0.75	979	23	946	32	1055	7
48	1.8672	0.0266	0.1724	0.0024	0.0786	0.0002	0.98	2.85	2.78	0.63	1069	9	1026	13	1161	6
49	2.0199	0.0303	0.1898	0.0028	0.0772	0.0002	0.98	3.00	2.94	0.60	1122	10	1121	15	1125	6
50	1.3506	0.0316	0.1352	0.0031	0.0725	0.0003	0.98	4.68	4.59	0.91	868	14	818	18	999	9
51	2.2276	0.0227	0.2038	0.0017	0.0793	0.0005	0.82	2.04	1.68	1.15	1190	7	1197	9	1179	11
52	3.0593	0.0380	0.2421	0.0029	0.0917	0.0003	0.96	2.48	2.38	0.70	1422	9	1399	15	1460	7
53	1.8132	0.0294	0.1784	0.0028	0.0737	0.0002	0.98	3.25	3.19	0.60	1050	11	1059	16	1034	6
54	1.7313	0.0193	0.1648	0.0017	0.0762	0.0003	0.94	2.23	2.10	0.75	1020	7	984	10	1100	7
55	1.4699	0.0284	0.1455	0.0028	0.0733	0.0003	0.98	3.87	3.80	0.72	918	12	876	16	1022	7
56	2.1867	0.0208	0.2045	0.0018	0.0776	0.0002	0.95	1.90	1.80	0.61	1177	7	1200	10	1136	6
57	1.8273	0.0222	0.1721	0.0020	0.0770	0.0003	0.95	2.43	2.31	0.74	1055	8	1024	11	1122	7

Table 4.1. (continued)

	CONCORDIA COLUMNS							±2σ			*AGES and 1 σ error (Ma)*					
analysis	**$^{207}Pb/^{235}U$**	**1σ**	**$^{206}Pb/^{238}U$**	**1σ**	**$^{207}Pb/^{206}Pb$**	**1σ**	**RHO**	**$^{207}Pb/^{235}U$**	**$^{206}Pb/^{238}U$**	**$^{207}Pb/^{206}Pb$**	**$^{207}Pb/^{235}U$**	**1σ**	**$^{206}Pb/^{238}U$**	**1σ**	**$^{207}Pb/^{206}Pb$**	**1σ**
Mount Musgrave Group - South Brook Formation (CB-230) (E 0447610/N 5416535)																
1	1.9811	0.0410	0.1925	0.0036	0.0746	0.0006	0.91	4.14	3.78	1.70	1109	14	1136	20	1058	17
2	1.7358	0.0392	0.1710	0.0036	0.0736	0.0006	0.94	4.52	4.25	1.54	1022	14	1018	20	1032	16
3	1.9568	0.0375	0.1827	0.0032	0.0777	0.0006	0.92	3.83	3.52	1.52	1101	13	1082	18	1139	15
4	2.4149	0.0415	0.2202	0.0034	0.0795	0.0006	0.89	3.44	3.08	1.54	1247	12	1284	18	1186	15
5	1.7406	0.0359	0.1704	0.0033	0.0741	0.0006	0.93	4.13	3.84	1.52	1024	13	1015	18	1043	15
6	1.6476	0.0303	0.1656	0.0028	0.0722	0.0005	0.91	3.68	3.37	1.49	988	12	989	15	991	15
7	1.0225	0.0191	0.1084	0.0016	0.0684	0.0008	0.80	3.73	2.99	2.24	715	10	664	9	881	23
8	1.8755	0.0422	0.1868	0.0039	0.0728	0.0006	0.92	4.50	4.13	1.78	1072	15	1105	21	1009	18
9	2.1334	0.0537	0.2103	0.0050	0.0736	0.0006	0.94	5.04	4.75	1.69	1160	17	1231	27	1030	17
10	1.4838	0.0272	0.1500	0.0025	0.0717	0.0005	0.91	3.66	3.33	1.53	924	11	902	14	978	16
11	1.7730	0.0401	0.1650	0.0035	0.0779	0.0006	0.94	4.52	4.24	1.57	1035	15	985	19	1145	16
12	1.6692	0.0303	0.1622	0.0026	0.0746	0.0006	0.90	3.63	3.26	1.60	997	11	970	15	1058	16
13	1.8370	0.0377	0.1739	0.0032	0.0766	0.0007	0.91	4.10	3.73	1.71	1059	13	1034	18	1111	17
14	1.9026	0.0386	0.1787	0.0034	0.0772	0.0006	0.93	4.06	3.76	1.54	1082	13	1061	18	1127	15
15	1.6735	0.0389	0.1617	0.0035	0.0750	0.0006	0.94	4.65	4.38	1.56	998	15	967	20	1070	16
16	1.7913	0.0453	0.1766	0.0041	0.0736	0.0007	0.93	5.05	4.69	1.88	1042	16	1049	23	1029	19
17	1.7652	0.0451	0.1736	0.0042	0.0738	0.0006	0.95	5.11	4.84	1.64	1033	16	1033	23	1035	17
18	1.6531	0.0322	0.1641	0.0029	0.0731	0.0006	0.90	3.89	3.51	1.67	991	12	980	16	1016	17
19	2.1412	0.0520	0.1979	0.0046	0.0785	0.0006	0.95	4.86	4.61	1.52	1162	17	1165	25	1159	15
20	2.2189	0.0370	0.2105	0.0031	0.0765	0.0006	0.89	3.33	2.96	1.53	1187	12	1232	17	1107	15
21	1.6431	0.0336	0.1661	0.0032	0.0717	0.0005	0.93	4.09	3.80	1.50	987	13	991	17	979	15
22	2.2165	0.0397	0.2099	0.0033	0.0766	0.0006	0.89	3.58	3.18	1.65	1186	12	1229	18	1110	16
23	2.0295	0.0423	0.1898	0.0037	0.0776	0.0006	0.93	4.17	3.87	1.55	1125	14	1121	20	1136	15
24	1.6851	0.0355	0.1702	0.0033	0.0718	0.0006	0.93	4.22	3.92	1.55	1003	13	1014	18	980	16
25	2.2266	0.0570	0.2083	0.0051	0.0775	0.0006	0.95	5.12	4.85	1.65	1189	18	1221	27	1135	16
26	1.7278	0.0400	0.1736	0.0038	0.0722	0.0005	0.95	4.63	4.38	1.49	1019	15	1033	21	991	15
27	1.8179	0.0431	0.1792	0.0040	0.0736	0.0006	0.94	4.74	4.47	1.57	1052	15	1064	22	1030	16
28	1.8706	0.0407	0.1832	0.0036	0.0741	0.0007	0.90	4.35	3.94	1.86	1071	14	1085	20	1043	19
29	2.5041	0.0471	0.2275	0.0039	0.0798	0.0006	0.91	3.76	3.44	1.54	1273	14	1322	21	1193	15

Table 4.1. (continued)

30	2.2183	0.0473	0.2025	0.0040	0.0794	0.0006	0.93	4.26	3.96	1.57	1187	15	1190	21	1183	16
31	1.8572	0.0467	0.1807	0.0043	0.0745	0.0006	0.95	5.03	4.80	1.51	1066	16	1072	24	1056	15
32	1.6196	0.0454	0.1587	0.0038	0.0740	0.0011	0.84	5.60	4.73	3.01	978	17	950	21	1042	30
33	1.8224	0.0448	0.1766	0.0041	0.0748	0.0006	0.94	4.92	4.60	1.73	1053	16	1049	22	1064	17
34	1.7295	0.0300	0.1750	0.0027	0.0717	0.0006	0.90	3.47	3.11	1.54	1019	11	1041	15	976	16
35	1.6599	0.0547	0.1630	0.0052	0.0739	0.0006	0.97	6.60	6.42	1.50	993	21	974	29	1037	15
36	2.2808	0.0479	0.2142	0.0042	0.0772	0.0006	0.93	4.20	3.92	1.51	1206	15	1252	22	1127	15
37	1.8209	0.0372	0.1754	0.0033	0.0753	0.0006	0.93	4.08	3.79	1.53	1053	13	1043	18	1076	15
38	1.5443	0.0325	0.1545	0.0029	0.0725	0.0007	0.89	4.21	3.76	1.91	948	13	927	16	1000	19
39	2.0627	0.0403	0.1912	0.0034	0.0782	0.0006	0.92	3.91	3.59	1.55	1136	13	1129	19	1153	15
40	2.0956	0.0444	0.1955	0.0039	0.0777	0.0006	0.93	4.24	3.96	1.50	1147	14	1152	21	1140	15
41	1.7492	0.0410	0.1720	0.0038	0.0737	0.0006	0.94	4.68	4.41	1.59	1027	15	1024	21	1034	16
42	2.6424	0.0616	0.2492	0.0055	0.0769	0.0006	0.94	4.67	4.41	1.53	1312	17	1435	28	1119	15
43	1.9623	0.0434	0.1857	0.0038	0.0766	0.0007	0.92	4.42	4.06	1.74	1103	15	1099	20	1112	17
44	1.7300	0.0428	0.1691	0.0039	0.0742	0.0006	0.94	4.95	4.64	1.74	1020	16	1008	22	1047	17
45	2.0766	0.0398	0.1913	0.0034	0.0787	0.0006	0.92	3.83	3.53	1.49	1141	13	1129	18	1165	15
46	2.1054	0.0445	0.1962	0.0038	0.0778	0.0007	0.92	4.23	3.88	1.67	1150	14	1156	21	1142	17
47	1.9658	0.0459	0.1884	0.0041	0.0757	0.0006	0.93	4.67	4.35	1.71	1104	16	1114	22	1087	17
48	1.3817	0.0406	0.1393	0.0039	0.0719	0.0006	0.96	5.88	5.64	1.63	881	17	841	22	984	17
49	1.7158	0.0366	0.1689	0.0033	0.0737	0.0006	0.92	4.27	3.93	1.65	1014	14	1007	18	1032	17
50	2.5941	0.1434	0.2207	0.0111	0.0853	0.0019	0.91	11.05	10.09	4.52	1299	40	1286	59	1322	44
51	2.0390	0.0299	0.1910	0.0027	0.0774	0.0003	0.97	2.93	2.85	0.68	1128	10	1128	15	1132	7
52	1.7352	0.0186	0.1716	0.0017	0.0733	0.0003	0.95	2.14	2.03	0.69	1022	7	1022	10	1023	7
53	1.7545	0.0204	0.1756	0.0019	0.0725	0.0003	0.95	2.33	2.20	0.74	1029	7	1044	11	999	8
54	1.9566	0.0356	0.1866	0.0033	0.0760	0.0003	0.97	3.64	3.54	0.83	1101	12	1104	18	1096	8

Table 4.1. (continued)

	CONCORDIA COLUMNS							±2σ			*AGES and 1 σ error (Ma)*					
analysis	**$^{207}Pb/^{235}U$**	**1σ**	**$^{206}Pb/^{238}U$**	**1σ**	**$^{207}Pb/^{206}Pb$**	**1σ**	**RHO**	**$^{207}Pb/^{235}U$**	**$^{206}Pb/^{238}U$**	**$^{207}Pb/^{206}Pb$**	**$^{207}Pb/^{235}U$**	**1σ**	**$^{206}Pb/^{238}U$**	**1σ**	**$^{207}Pb/^{206}Pb$**	**1σ**
Curling Group - Summerside Formation (CB-219) (E 0429615/N 5425259)																
1	2.0495	0.0370	0.1904	0.0034	0.0781	0.0003	0.98	3.61	3.53	0.77	1132	12	1124	18	1149	8
2	1.8030	0.0378	0.1766	0.0036	0.0740	0.0003	0.98	4.19	4.12	0.79	1046	14	1049	20	1042	8
3	1.9135	0.0354	0.1798	0.0033	0.0772	0.0003	0.98	3.70	3.64	0.67	1086	12	1067	18	1126	7
4	1.6548	0.0270	0.1627	0.0026	0.0738	0.0003	0.96	3.26	3.15	0.86	991	10	972	14	1035	9
5	1.7071	0.0345	0.1672	0.0033	0.0740	0.0003	0.99	4.04	3.98	0.68	1011	13	998	18	1042	7
6	2.0052	0.0363	0.1867	0.0033	0.0779	0.0002	0.99	3.62	3.57	0.60	1117	12	1104	18	1144	6
7	1.6960	0.0348	0.1675	0.0033	0.0734	0.0004	0.97	4.11	3.98	1.04	1007	13	999	18	1026	11
8	3.0639	0.0411	0.2348	0.0031	0.0947	0.0003	0.98	2.68	2.62	0.58	1424	10	1361	16	1521	5
9	3.0214	0.0534	0.2379	0.0041	0.0921	0.0003	0.98	3.53	3.47	0.66	1413	13	1377	21	1470	6
10	1.9645	0.0330	0.1824	0.0030	0.0781	0.0002	0.98	3.36	3.30	0.62	1103	11	1081	16	1149	6
11	2.0681	0.0381	0.1894	0.0034	0.0792	0.0004	0.96	3.68	3.54	1.01	1138	13	1119	18	1177	10
12	2.0827	0.0648	0.1796	0.0053	0.0841	0.0008	0.95	6.22	5.93	1.89	1143	21	1065	29	1295	18
13	1.6449	0.0244	0.1557	0.0022	0.0766	0.0003	0.95	2.97	2.83	0.91	987	9	934	12	1111	9
14	1.6853	0.0282	0.1653	0.0027	0.0739	0.0002	0.98	3.35	3.29	0.65	1003	11	987	15	1040	7
15	1.6481	0.0298	0.1612	0.0028	0.0741	0.0003	0.97	3.62	3.50	0.91	989	11	964	16	1045	9
16	2.8875	0.0441	0.2285	0.0034	0.0916	0.0003	0.97	3.05	2.96	0.73	1378	11	1328	18	1460	7
17	1.5671	0.0669	0.1533	0.0064	0.0741	0.0006	0.98	8.54	8.40	1.51	957	26	920	36	1045	15
18	2.0690	0.0325	0.1914	0.0030	0.0784	0.0002	0.98	3.15	3.09	0.57	1138	11	1130	16	1157	6
19	2.1968	0.0410	0.1991	0.0037	0.0800	0.0003	0.98	3.73	3.67	0.68	1180	13	1171	20	1198	7
20	1.6430	0.0298	0.1613	0.0028	0.0739	0.0004	0.96	3.63	3.50	0.96	987	11	965	16	1039	10
21	1.9862	0.0376	0.1853	0.0035	0.0777	0.0002	0.99	3.79	3.74	0.60	1111	13	1097	19	1140	6
22	2.1666	0.0355	0.2033	0.0033	0.0773	0.0002	0.98	3.28	3.21	0.64	1170	11	1194	17	1129	6
23	1.6821	0.0290	0.1644	0.0028	0.0742	0.0003	0.98	3.45	3.38	0.68	1002	11	982	15	1048	7
24	1.9155	0.0317	0.1791	0.0029	0.0776	0.0002	0.98	3.31	3.25	0.60	1086	11	1063	16	1136	6
25	0.7872	0.0138	0.0944	0.0016	0.0605	0.0003	0.97	3.52	3.39	0.92	589	8	582	9	622	10
26	1.7554	0.0306	0.1598	0.0025	0.0797	0.0006	0.91	3.48	3.17	1.44	1029	11	956	14	1189	14
27	1.7713	0.0213	0.1746	0.0021	0.0736	0.0002	0.98	2.40	2.35	0.50	1035	8	1038	11	1030	5
28	1.9979	0.0230	0.1843	0.0020	0.0786	0.0003	0.94	2.30	2.16	0.78	1115	8	1091	11	1163	8
29	2.1753	0.0272	0.1997	0.0025	0.0790	0.0002	0.98	2.50	2.46	0.46	1173	9	1175	13	1172	5
30	2.0754	0.0370	0.1940	0.0034	0.0776	0.0002	0.99	3.56	3.54	0.42	1141	12	1144	19	1137	4

Table 4.1. (continued)

31	1.6927	0.0328	0.1658	0.0031	0.0740	0.0004	0.97	3.87	3.75	0.96	1006	12	990	17	1042	10
32	1.7693	0.0275	0.1733	0.0025	0.0741	0.0004	0.92	3.11	2.87	1.19	1034	10	1031	14	1043	12
33	2.1192	0.0375	0.1857	0.0032	0.0828	0.0003	0.98	3.54	3.48	0.61	1155	12	1099	18	1264	6
34	1.7755	0.0326	0.1709	0.0028	0.0753	0.0006	0.91	3.67	3.33	1.55	1036	12	1018	16	1077	16
35	1.8792	0.0479	0.1636	0.0025	0.0833	0.0017	0.59	5.09	3.02	4.10	1074	17	977	14	1277	40
36	1.6982	0.0310	0.1666	0.0030	0.0739	0.0002	0.99	3.66	3.63	0.48	1008	12	994	17	1040	5
37	1.6119	0.0258	0.1627	0.0026	0.0719	0.0002	0.98	3.20	3.14	0.57	975	10	973	14	982	6
38	1.7622	0.0261	0.1704	0.0025	0.0750	0.0002	0.98	2.96	2.91	0.54	1032	10	1015	14	1069	5
39	2.2535	0.0205	0.2111	0.0018	0.0774	0.0002	0.96	1.82	1.74	0.53	1198	6	1235	10	1132	5
40	1.6164	0.0356	0.1585	0.0035	0.0740	0.0002	0.99	4.41	4.38	0.50	976	14	949	19	1041	5
41	0.8509	0.0152	0.0994	0.0016	0.0621	0.0004	0.92	3.56	3.27	1.40	625	8	612	10	676	15
42	2.0032	0.0312	0.1867	0.0029	0.0778	0.0002	0.99	3.12	3.08	0.49	1116	10	1104	16	1142	5
43	1.8017	0.0168	0.1762	0.0016	0.0742	0.0002	0.96	1.86	1.78	0.54	1046	6	1047	9	1046	5
44	1.9782	0.0284	0.1844	0.0026	0.0778	0.0002	0.98	2.87	2.82	0.53	1108	10	1092	14	1141	5
45	2.0044	0.0227	0.1882	0.0021	0.0772	0.0002	0.98	2.26	2.22	0.44	1117	8	1112	11	1128	4
46	1.7549	0.0336	0.1634	0.0025	0.0779	0.0009	0.79	3.83	3.02	2.36	1029	12	977	14	1144	23
47	1.8983	0.0296	0.1866	0.0029	0.0738	0.0002	0.99	3.12	3.08	0.52	1080	10	1104	16	1035	5
48	2.1446	0.0294	0.2002	0.0026	0.0777	0.0003	0.96	2.74	2.63	0.76	1163	9	1177	14	1139	8
49	2.0158	0.0220	0.1885	0.0020	0.0776	0.0002	0.97	2.19	2.13	0.51	1121	7	1114	11	1135	5
50	2.0531	0.0253	0.1927	0.0023	0.0773	0.0003	0.95	2.47	2.35	0.74	1133	8	1137	12	1128	7
51	2.2361	0.0311	0.2081	0.0028	0.0779	0.0002	0.98	2.78	2.72	0.59	1192	10	1220	15	1145	6
52	1.9992	0.0234	0.1889	0.0022	0.0768	0.0002	0.98	2.34	2.30	0.42	1115	8	1116	12	1115	4
53	1.6931	0.0229	0.1655	0.0022	0.0742	0.0002	0.98	2.71	2.67	0.48	1006	9	988	12	1047	5
54	1.9947	0.0284	0.1860	0.0026	0.0778	0.0002	0.98	2.84	2.80	0.51	1114	10	1100	14	1142	5
55	2.0404	0.0260	0.1902	0.0023	0.0778	0.0002	0.97	2.55	2.47	0.64	1129	9	1123	13	1142	6
56	3.0765	0.0370	0.2449	0.0029	0.0911	0.0002	0.99	2.41	2.38	0.38	1427	9	1413	15	1449	4
57	1.6210	0.0286	0.1586	0.0027	0.0741	0.0003	0.98	3.52	3.44	0.74	978	11	950	15	1045	7
58	1.6661	0.0251	0.1632	0.0024	0.0740	0.0003	0.97	3.01	2.91	0.77	996	10	976	13	1042	8
59	2.0667	0.0291	0.1885	0.0026	0.0795	0.0002	0.98	2.82	2.77	0.52	1138	10	1114	14	1186	5
60	1.6849	0.0244	0.1632	0.0022	0.0749	0.0004	0.93	2.90	2.70	1.06	1003	9	975	12	1065	11
61	2.0386	0.0313	0.1902	0.0029	0.0777	0.0002	0.99	3.07	3.03	0.53	1128	10	1123	16	1140	5
62	1.8838	0.0186	0.1863	0.0017	0.0733	0.0003	0.91	1.97	1.80	0.80	1075	7	1102	9	1024	8
63	1.9975	0.0296	0.1877	0.0027	0.0772	0.0003	0.97	2.97	2.87	0.74	1115	10	1110	15	1126	7

Table 4.1. (continued)

	CONCORDIA COLUMNS							±2σ			AGES and 1 σ error (Ma)					
analysis	$^{207}Pb/^{235}U$	1σ	$^{206}Pb/^{238}U$	1σ	$^{207}Pb/^{206}Pb$	1σ	RHO	$^{207}Pb/^{235}U$	$^{206}Pb/^{238}U$	$^{207}Pb/^{206}Pb$	$^{207}Pb/^{235}U$	1σ	$^{206}Pb/^{238}U$	1σ	$^{207}Pb/^{206}Pb$	1σ
Curling Group - Summerside Formation (CB-259) (E 0427575/N 5425635)																
1	1.7923	0.0300	0.1717	0.0028	0.0757	0.0004	0.96	3.34	3.21	0.95	1043	11	1022	15	1088	9
2	1.5377	0.0203	0.1560	0.0020	0.0715	0.0002	0.97	2.65	2.56	0.67	945	8	935	11	972	7
3	12.0561	0.3003	0.4651	0.0115	0.1880	0.0004	1.00	4.98	4.96	0.46	2608	23	2464	51	2725	4
4	1.6683	0.0220	0.1647	0.0021	0.0735	0.0002	0.98	2.63	2.58	0.55	996	8	984	12	1027	6
5	1.7664	0.0282	0.1703	0.0027	0.0752	0.0002	0.98	3.19	3.13	0.61	1033	10	1015	15	1074	6
6	10.5791	0.3344	0.4260	0.0132	0.1801	0.0010	0.98	6.32	6.22	1.16	2486	29	2290	60	2654	10
7	1.6208	0.0262	0.1601	0.0024	0.0734	0.0005	0.92	3.23	2.97	1.28	978	10	958	13	1025	13
8	1.8195	0.0264	0.1735	0.0025	0.0761	0.0002	0.98	2.90	2.83	0.63	1052	9	1032	14	1097	6
9	2.6662	0.0583	0.2215	0.0047	0.0873	0.0004	0.98	4.37	4.29	0.85	1319	16	1291	25	1367	8
10	3.3320	0.0405	0.2518	0.0030	0.0960	0.0002	0.98	2.43	2.38	0.49	1488	9	1449	15	1547	5
11	2.8470	0.0506	0.2347	0.0041	0.0880	0.0002	0.99	3.56	3.52	0.52	1368	13	1360	22	1382	5
12	3.0865	0.0553	0.2449	0.0043	0.0914	0.0002	0.99	3.58	3.55	0.49	1429	14	1413	22	1455	5
13	1.6440	0.0280	0.1625	0.0027	0.0734	0.0003	0.98	3.41	3.33	0.76	987	11	971	15	1024	8
14	3.1316	0.0639	0.2407	0.0047	0.0944	0.0005	0.97	4.08	3.94	1.06	1440	16	1391	25	1516	10
15	1.7715	0.0329	0.1701	0.0031	0.0755	0.0003	0.97	3.71	3.61	0.87	1035	12	1013	17	1083	9
16	3.9750	0.0799	0.2867	0.0057	0.1005	0.0003	0.99	4.02	3.99	0.52	1629	16	1627	29	1634	5
17	1.5501	0.0271	0.1563	0.0027	0.0719	0.0003	0.98	3.49	3.42	0.72	950	11	937	15	984	7
18	1.7032	0.0338	0.1689	0.0033	0.0732	0.0002	0.99	3.97	3.93	0.60	1010	13	1007	18	1018	6
19	1.7511	0.0265	0.1696	0.0025	0.0749	0.0002	0.98	3.03	2.96	0.63	1027	10	1011	14	1066	6
20	14.5894	0.2395	0.5162	0.0083	0.2050	0.0006	0.98	3.28	3.23	0.58	2788	15	2685	35	2866	5
21	16.3864	0.2462	0.5568	0.0083	0.2134	0.0005	0.99	3.01	2.97	0.47	2899	14	2856	34	2932	4
22	2.3150	0.0293	0.2144	0.0025	0.0783	0.0004	0.94	2.53	2.37	0.90	1217	9	1253	13	1155	9
23	1.7964	0.0295	0.1707	0.0027	0.0763	0.0004	0.95	3.28	3.13	0.99	1044	11	1017	15	1104	10
24	1.8045	0.0260	0.1739	0.0025	0.0753	0.0002	0.98	2.88	2.83	0.53	1047	9	1034	14	1076	5
25	11.8995	0.1681	0.4552	0.0063	0.1896	0.0005	0.98	2.83	2.78	0.53	2596	13	2420	28	2739	4
26	1.6631	0.0278	0.1642	0.0027	0.0734	0.0002	0.99	3.35	3.30	0.55	994	11	981	15	1026	6
27	3.9782	0.0584	0.2810	0.0040	0.1027	0.0004	0.97	2.94	2.85	0.72	1630	12	1598	20	1673	7
28	2.5663	0.0303	0.2184	0.0025	0.0852	0.0002	0.97	2.36	2.30	0.53	1291	9	1274	13	1321	5
29	2.6870	0.0503	0.2243	0.0042	0.0869	0.0002	0.99	3.75	3.71	0.51	1325	14	1306	22	1358	5

Table 4.1. (continued)

30	4.9262	0.0751	0.3207	0.0048	0.1114	0.0003	0.99	3.05	3.01	0.47	1806	13	1795	24	1822	4
31	3.7272	0.0492	0.2719	0.0035	0.0994	0.0003	0.98	2.64	2.59	0.52	1577	11	1552	18	1613	5
32	1.7187	0.0297	0.1666	0.0027	0.0748	0.0004	0.95	3.46	3.27	1.12	1015	11	994	15	1063	11
33	1.7288	0.0270	0.1665	0.0025	0.0753	0.0003	0.96	3.12	2.99	0.90	1019	10	994	14	1077	9
34	1.6711	0.0272	0.1614	0.0025	0.0751	0.0004	0.94	3.26	3.05	1.14	997	10	965	14	1071	11
35	3.4228	0.0478	0.2535	0.0035	0.0979	0.0003	0.98	2.79	2.73	0.56	1509	11	1458	18	1585	5
36	1.6980	0.0265	0.1649	0.0024	0.0747	0.0004	0.93	3.13	2.92	1.12	1008	10	985	13	1060	11
37	1.7504	0.0288	0.1683	0.0027	0.0754	0.0002	0.99	3.29	3.25	0.55	1027	11	1003	15	1080	6
38	1.6493	0.0248	0.1628	0.0024	0.0735	0.0002	0.98	3.01	2.94	0.64	989	9	973	13	1028	6
39	2.0263	0.0327	0.1882	0.0030	0.0781	0.0002	0.99	3.22	3.19	0.47	1124	11	1112	16	1149	5
40	1.8001	0.0326	0.1700	0.0030	0.0768	0.0003	0.97	3.62	3.51	0.88	1045	12	1013	16	1115	9
41	2.1001	0.0335	0.1882	0.0029	0.0810	0.0003	0.97	3.19	3.11	0.73	1149	11	1112	16	1220	7
42	2.9249	0.0387	0.2342	0.0030	0.0906	0.0003	0.97	2.65	2.56	0.68	1388	10	1357	16	1438	7
43	1.8015	0.0291	0.1692	0.0026	0.0772	0.0004	0.94	3.23	3.05	1.06	1046	10	1008	14	1127	11
44	2.5045	0.0393	0.2129	0.0033	0.0853	0.0002	0.98	3.14	3.09	0.54	1273	11	1245	17	1322	5
45	3.1270	0.0766	0.2493	0.0059	0.0910	0.0006	0.96	4.90	4.69	1.39	1439	19	1436	30	1446	13
46	1.6111	0.0441	0.1602	0.0041	0.0729	0.0007	0.93	5.47	5.11	1.97	974	17	959	23	1013	20
47	2.2775	0.0577	0.1990	0.0049	0.0830	0.0005	0.97	5.07	4.92	1.20	1205	18	1171	26	1270	12
48	1.6221	0.0408	0.1599	0.0039	0.0736	0.0005	0.97	5.02	4.86	1.28	979	16	957	22	1030	13
49	1.7808	0.0431	0.1720	0.0040	0.0751	0.0005	0.97	4.84	4.68	1.23	1038	16	1024	22	1071	12
50	1.7585	0.0448	0.1685	0.0041	0.0757	0.0005	0.96	5.10	4.91	1.35	1030	16	1005	23	1087	14
51	2.6080	0.0621	0.2197	0.0051	0.0861	0.0005	0.97	4.76	4.62	1.15	1303	17	1282	27	1340	11
52	2.0653	0.0517	0.1915	0.0047	0.0782	0.0005	0.97	5.01	4.87	1.16	1137	17	1130	25	1153	11
53	1.8389	0.0455	0.1782	0.0043	0.0748	0.0004	0.97	4.94	4.80	1.19	1059	16	1058	23	1064	12
54	1.7683	0.0457	0.1716	0.0043	0.0748	0.0005	0.97	5.17	5.01	1.29	1034	17	1022	24	1062	13
55	13.1315	0.3102	0.5351	0.0121	0.1780	0.0012	0.96	4.73	4.53	1.34	2689	22	2765	51	2634	11
56	1.5931	0.0403	0.1594	0.0039	0.0725	0.0004	0.97	5.06	4.92	1.19	967	16	954	22	1000	12
57	2.3933	0.0599	0.2039	0.0049	0.0851	0.0005	0.97	5.01	4.85	1.26	1240	18	1197	26	1319	12
58	2.7405	0.0695	0.2283	0.0056	0.0871	0.0005	0.97	5.07	4.94	1.15	1339	19	1327	30	1362	11
59	10.3519	0.2512	0.4635	0.0109	0.1620	0.0010	0.97	4.85	4.70	1.19	2466	22	2457	48	2477	10
60	1.7639	0.0481	0.1671	0.0044	0.0765	0.0006	0.96	5.46	5.24	1.51	1032	18	997	24	1109	15
61	1.7085	0.0472	0.1648	0.0043	0.0752	0.0006	0.95	5.52	5.27	1.65	1012	18	984	24	1074	17
62	2.5540	0.0651	0.2174	0.0053	0.0852	0.0006	0.96	5.10	4.91	1.36	1287	18	1269	28	1320	13

Table 4.1. (continued)

63	2.5611	0.0631	0.2163	0.0051	0.0859	0.0006	0.96	4.93	4.75	1.33	1289	18	1263	27	1335	13
64	1.8840	0.0482	0.1829	0.0045	0.0747	0.0005	0.96	5.12	4.92	1.39	1075	17	1084	25	1060	14

Table 4.1. (continued)

	CONCORDIA COLUMNS							±2σ			*AGES and 1 σ error (Ma)*					
analysis	**$^{207}Pb/^{235}U$**	**1σ**	**$^{206}Pb/^{238}U$**	**1σ**	**$^{207}Pb/^{206}Pb$**	**1σ**	**RHO**	**$^{207}Pb/^{235}U$**	**$^{206}Pb/^{238}U$**	**$^{207}Pb/^{206}Pb$**	**$^{207}Pb/^{235}U$**	**1σ**	**$^{206}Pb/^{238}U$**	**1σ**	**$^{207}Pb/^{206}Pb$**	**1σ**
Curling Group - Irishtown Formation (CB-260) (E 0431325/N 5423257)																
1	0.7216	0.0120	0.0880	0.0014	0.0595	0.0003	0.95	3.32	3.15	1.05	552	7	544	8	584	11
2	1.7641	0.0305	0.1690	0.0028	0.0757	0.0004	0.96	3.45	3.30	1.01	1032	11	1008	15	1087	10
3	4.9041	0.0716	0.3149	0.0044	0.1130	0.0004	0.96	2.92	2.81	0.79	1803	12	1766	22	1848	7
4	12.6877	0.2125	0.4981	0.0082	0.1847	0.0006	0.98	3.35	3.28	0.70	2656	16	2608	35	2696	6
5	11.5926	0.1761	0.4684	0.0069	0.1795	0.0006	0.97	3.04	2.96	0.71	2572	14	2479	30	2648	6
6	4.9270	0.0822	0.3168	0.0051	0.1128	0.0005	0.97	3.34	3.24	0.80	1807	14	1775	25	1845	7
7	1.7829	0.0284	0.1743	0.0027	0.0742	0.0003	0.97	3.18	3.10	0.73	1039	10	1037	15	1046	7
8	1.9653	0.0365	0.1836	0.0033	0.0776	0.0003	0.98	3.71	3.64	0.71	1104	12	1088	18	1137	7
9	14.8968	0.2251	0.5347	0.0078	0.2021	0.0007	0.97	3.02	2.93	0.73	2808	14	2763	33	2843	6
10	3.1599	0.0482	0.2358	0.0034	0.0972	0.0005	0.94	3.05	2.87	1.03	1447	12	1366	18	1571	10
11	1.7578	0.0330	0.1698	0.0031	0.0751	0.0003	0.97	3.76	3.64	0.93	1030	12	1012	17	1071	9
12	2.2821	0.0430	0.2002	0.0036	0.0827	0.0004	0.96	3.77	3.61	1.07	1207	13	1177	19	1261	10
13	13.1816	0.2051	0.5026	0.0076	0.1902	0.0007	0.97	3.11	3.03	0.72	2692	15	2627	33	2744	6
14	1.9852	0.0362	0.1842	0.0033	0.0782	0.0003	0.98	3.64	3.55	0.81	1110	12	1090	18	1152	8
15	2.4807	0.0440	0.2108	0.0036	0.0853	0.0005	0.95	3.55	3.37	1.11	1266	13	1234	19	1323	11
16	1.6665	0.0294	0.1640	0.0028	0.0737	0.0003	0.98	3.53	3.44	0.78	996	11	980	16	1033	8
17	2.5653	0.0433	0.2173	0.0035	0.0856	0.0005	0.95	3.37	3.19	1.09	1291	12	1268	18	1330	10
18	2.4163	0.0432	0.2037	0.0034	0.0860	0.0005	0.94	3.57	3.36	1.21	1247	13	1196	18	1339	12
19	1.7627	0.0332	0.1708	0.0031	0.0748	0.0004	0.96	3.77	3.62	1.02	1032	12	1017	17	1064	10
20	4.7190	0.0767	0.3121	0.0050	0.1097	0.0004	0.98	3.25	3.17	0.70	1770	14	1753	24	1794	6
21	5.1332	0.0781	0.3265	0.0048	0.1140	0.0004	0.97	3.04	2.96	0.72	1841	13	1823	23	1865	6
22	4.9666	0.0763	0.3210	0.0048	0.1122	0.0004	0.97	3.07	2.98	0.76	1813	13	1796	23	1836	7
23	12.0348	0.1990	0.4777	0.0077	0.1827	0.0007	0.98	3.31	3.23	0.71	2607	15	2519	34	2678	6
24	5.0710	0.0787	0.3222	0.0048	0.1141	0.0004	0.97	3.10	3.01	0.76	1831	13	1802	24	1866	7
25	1.7489	0.0324	0.1673	0.0030	0.0758	0.0004	0.97	3.70	3.58	0.95	1027	12	998	17	1090	9
26	1.7118	0.0333	0.1663	0.0031	0.0747	0.0005	0.95	3.89	3.68	1.26	1013	12	992	17	1059	13
27	3.7733	0.0700	0.2681	0.0047	0.1021	0.0006	0.95	3.71	3.53	1.14	1587	15	1532	24	1663	10
28	3.2829	0.0579	0.2496	0.0043	0.0954	0.0004	0.98	3.53	3.44	0.78	1477	14	1438	22	1536	7
29	1.6470	0.0289	0.1645	0.0028	0.0726	0.0003	0.98	3.51	3.43	0.73	988	11	983	16	1003	7

Table 4.1. (continued)

30	1.8178	0.0360	0.1724	0.0033	0.0765	0.0003	0.98	3.96	3.87	0.83	1052	13	1026	18	1108	8
31	1.6423	0.0313	0.1602	0.0029	0.0744	0.0004	0.96	3.82	3.67	1.04	986	12	958	16	1051	11
32	3.7908	0.0629	0.2676	0.0043	0.1027	0.0004	0.97	3.32	3.22	0.82	1591	13	1530	22	1674	8
33	1.7680	0.0375	0.1657	0.0033	0.0774	0.0006	0.94	4.24	3.97	1.48	1034	14	989	18	1132	15
34	3.7839	0.0611	0.2714	0.0043	0.1011	0.0004	0.97	3.23	3.15	0.73	1589	13	1549	22	1645	7
35	14.2480	0.2483	0.5158	0.0088	0.2003	0.0007	0.98	3.49	3.41	0.72	2766	16	2684	37	2829	6
36	2.7908	0.0531	0.2180	0.0040	0.0928	0.0005	0.96	3.80	3.65	1.07	1353	14	1272	21	1485	10
37	1.8009	0.0355	0.1709	0.0032	0.0764	0.0005	0.94	3.94	3.71	1.31	1046	13	1018	17	1106	13
38	1.7020	0.0345	0.1662	0.0033	0.0743	0.0003	0.98	4.06	3.97	0.86	1009	13	992	18	1049	9
39	3.0058	0.0498	0.2396	0.0039	0.0910	0.0003	0.97	3.31	3.22	0.76	1409	13	1386	20	1447	7
40	1.6348	0.0306	0.1613	0.0029	0.0735	0.0003	0.98	3.74	3.66	0.78	984	12	965	16	1028	8
41	1.9147	0.0333	0.1732	0.0029	0.0802	0.0004	0.96	3.48	3.34	0.96	1086	12	1031	16	1201	9
42	14.0436	0.2021	0.5205	0.0072	0.1957	0.0007	0.97	2.88	2.78	0.73	2752	14	2703	31	2791	6
43	1.6292	0.0348	0.1601	0.0033	0.0738	0.0003	0.98	4.27	4.17	0.92	981	13	958	19	1036	9
44	32.0859	0.5441	0.7107	0.0118	0.3274	0.0011	0.98	3.39	3.32	0.69	3552	17	3464	44	3605	5
45	5.1019	0.0880	0.3183	0.0053	0.1163	0.0005	0.97	3.45	3.36	0.78	1836	15	1783	26	1899	7
46	12.8050	0.2033	0.4909	0.0076	0.1892	0.0007	0.97	3.17	3.08	0.77	2665	15	2577	33	2735	6
47	2.4374	0.0455	0.2076	0.0037	0.0851	0.0004	0.97	3.73	3.61	0.93	1254	13	1217	20	1319	9
48	1.7518	0.0344	0.1679	0.0032	0.0757	0.0003	0.98	3.92	3.85	0.79	1028	13	1002	18	1086	8
49	12.7083	0.1958	0.4885	0.0073	0.1887	0.0007	0.97	3.08	2.98	0.77	2658	14	2566	32	2731	6
50	1.7749	0.0342	0.1763	0.0034	0.0730	0.0002	0.99	3.86	3.82	0.54	1036	12	1048	18	1014	5
51	2.2117	0.0434	0.1932	0.0037	0.0830	0.0002	0.99	3.93	3.88	0.60	1185	14	1139	20	1270	6
52	4.5152	0.0839	0.2977	0.0055	0.1100	0.0003	0.99	3.72	3.68	0.50	1734	15	1681	27	1800	5
53	3.6838	0.0673	0.2623	0.0047	0.1019	0.0003	0.98	3.65	3.59	0.64	1568	14	1503	24	1658	6
54	2.3135	0.0457	0.1977	0.0039	0.0849	0.0002	0.99	3.95	3.91	0.58	1216	14	1164	21	1312	6
55	4.1148	0.0746	0.2816	0.0050	0.1060	0.0004	0.98	3.62	3.56	0.67	1657	15	1601	25	1731	6
56	1.6269	0.0326	0.1585	0.0030	0.0745	0.0004	0.96	4.01	3.83	1.19	980	13	949	17	1054	12
57	6.6343	0.1168	0.3659	0.0064	0.1315	0.0004	0.99	3.52	3.48	0.54	2064	15	2012	30	2118	5
58	5.0713	0.0930	0.3210	0.0058	0.1146	0.0003	0.99	3.67	3.63	0.50	1831	15	1796	28	1873	5
59	1.6640	0.0325	0.1637	0.0032	0.0737	0.0002	0.99	3.91	3.85	0.63	995	12	978	17	1034	6
60	1.7382	0.0370	0.1666	0.0035	0.0757	0.0002	0.99	4.26	4.21	0.64	1023	14	994	19	1087	6
61	3.1038	0.0630	0.2361	0.0047	0.0953	0.0003	0.99	4.06	4.02	0.58	1433	15	1368	25	1535	5
62	2.4941	0.0490	0.2102	0.0041	0.0860	0.0003	0.99	3.93	3.87	0.66	1270	14	1231	22	1339	6

Table 4.1. (continued)

63	1.5521	0.0310	0.1551	0.0030	0.0726	0.0004	0.97	4.00	3.86	1.04	951	12	930	17	1002	11
64	16.9175	0.2934	0.5499	0.0094	0.2231	0.0007	0.98	3.47	3.41	0.63	2930	16	2827	39	3003	5
65	4.9270	0.0966	0.3138	0.0061	0.1139	0.0003	0.99	3.92	3.88	0.56	1807	16	1761	30	1862	5
66	2.3044	0.0459	0.1946	0.0038	0.0859	0.0004	0.97	3.98	3.87	0.94	1213	14	1147	20	1335	9
67	13.0196	0.2283	0.4956	0.0086	0.1905	0.0005	0.99	3.51	3.47	0.50	2681	16	2597	37	2747	4
68	1.6199	0.0328	0.1582	0.0032	0.0743	0.0003	0.98	4.05	3.98	0.74	978	13	947	18	1049	7
69	1.7507	0.0349	0.1691	0.0033	0.0751	0.0002	0.99	3.99	3.95	0.53	1027	13	1008	18	1071	5

Table 4.1. (continued)

	CONCORDIA COLUMNS							±2σ			AGES and 1 σ error (Ma)					
analysis	$^{207}Pb/^{235}U$	1σ	$^{206}Pb/^{238}U$	1σ	$^{207}Pb/^{206}Pb$	1σ	RHO	$^{207}Pb/^{235}U$	$^{206}Pb/^{238}U$	$^{207}Pb/^{206}Pb$	$^{207}Pb/^{235}U$	1σ	$^{206}Pb/^{238}U$	1σ	$^{207}Pb/^{206}Pb$	1σ
Crystalline Basement - Long Range Massif (NP-10A) (E 0512691/N 5529368)																
1	1.7766	0.0797	0.1744	0.0078	0.0739	0.0002	1.00	8.97	8.94	0.65	1037	29	1037	43	1039	7
2	1.8165	0.0809	0.1767	0.0078	0.0746	0.0002	1.00	8.91	8.88	0.64	1051	29	1050	43	1057	6
3	1.8099	0.0808	0.1770	0.0079	0.0741	0.0002	1.00	8.93	8.91	0.67	1049	29	1052	43	1045	7
4	1.7204	0.0784	0.1686	0.0077	0.0740	0.0002	1.00	9.12	9.10	0.62	1016	29	1005	42	1041	6
5	1.7674	0.0777	0.1737	0.0076	0.0738	0.0003	1.00	8.79	8.76	0.69	1033	28	1033	42	1036	7
6	1.8114	0.0797	0.1535	0.0067	0.0856	0.0003	1.00	8.80	8.77	0.75	1049	28	922	38	1328	7
7	1.7932	0.0796	0.1735	0.0077	0.0750	0.0003	1.00	8.88	8.84	0.79	1043	29	1032	42	1068	8
8	1.8114	0.0802	0.1768	0.0078	0.0743	0.0002	1.00	8.86	8.84	0.63	1049	29	1050	43	1050	6
9	1.7825	0.0798	0.1598	0.0071	0.0809	0.0004	0.99	8.96	8.90	1.00	1039	29	956	39	1219	10
10	1.7636	0.0772	0.1720	0.0075	0.0744	0.0003	1.00	8.75	8.72	0.75	1032	28	1024	41	1052	8
11	1.7435	0.0788	0.1720	0.0077	0.0735	0.0003	1.00	9.04	9.01	0.69	1025	29	1024	43	1029	7
12	1.5196	0.0679	0.1503	0.0067	0.0733	0.0003	1.00	8.94	8.90	0.88	938	27	903	37	1023	9
13	1.7226	0.0769	0.1685	0.0075	0.0742	0.0002	1.00	8.93	8.90	0.65	1017	28	1004	41	1046	7
14	1.5674	0.0702	0.1431	0.0064	0.0794	0.0003	1.00	8.96	8.92	0.82	957	27	863	36	1182	8
15	1.7145	0.0768	0.1671	0.0075	0.0744	0.0003	1.00	8.96	8.94	0.69	1014	28	997	41	1052	7
16	1.7172	0.0765	0.1675	0.0074	0.0744	0.0002	1.00	8.90	8.88	0.66	1015	28	999	41	1051	7
17	1.6545	0.0833	0.1633	0.0082	0.0735	0.0003	1.00	10.07	10.05	0.69	991	31	976	45	1027	7
18	1.7443	0.0774	0.1701	0.0075	0.0744	0.0003	1.00	8.88	8.85	0.70	1025	28	1014	41	1051	7
19	1.7412	0.0769	0.1708	0.0075	0.0739	0.0002	1.00	8.83	8.80	0.67	1024	28	1017	41	1040	7
20	1.6755	0.0737	0.1649	0.0072	0.0737	0.0003	1.00	8.80	8.77	0.74	999	28	984	40	1034	7
21	1.7119	0.0754	0.1677	0.0074	0.0740	0.0002	1.00	8.81	8.79	0.67	1013	28	1000	41	1043	7
22	1.7526	0.0776	0.1627	0.0072	0.0781	0.0004	0.99	8.86	8.79	1.05	1028	28	972	40	1150	10
23	1.6735	0.0741	0.1639	0.0072	0.0741	0.0002	1.00	8.86	8.84	0.63	998	28	979	40	1043	6
24	1.7760	0.0780	0.1708	0.0075	0.0754	0.0002	1.00	8.79	8.76	0.65	1037	28	1017	41	1079	7
25	1.6663	0.0737	0.1632	0.0072	0.0741	0.0002	1.00	8.84	8.82	0.66	996	28	975	40	1043	7
26	1.5707	0.0714	0.1595	0.0072	0.0714	0.0004	0.99	9.09	9.03	0.99	959	28	955	40	969	10
27	1.6851	0.0755	0.1543	0.0069	0.0792	0.0004	0.99	8.97	8.92	0.93	1003	28	926	38	1178	9
28	1.6711	0.0744	0.1613	0.0072	0.0751	0.0003	1.00	8.90	8.87	0.77	997	28	965	40	1072	8
29	1.6930	0.0752	0.1660	0.0074	0.0740	0.0002	1.00	8.88	8.86	0.64	1006	28	991	41	1040	6

Table 4.1. (continued)

30	1.6342	0.0719	0.1608	0.0071	0.0737	0.0002	1.00	8.80	8.78	0.67	983	27	962	39	1033	7
31	1.7016	0.0752	0.1628	0.0072	0.0758	0.0003	1.00	8.84	8.79	0.86	1009	28	973	40	1089	9
32	1.6656	0.0731	0.1615	0.0071	0.0748	0.0003	1.00	8.78	8.74	0.77	995	27	966	39	1063	8
33	1.6329	0.0719	0.1587	0.0070	0.0746	0.0003	1.00	8.81	8.78	0.69	983	27	951	39	1058	7
34	1.6311	0.0720	0.1593	0.0070	0.0743	0.0003	1.00	8.83	8.80	0.73	982	27	953	39	1049	7
35	1.6373	0.0724	0.1603	0.0071	0.0741	0.0003	1.00	8.85	8.82	0.70	985	28	959	39	1043	7
36	1.7759	0.0796	0.1744	0.0078	0.0739	0.0002	1.00	8.97	8.94	0.65	1037	29	1037	43	1038	7
37	1.8454	0.0819	0.1809	0.0080	0.0740	0.0002	1.00	8.87	8.85	0.62	1062	29	1072	44	1042	6
38	1.7562	0.0801	0.1656	0.0075	0.0769	0.0004	0.99	9.12	9.08	0.95	1029	29	988	41	1120	9
39	1.6849	0.0761	0.1641	0.0074	0.0745	0.0003	1.00	9.04	9.01	0.69	1003	28	980	41	1054	7
40	1.7973	0.0816	0.1767	0.0080	0.0738	0.0002	1.00	9.08	9.06	0.66	1044	29	1050	44	1035	7

Table 4.1. (continued)

	CONCORDIA COLUMNS							±2σ			*AGES and 1 σ error (Ma)*					
analysis	**$^{207}Pb/^{235}U$**	**1σ**	**$^{206}Pb/^{238}U$**	**1σ**	**$^{207}Pb/^{206}Pb$**	**1σ**	**RHO**	**$^{207}Pb/^{235}U$**	**$^{206}Pb/^{238}U$**	**$^{207}Pb/^{206}Pb$**	**$^{207}Pb/^{235}U$**	**1σ**	**$^{206}Pb/^{238}U$**	**1σ**	**$^{207}Pb/^{206}Pb$**	**1σ**
Labrador Group - Bradore Formation (NP-10) (E 0512691/N 5529368)																
1	2.0615	0.0747	0.1906	0.0069	0.0784	0.0002	1.00	7.25	7.24	0.43	1136	24	1125	37	1158	4
2	2.1802	0.0794	0.2068	0.0075	0.0765	0.0002	1.00	7.28	7.26	0.47	1175	25	1213	40	1107	5
3	2.1991	0.0802	0.2058	0.0075	0.0775	0.0001	1.00	7.30	7.29	0.37	1181	25	1207	40	1134	4
4	2.1954	0.0804	0.2047	0.0075	0.0778	0.0002	1.00	7.33	7.31	0.45	1179	25	1202	40	1141	4
5	1.9010	0.1150	0.1751	0.0105	0.0787	0.0007	0.99	12.10	11.98	1.73	1081	39	1041	57	1166	17
6	1.9468	0.0710	0.1863	0.0068	0.0758	0.0002	1.00	7.29	7.27	0.52	1097	24	1102	37	1089	5
7	1.8297	0.0675	0.1816	0.0067	0.0731	0.0002	1.00	7.38	7.37	0.42	1056	24	1076	36	1017	4
8	2.1310	0.0782	0.2073	0.0075	0.0746	0.0003	0.99	7.34	7.28	0.89	1159	25	1215	40	1057	9
9	2.1164	0.0803	0.1966	0.0074	0.0781	0.0002	1.00	7.59	7.57	0.51	1154	26	1158	40	1149	5
10	1.8244	0.0685	0.1774	0.0066	0.0746	0.0003	1.00	7.51	7.48	0.67	1054	24	1054	36	1057	7
11	1.7838	0.0673	0.1742	0.0066	0.0743	0.0002	1.00	7.54	7.53	0.50	1039	24	1036	36	1049	5
12	2.1018	0.0770	0.1955	0.0072	0.0780	0.0001	1.00	7.33	7.32	0.38	1149	25	1152	38	1146	4
13	1.9351	0.0726	0.1873	0.0070	0.0749	0.0001	1.00	7.50	7.49	0.37	1093	25	1108	38	1066	4
14	1.6825	0.0624	0.1661	0.0061	0.0735	0.0002	1.00	7.41	7.40	0.46	1002	23	991	34	1027	5
15	2.2823	0.0816	0.2145	0.0077	0.0772	0.0001	1.00	7.15	7.14	0.39	1207	25	1254	41	1125	4
16	2.0476	0.0748	0.1928	0.0070	0.0770	0.0001	1.00	7.31	7.30	0.38	1131	25	1138	38	1121	4
17	3.5445	0.1274	0.2714	0.0097	0.0947	0.0002	1.00	7.19	7.17	0.45	1537	28	1549	49	1523	4
18	2.1591	0.0780	0.2022	0.0073	0.0774	0.0002	1.00	7.23	7.21	0.45	1168	25	1188	39	1132	4
19	1.8125	0.0642	0.1706	0.0060	0.0771	0.0002	1.00	7.09	7.06	0.56	1050	23	1016	33	1123	6
20	2.1128	0.0780	0.1969	0.0073	0.0778	0.0002	1.00	7.38	7.36	0.49	1153	25	1160	39	1142	5
21	1.7746	0.0665	0.1753	0.0066	0.0734	0.0001	1.00	7.50	7.49	0.41	1036	24	1042	36	1025	4
22	1.4332	0.0595	0.1396	0.0057	0.0744	0.0005	0.99	8.31	8.21	1.29	903	25	843	32	1054	13
23	1.9123	0.0676	0.1882	0.0066	0.0737	0.0001	1.00	7.07	7.06	0.39	1085	23	1112	36	1033	4
24	1.7762	0.0744	0.1713	0.0072	0.0752	0.0002	1.00	8.38	8.37	0.41	1037	27	1020	39	1075	4
25	2.1337	0.0767	0.2004	0.0072	0.0772	0.0001	1.00	7.19	7.18	0.37	1160	25	1178	39	1127	4
26	2.0664	0.0746	0.1932	0.0070	0.0776	0.0002	1.00	7.22	7.21	0.40	1138	24	1139	38	1136	4
27	3.0599	0.1129	0.2413	0.0089	0.0920	0.0002	1.00	7.38	7.37	0.42	1423	28	1394	46	1467	4
28	1.7828	0.0652	0.1755	0.0064	0.0737	0.0002	1.00	7.31	7.30	0.41	1039	24	1043	35	1033	4
29	2.0625	0.0768	0.1926	0.0072	0.0777	0.0001	1.00	7.45	7.44	0.37	1136	25	1136	39	1138	4

Table 4.1. (continued)

30	3.0803	0.1135	0.2380	0.0088	0.0939	0.0002	1.00	7.37	7.36	0.43	1428	28	1377	45	1506	4
31	1.6412	0.0608	0.1609	0.0059	0.0740	0.0002	1.00	7.40	7.39	0.48	986	23	963	33	1040	5
32	1.6920	0.0623	0.1679	0.0062	0.0731	0.0001	1.00	7.37	7.36	0.40	1005	23	1002	34	1016	4
33	1.7795	0.0697	0.1721	0.0067	0.0750	0.0002	1.00	7.84	7.82	0.52	1038	25	1025	37	1068	5
34	1.6957	0.0629	0.1706	0.0063	0.0721	0.0001	1.00	7.42	7.41	0.38	1007	23	1016	35	988	4
35	1.6653	0.0635	0.1630	0.0062	0.0741	0.0002	1.00	7.62	7.60	0.60	995	24	974	34	1045	6
36	2.3019	0.0962	0.1921	0.0071	0.0869	0.0017	0.88	8.36	7.38	3.91	1213	29	1134	38	1359	38
37	1.9706	0.0748	0.1842	0.0070	0.0776	0.0002	1.00	7.59	7.57	0.51	1105	25	1091	38	1136	5
38	1.9425	0.0721	0.1831	0.0068	0.0769	0.0001	1.00	7.43	7.42	0.37	1096	25	1085	37	1120	4
39	2.2831	0.0822	0.1998	0.0072	0.0829	0.0003	0.99	7.20	7.16	0.74	1207	25	1175	38	1266	7
40	1.8092	0.0674	0.1776	0.0066	0.0739	0.0002	1.00	7.46	7.44	0.44	1049	24	1055	36	1038	4
41	1.9457	0.0780	0.1830	0.0073	0.0771	0.0001	1.00	8.02	8.01	0.34	1097	27	1084	40	1125	3
42	2.0288	0.0824	0.1916	0.0078	0.0768	0.0001	1.00	8.12	8.11	0.36	1125	27	1131	42	1116	4
43	1.6891	0.0679	0.1657	0.0066	0.0740	0.0003	1.00	8.05	8.02	0.68	1004	25	989	37	1040	7
44	1.8268	0.0727	0.1773	0.0070	0.0747	0.0001	1.00	7.96	7.95	0.30	1055	26	1053	39	1061	3
45	2.0126	0.0809	0.1880	0.0075	0.0776	0.0002	1.00	8.04	8.02	0.58	1120	27	1112	41	1137	6
46	1.5980	0.0624	0.1577	0.0061	0.0735	0.0002	1.00	7.81	7.80	0.41	969	24	945	34	1028	4
47	1.8259	0.0732	0.1752	0.0070	0.0756	0.0001	1.00	8.01	8.01	0.26	1055	26	1042	38	1084	3
48	1.6537	0.0675	0.1630	0.0067	0.0736	0.0001	1.00	8.17	8.16	0.39	991	26	974	37	1029	4
49	1.5846	0.0657	0.1564	0.0065	0.0735	0.0002	1.00	8.30	8.28	0.57	964	25	938	36	1027	6
50	2.3933	0.1478	0.2028	0.0122	0.0856	0.0011	0.98	12.35	12.06	2.65	1240	43	1191	65	1329	26
51	1.6400	0.0670	0.1618	0.0066	0.0735	0.0002	1.00	8.18	8.16	0.44	986	25	968	37	1028	4
52	2.0093	0.0809	0.1879	0.0076	0.0775	0.0001	1.00	8.05	8.04	0.30	1118	27	1111	41	1135	3
53	1.6545	0.0682	0.1628	0.0067	0.0737	0.0002	1.00	8.25	8.23	0.49	991	26	973	37	1034	5
54	1.9308	0.0772	0.1807	0.0072	0.0775	0.0002	1.00	8.00	7.99	0.42	1092	26	1071	39	1134	4
55	1.6509	0.0660	0.1631	0.0065	0.0734	0.0001	1.00	8.00	8.00	0.28	990	25	975	36	1025	3
56	1.8309	0.0750	0.1730	0.0071	0.0767	0.0002	1.00	8.19	8.17	0.53	1056	27	1030	39	1114	5
57	1.6601	0.0678	0.1629	0.0066	0.0739	0.0001	1.00	8.17	8.16	0.35	993	26	974	37	1039	4
58	1.9116	0.0772	0.1817	0.0073	0.0763	0.0001	1.00	8.07	8.07	0.27	1085	27	1077	40	1103	3
59	1.7602	0.0710	0.1702	0.0069	0.0750	0.0001	1.00	8.07	8.06	0.36	1031	26	1014	38	1068	4
60	1.6344	0.0659	0.1626	0.0066	0.0729	0.0001	1.00	8.07	8.06	0.35	983	25	972	36	1012	4

Table 4.1. (continued)

	CONCORDIA COLUMNS							±2σ			AGES and 1 σ error (Ma)					
analysis	$^{207}Pb/^{235}U$	1σ	$^{206}Pb/^{238}U$	1σ	$^{207}Pb/^{206}Pb$	1σ	RHO	$^{207}Pb/^{235}U$	$^{206}Pb/^{238}U$	$^{207}Pb/^{206}Pb$	$^{207}Pb/^{235}U$	1σ	$^{206}Pb/^{238}U$	1σ	$^{207}Pb/^{206}Pb$	1σ
Crystalline Basement - Indian Head Range (STV-30A) (E 0393708/N 5394102)																
1	3.3670	0.0450	0.2606	0.0034	0.0937	0.0002	0.99	2.67	2.65	0.37	1497	10	1494	18	1502	4
2	3.3165	0.0427	0.2577	0.0033	0.0933	0.0002	0.98	2.57	2.54	0.44	1485	10	1479	17	1495	4
3	3.2874	0.0459	0.2553	0.0035	0.0934	0.0002	0.98	2.79	2.75	0.52	1478	11	1467	18	1495	5
4	3.3694	0.0685	0.2610	0.0053	0.0936	0.0002	0.99	4.07	4.05	0.41	1497	16	1496	27	1500	4
5	3.3395	0.0440	0.2592	0.0034	0.0935	0.0002	0.98	2.63	2.59	0.48	1490	10	1487	17	1497	5
6	3.3316	0.0437	0.2591	0.0034	0.0932	0.0002	0.99	2.63	2.59	0.43	1488	10	1487	17	1493	4
7	3.3062	0.0416	0.2568	0.0032	0.0934	0.0002	0.99	2.51	2.48	0.43	1482	10	1475	16	1495	4
8	3.2829	0.0395	0.2545	0.0030	0.0936	0.0002	0.98	2.41	2.37	0.44	1477	9	1463	15	1499	4
9	3.1487	0.0605	0.2496	0.0048	0.0915	0.0002	0.99	3.84	3.82	0.47	1444	15	1438	25	1457	4
10	3.2819	0.0404	0.2552	0.0031	0.0933	0.0002	0.99	2.46	2.42	0.41	1477	10	1466	16	1494	4
11	3.3218	0.0396	0.2575	0.0030	0.0936	0.0002	0.99	2.38	2.35	0.39	1486	9	1478	16	1499	4
12	3.2806	0.0364	0.2555	0.0028	0.0931	0.0002	0.99	2.22	2.19	0.38	1476	9	1468	14	1491	4
13	3.2473	0.0403	0.2528	0.0031	0.0932	0.0002	0.98	2.48	2.44	0.48	1468	10	1454	16	1491	5
14	3.2672	0.0366	0.2540	0.0028	0.0933	0.0002	0.98	2.24	2.19	0.46	1473	9	1460	14	1493	4
15	3.2750	0.0425	0.2544	0.0032	0.0934	0.0002	0.98	2.60	2.56	0.46	1475	10	1462	17	1496	4
16	3.2610	0.0373	0.2543	0.0029	0.0930	0.0002	0.98	2.29	2.25	0.43	1472	9	1462	15	1488	4
17	3.2147	0.0403	0.2495	0.0031	0.0934	0.0002	0.98	2.51	2.45	0.52	1460	10	1437	16	1497	5
18	3.1344	0.0395	0.2455	0.0030	0.0926	0.0002	0.98	2.52	2.48	0.45	1441	10	1416	16	1480	4
19	3.2271	0.0676	0.2519	0.0053	0.0929	0.0002	1.00	4.19	4.17	0.38	1463	16	1449	27	1486	4
20	3.1171	0.0467	0.2445	0.0036	0.0925	0.0002	0.99	3.00	2.97	0.40	1437	11	1411	19	1477	4
21	3.2209	0.0547	0.2526	0.0036	0.0925	0.0008	0.85	3.40	2.89	1.79	1462	13	1453	19	1477	17
22	3.4571	0.0629	0.2716	0.0043	0.0923	0.0008	0.87	3.64	3.15	1.82	1517	14	1550	22	1474	17
23	3.6714	0.0602	0.2871	0.0039	0.0927	0.0008	0.84	3.28	2.75	1.79	1565	13	1628	20	1483	17
24	3.2739	0.0841	0.2550	0.0061	0.0931	0.0008	0.94	5.14	4.81	1.81	1475	20	1465	31	1490	17
25	3.5267	0.0637	0.2746	0.0043	0.0931	0.0008	0.87	3.61	3.13	1.80	1533	14	1565	22	1491	17
26	3.5503	0.0607	0.2784	0.0041	0.0925	0.0008	0.85	3.42	2.92	1.79	1538	13	1585	20	1477	17
27	3.4927	0.0616	0.2727	0.0041	0.0929	0.0008	0.86	3.53	3.04	1.79	1525	14	1556	21	1486	17
28	3.4270	0.0642	0.2676	0.0044	0.0929	0.0008	0.88	3.75	3.28	1.80	1510	15	1530	22	1485	17
29	3.3483	0.0582	0.2555	0.0038	0.0950	0.0009	0.86	3.48	2.98	1.80	1492	14	1468	20	1529	17

Table 4.1. (continued)

30	3.3114	0.0565	0.2614	0.0038	0.0919	0.0008	0.85	3.41	2.90	1.80	1484	13	1498	19	1465	17
31	3.2701	0.0615	0.2575	0.0042	0.0921	0.0008	0.88	3.76	3.30	1.81	1474	15	1478	22	1470	17
32	3.3400	0.0600	0.2601	0.0040	0.0931	0.0008	0.87	3.60	3.11	1.80	1490	14	1492	21	1491	17
33	3.3605	0.0609	0.2630	0.0041	0.0927	0.0008	0.87	3.63	3.15	1.79	1495	14	1506	21	1481	17
34	3.4151	0.0610	0.2656	0.0041	0.0932	0.0008	0.86	3.57	3.08	1.81	1508	14	1520	21	1493	17
35	3.3855	0.0582	0.2649	0.0039	0.0927	0.0008	0.85	3.44	2.93	1.79	1501	13	1516	20	1482	17
36	3.3418	0.0614	0.2618	0.0042	0.0926	0.0008	0.87	3.68	3.21	1.79	1491	14	1500	21	1479	17
37	3.3408	0.0590	0.2628	0.0040	0.0922	0.0008	0.86	3.53	3.04	1.79	1490	14	1506	20	1471	17
38	3.2853	0.0644	0.2561	0.0045	0.0930	0.0008	0.89	3.92	3.49	1.79	1477	15	1471	23	1489	17
39	3.3730	0.0587	0.2635	0.0039	0.0928	0.0008	0.86	3.48	2.99	1.78	1498	14	1509	20	1485	17
40	3.1477	0.0506	0.2610	0.0035	0.0875	0.0008	0.83	3.21	2.67	1.79	1444	12	1496	18	1371	17

Table 4.1. (continued)

	CONCORDIA COLUMNS							±2σ			*AGES and 1 σ error (Ma)*					
analysis	**$^{207}Pb/^{235}U$**	**1σ**	**$^{206}Pb/^{238}U$**	**1σ**	**$^{207}Pb/^{206}Pb$**	**1σ**	**RHO**	**$^{207}Pb/^{235}U$**	**$^{206}Pb/^{238}U$**	**$^{207}Pb/^{206}Pb$**	**$^{207}Pb/^{235}U$**	**1σ**	**$^{206}Pb/^{238}U$**	**1σ**	**$^{207}Pb/^{206}Pb$**	**1σ**
Labrador Group - Bradore Formation (STV-30) (E 0393708/N 5394102)																
1	1.7223	0.0281	0.1661	0.0027	0.0752	0.0002	0.99	3.26	3.21	0.55	1017	10	991	15	1074	5
2	1.9695	0.0306	0.1836	0.0028	0.0778	0.0002	0.98	3.11	3.06	0.55	1105	10	1087	15	1142	5
3	2.0954	0.0233	0.1969	0.0021	0.0772	0.0003	0.95	2.22	2.10	0.71	1147	8	1160	11	1126	7
4	2.1739	0.0191	0.2054	0.0017	0.0768	0.0002	0.93	1.76	1.64	0.63	1173	6	1205	9	1115	6
5	1.9537	0.0365	0.1826	0.0033	0.0776	0.0003	0.98	3.73	3.65	0.80	1100	12	1082	18	1137	8
6	2.0629	0.0193	0.1943	0.0017	0.0770	0.0002	0.95	1.87	1.78	0.58	1136	6	1145	9	1122	6
7	2.1483	0.0340	0.2032	0.0031	0.0767	0.0003	0.97	3.16	3.08	0.71	1164	11	1194	17	1112	7
8	1.9955	0.0277	0.1844	0.0025	0.0785	0.0003	0.97	2.78	2.69	0.70	1114	9	1092	13	1159	7
9	1.9326	0.0248	0.1872	0.0023	0.0749	0.0002	0.97	2.57	2.49	0.64	1092	9	1107	13	1065	6
10	1.5773	0.0243	0.1577	0.0024	0.0725	0.0002	0.98	3.08	3.03	0.59	961	10	945	13	1001	6
11	2.0820	0.0344	0.1954	0.0032	0.0773	0.0002	0.98	3.31	3.25	0.63	1143	11	1151	17	1128	6
12	1.9128	0.0334	0.1792	0.0031	0.0774	0.0002	0.98	3.49	3.44	0.63	1085	12	1063	17	1132	6
13	2.0221	0.0256	0.1901	0.0023	0.0772	0.0002	0.98	2.53	2.47	0.55	1123	9	1123	13	1125	5
14	1.9369	0.0309	0.1805	0.0028	0.0778	0.0003	0.97	3.19	3.09	0.79	1094	11	1070	15	1143	8
15	1.9531	0.0410	0.1828	0.0038	0.0775	0.0002	0.99	4.20	4.17	0.53	1099	14	1083	21	1134	5
16	1.9914	0.0322	0.1868	0.0030	0.0773	0.0002	0.99	3.23	3.18	0.54	1112	11	1105	16	1130	5
17	1.9102	0.0325	0.1796	0.0030	0.0771	0.0002	0.98	3.40	3.35	0.61	1084	11	1066	16	1125	6
18	1.9461	0.0325	0.1813	0.0029	0.0778	0.0003	0.97	3.35	3.24	0.82	1097	11	1075	16	1143	8
19	1.7937	0.0296	0.1701	0.0027	0.0765	0.0003	0.97	3.30	3.20	0.80	1043	11	1014	15	1107	8
20	1.9539	0.0336	0.1824	0.0031	0.0777	0.0002	0.99	3.44	3.39	0.54	1100	11	1081	17	1139	5
21	2.2466	0.0357	0.2184	0.0033	0.0746	0.0003	0.96	3.17	3.04	0.92	1196	11	1274	18	1058	9
22	1.5906	0.0299	0.1599	0.0030	0.0721	0.0002	0.99	3.76	3.72	0.56	966	12	957	17	990	6
23	1.9865	0.0338	0.1857	0.0031	0.0776	0.0002	0.99	3.40	3.36	0.55	1111	11	1099	17	1136	5
24	1.8779	0.0329	0.1782	0.0031	0.0764	0.0002	0.99	3.50	3.45	0.59	1073	12	1058	17	1107	6
25	1.9385	0.0346	0.1805	0.0032	0.0779	0.0003	0.98	3.57	3.50	0.68	1094	12	1070	17	1144	7
26	1.8737	0.0393	0.1780	0.0037	0.0763	0.0002	0.99	4.20	4.16	0.54	1072	14	1057	20	1104	5
27	1.8978	0.0349	0.1771	0.0032	0.0777	0.0002	0.99	3.68	3.64	0.54	1080	12	1052	18	1139	5
28	1.8876	0.0327	0.1759	0.0030	0.0778	0.0003	0.98	3.46	3.39	0.71	1077	11	1045	16	1143	7
29	1.9356	0.0352	0.1809	0.0032	0.0776	0.0002	0.99	3.63	3.58	0.61	1093	12	1073	18	1136	6

Table 4.1. (continued)

30	1.5774	0.0253	0.1590	0.0025	0.0719	0.0002	0.99	3.20	3.16	0.52	961	10	952	14	984	5
31	1.9110	0.0334	0.1792	0.0031	0.0773	0.0002	0.98	3.50	3.43	0.65	1085	12	1064	17	1130	6
32	1.8039	0.0299	0.1728	0.0028	0.0757	0.0002	0.98	3.32	3.26	0.63	1047	11	1028	15	1088	6
33	1.8805	0.0284	0.1783	0.0026	0.0765	0.0002	0.98	3.02	2.96	0.59	1074	10	1059	14	1108	6
34	1.7385	0.0304	0.1708	0.0030	0.0738	0.0002	0.99	3.49	3.46	0.50	1023	11	1018	16	1036	5
35	2.0796	0.0252	0.1947	0.0023	0.0775	0.0002	0.97	2.42	2.34	0.63	1142	8	1148	12	1133	6
36	2.2055	0.0323	0.2074	0.0030	0.0771	0.0002	0.98	2.93	2.86	0.61	1183	10	1216	16	1124	6
37	1.9445	0.0394	0.1819	0.0036	0.0775	0.0003	0.99	4.06	4.00	0.65	1096	14	1078	20	1135	6
38	1.9524	0.0386	0.1799	0.0035	0.0787	0.0003	0.98	3.95	3.86	0.86	1099	13	1067	19	1165	8
39	1.9517	0.0389	0.1813	0.0036	0.0781	0.0003	0.99	3.98	3.93	0.66	1099	13	1075	19	1149	7
40	1.9155	0.0368	0.1794	0.0034	0.0775	0.0003	0.98	3.84	3.78	0.69	1086	13	1064	19	1133	7
41	2.0056	0.0332	0.1867	0.0030	0.0779	0.0002	0.98	3.31	3.26	0.57	1117	11	1104	17	1144	6
42	2.1476	0.0346	0.2018	0.0031	0.0772	0.0003	0.96	3.23	3.11	0.85	1164	11	1186	17	1126	8
43	2.0307	0.0320	0.1918	0.0029	0.0768	0.0003	0.97	3.15	3.06	0.76	1126	11	1132	16	1115	8
44	1.8508	0.0307	0.1749	0.0028	0.0768	0.0003	0.98	3.32	3.23	0.73	1064	11	1040	16	1115	7
45	1.9212	0.0303	0.1794	0.0028	0.0777	0.0002	0.98	3.16	3.10	0.57	1088	10	1064	15	1139	6
46	2.0538	0.0348	0.1929	0.0032	0.0772	0.0002	0.99	3.39	3.35	0.51	1133	12	1138	17	1127	5
47	1.9880	0.0269	0.1861	0.0024	0.0775	0.0003	0.97	2.71	2.61	0.71	1111	9	1101	13	1133	7
48	1.8752	0.0306	0.1763	0.0028	0.0771	0.0002	0.99	3.26	3.22	0.55	1072	11	1048	16	1125	5
49	1.9006	0.0332	0.1790	0.0031	0.0770	0.0002	0.98	3.49	3.44	0.63	1081	12	1062	17	1122	6
50	1.9695	0.0301	0.1837	0.0027	0.0778	0.0003	0.98	3.05	2.98	0.64	1105	10	1088	15	1141	6
51	1.9119	0.0331	0.1714	0.0022	0.0809	0.0009	0.74	3.47	2.57	2.33	1085	11	1021	12	1219	23
52	1.8620	0.0300	0.1753	0.0028	0.0770	0.0003	0.98	3.23	3.15	0.71	1068	11	1042	15	1122	7
53	1.8651	0.0363	0.1743	0.0034	0.0776	0.0002	0.99	3.90	3.86	0.55	1069	13	1037	18	1136	5
54	1.8950	0.0326	0.1772	0.0030	0.0776	0.0003	0.98	3.44	3.38	0.65	1079	11	1052	16	1136	6
55	1.9762	0.0339	0.1826	0.0030	0.0785	0.0003	0.97	3.43	3.31	0.88	1107	11	1082	16	1160	9
56	1.6130	0.0249	0.1614	0.0025	0.0725	0.0002	0.98	3.09	3.04	0.55	975	10	965	14	999	6
57	1.9446	0.0289	0.1821	0.0027	0.0775	0.0002	0.98	2.97	2.92	0.52	1096	10	1079	15	1133	5
58	1.7356	0.0229	0.1724	0.0022	0.0730	0.0002	0.97	2.64	2.56	0.64	1022	8	1026	12	1014	7
59	1.7617	0.0353	0.1703	0.0033	0.0750	0.0003	0.98	4.01	3.93	0.79	1031	13	1014	18	1070	8

Table 4.2. Lu-Hf isotopic data of LAM-ICP-MS analysis of detrital and igneous zircons

analysis	Age (Ma)	$^{176}Hf/^{177}Hf_{(0)}$	1σ	$^{176}Lu/^{177}Lu$	$^{176}Hf/^{177}Hf_{initial}$	$\varepsilon_{Hf}(t)$	T_{CHUR} (Ga)	T_{DM} (Ga)
Mount Musgrave Group - South Brook Fm (CB-212)								
1	1045	0.282205	0.000011	0.000468	0.282196	2.4	0.94	1.42
2	1064	0.282208	0.000014	0.000808	0.282192	2.7	0.94	1.43
3	1057	0.282214	0.000012	0.000623	0.282202	2.9	0.93	1.42
4	1052	0.282199	0.000011	0.001132	0.282177	1.9	0.97	1.46
5	1054	0.282205	0.000012	0.000771	0.282190	2.4	0.95	1.43
6	1000	0.282193	0.000010	0.001881	0.282158	0.0	1.00	1.49
7	1066	0.282212	0.000012	0.000690	0.282198	3.0	0.93	1.42
8	1054	0.282203	0.000013	0.000696	0.282189	2.4	0.95	1.43
9	1070	0.282216	0.000013	0.000819	0.282199	3.1	0.93	1.42
10	1148	0.282236	0.000012	0.001232	0.282209	5.2	0.91	1.41
11	1006	0.282193	0.000010	0.000543	0.282183	1.0	0.96	1.44
12	1208	0.282195	0.000013	0.000703	0.282179	5.5	0.96	1.45
13	1006	0.282303	0.000012	0.000875	0.282286	4.7	0.79	1.30
14	1145	0.282205	0.000021	0.000620	0.282192	4.5	0.94	1.43
15	988	0.282205	0.000012	0.000649	0.282193	1.0	0.94	1.43
16	1431	0.282082	0.000014	0.000904	0.282058	6.3	1.15	1.61
17	1153	0.282220	0.000012	0.000918	0.282200	5.0	0.93	1.42
18	1032	0.282165	0.000012	0.000758	0.282150	0.5	1.01	1.49
19	1140	0.282121	0.000013	0.000521	0.282110	1.5	1.07	1.54
20	1059	0.282210	0.000013	0.000693	0.282196	2.7	0.94	1.42
21	1162	0.282145	0.000013	0.000741	0.282129	2.7	1.04	1.52
22	1010	0.282158	0.000011	0.000941	0.282140	-0.4	1.03	1.51
23	1010	0.282205	0.000014	0.000430	0.282197	1.6	0.94	1.42
24	1012	0.282184	0.000014	0.001163	0.282162	0.4	0.99	1.48
25	1333	0.282160	0.000014	0.000622	0.282144	7.1	1.01	1.49
26	1145	0.282164	0.000013	0.000706	0.282149	3.0	1.01	1.49
27	1147	0.282222	0.000012	0.001055	0.282199	4.8	0.93	1.42
28	1162	0.282248	0.000012	0.000929	0.282228	6.2	0.88	1.38
29	1141	0.282157	0.000015	0.000914	0.282137	2.5	1.03	1.51
30	1083	0.282235	0.000013	0.001348	0.282207	3.7	0.91	1.41
31	1148	0.282275	0.000015	0.001373	0.282245	6.5	0.85	1.36
32	1035	0.282237	0.000011	0.001188	0.282214	2.8	0.91	1.41
33	1044	0.282210	0.000012	0.000914	0.282192	2.2	0.94	1.43
34	1019	0.282202	0.000016	0.001490	0.282173	1.0	0.97	1.47
35	1197	0.282151	0.000013	0.001021	0.282128	3.4	1.04	1.52
36	1154	0.282178	0.000016	0.000688	0.282163	3.7	0.99	1.47
37	1053	0.282192	0.000017	0.000855	0.282175	1.8	0.97	1.46
38	1472	0.282194	0.000014	0.002069	0.282136	10.0	1.00	1.50
39	1499	0.282111	0.000009	0.001709	0.282062	8.0	1.13	1.60
40	1497	0.282004	0.000009	0.000822	0.281981	5.1	1.27	1.71
41	999	0.282269	0.000014	0.001625	0.282238	2.9	0.87	1.38
42	1179	0.282146	0.000013	0.000740	0.282130	3.1	1.04	1.51
43	1460	0.282089	0.000014	0.001266	0.282054	6.8	1.15	1.62
44	1034	0.282177	0.000013	0.000690	0.282164	1.0	0.99	1.47

Table 4.2. (continued)

analysis	Age (Ma)	$^{176}Hf/^{177}Hf_{(0)}$	1σ	$^{176}Lu/^{177}Lu$	$^{176}Hf/^{177}Hf_{initial}$	$\varepsilon_{Hf}(t)$	T_{CHUR} (Ga)	T_{DM} (Ga)
Mount Musgrave Group - South Brook Fm (CB-230)								
1	1058	0.282183	0.000015	0.001136	0.282160	1.4	0.99	1.48
2	1032	0.282218	0.000011	0.000565	0.282207	2.5	0.92	1.41
3	1139	0.282220	0.000013	0.001113	0.282196	4.5	0.93	1.43
4	1186	0.282154	0.000013	0.000713	0.282138	3.5	1.03	1.50
5	1043	0.282195	0.000012	0.000463	0.282186	2.0	0.95	1.44
6	991	0.282215	0.000009	0.001518	0.282187	0.8	0.95	1.45
7	881	0.282223	0.000009	0.000649	0.282212	-0.7	0.91	1.40
8	1009	0.282225	0.000012	0.001008	0.282206	1.9	0.92	1.42
9	1030	0.282186	0.000011	0.000733	0.282172	1.2	0.98	1.46
10	978	0.282252	0.000013	0.000599	0.282241	2.5	0.87	1.36
11	1145	0.282199	0.000014	0.000665	0.282185	4.3	0.95	1.44
12	1058	0.282161	0.000011	0.000463	0.282152	1.1	1.01	1.48
13	1111	0.282187	0.000014	0.000926	0.282168	2.9	0.98	1.47
14	1127	0.282182	0.000013	0.000447	0.282172	3.4	0.97	1.45
15	1070	0.282157	0.000017	0.000776	0.282141	1.0	1.02	1.50
16	1029	0.282218	0.000014	0.000484	0.282209	2.5	0.92	1.41
17	1035	0.282208	0.000014	0.000507	0.282198	2.2	0.93	1.42
18	1016	0.282222	0.000013	0.000589	0.282211	2.3	0.91	1.40
19	1159	0.282246	0.000013	0.001356	0.282216	5.7	0.90	1.40
20	1110	0.282129	0.000014	0.000875	0.282111	0.9	1.07	1.54
21	1136	0.282189	0.000014	0.001176	0.282164	3.3	0.98	1.47
22	980	0.282191	0.000014	0.000536	0.282181	0.4	0.96	1.44
23	1135	0.282196	0.000014	0.000850	0.282178	3.8	0.96	1.45
24	991	0.282214	0.000013	0.001083	0.282194	1.1	0.94	1.43
25	1030	0.282201	0.000011	0.000635	0.282189	1.8	0.95	1.43
26	1043	0.282192	0.000014	0.000702	0.282178	1.7	0.96	1.45
27	1193	0.282227	0.000013	0.000675	0.282212	6.3	0.91	1.40
28	1183	0.282221	0.000013	0.000620	0.282207	5.9	0.92	1.41
29	1056	0.282301	0.000015	0.001122	0.282279	5.6	0.80	1.31
30	1042	0.282254	0.000013	0.000338	0.282247	4.2	0.86	1.35
31	976	0.282217	0.000012	0.000473	0.282208	1.3	0.92	1.41
32	1037	0.282183	0.000011	0.000808	0.282167	1.2	0.98	1.47
33	1127	0.282256	0.000010	0.001200	0.282230	5.5	0.88	1.38
34	1076	0.282164	0.000015	0.001385	0.282136	1.0	1.03	1.52
35	1000	0.282240	0.000012	0.000393	0.282233	2.7	0.88	1.37
36	1153	0.282259	0.000017	0.002089	0.282214	5.5	0.90	1.41
37	984	0.282188	0.000014	0.000743	0.282174	0.3	0.97	1.46
38	1032	0.282230	0.000013	0.000860	0.282213	2.7	0.91	1.40
39	1322	0.282093	0.000012	0.001350	0.282059	3.9	1.15	1.61
40	999	0.282193	0.000014	0.000532	0.282183	0.9	0.96	1.44

Table 4.2. (continued)

analysis	Age (Ma)	$^{176}Hf/^{177}Hf_{(0)}$	1σ	$^{176}Lu/^{177}Lu$	$^{176}Hf/^{177}Hf_{initial}$	$\varepsilon_{Hf}(t)$	T_{CHUR} (Ga)	T_{DM} (Ga)
Curling Group - Summerside Fm (CB-219)								
1	1149	0.282183	0.000012	0.001488	0.282151	3.2	1.00	1.49
2	1042	0.282168	0.000013	0.000733	0.282154	0.8	1.00	1.48
3	1126	0.282161	0.000015	0.000573	0.282149	2.6	1.01	1.49
4	1035	0.282119	0.000016	0.000691	0.282106	-1.0	1.08	1.55
5	1042	0.282223	0.000010	0.001210	0.282199	2.5	0.93	1.43
6	1144	0.282168	0.000011	0.001202	0.282142	2.7	1.02	1.50
7	1026	0.282226	0.000023	0.000465	0.282217	2.7	0.90	1.39
8	1521	0.282065	0.000009	0.001569	0.282020	7.0	1.20	1.66
9	1470	0.282095	0.000012	0.001554	0.282052	7.0	1.15	1.62
10	1149	0.282139	0.000013	0.000682	0.282124	2.2	1.05	1.52
11	1177	0.282126	0.000011	0.000666	0.282111	2.4	1.07	1.54
12	1295	0.282075	0.000029	0.005904	0.281931	-1.3	1.37	1.86
13	1111	0.282175	0.000013	0.000798	0.282158	2.6	0.99	1.48
14	1040	0.282239	0.000011	0.000572	0.282228	3.4	0.89	1.38
15	1045	0.282178	0.000014	0.000497	0.282168	1.4	0.98	1.46
16	1460	0.282121	0.000011	0.000500	0.282107	8.7	1.07	1.54
17	1045	0.282138	0.000009	0.001500	0.282108	-0.7	1.08	1.56
18	1157	0.282239	0.000012	0.001261	0.282211	5.5	0.90	1.41
19	1198	0.282232	0.000010	0.001433	0.282200	6.0	0.92	1.42
20	1039	0.282225	0.000010	0.000699	0.282211	2.8	0.91	1.40
21	1140	0.282193	0.000014	0.000898	0.282174	3.8	0.97	1.46
22	1129	0.282157	0.000010	0.000979	0.282136	2.2	1.03	1.51
23	1048	0.281924	0.000015	0.000421	0.281916	-7.5	1.38	1.80
24	1136	0.282187	0.000012	0.000649	0.282173	3.7	0.97	1.45
25	622	0.282395	0.000013	0.001438	0.282378	-0.7	0.65	1.19
26	1189	0.282155	0.000011	0.000345	0.282147	3.9	1.01	1.49
27	1030	0.282166	0.000012	0.000487	0.282157	0.7	1.00	1.48
28	1163	0.282174	0.000014	0.000883	0.282155	3.6	1.00	1.48
29	1172	0.282251	0.000014	0.001852	0.282210	5.8	0.90	1.41
30	1137	0.282182	0.000011	0.000847	0.282164	3.3	0.99	1.47
31	1042	0.282223	0.000010	0.000779	0.282208	2.8	0.92	1.41
32	1043	0.282213	0.000013	0.000627	0.282201	2.5	0.93	1.42
33	1264	0.282121	0.000012	0.000584	0.282107	4.2	1.07	1.54
34	1077	0.282199	0.000010	0.000516	0.282189	2.9	0.95	1.43
35	1277	0.282234	0.000012	0.000616	0.282219	8.5	0.90	1.39
36	1040	0.282185	0.000011	0.000730	0.282171	1.4	0.98	1.46
37	982	0.282152	0.000013	0.000738	0.282138	-1.1	1.03	1.51
38	1069	0.282132	0.000008	0.000818	0.282116	0.1	1.06	1.54
39	1132	0.282145	0.000012	0.000729	0.282129	2.0	1.04	1.52
40	1041	0.282166	0.000017	0.001309	0.282140	0.3	1.03	1.51
41	676	0.282456	0.000012	0.001063	0.282442	2.8	0.55	1.09
42	1142	0.282181	0.000010	0.000782	0.282164	3.5	0.98	1.47
43	1046	0.282209	0.000011	0.000763	0.282194	2.3	0.94	1.43
44	1141	0.282150	0.000010	0.000813	0.282133	2.3	1.04	1.51
45	1449	0.282070	0.000009	0.001204	0.282037	6.0	1.18	1.64

Table 4.2. (continued)

analysis	Age (Ma)	$^{176}Hf/^{177}Hf_{(0)}$	1σ	$^{176}Lu/^{177}Lu$	$^{176}Hf/^{177}Hf_{initial}$	$\varepsilon_{Hf}(t)$	T_{CHUR} (Ga)	T_{DM} (Ga)
Curling Group - Summerside Fm (CB-259)								
1	1088	0.282209	0.000010	0.000575	0.282197	3.4	0.93	1.42
2	972	0.282106	0.000012	0.000799	0.282091	-3.0	1.11	1.57
3	2725	0.281112	0.000013	0.000548	0.281083	1.7	2.65	2.91
4	1027	0.282130	0.000014	0.000576	0.282119	-0.7	1.06	1.53
5	1074	0.282181	0.000011	0.000773	0.282165	2.0	0.98	1.47
6	2654	0.281218	0.000027	0.003618	0.281034	-1.8	2.74	3.00
7	1025	0.282267	0.000018	0.000412	0.282259	4.2	0.84	1.34
8	1097	0.282211	0.000014	0.000421	0.282202	3.8	0.93	1.41
9	1367	0.282000	0.000014	0.000625	0.281984	2.2	1.27	1.71
10	1547	0.281769	0.000012	0.001255	0.281732	-2.6	1.66	2.06
11	1382	0.281898	0.000014	0.000607	0.281882	-1.1	1.43	1.85
12	1455	0.282157	0.000014	0.002018	0.282101	8.4	1.06	1.55
13	1024	0.282108	0.000014	0.000236	0.282103	-1.3	1.08	1.55
14	1516	0.281954	0.000008	0.000838	0.281930	3.7	1.35	1.78
15	1083	0.282164	0.000016	0.000208	0.282160	2.0	0.99	1.47
16	1634	0.281870	0.000010	0.001688	0.281818	2.4	1.52	1.94
17	984	0.282060	0.000011	0.000351	0.282053	-4.0	1.16	1.62
18	1018	0.282179	0.000012	0.000650	0.282167	0.8	0.98	1.47
19	1066	0.282177	0.000014	0.000553	0.282166	1.8	0.98	1.46
20	2866	0.281065	0.000015	0.000382	0.281044	3.6	2.71	2.96
21	2932	0.281026	0.000013	0.000830	0.280979	2.8	2.81	3.04
22	1155	0.282187	0.000008	0.000451	0.282177	4.2	0.97	1.45
23	1104	0.282198	0.000013	0.000872	0.282180	3.2	0.96	1.45
24	1076	0.282223	0.000012	0.000660	0.282210	3.6	0.91	1.41
25	2739	0.280929	0.000008	0.001005	0.280876	-5.4	2.97	3.19
26	1026	0.282042	0.000013	0.000509	0.282032	-3.8	1.20	1.65
27	1673	0.281859	0.000012	0.001078	0.281825	3.6	1.51	1.93
28	1321	0.281981	0.000011	0.000823	0.281960	0.3	1.31	1.74
29	1358	0.282146	0.000019	0.000410	0.282135	7.4	1.03	1.50
30	1822	0.281618	0.000008	0.001408	0.281569	-2.1	1.92	2.28
31	1613	0.281840	0.000012	0.000571	0.281823	2.1	1.52	1.93
32	1063	0.282256	0.000015	0.000753	0.282241	4.4	0.86	1.36
33	1077	0.282200	0.000014	0.000330	0.282193	3.0	0.94	1.42
34	1071	0.282170	0.000016	0.000444	0.282161	1.7	0.99	1.47
35	1585	0.281735	0.000013	0.000957	0.281706	-2.7	1.70	2.09
36	1060	0.282153	0.000013	0.000478	0.282143	0.9	1.02	1.49
37	1080	0.282113	0.000014	0.000027	0.282112	0.2	1.07	1.53
38	1028	0.282288	0.000014	0.000420	0.282280	5.0	0.80	1.31
39	1149	0.282203	0.000013	0.000767	0.282186	4.4	0.95	1.44
40	1115	0.282243	0.000016	0.000731	0.282228	5.1	0.88	1.38
41	1220	0.282173	0.000017	0.000695	0.282157	5.0	1.00	1.48
42	1438	0.281947	0.000019	0.000550	0.281932	2.0	1.35	1.78
43	1127	0.282156	0.000014	0.000442	0.282147	2.5	1.01	1.49
44	1322	0.282219	0.000014	0.000705	0.282201	8.9	0.92	1.41
45	1446	0.281950	0.000011	0.001316	0.281914	1.5	1.38	1.81
46	1013	0.282141	0.000014	0.000535	0.282131	-0.6	1.04	1.51

Table 4.2. (continued)

47	1270	0.282087	0.000009	0.001018	0.282063	2.8	1.14	1.61
48	1030	0.282119	0.000011	0.000916	0.282101	-1.3	1.09	1.56
49	1071	0.282158	0.000014	0.000656	0.282145	1.2	1.02	1.49
50	1087	0.282254	0.000015	0.000502	0.282244	5.0	0.86	1.36
51	1340	0.281977	0.000011	0.001086	0.281950	0.4	1.32	1.76
52	1153	0.282196	0.000014	0.000809	0.282178	4.2	0.96	1.45
53	2634	0.281058	0.000014	0.000683	0.281024	-2.6	2.75	2.99
54	1000	0.282107	0.000016	0.000504	0.282098	-2.1	1.09	1.56
55	1362	0.282153	0.000010	0.001327	0.282119	6.9	1.05	1.53
56	2477	0.281237	0.000019	0.000391	0.281218	0.7	2.45	2.73
57	1320	0.281861	0.000013	0.000660	0.281845	-3.8	1.49	1.90
58	1335	0.282053	0.000012	0.000972	0.282028	3.1	1.20	1.65

Table 4.2. (continued)

analysis	Age (Ma)	$^{176}Hf/^{177}Hf_{(0)}$	1σ	$^{176}Lu/^{177}Lu$	$^{176}Hf/^{177}Hf_{initial}$	$\varepsilon_{Hf}(t)$	T_{CHUR} (Ga)	T_{DM} (Ga)
Curling Group - Irishtown Fm (CB-260)								
1	544	0.282556	0.000012	0.000956	0.282546	3.5	0.38	0.95
2	1087	0.282217	0.000013	0.000473	0.282207	3.8	0.92	1.41
3	1848	0.281602	0.000014	0.000745	0.281576	-1.2	1.90	2.26
4	2696	0.281069	0.000014	0.000156	0.281061	0.2	2.69	2.93
5	2648	0.281230	0.000011	0.001204	0.281169	2.9	2.52	2.80
6	1845	0.281599	0.000013	0.000525	0.281581	-1.1	1.89	2.25
7	1046	0.282086	0.000013	0.000310	0.282080	-1.7	1.12	1.58
8	1137	0.282211	0.000017	0.001518	0.282178	3.9	0.96	1.45
9	2843	0.281088	0.000015	0.000453	0.281063	3.7	2.68	2.93
10	1571	0.281758	0.000013	0.000963	0.281729	-2.2	1.67	2.06
11	1071	0.282294	0.000012	0.000504	0.282284	6.1	0.80	1.30
12	1261	0.282184	0.000020	0.001164	0.282156	5.9	0.99	1.48
13	2744	0.281119	0.000014	0.000265	0.281105	2.9	2.62	2.88
14	1152	0.282205	0.000012	0.000807	0.282187	4.5	0.95	1.44
15	1323	0.281947	0.000010	0.000795	0.281927	-0.8	1.36	1.79
16	1033	0.282191	0.000012	0.000715	0.282177	1.5	0.97	1.45
17	1330	0.281723	0.000014	0.000451	0.281712	-8.3	1.70	2.08
18	1339	0.281996	0.000014	0.000594	0.281981	1.5	1.27	1.71
19	1064	0.282185	0.000010	0.000521	0.282175	2.1	0.97	1.45
20	1794	0.281415	0.000013	0.000247	0.281407	-8.5	2.16	2.48
21	1865	0.281311	0.000011	0.000440	0.281295	-10.8	2.34	2.63
22	1836	0.281227	0.000014	0.000260	0.281218	-14.2	2.45	2.73
23	2678	0.281162	0.000018	0.000453	0.281139	2.5	2.57	2.83
24	1866	0.281133	0.000012	0.000883	0.281102	-17.7	2.65	2.90
25	1090	0.282161	0.000013	0.000492	0.282151	1.8	1.01	1.48
26	1059	0.282137	0.000013	0.000470	0.282128	0.3	1.05	1.52
27	1663	0.281870	0.000014	0.001611	0.281819	3.1	1.52	1.94
28	1536	0.282065	0.000014	0.000335	0.282055	8.6	1.15	1.61
29	1003	0.282046	0.000012	0.000301	0.282040	-4.1	1.18	1.63
30	1108	0.282253	0.000011	0.000637	0.282240	5.4	0.87	1.36
31	1051	0.282136	0.000012	0.000454	0.282127	0.1	1.05	1.52
32	1674	0.281943	0.000014	0.000906	0.281914	6.8	1.37	1.80
33	1132	0.282221	0.000016	0.000550	0.282209	4.8	0.91	1.40
34	1645	0.281774	0.000014	0.000823	0.281748	0.2	1.64	2.03
35	2829	0.281098	0.000011	0.000369	0.281078	3.9	2.66	2.91
36	1485	0.281783	0.000014	0.001631	0.281737	-3.9	1.66	2.06
37	1106	0.282239	0.000014	0.000576	0.282227	4.9	0.89	1.38
38	1049	0.282208	0.000013	0.000631	0.282196	2.5	0.94	1.42
39	1447	0.282055	0.000012	0.000691	0.282036	5.9	1.18	1.64
40	1028	0.282039	0.000014	0.001080	0.282018	-4.3	1.22	1.68
41	1201	0.282203	0.000011	0.000699	0.282187	5.6	0.95	1.43
42	2791	0.281115	0.000011	0.000288	0.281100	3.8	2.63	2.88
43	1036	0.282114	0.000010	0.000582	0.282103	-1.1	1.09	1.55
44	3605	0.280439	0.000012	0.000510	0.280403	-1.7	3.68	3.79
45	1899	0.281569	0.000016	0.000606	0.281547	-1.1	1.95	2.30
46	2735	0.281040	0.000011	0.000343	0.281022	-0.3	2.75	2.99

Table 4.2. (continued)

47	1086	0.282210	0.000013	0.000887	0.282192	3.2	0.94	1.43
48	2731	0.280803	0.000012	0.000175	0.280794	-8.5	3.09	3.29
49	1014	0.282004	0.000013	0.001961	0.281967	-6.4	1.31	1.77
50	1270	0.282208	0.000013	0.000589	0.282194	7.5	0.94	1.42
51	1800	0.281340	0.000013	0.000482	0.281324	-11.3	2.30	2.60
52	1658	0.281749	0.000013	0.001064	0.281716	-0.6	1.69	2.08
53	1731	0.281768	0.000014	0.001019	0.281735	1.7	1.65	2.05
54	1054	0.282196	0.000014	0.000588	0.282184	2.2	0.96	1.44
55	2118	0.281483	0.000014	0.001549	0.281421	-0.5	2.14	2.47
56	1873	0.281570	0.000014	0.000847	0.281540	-1.9	1.96	2.31
57	1034	0.282129	0.000017	0.000287	0.282123	-0.4	1.05	1.52
58	1087	0.282252	0.000016	0.000593	0.282240	4.9	0.87	1.36
59	1535	0.281768	0.000010	0.000501	0.281753	-2.1	1.63	2.02
60	3003	0.280882	0.000014	0.000489	0.280854	0.1	3.00	3.21
61	1862	0.281585	0.000013	0.000664	0.281562	-1.4	1.92	2.28
62	2747	0.280736	0.000013	0.000581	0.280705	-11.3	3.23	3.41

Table 4.2. (continued)

analysis	Age (Ma)	$^{176}Hf/^{177}Hf_{(0)}$	1σ	$^{176}Lu/^{177}Lu$	$^{176}Hf/^{177}Hf_{initial}$	$\varepsilon_{Hf}(t)$	T_{CHUR} (Ga)	T_{DM} (Ga)
Crystalline Basement - Long Range Massif (NP-10A)								
1	1039	0.282161	0.000010	0.000641	0.282148	0.6	1.01	1.49
2	1057	0.282185	0.000011	0.001130	0.282162	1.5	0.99	1.48
3	1045	0.282184	0.000013	0.000576	0.282173	1.6	0.97	1.46
4	1041	0.282173	0.000014	0.000676	0.282160	1.0	0.99	1.47
5	1036	0.282178	0.000015	0.000666	0.282165	1.1	0.99	1.47
6	1062	0.282150	0.000011	0.000591	0.282138	0.7	1.03	1.50
7	1068	0.282218	0.000013	0.000957	0.282199	3.0	0.93	1.42
8	1050	0.282148	0.000013	0.000604	0.282136	0.4	1.03	1.51
9	1052	0.282170	0.000013	0.000495	0.282160	1.3	0.99	1.47
10	1029	0.282167	0.000013	0.000650	0.282154	0.6	1.00	1.48
11	1023	0.282180	0.000018	0.001564	0.282150	0.3	1.01	1.50
12	1046	0.282162	0.000014	0.000464	0.282153	0.9	1.01	1.48
13	1062	0.282163	0.000010	0.000615	0.282151	1.2	1.01	1.49
14	1052	0.282153	0.000010	0.000759	0.282138	0.5	1.03	1.51
15	1051	0.282156	0.000012	0.000666	0.282143	0.7	1.02	1.50
16	1027	0.282170	0.000012	0.001485	0.282141	0.1	1.02	1.51
17	1040	0.282179	0.000014	0.000435	0.282170	1.4	0.98	1.46
18	1043	0.282146	0.000014	0.000623	0.282134	0.1	1.04	1.51
19	1150	0.282152	0.000013	0.001039	0.282129	2.4	1.04	1.52
20	1043	0.282184	0.000008	0.000704	0.282170	1.4	0.98	1.46
21	1079	0.282160	0.000012	0.000812	0.282143	1.3	1.02	1.50
22	1043	0.282162	0.000013	0.000660	0.282149	0.7	1.01	1.49
23	969	0.282149	0.000016	0.000418	0.282141	-1.3	1.02	1.50
24	1178	0.282171	0.000010	0.000720	0.282155	4.0	1.00	1.48
25	1072	0.282169	0.000013	0.000523	0.282158	1.7	1.00	1.47
26	1040	0.282205	0.000014	0.000818	0.282189	2.0	0.95	1.44
27	1120	0.282189	0.000011	0.002228	0.282142	2.2	1.02	1.51
28	1054	0.282240	0.000012	0.000926	0.282222	3.5	0.89	1.39
29	1035	0.282194	0.000013	0.000565	0.282183	1.7	0.96	1.44

Table 4.2. (continued)

analysis	Age (Ma)	$^{176}Hf/^{177}Hf_{(0)}$	1σ	$^{176}Lu/^{177}Lu$	$^{176}Hf/^{177}Hf_{initial}$	$\varepsilon_{Hf}(t)$	T_{CHUR} (Ga)	T_{DM} (Ga)
Labrador Group - Bradore Fm (NP-10)								
1	1158	0.282197	0.000012	0.000742	0.282181	4.4	0.96	1.44
2	1107	0.282240	0.000014	0.002012	0.282198	3.9	0.92	1.43
3	1134	0.282229	0.000013	0.001294	0.282201	4.6	0.92	1.42
4	1141	0.282208	0.000015	0.000713	0.282193	4.5	0.94	1.43
5	1166	0.282081	0.000013	0.001012	0.282059	0.3	1.15	1.62
6	1089	0.282226	0.000014	0.001274	0.282200	3.5	0.93	1.42
7	1017	0.282207	0.000015	0.000495	0.282198	1.8	0.94	1.42
8	1057	0.282235	0.000013	0.000400	0.282227	3.8	0.89	1.38
9	1149	0.282210	0.000012	0.000723	0.282194	4.7	0.94	1.43
10	1057	0.282195	0.000016	0.000497	0.282185	2.3	0.95	1.44
11	1049	0.282234	0.000011	0.000815	0.282218	3.3	0.90	1.40
12	1146	0.282212	0.000020	0.000888	0.282193	4.6	0.94	1.43
13	1066	0.282155	0.000017	0.001047	0.282134	0.7	1.03	1.51
14	1027	0.282175	0.000020	0.000482	0.282166	0.9	0.99	1.46
15	1125	0.282222	0.000012	0.001002	0.282201	4.4	0.93	1.42
16	1121	0.282211	0.000012	0.000558	0.282199	4.2	0.93	1.42
17	1523	0.282098	0.000016	0.000929	0.282071	8.9	1.12	1.59
18	1132	0.282174	0.000015	0.000987	0.282153	2.9	1.00	1.49
19	1123	0.282155	0.000016	0.000723	0.282140	2.2	1.02	1.50
20	1142	0.282223	0.000011	0.000691	0.282208	5.0	0.91	1.41
21	1025	0.282199	0.000012	0.000581	0.282188	1.7	0.95	1.44
22	1054	0.282226	0.000013	0.000932	0.282207	3.0	0.92	1.41
23	1033	0.282180	0.000013	0.000519	0.282170	1.2	0.98	1.46
24	1075	0.282197	0.000015	0.000578	0.282185	2.7	0.95	1.44
25	1127	0.282211	0.000015	0.000966	0.282190	4.1	0.94	1.43
26	1136	0.282238	0.000014	0.000989	0.282217	5.2	0.90	1.40
27	1467	0.282177	0.000014	0.001136	0.282145	10.2	1.00	1.49
28	1033	0.282197	0.000014	0.000366	0.282190	1.9	0.95	1.43
29	1138	0.282179	0.000015	0.000737	0.282163	3.4	0.99	1.47
30	1506	0.282102	0.000017	0.001468	0.282060	8.1	1.13	1.61
31	1359	0.282231	0.000014	0.000708	0.282213	10.1	0.90	1.40
32	988	0.282159	0.000011	0.000879	0.282143	-0.8	1.02	1.50
33	1266	0.282270	0.000010	0.001814	0.282227	8.5	0.87	1.38
34	1125	0.282204	0.000016	0.000690	0.282189	4.0	0.95	1.43
35	1116	0.282212	0.000013	0.000965	0.282192	3.9	0.94	1.43
36	1040	0.282240	0.000014	0.000355	0.282233	3.6	0.88	1.37
37	1061	0.282231	0.000013	0.000631	0.282218	3.6	0.90	1.39
38	1137	0.282179	0.000014	0.000536	0.282168	3.5	0.98	1.46
39	1027	0.282221	0.000014	0.000425	0.282213	2.6	0.91	1.40
40	1329	0.282136	0.000011	0.002006	0.282086	5.0	1.10	1.58

Table 4.2. (continued)

analysis	Age (Ma)	$^{176}Hf/^{177}Hf_{(0)}$	1σ	$^{176}Lu/^{177}Lu$	$^{176}Hf/^{177}Hf_{initial}$	$\varepsilon_{Hf}(t)$	T_{CHUR} (Ga)	T_{DM} (Ga)
Crystalline Basement - Indian Head Range (STV-30A)								
1	1502	0.282058	0.000012	0.001872	0.282005	6.0	1.22	1.69
2	1495	0.282016	0.000011	0.001090	0.281985	5.2	1.26	1.71
3	1495	0.282038	0.000009	0.001809	0.281987	5.2	1.25	1.71
4	1500	0.282030	0.000015	0.001008	0.282001	5.9	1.23	1.69
5	1497	0.282024	0.000013	0.001106	0.281993	5.5	1.25	1.70
6	1493	0.282049	0.000009	0.002034	0.281992	5.4	1.24	1.71
7	1495	0.282072	0.000012	0.002054	0.282014	6.2	1.21	1.67
8	1499	0.282024	0.000012	0.000943	0.281997	5.7	1.24	1.69
9	1457	0.281999	0.000020	0.000956	0.281973	3.9	1.28	1.73
10	1494	0.282009	0.000013	0.001336	0.281971	4.7	1.28	1.73
11	1499	0.282037	0.000014	0.001512	0.281994	5.6	1.24	1.70
12	1491	0.282075	0.000010	0.001364	0.282037	6.9	1.18	1.64
13	1491	0.282015	0.000014	0.001266	0.281979	4.9	1.27	1.72
14	1493	0.282035	0.000018	0.001339	0.281997	5.6	1.24	1.69
15	1496	0.282017	0.000012	0.001303	0.281980	5.0	1.27	1.72
16	1488	0.282010	0.000016	0.001027	0.281981	4.9	1.27	1.71
17	1497	0.282051	0.000009	0.001937	0.281996	5.6	1.24	1.70
18	1480	0.282040	0.000008	0.001208	0.282006	5.6	1.23	1.68
19	1486	0.282021	0.000014	0.000876	0.281996	5.4	1.24	1.69
20	1477	0.282109	0.000011	0.002436	0.282041	6.8	1.16	1.64
21	1477	0.282077	0.000010	0.001997	0.282021	6.1	1.19	1.66
22	1474	0.282026	0.000010	0.001538	0.281983	4.6	1.26	1.72
23	1483	0.282027	0.000012	0.001262	0.281992	5.1	1.25	1.70
24	1490	0.282052	0.000013	0.001472	0.282010	6.0	1.22	1.68
25	1491	0.282005	0.000011	0.000642	0.281987	5.1	1.26	1.70
26	1477	0.282060	0.000009	0.001700	0.282012	5.7	1.21	1.67
27	1486	0.282054	0.000011	0.001516	0.282011	5.9	1.21	1.67
28	1485	0.282080	0.000009	0.000972	0.282053	7.4	1.15	1.62
29	1529	0.282025	0.000013	0.001736	0.281975	5.6	1.27	1.73
30	1465	0.282025	0.000013	0.001641	0.281980	4.3	1.27	1.72

Table 4.2. (continued)

analysis	Age (Ma)	$^{176}Hf/^{177}Hf_{(0)}$	1σ	$^{176}Lu/^{177}Lu$	$^{176}Hf/^{177}Hf_{initial}$	$\varepsilon_{Hf}(t)$	T_{CHUR} (Ga)	T_{DM} (Ga)
Labrador Group - Bradore Fm (STV-30)								
1	1074	0.282171	0.000012	0.000680	0.282157	1.7	1.00	1.48
2	1142	0.282181	0.000010	0.001105	0.282157	3.2	0.99	1.48
3	1126	0.282190	0.000014	0.001176	0.282165	3.1	0.98	1.47
4	1115	0.282194	0.000012	0.000986	0.282173	3.2	0.97	1.46
5	1137	0.282205	0.000012	0.001156	0.282180	3.9	0.96	1.45
6	1122	0.282188	0.000011	0.000966	0.282168	3.1	0.98	1.47
7	1112	0.282193	0.000013	0.000660	0.282179	3.3	0.96	1.45
8	1159	0.282190	0.000012	0.001157	0.282165	3.9	0.98	1.47
9	1065	0.282177	0.000014	0.001118	0.282155	1.4	1.00	1.49
10	1001	0.282203	0.000011	0.001497	0.282175	0.6	0.97	1.46
11	1128	0.282191	0.000014	0.000993	0.282170	3.4	0.98	1.46
12	1132	0.282176	0.000012	0.000749	0.282160	3.1	0.99	1.47
13	1125	0.282205	0.000011	0.000707	0.282190	4.0	0.94	1.43
14	1143	0.282184	0.000011	0.000650	0.282170	3.7	0.98	1.46
15	1134	0.282191	0.000013	0.000731	0.282175	3.7	0.97	1.45
16	1130	0.282200	0.000012	0.001626	0.282165	3.2	0.98	1.47
17	1125	0.282219	0.000013	0.001684	0.282183	3.8	0.95	1.45
18	1143	0.282169	0.000006	0.000662	0.282155	3.2	1.00	1.48
19	1107	0.282199	0.000014	0.000944	0.282179	3.2	0.96	1.45
20	1139	0.282197	0.000013	0.000728	0.282181	4.0	0.96	1.44
21	1058	0.282198	0.000012	0.001320	0.282172	1.8	0.97	1.46
22	990	0.282183	0.000012	0.000732	0.282169	0.2	0.98	1.46
23	1136	0.282162	0.000012	0.000697	0.282147	2.7	1.01	1.49
24	1107	0.282174	0.000013	0.001089	0.282151	2.2	1.01	1.49
25	984	0.282132	0.000013	0.000640	0.282120	-1.7	1.06	1.53
26	1088	0.282242	0.000014	0.001551	0.282210	3.9	0.91	1.41
27	1108	0.282200	0.000014	0.001042	0.282178	3.2	0.96	1.45
28	1036	0.282201	0.000011	0.000558	0.282190	2.0	0.95	1.43
29	1133	0.282202	0.000012	0.000613	0.282189	4.1	0.95	1.43
30	1124	0.282118	0.000013	0.000816	0.282101	0.8	1.09	1.56
31	1135	0.282193	0.000012	0.001012	0.282171	3.6	0.97	1.46
32	1165	0.282242	0.000015	0.001173	0.282216	5.8	0.90	1.40
33	1149	0.282210	0.000012	0.000779	0.282193	4.7	0.94	1.43
34	1125	0.282181	0.000014	0.000708	0.282166	3.1	0.98	1.46
35	1122	0.282164	0.000009	0.000526	0.282153	2.6	1.00	1.48
36	1219	0.282199	0.000012	0.000971	0.282177	5.7	0.96	1.45
37	1122	0.282271	0.000017	0.000972	0.282250	6.1	0.85	1.35
38	999	0.282178	0.000014	0.000629	0.282166	0.3	0.99	1.47
39	1014	0.282200	0.000014	0.000578	0.282189	1.4	0.95	1.43
40	1070	0.282189	0.000013	0.000663	0.282176	2.2	0.97	1.45

Table 4.3. U-Pb age statistics for analyzed detrital zircons.

Sample	*n*	Population	n_i	Detection limits (%) probablity level		Zircon fraction size			Category
				p_L = 0.5	p_L = 0.95	%	2*s* Absolute	Relative (%)	
Total Synrift	427	Neoprot (543-980 Ma)	4			1	2.0	50	Accessory
		l. Meso (980-1250 Ma)	333			78	8.6	3	Large
		m. Meso (1250-1400 Ma)	28			7	5.1	18	Minor
		e. Meso (1400-1600 Ma)	23			5	4.7	20	Minor
		l. Paleo (1600-2000 Ma)	19			4	4.3	22	Accessory
		e. Paleo (2000-2500 Ma)	2			0.5	1.4	71	Accessory
		l. Archean (2500-2900 Ma)	16			4	3.9	25	Accessory
		Archean (>3000 Ma)	2			0.5	1.4	71	Accessory
Summerside	63			1	5				
CB-219		Neoprot	2			3	1.4	70	Accessory
		late Meso	54			86	2.8	5	Dominant
		mid Meso	3			5	1.7	56	Accessory
		early Meso	4			6	1.9	48	Minor
Summerside	64			1	5				
CB-259		late Meso	36			56	4.0	11	Large
		mid Meso	11			17	3.0	27	Minor
		early Meso	6			9	2.3	39	Minor
		late Paleo	4			6	1.9	48	Minor
		early Paleo	1			2	1.0	99	Accessory
		late Archean	6			9	2.3	39	Minor
Irishtown	69			1	4				
CB-260		Neoprot	1			1	1.0	99	Accessory
		late Meso	26			38	4.0	15	Major
		mid Meso	9			13	2.8	31	Minor
		early Meso	5			7	2.2	43	Minor
		late Paleo	15			22	3.4	23	Major
		early Paleo	1			1	1.0	99	Accessory
		late Archean	10			14	2.9	29	Minor
		Archean	2			3	1.4	70	Accessory
South Brook	57			1	5				
CB-212		late Meso	51			89	2.3	5	Dominant
		mid Meso	1			2	1.0	99	Accessory
		early Meso	5			9	2.1	43	Minor
South Brook	54			1	5				
CB-230		Neoprot	1			2	1.0	99	Accessory
		late Meso	52			96	1.4	3	Dominant
		mid Meso	1			2	1.0	99	Accessory
Bradore	59			1	5				
STV-30		late Meso	59			100	0.0	N/A	Dominant
Bradore	60			1	5				
NP-10		late Meso	54			90	2.3	4	Dominant
		mid Meso	3			5	1.7	56	Accessory
		early Meso	3			5	1.7	56	Accessory

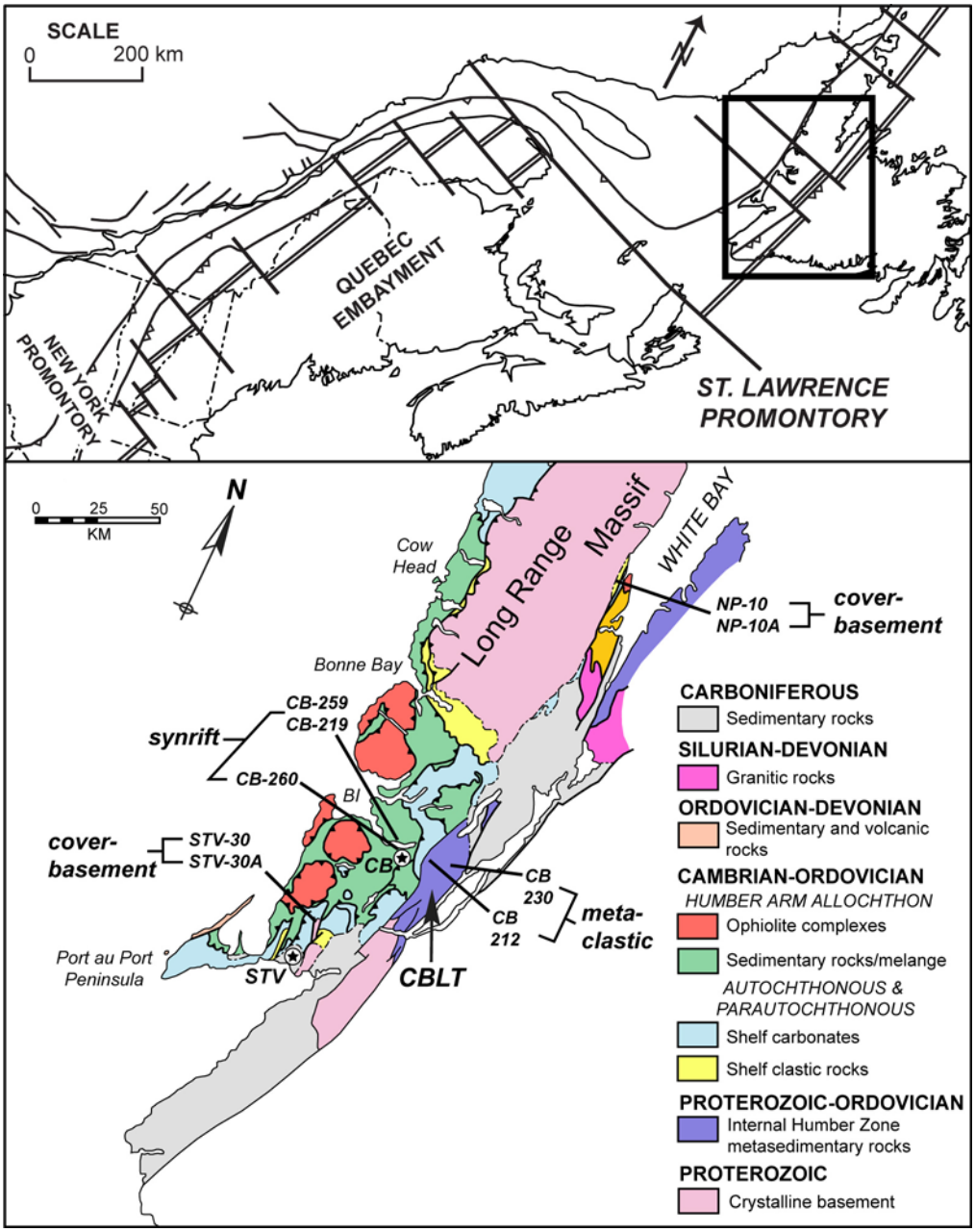

Figure 4.1. *Top*: Outline map of the interpreted Neoproterozoic-Early Cambrian continental margin defined by rift segments and transform faults (modified from Thomas, 1977), as well as illustrating the distribution of promontonories and embayments in the northern Appalachian orogen. *Bottom*: Simplified geologic map of western Newfoundland showing the locations of the analyzed samples. BI = Bay of Islands; CB = City of Corner Brook; CBLT = Corner Brook Lake terrane; STV = City of Stephenville.

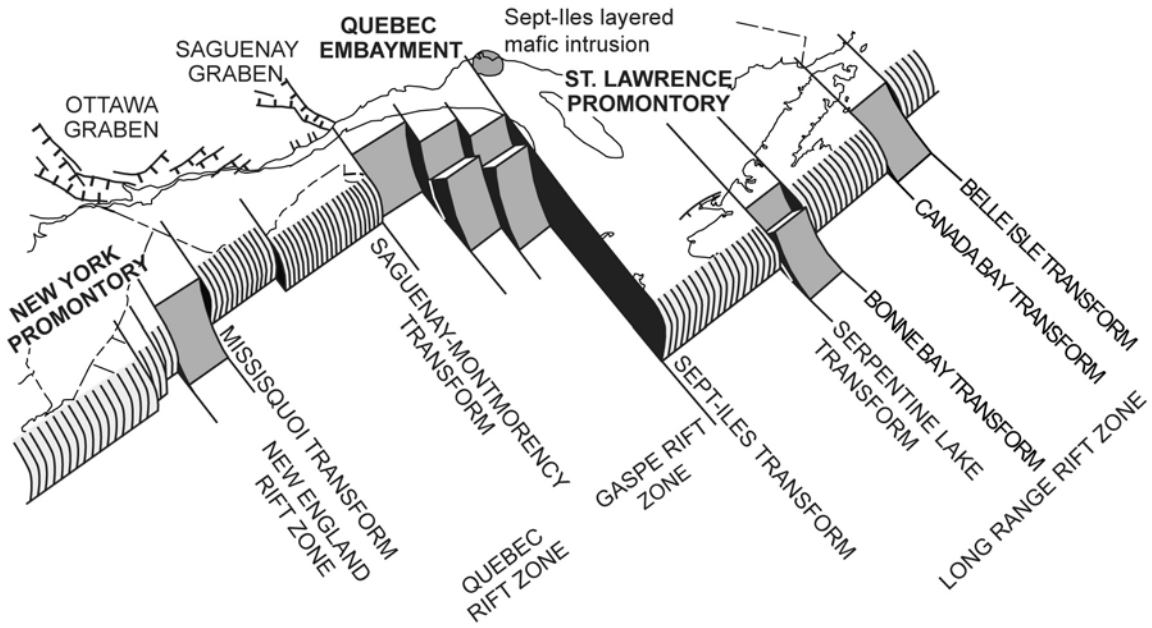

Figure 4.2. Schematic block diagram illustrating the 3-D structure of the eastern Laurentian rifted continental margin of northeastern North America (present coordinates) in the context of a low-angle detachment rift system (see Chapter 2). SILMI = Sept-Iles layered mafic intrusion.

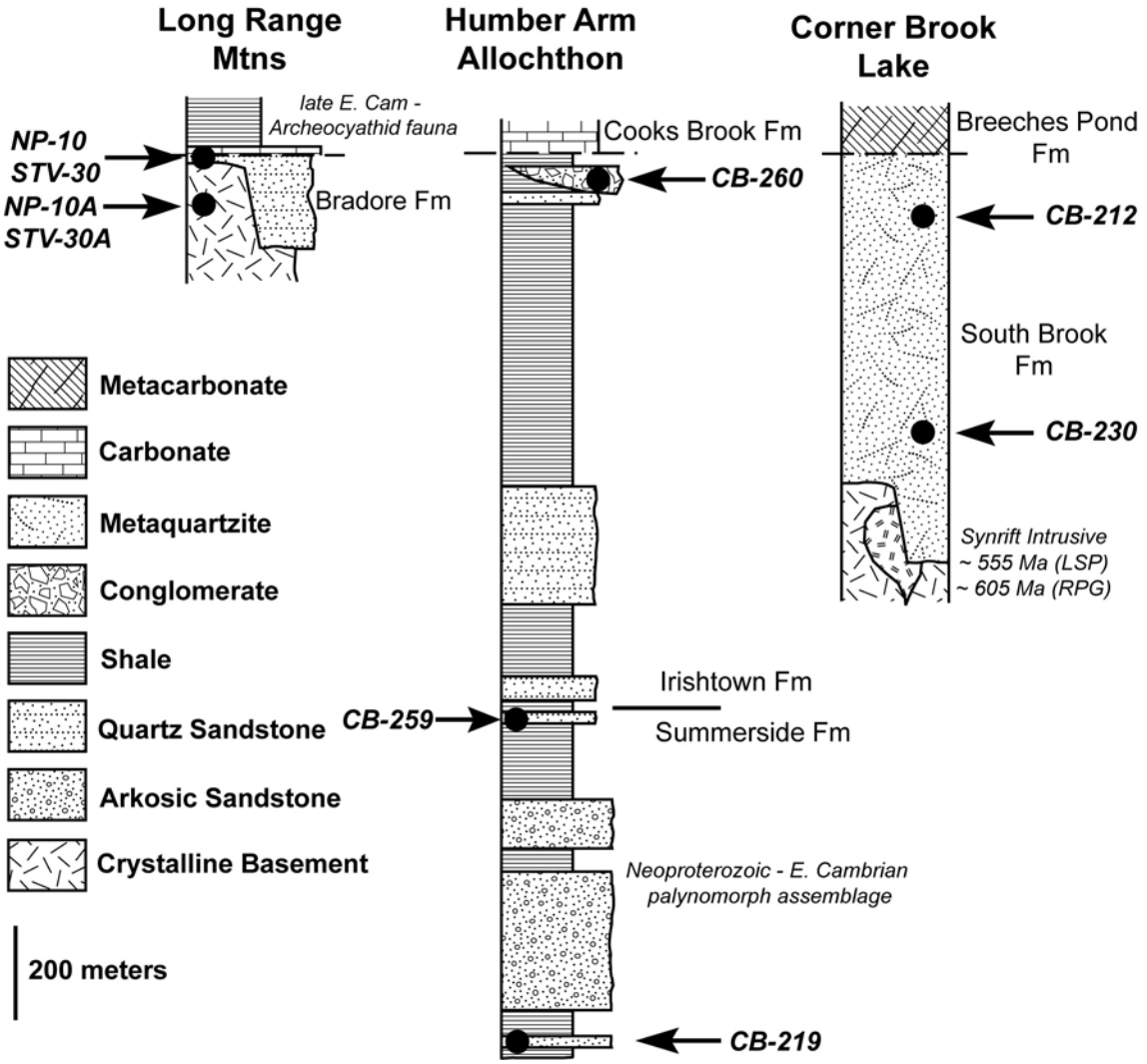

Figure 4.3. Stratigraphic sections across the Humber zone illustrating the late Neoproterozoic-Early Cambrian synrift stratigraphy in the parautochthon (Long Range Mtns), the Humber Arm allochthon, and in the eastern internal domain (Corner Brook Lake). Sample locations identified by sample numbers and illustrated (black circles) with respect to location in the vertical stratigraphic section.

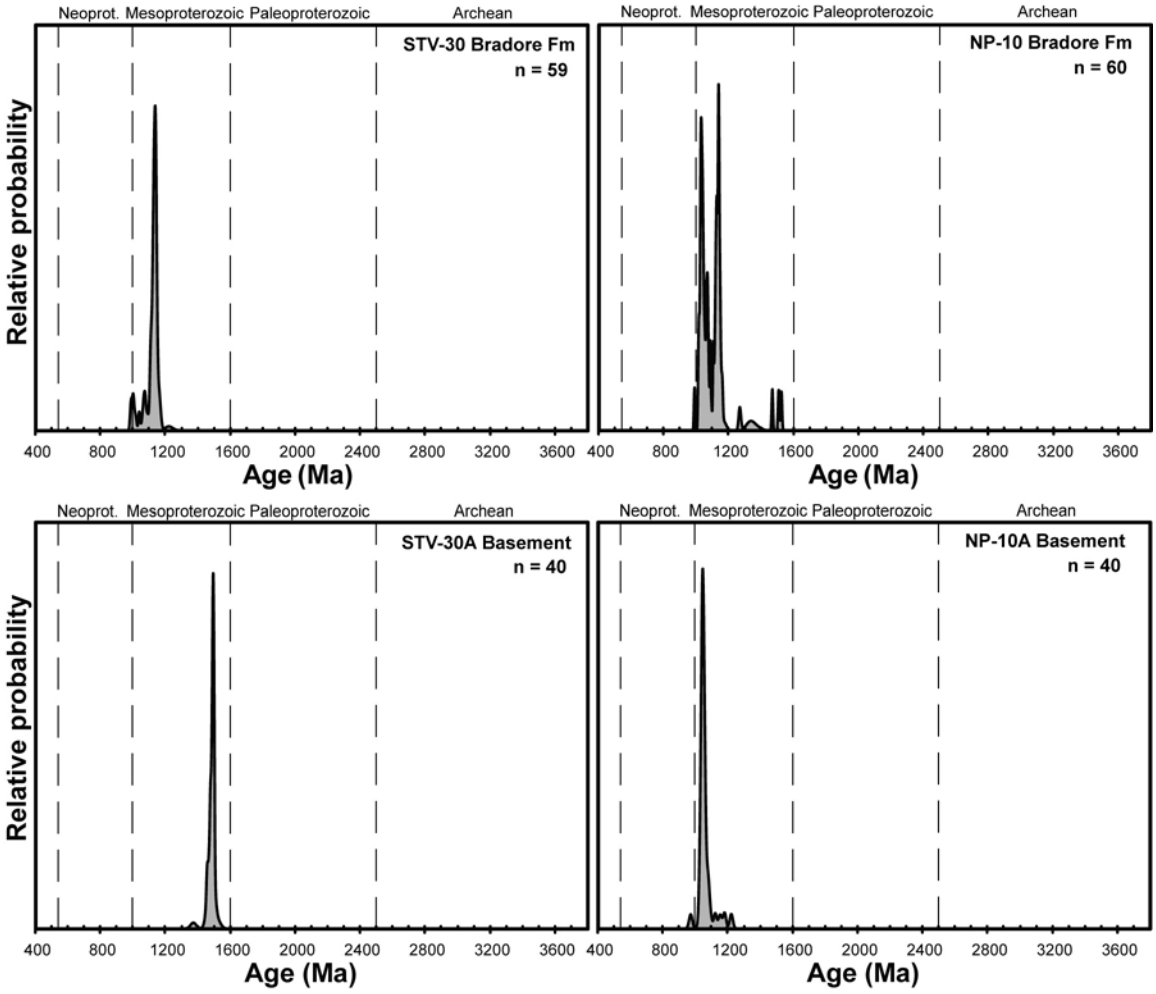

Figure 4.4. Cumulative probability density diagrams for U-Pb isotopic ages in zircon from the basement-cover samples. Only those analyses within ±10% discordance are plotted.

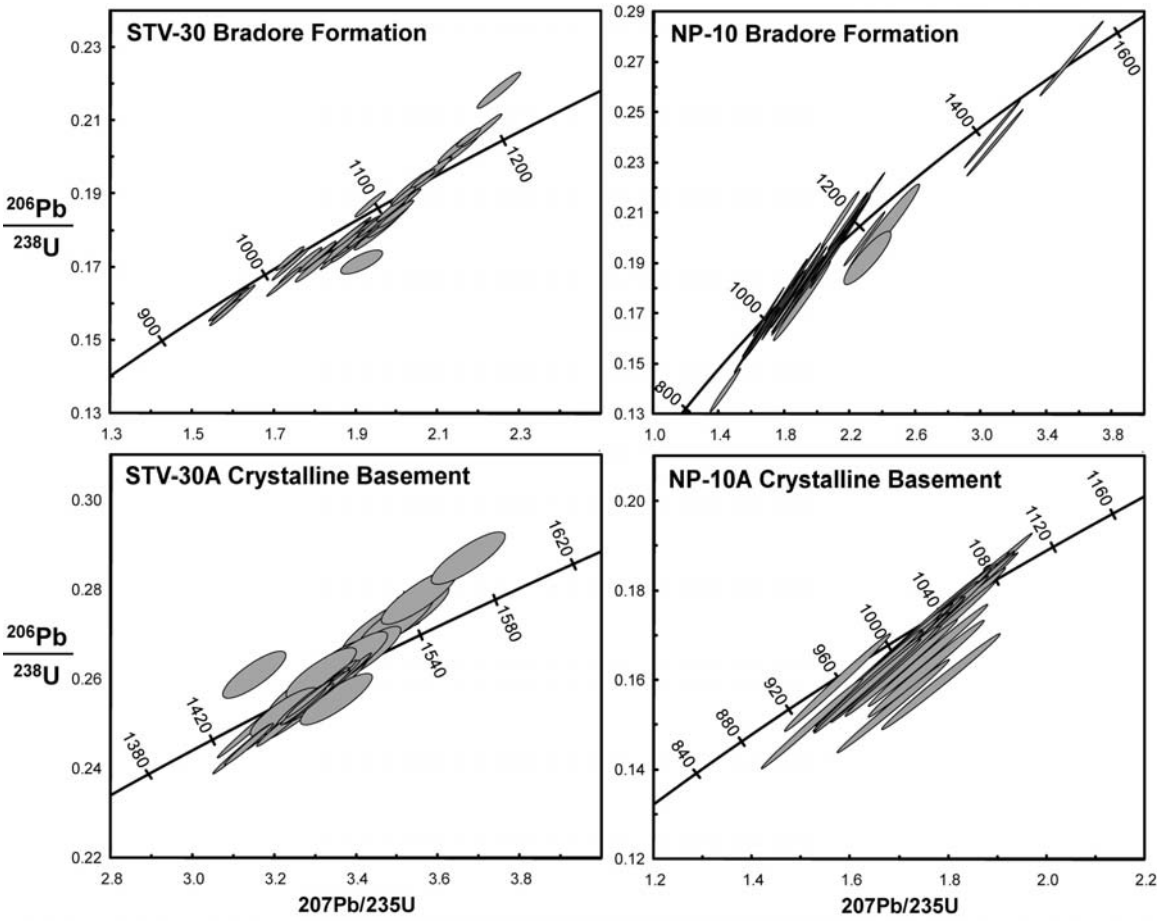

Figure 4.5. U-Pb Concordia diagrams for zircon analyzed in the basement-cover samples; error ellipses are 1σ.

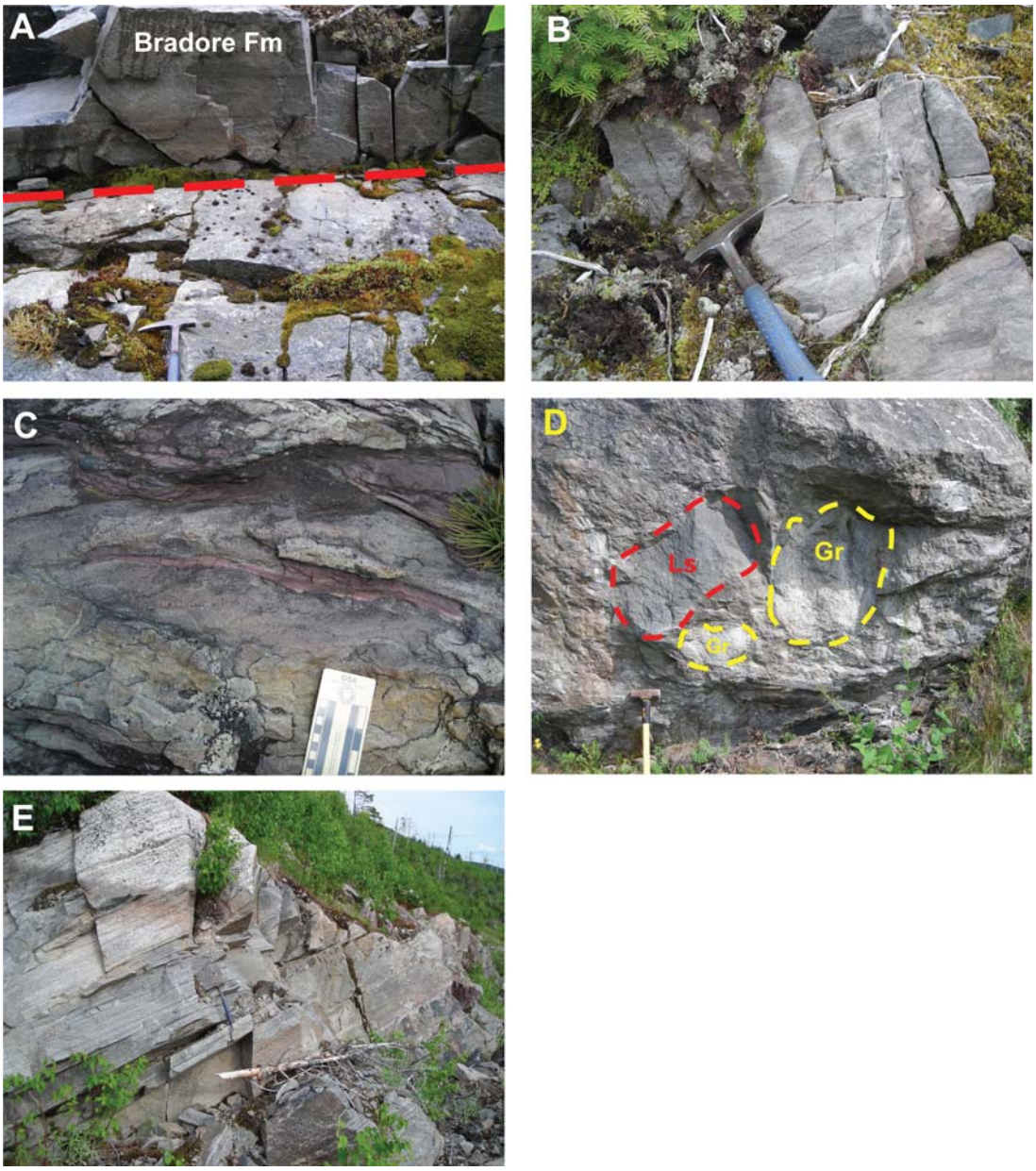

Figure 4.6. Representative outcrop samples for detrital-zircon analysis. *A)* Proterozoic-Paleozoic unconformity (red dotted line) between Bradore Formation (NP-10) and underlying crystalline basement (NP-10A); *B)* Bradore Formation sandstone with cross beds (STV-30); *C)* Summerside Formation (CB-219); *D)* conglomerate in the Irishtown Formation (CB-260) with boulders of shelf limestone (Ls) and granitic basement (Gr); *E)* South Brook Formation (CB-230).

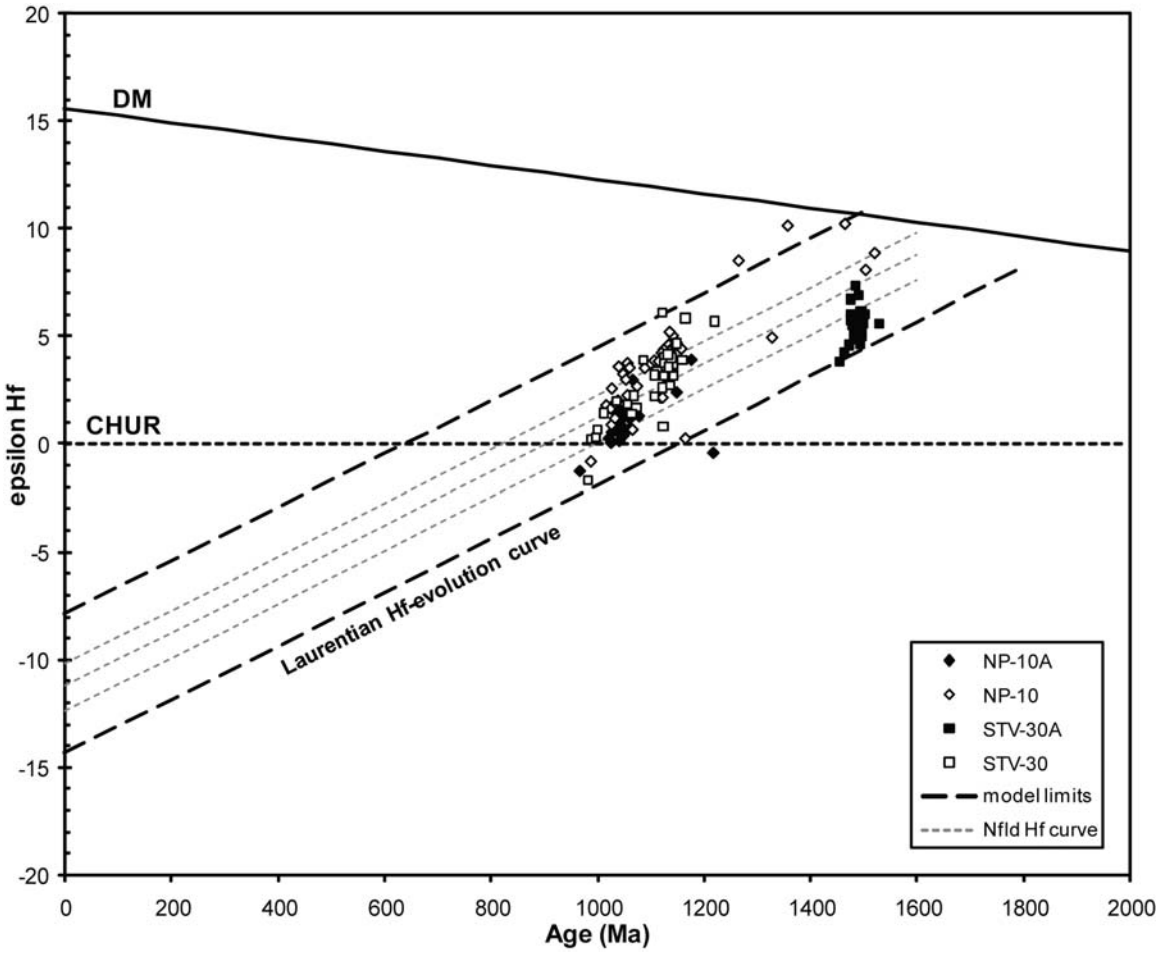

Figure 4.7. $^{177}Hf/^{176}Hf$ displayed as εHf versus U-Pb age for basement-cover samples. Reference lines representing CHUR Hf evolution and the depleted mantle (DM) (Bouvier et al., 2008) are shown, as is the range of crustal reservoirs corresponding to Laurentian crust on the St. Lawrence promontory (bold dotted line), which is based on the measured range of εHf values from the analyzed basement-cover zircons. The temporal evolution of the Hf reservoir for the St. Lawrence promontory is calculated with an assumed Lu/Hf whole rock ratio of 0.015, which corresponds to average crustal values.

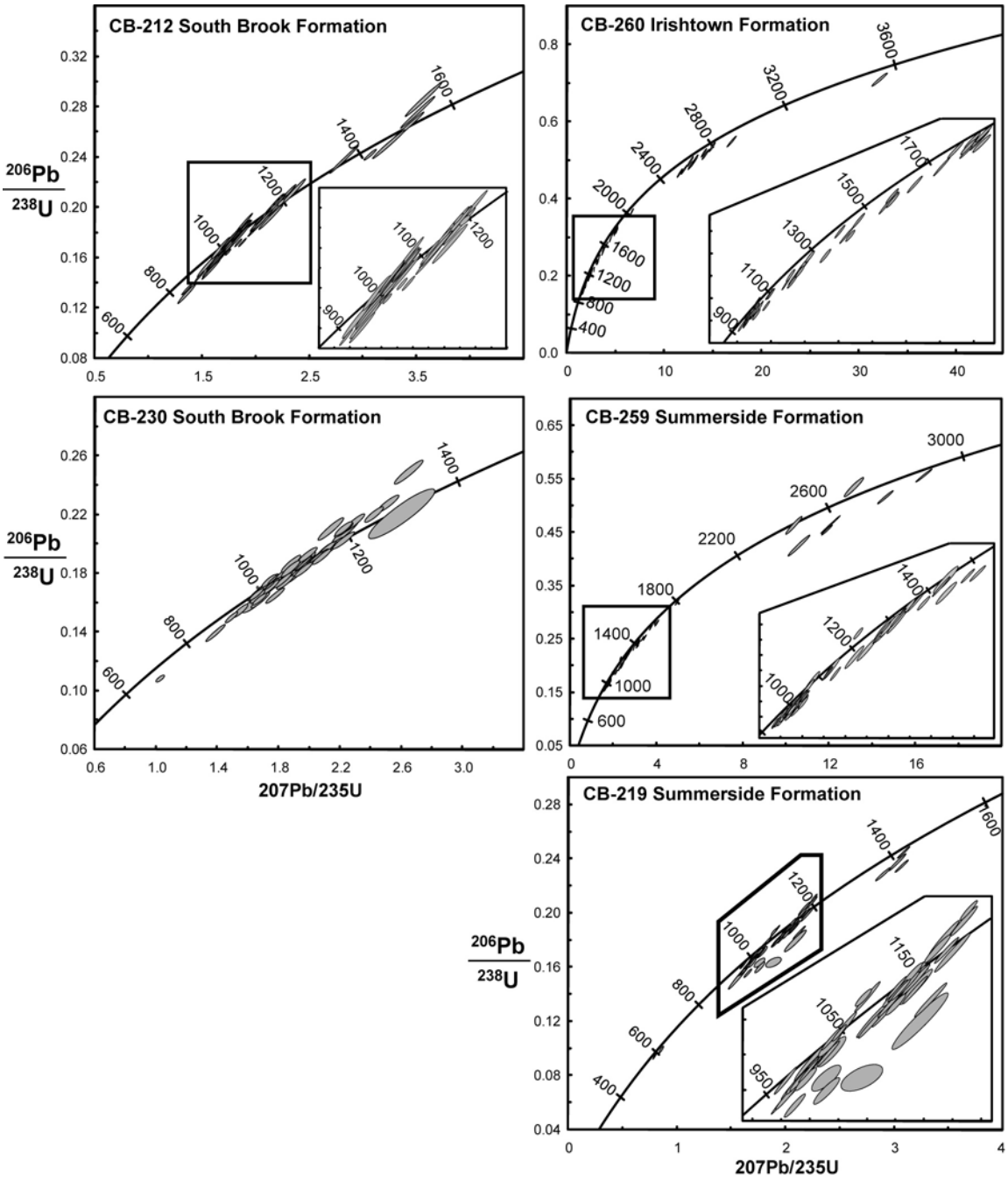

Figure 4.8. U-Pb Concordia diagrams for zircon analyzed in the synrift and metaclastic samples; error ellipses are 1σ.

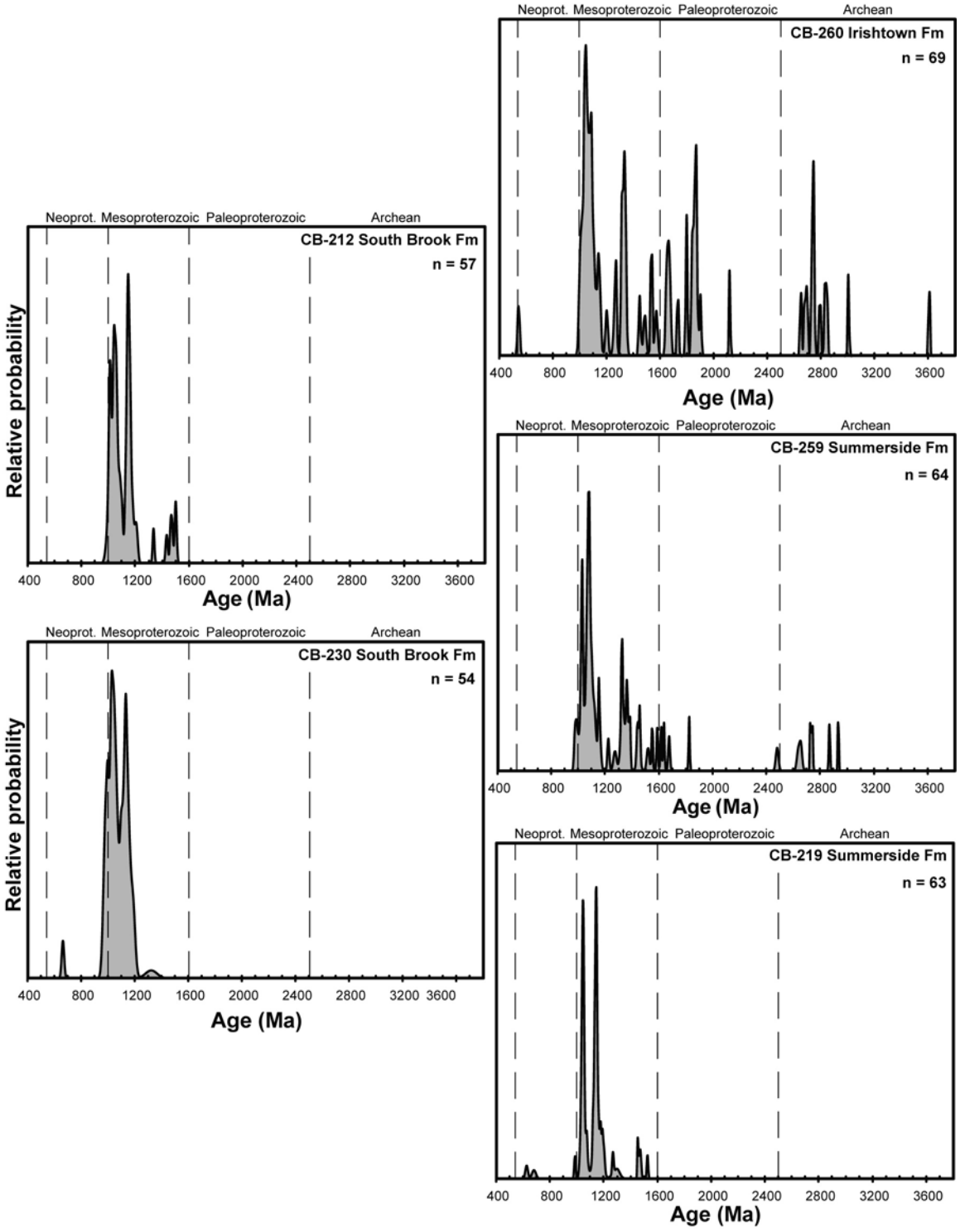

Figure 4.9. Cumulative probability density diagrams for U-Pb isotopic ages in zircon from the synrift and metaclastic samples. Only those analyses within ±10% discordance are plotted.

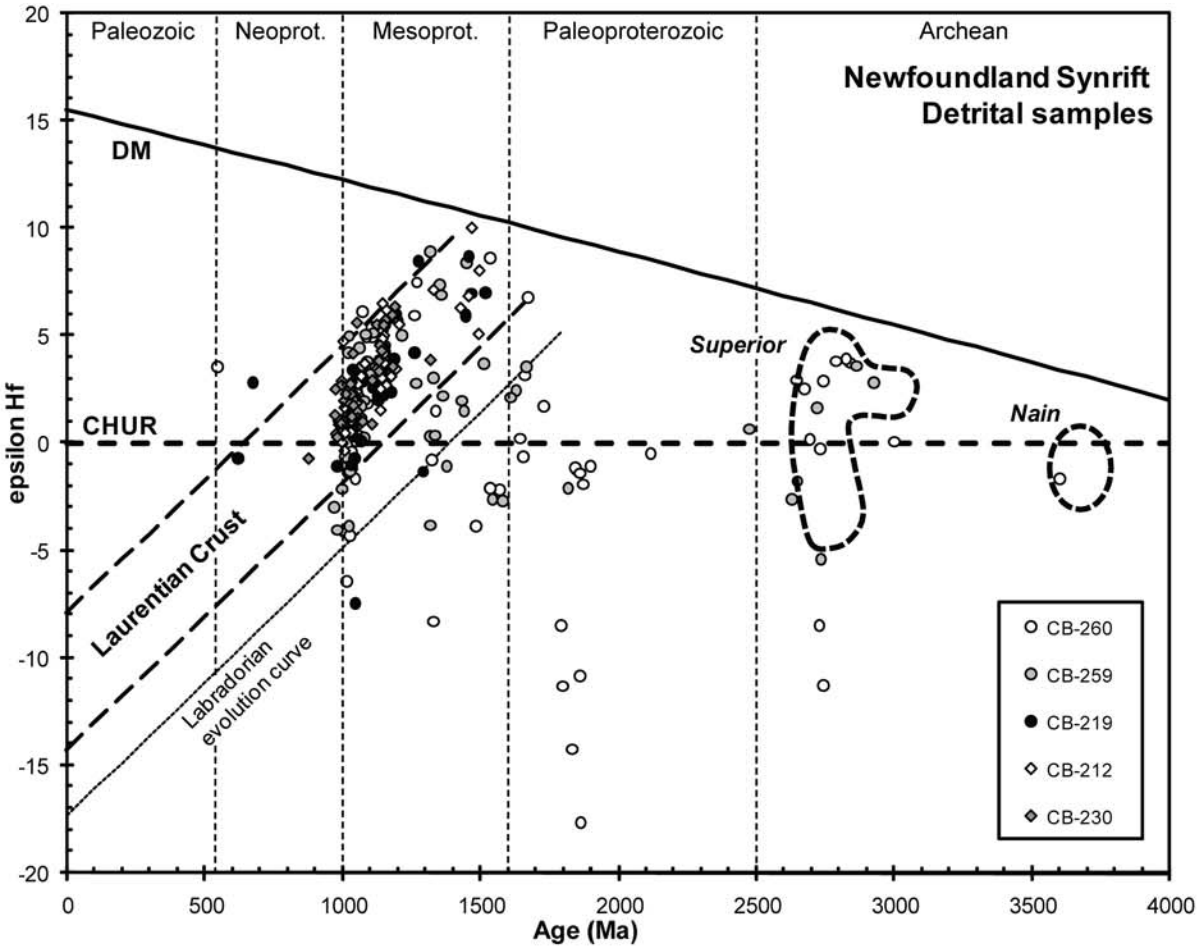

Figure 4.10. $^{177}Hf/^{176}Hf$ from the metaclastic and synrift samples displayed as εHf versus U-Pb age. Evolution curves for CHUR and depleted mantle (DM) are plotted, along with the modeled range of Hf crustal reservoirs for Laurentian crust on the St. Lawrence promontory (bold straight dotted lines). Also shown is a Hf-evolution curve for Labradorian crust (thin dotted line). Fields for initial Hf ratios that correspond to the Superior and Nain provinces are taken from references in the text.

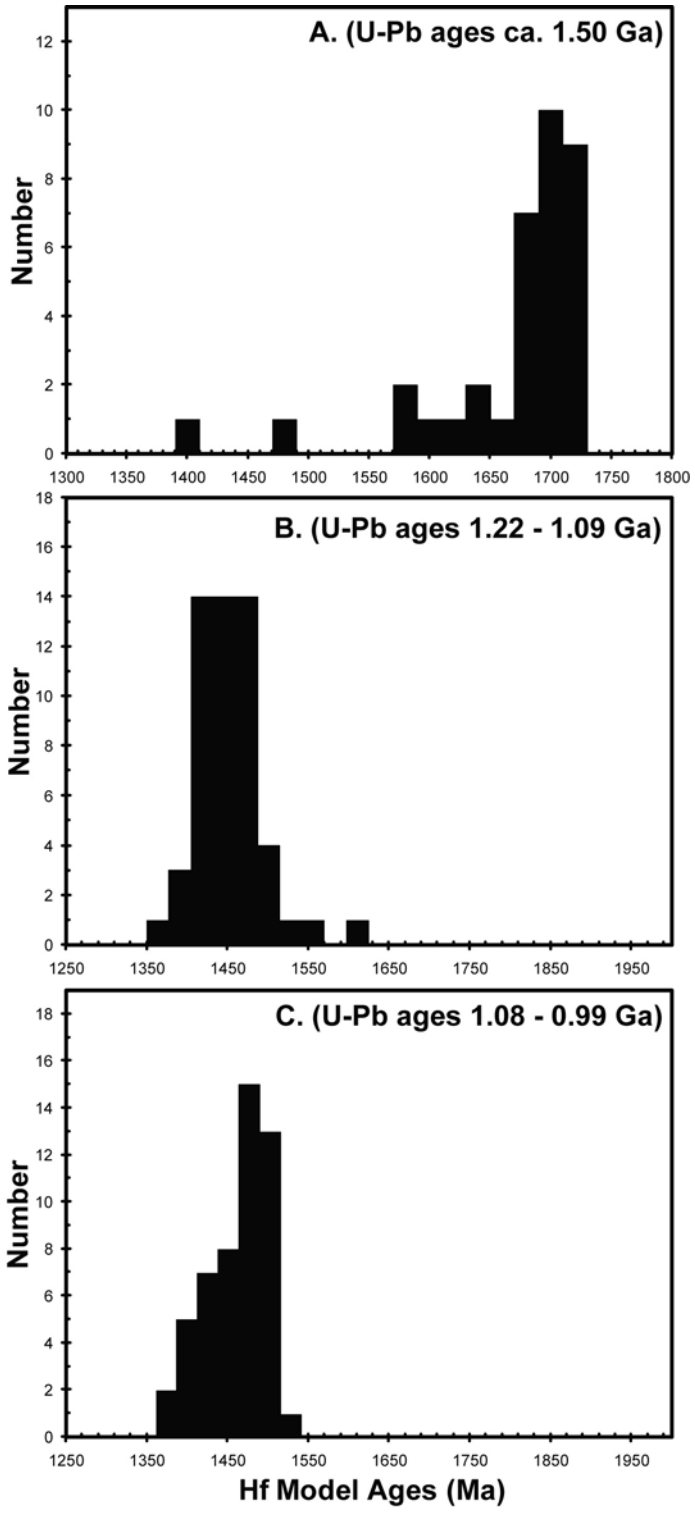

Figure 4.11. Cumulative histograms of the depleted mantle model ages (T_{DM}) calculated from analyzed detrital zircon that correspond to a *A)* ca. 1.50 Ga population; *B)* 1.22-1.09 Ga population; and *C)* 1.08-0.99 population.

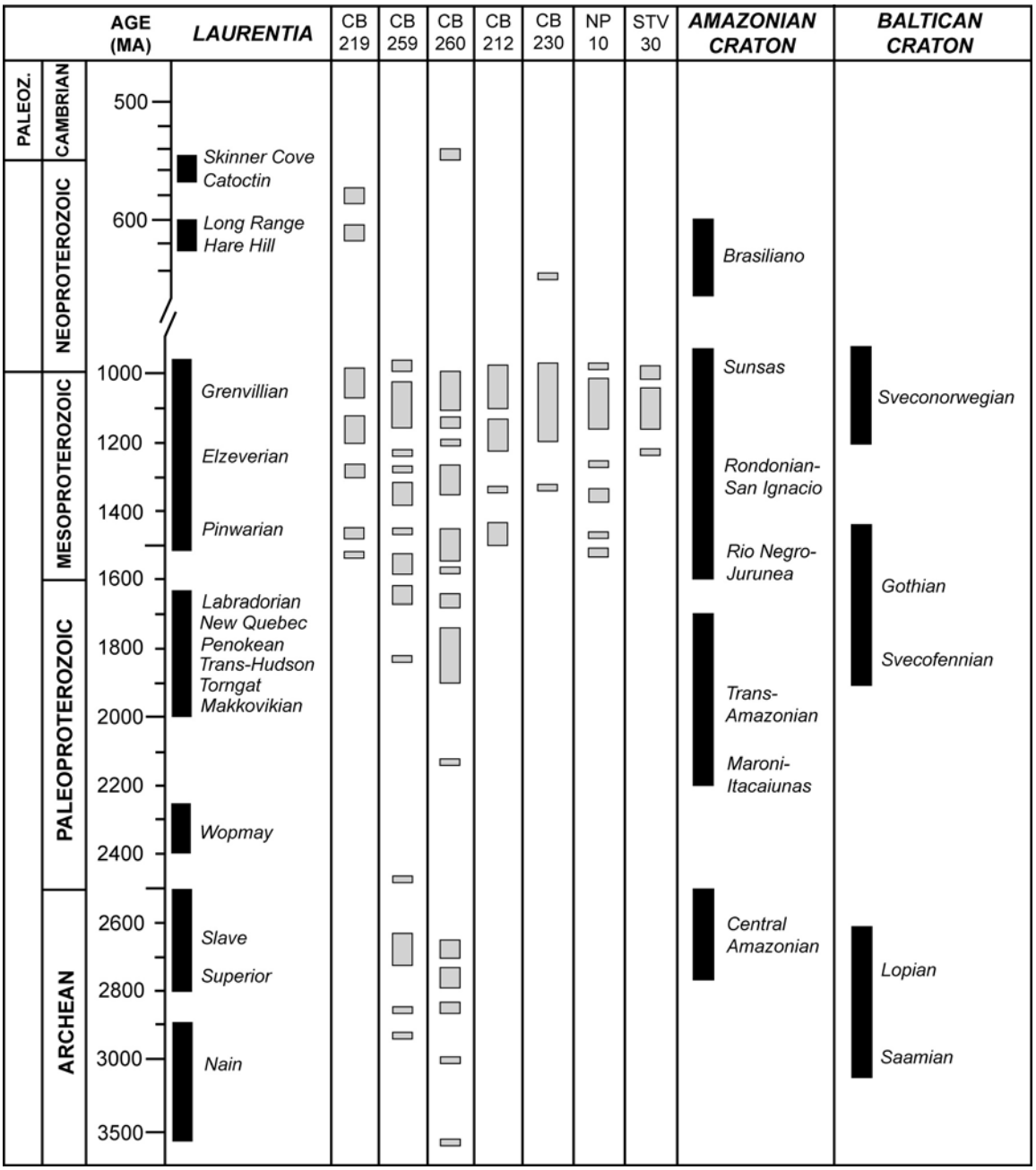

Figure 4.12. Composite chart illustrating detrital-zircon ages from the late Neoproterozoic-Early Cambrian synrift succession from the St. Lawrence promontory, as well as the ages of magmatic, metamorphic, and orogenic events on Laurentia (e.g., Gower and Krogh, 2002), the Amazon craton (e.g., Cordani and Teixeira, 2007), and the Baltican craton (e.g., Gorbatschev and Bogdanova, 1993; Andersen, 2005).

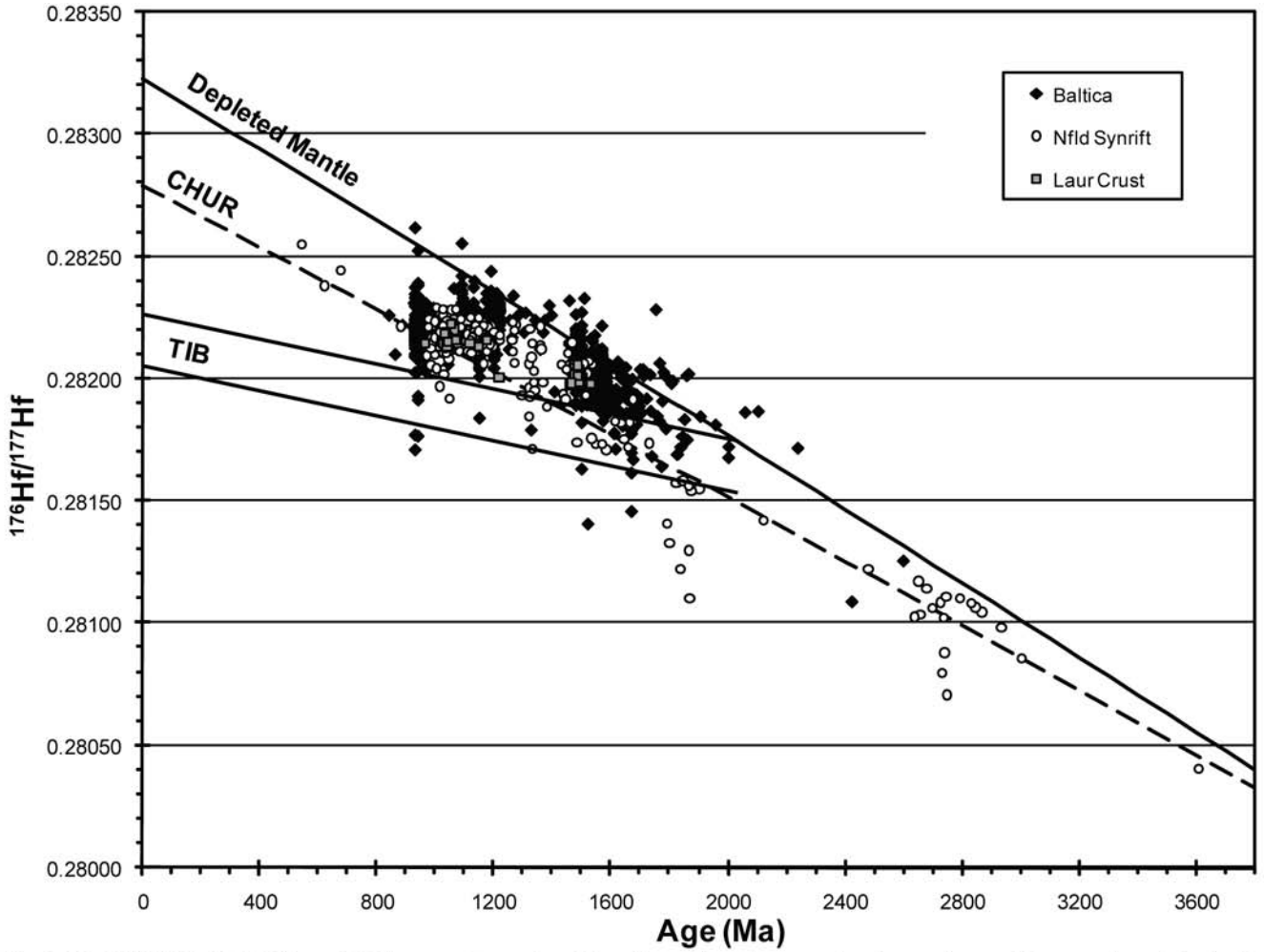

Figure 4.13. Initial 177Hf/176Hf vs. U-Pb age from the Newfoundland metaclastic and synrift samples (circles) and basement samples (squares) plotted against zircon from igneous suites on the Baltican craton (diamonds; references in text). Reference lines representing CHUR Hf evolution and the depleted mantle (DM) (Bouvier et al., 2008) are shown, as well as the range of crustal reservoirs corresponding to the Trans-Scandinavian Igneous Belt (TIB).

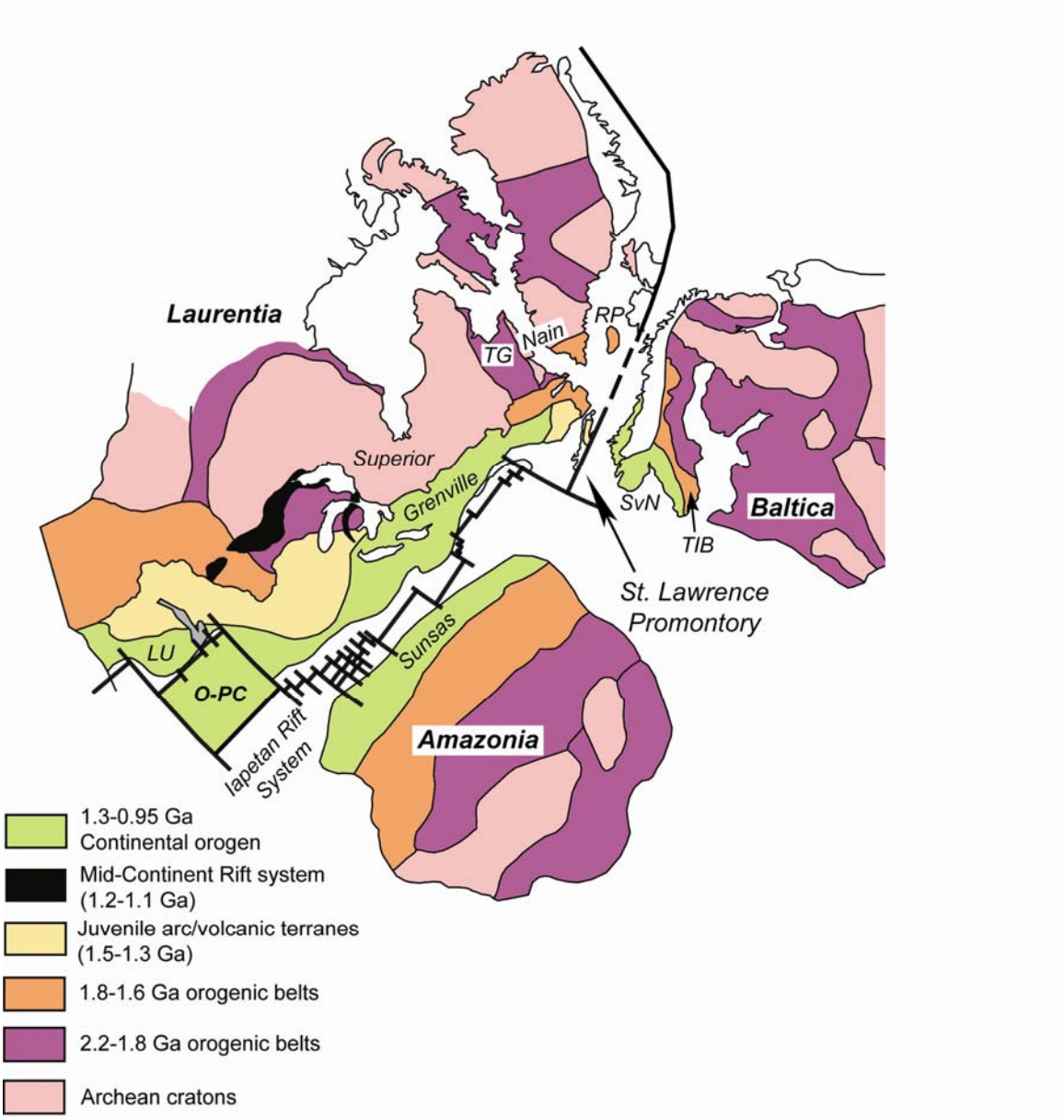

Figure 4.14. The Laurentia-Baltica-Amazonia reconstruction at around 600 Ma based on the results of this investigation, immediately prior to the opening of the Iapetus Ocean. Archean, Paleproterozoic, and Mesoproterozoic elements of each of the three cratons are displayed along with the outline of the Iapetan rift (bold black line, based on Thomas, 2006). LU = Llano uplift; O-PC = Ouachita-Argentine Precordillera; TIB = Trans-Scandinavian Igneous Belt; TG = Torngat province; RP = Rockall Platform; SvN = Sveconorwegian orogen.

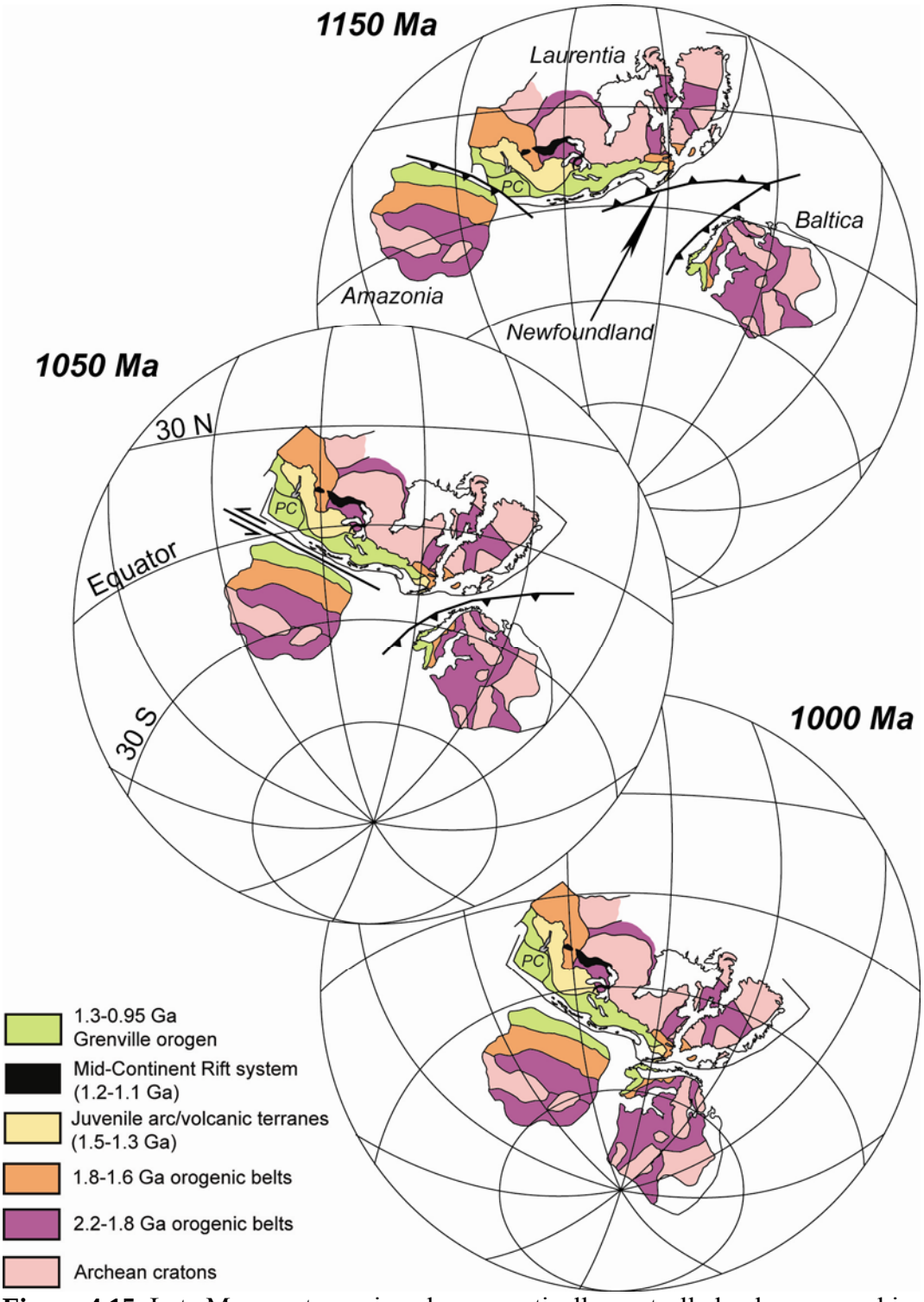

Figure 4.15. Late Mesoproterozoic paleomagnetically controlled paleogeographic continental reconstructions of eastern Laurentia, Baltica, and Amazonia in the time leading up to the Rodinia assembly. Final positions of Baltica and Amazonia with respect to western Newfoundland are controlled by the detrital-zircon data of this study, as well as by paleomagnetic data (Tohver et al., 2004; Cawood and Pisarevsky, 2006; Li et al., 2008). PC = Ouachita-Argentine Precordillera.

CHAPTER 5 - SUMMARY OF CONCLUSIONS

5.1 INTRODUCTION

The results of this dissertation provide a detailed paleogeographic reconstruction of the pre- and post-Iapetan rift history for the eastern Laurentian continental margin in western Newfoundland. Continental margins are formed by continental rifts that either break apart supercontinents or fracture continents into smaller microcontinental masses (Dewey and Burke, 1974; Rogers and Santosh, 2004; Condie, 2005). There is still some debate as to how exactly continental rifts are initiated and evolve structurally, primarily because active rifts and modern continental margins are buried under thick sedimentary accumulations. The geology of western Newfoundland offers a unique opportunity to study the stratigraphy of an ancient rift and passive continental margin and test hypothetical models for the evolution of continental rifting, as well as expand our understanding of the Proterozoic and Paleozoic evolution of the Appalachian orogen.

This chapter presents a summary of the findings of this dissertation. The hypotheses and the objectives of study will be revisited in light of the new data produced by the dissertation. An outline of the Proterozoic and Paleozoic geologic history of western Newfoundland will be proposed on the basis of the data and interpretations generated in Chapters 2, 3, and 4. This chapter will conclude by briefly discussing remaining unanswered questions concerning the tectonic evolution of the St. Lawrence promontory and the eastern Laurentian continental margin.

5.2 SUMMARY OF HYPOTHESES AND OBJECTIVES

Hypothesis 1: The Neoproterozoic-early Paleozoic eastern Laurentian margin in the northern Appalachians, with specific reference to the St. Lawrence promontory of western Newfoundland, developed from a simple shear, low-angle detachment rift system.

The results of this investigation demonstrate important along-strike changes in the structure and subsidence of eastern Laurentian basement, and in the stratigraphy of overlying Neoproterozoic-early Paleozoic synrift and post-rift sedimentary deposits in

western Newfoundland. Important along-strike contrasts in the development of the middle and late Paleozoic Appalachian collisional orogen are also demonstrated in balanced cross sections. All of the available data from this part of the investigation indicate that the eastern Laurentian rift along the St. Lawrence promontory developed as a simple-shear, low-angle detachment system. Observations from the Quebec embayment and the New York promontory also suggest that in those locations, the eastern Laurentian rift developed as a low-angle detachment.

Objective A: Determine if regional lateral variations in the age, thickness, facies, composition, and geophysical attributes of synrift and post-rift successions distributed along the deformed northern Appalachian margin conform to proposed models for a low-angle detachment rift model.

Chapter 2 presents a complete history of the eastern Laurentian margin during the early Paleozoic, from the initiation of continental rifting in the late Neoproterozoic to passive-margin thermal subsidence through the Early Ordovician. Synthesis of the available data reveals significant, abrupt, along-strike variations in the thickness, composition, age, and facies of important synrift and post-rift stratigraphic successions between different northern Appalachian rift zones. Furthermore, differences in the ages of synrift accumulations and the paleomagnetic data set for eastern Laurentia around the end of the Neoproterozoic require a multi-stage continental rift system, with break out Laurentia from the supercontinent Rodinia around 570 Ma, followed by rifting of microcontinents from the margin at 550 Ma (Cawood et al., 2001). The along-strike variations in the Laurentian margin stratigraphy observed in the northern Appalachians are consistent with models for low-angle detachment rift systems and allow for the resolution of the underlying architecture of the eastern Laurentian margin specific to low-angle detachments (i.e., upper-plate margins, lower-plate margins, and transform faults). The model proposed in Chapter 2 is consistent with previously proposed models for the evolution of the eastern Laurentian rift in the southern Appalachians (e.g., Thomas, 1993; Thomas and Astini, 1999).

Objective B: Palinspastically reconstruct the St. Lawrence promontory to test if the distribution of synrift and post-rift sediments and structures fit a low-angle detachment model for this segment of the eastern Laurentian margin.

The results of Chapter 3 verify the observations made in Chapter 2 concerning the structural architecture of the St. Lawrence promontory. Restoration of deformed continental-margin successions through the use of balanced cross sections demonstrates significant along-strike variation in the palinspastic extent of synrift and post-rift stratigraphy on the St. Lawrence promontory. The stark along-strike contrasts in the thickness and extent of palinspastically restored Neoproterozoic-Early Cambrian sediments on the promontory is best explained by synrift sediment dispersal into upper- and lower-plate domains along a low-angle detachment margin. Furthermore, distinct differences in the subsidence history of specific segments of the St. Lawrence promontory indicate an asymmetrically rifted continental margin, which mimics proposed models for simple-shear, low-angle detachment rifts. Balanced cross sections across the deformed St. Lawrence promontory also elucidate the tectonic evolution of western Newfoundland by resolving the sequence of stratigraphic and structural events on the promontory during the Ordovician, Silurian, Devonian, and Carboniferous.

Hypothesis 2: During the breakup of Rodinia and opening of the Iapetus Ocean, departing conjugate cratons may have left a geochemical fingerprint on the eastern Laurentian margin in the synrift sedimentary detritus, which is currently exposed as a result of the Appalachian orogenic cycle. Thus, isotopic tracers in detrital zircon deposited as part of the synrift sedimentary system on the St. Lawrence promontory can be used to identify Proterozoic conjugate cratons to the eastern Laurentian margin in that region.

The results of the detrital zircon study demonstrate that combined radiometric U-Pb ages and Hf-isotopic data from individual zircons sampled from crystalline and detrital sources provides useful information concerning the provenance of sediment deposited into an active rift and early passive-margin system. The study also

demonstrates that a provenance component for detrital zircons can only be uniquely determined if a suitable Lu/Hf record is available for potential source terranes/cratons. For the synrift deposits on the St. Lawrence promontory, a large Lu/Hf database exists for both Archean and Proterozoic terranes on the Laurentian and Baltican cratons. Therefore, zircons of Laurentian and Baltican origin can be identified on the basis of U-Pb age and Lu/Hf isotopy.

Objective C: Conduct modern isotopic analyses (i.e., U-Pb ages and Lu/Hf ratios) of detrital zircons from synrift sediments to test the alternatives for provenance in the context of conjugate cratons to the St. Lawrence promontory.

Chapter 4 goes beyond the architecture of the eastern Laurentian margin to address the question of which craton in the mosaic of continental cratons in the Rodinia assembly was conjugate to the St. Lawrence promontory prior to continental rifting at the end of the Neoproterozoic. Previous paleomagnetic investigations have narrowed candidates to either Baltica or Amazonia. The hypothesis at the beginning of the study was that either of these cratons may have left a geochemical fingerprint on the St. Lawrence promontory preserved in the form of U-Pb ages and Lu-Hf isotopes in detrital zircon deposited as part of the synrift sedimentary record. Detrital zircons analyzed from seven synrift clastic samples are overwhelmingly late Mesoproterozoic in age, which is unsurprising considering that most Paleozoic sediments in the Appalachian orogen appear to be flooded with “Grenville-age” detritus (e.g., Moecher and Samson, 2006). However, when coupled with Hf analyses, the detrital zircons from the Newfoundland synrift succession demonstrate a clear shift in provenance of synrift sedimentary detritus through time. Furthermore, similarity in the Lu-Hf geochemistry of synrift detrital zircons from the St. Lawrence promontory to that of Mesoproterozoic zircons previously analyzed from the Baltican craton indicates that Baltica was conjugate to the St. Lawrence promontory during the Mesoproterozoic assembly of Rodinia.

5.3 PALEOGEOGRAPHIC HISTORY OF THE ST. LAWRENCE PROMONTORY, WESTERN NEWFOUNDLAND

Paleogeography is the study of the evolution of the Earth's surface through geologic time. In this investigation, emphasis is focused primarily on the changing positions and geologic environments of Earth's ancient continental cratons. Data and interpretations produced by this dissertation add valuable information regarding the paleogeographic evolution of eastern Laurentia and the continental margin with respect to other neighboring cratons during the Proterozoic and Paleozoic. The paleogeographic summary below highlights important tectonic events that affected eastern Laurentia in the region around the St. Lawrence promontory of western Newfoundland.

- *1)* During the early and middle Mesoproterozoic (ca. 1520-1200 Ma), northeastern Laurentia (present coordinates) experienced several pulses of intense magmatic and metamorphic events related to continental-arc magmatism and juvenile-arc accretion along the eastern margin (e.g., Pinwarian, Elsonian, Elzevirian orogens) (Gower and Krogh, 2002). Juvenille-arc accretion and continental-arc magmatism along the eastern Laurentian margin are related to the symmetrical closure of a major Pacific-style ocean basin between Laurentia and Baltica.

- *2)* Late Mesoproterozoic (1200-1000 Ma) arc magmatism along the northeastern Laurentian margin culminated in a continent-continent collision between Baltica and northeastern Laurentia (Grenville orogen) as the supercontinent Rodinia was being assembled. Previous studies have suggested that Amazonia was conjugate to the northeastern Laurentia (Dalziel, 1997); however, U-Pb and Hf isotopic data from detrital zircons sampled on the St. Lawrence promontory indicate a better match with Baltica. Furthermore, new paleomagnetic and geochemical data indicate Amazonia collided with the southern Laurentian margin during the assembly of Rodinia (Tohver et al., 2002; 2004; Lowey et al., 2003)

- *3)* The supercontinent Rodinia persisted for ~250 m.y. after the Grenville orogeny. Breakup of Rodinia along the eastern Laurentian margin began during the

Neoproterozoic. Synrift sedimentary accumulations and igneous suites in the southern Appalachians suggest that continental extension began as early as 760 Ma (lower Ocoee Supergroup; Mount Rogers suite) (Thomas, 2006). Pervasive rifting along the entire length of the eastern Laurentian margin began around 620 Ma. In the northern Appalachians, the Neoproterozoic paleomagnetic reconstruction for eastern Laurentia, coupled with differences in the ages of rift-related rocks, require a multi-stage continental rift system, punctuated by early breakout of Laurentia from Rodinia around ca. 570 Ma, followed by late-stage rifting of microcontinents around ca. 550 Ma (Cawood et al., 2001, Waldron and van Staal, 2001; Thomas, 2006).

- *4)* Breakout of a strand of microcontinents at approximately 550 Ma affected the entire margin of eastern Laurentia and produced the St. Lawrence promontory, as well as other promontories and embayments along the eastern margin (e.g., Thomas, 1977). Promontories and embayments were defined by northeast-trending rift segments in continental crust, which were offset along strike by northwest-trending transforms. Significant along-strike asymmetry in synrift sedimentary accumulations, crustal structure, and subsidence history indicate that the eastern Laurentian rifted margin was founded on a low-angle detachment rift system.

- *5)* A late-Early Cambrian clastic/carbonate transgressive sequence marks the end of rifting along the St. Lawrence promontory. The newly formed eastern Laurentian passive margin was flanked by a narrow seaway (Humber Seaway) that separated it from the strand of microcontinents. Outboard of the strand of microcontinents was the Iapetus Ocean, which is estimated to have been approximately 3000 km wide and separated Laurentia from the then assembling Gondwanan supercontinent (Cawood et al., 2001).

- *6)* By the Middle Cambrian, the entire length of the eastern Laurentian margin, including the St. Lawrence promontory, had evolved into a full-fledged carbonate bank. Passive-margin carbonate deposition persisted on the shelf of the St. Lawrence promontory approximately 40 m.y., from the Middle Cambrian through the early

Middle Ordovician (Llanvirn). Closure of the Iapetus Ocean had begun by the Late Cambrian. Obducted oceanic igneous suites and intense Late Cambrian deformation in the Dashwoods block in the Dunnage zone indicate attempted subduction of the outboard strand of microcontinents by the end of the Cambrian (Waldron and van Staal, 2001).

- *7)* Initiation of subduction of the leading edge of the St. Lawrence promontory beneath Iapetan oceanic island arcs is indicated by the influx of early Middle Ordovician (Arenig) flysch along the most distal parts of the slope (e.g., Eagle Island Formation). Full-fledged subsidence of the shelf as a result of collision with oceanic island arcs began by the Llanvirnian with the influx of sandstone and shale in the Goose Tickle Group.

- *8)* The Middle Ordovician "Taconic" orogeny on the St. Lawrence promontory is marked by the obduction of ophiolites and thin-skinned emplacement of the Humber Arm allochthon onto the very leading edge of the continental margin as the Iapetus Ocean basin was closing. Emplacement of the allochthon onto the very leading edge of the margin resulted in a relatively thin Middle Ordovician foreland basin except where flexural-subsidence-induced extension in the foreland was sufficient to reactivate older rift graben (i.e., Round Head fault, Parson's Pond thrust).

- *9)* Following a brief time of tectonic quiescence, shortening along the St. Lawrence promontory during the Late Ordovician-Early Silurian "Salinic" orogeny thrust the Humber Arm allochthon farther up onto the margin. The result was foreland subsidence and accumulation of a thick, Late Ordovician-Early Silurian foreland basin succession followed by intense metamorphism of part of the distal margin as it was buried deep underneath the advancing Humber Arm allochthon.

- *10)* Latest Silurian-Early Devonian subsidence of the St. Lawrence promontory is indicated by deposition of red beds in the Clam Bank and Red Island Road Formations. Final westward emplacement of the Humber Arm allochthon into a

tectonic wedge beneath the Late Ordovician-Early Devonian foreland basin is constrained to post-Early Devonian because Emsian age strata in the Red Island Road Formation are deformed by the roof thrust of the tectonic wedge.

• *11)* The final major tectonic event to affect rocks on the St. Lawrence promontory is the wholesale thick-skinned reactivation of earlier basement faults, which in some locations structurally inverted previous graben systems in the shelf succession. Stratigraphic relationships on the promontory loosely constrain the timing of thick-skinned tectonism to between the Early Devonian and Early Mississippian. As a result, this final event may be related either to late "Acadian" compression as Avalonia was being accreted to the eastern Laurentian margin; or to early "Alleghanian" transpression on the promontory resulting from deformation along major Carboniferious strike slip faults in western Newfoundland.

5.4 FUTURE RESEARCH

The investigations of this dissertation have provided new observations and data that elucidate the tectonic and paleogeographic evolution of western Newfoundland and the St. Lawrence promontory during the span of time from the early Mesoproterozoic through the late Paleozoic. Although many questions may have been answered by this dissertation, some questions remain unanswered and many new questions have been generated. Listed below are topics that required further investigation, which may confirm, disprove, and/or expand the interpretations of this study, as well as aid in our overall understanding of continental rifts and the evolution of the eastern Laurentian continental margin.

1) Subsidence curves and palinspastic restoration of the Paleozoic stratigraphy on the St. Lawrence promontory by balanced cross sections confirms the low-angle detachment architecture of the eastern Laurentian rift in that part of the northern Appalachians. The results imply, yet do not demonstrate, a similar geometry for the eastern Laurentian rift in Quebec and New England. Thus, the question still remains: Did the eastern Laurentian margin in the Quebec embayment and the New York promontory develop as a low-angle

detachment rift? To answer this question, balanced cross sections and subsidence histories need to be complied for these parts of the northern Appalachian margin.

2) Much of this dissertation focuses on the geology of southwestern Newfoundland and the coastal lowlands west of the Long Range Mountains on the Northern Peninsula. Another complex allochthonous mass of Neoproterozoic-Ordovician slope stratigraphy, however, with structurally overlying ophiolites, is exposed on the eastern coastlands of the Northern Peninsula around Hare Bay. What is the structure and stratigraphy of thrust sheets in the Hare Bay allochthon and how far off the edge of the continental shelf does the allochthon palinspastically restore? What do the Neoproterozoic-Early Cambrian sedimentary accumulations in the allochthon reveal about the rift and post-rift subsidence history of the margin along this segment of the promontory? Subsidence curves and construction of balanced cross sections across the northern tip of the Northern Peninsula can resolve some of these questions, as well as produce a more complete picture of the early Paleozoic history of the St. Lawrence promontory.

3) U-Pb and Hf isotopic analysis of detrital zircon from the St. Lawrence promontory indicate that Baltica, and not Amazonia, was directly adjacent to western Newfoundland in the assembly of Rodinia. Was the Baltican craton also adjacent the Quebec embayment and New York promontory segments of the margin? Isotopic and paleomagnetic investigations indicate that Amazonia was adjacent to the southern Appalachian part of the Laurentian margin. Where is the boundary between Baltica and Amazonia in the Rodinia assembly with respect to the eastern Laurentian margin? Further isotopic tests, including U-Pb and Lu-Hf zircon investigations, may provide answers to this question. In particular, the New York promontory contains synrift sedimentary accumulations deposited on Mesoproterozoic basement. Thus, a study similar to the one presented in this dissertation can be performed on the deformed synrift rocks in New York and New England.

4) U-Pb and Hf isotopic analysis of detrital zircons from the synrift succession on the St. Lawrnece promontory indicate a change in provenance of rift accumulations from local sedimentary input at the initiation of rifting to sedimentary drainage across most of the northern Laurentian craton by the onset of passive-margin thermal subsidence. How does the provenance of sedimentary accumulations change on the promontory during development of an active collisional orogen during the Ordovician, Silurian, and Devonian? A detailed U-Pb and Lu-Hf detrital zircon study through the entire Paleozoic foreland-basin succession (i.e., Goose Tickle Group, Long Point Group, and Clam Bank-Red Island Road Formations) can answer these questions.

5) Are the Chain Lakes massif and Dashwoods block manifestations of the strand of microcontinents that were rifted off the eastern Laurentian margin as Rodinia broke apart? U-Pb and Hf isotopic analysis of detrital zircons in the metasedimentary accumulations in these two deformed crustal blocks can evaluate a potential geochemical and isotopic link to eastern Laurentia.

Appendix A. Calculation of Lu/Hf evolution curves, depleted mantle model ages, and epsilon-Hf notation.

Lutetium-176 (^{176}Lu) is one of two naturally occurring isotopes in the Lutetium system, and decays to Hafnium-176 (^{176}Hf) by β-emission with a half-life of 35.7×10^9 years (Faure and Mensing, 2005). The abundance of ^{176}Hf, expressed as the ratio of radiogenic ^{176}Hf vs non-radiogenic ^{177}Hf (i.e., ^{176}Hf/^{177}Hf), increases with time at a rate that is proportional to the atomic ^{176}Lu/^{177}Hf ratio of the rock or mineral:

$$\frac{^{176}\mathrm{Hf}}{^{177}\mathrm{Hf}} = \left(\frac{^{176}\mathrm{Hf}}{^{177}\mathrm{Hf}}\right)_i + \frac{^{176}\mathrm{Lu}}{^{177}\mathrm{Hf}}\left(e^{\lambda t} - 1\right) \qquad \text{(eq. A.1)}$$

where ^{176}Hf/^{177}Hf = ratio of these isotopes in a sample of rock or mineral at the present time

$(^{176}\mathrm{Hf}/^{177}\mathrm{Hf})_i$ = ratio of these isotopes at the time of formation in the Lu-bearing rock or mineral

^{176}Lu/^{177}Hf = ratio of these isotopes in the Lu-bearing rock or mineral at the present time

λ = the decay constant of ^{176}Lu (1.867×10^{-11} yr^{-1}); after Soderlund et al. (2004).

The ^{176}Hf/^{177}Hf ratio of the depleted mantle (DM) can be calculated at any time t by means of equation A.2:

$$\left(\frac{^{176}\mathrm{Hf}}{^{177}\mathrm{Hf}}\right)^0_{\mathrm{DM}} = \left(\frac{^{176}\mathrm{Hf}}{^{177}\mathrm{Hf}}\right)^t_{\mathrm{DM}} + \left(\frac{^{176}\mathrm{Lu}}{^{177}\mathrm{Hf}}\right)^0_{\mathrm{DM}}\left(e^{\lambda t} - 1\right) \qquad \text{(eq. A.2)}$$

where the superscript zero signifies the depleted mantle ^{176}Hf/^{177}Hf and ^{176}Lu/^{177}Hf ratios at the present (i.e., $t = 0$) and the superscript t refers to the depleted mantle ^{176}Hf/^{177}Hf ratio at a time in the past. Therefore:

$$\left(\frac{^{176}\mathrm{Hf}}{^{177}\mathrm{Hf}}\right)^t_{\mathrm{DM}} = \left(\frac{^{176}\mathrm{Hf}}{^{177}\mathrm{Hf}}\right)^0_{\mathrm{DM}} - \left(\frac{^{176}\mathrm{Lu}}{^{177}\mathrm{Hf}}\right)^0_{\mathrm{DM}}\left(e^{\lambda t} - 1\right) \qquad \text{(eq. A.3)}$$

The depleted mantle model can be used to calculate the time at which the Hf contained within the rock or mineral sample was separated from the "depleted mantle reservoir". For this purpose, equation A.2 is used to express the $^{176}Hf/^{177}Hf$ ratio of the rock (*R*) at some time *t* in the past analogous to equation A.3 for DM:

$$\left(\frac{^{176}\mathrm{Hf}}{^{177}\mathrm{Hf}}\right)_R^t = \left(\frac{^{176}\mathrm{Hf}}{^{177}\mathrm{Hf}}\right)_R^0 - \left(\frac{^{176}\mathrm{Lu}}{^{177}\mathrm{Hf}}\right)_R^0 \left(e^{\lambda t} - 1\right) \qquad \text{(eq. A.4)}$$

Because $\left(\frac{^{176}\mathrm{Hf}}{^{177}\mathrm{Hf}}\right)_R^t = \left(\frac{^{176}\mathrm{Hf}}{^{177}\mathrm{Hf}}\right)_{\mathrm{DM}}^t$ the right sides of equations A.3 and A.4 can be set equal to one another. Therefore, solving for t and substituting values for the isotope ratios for DM:

$$\left(\frac{^{176}\mathrm{Hf}}{^{177}\mathrm{Hf}}\right)_{\mathrm{DM}}^0 = 0.28323$$

$$\left(\frac{^{176}\mathrm{Lu}}{^{177}\mathrm{Hf}}\right)_{\mathrm{DM}}^0 = 0.03854$$

yields the equation for a depleted mantle model age (T_{DM}):

$$t = \frac{1}{\lambda}\ln\left[\frac{\left(^{176}\mathrm{Hf}/^{177}\mathrm{Hf}\right)_R^0 - 0.28279}{\left(^{176}\mathrm{Lu}/^{177}\mathrm{Hf}\right)_R^0 - 0.0336} + 1\right] \qquad \text{(eq. A.5)}$$

The $^{176}Hf/^{177}Hf$ ratios of terrestrial rocks are commonly evaluated by comparison to the present isotope ratio of CHUR. This comparison is facilitated by the epsilon notation (i.e. ε_{Hf}) of DePaolo and Wasserberg (1976):

$$\varepsilon^t(\mathrm{Hf}) = \left[\frac{(^{176}\mathrm{Hf}/^{177}\mathrm{Hf})_R^t}{(^{176}\mathrm{Hf}/^{177}\mathrm{Hf})_{\mathrm{CHUR}}^t} - 1\right] \times 10^4 \qquad \text{(eq. A.6)}$$

where $\left(\frac{^{176}\mathrm{Hf}}{^{177}\mathrm{Hf}}\right)_{\mathrm{CHUR}}^t = 0.28279 - 0.0336\left(e^{\lambda t} - 1\right)$; the $^{176}Hf/^{177}Hf$ ratio of CHUR calculated at some time *t*

and $\left(\frac{^{176}\mathrm{Hf}}{^{177}\mathrm{Hf}}\right)_R^t$ = the calculated ratio of $^{176}Hf/^{177}Hf$ for the rock or mineral sample at time *t*

Where ε_{Hf} is positive, the protoliths of the rock/mineral of age *t* originated from a depleted mantle source. Where ε_{Hf} is negative, protoliths for the rock/mineral of age *t* were derived from continental crust.

REFERENCES

Allen, J.S., Thomas, W.A., and Lavoie, D., 2009, Stratigraphy and structure of the Laurentian rifted margin in the northern Appalachians: a low-angle detachment rift system: Geology, v. 37, p. 335-338.

Amelin, Y., Lee, D.C., and Halliday, A.N., 2000, Early-middle Archaean crustal evolution deduced from Lu-Hf and U-Pb isotopic studies of single zircon grains: Geochimica et Cosmochimica Acta, v. 64, p. 4205-4225.

Andersen, T., 2005, Detrital zircons as tracers of sedimentary provenance: limiting conditions from statistics and numerical simulation: Chemical Geology, v. 216, p. 249-270.

Andersen, T., and Griffin, W.L., 2004, Lu-Hf and U-Pb isotope systematics of zircons from the Storgangen intrusion, Rogaland Intrusive Complex, SW Norway: implications for the composition and evolution of Precambrian lower crust in the Baltic Shield, Lithos, v. 73, p. 271-288.

Andersen, T., Griffin, W.L., and Pearson, N.J., 2002, Crustal evolution in the SW part of the Baltic Shield: the Hf isotope evidence: Journal of Petrology, v. 43, p. 1725-1747.

Andersen, T., Griffin, W.L., Jackson, S.E., and Knudsen T.L., 2004, Mid-Proterozoic magmatic arc evolution at the southwest margin of the Baltic Shield: Lithos, v. 73, p. 289-313.

Andersen, T., Griffin, W.L., and Sylvester, A.G., 2007, Sveconorwegian crustal underplating in southwestern Fennoscandia: LAM-ICPMS U-Pb and Lu-Hf isotope evidence from granites and gneisses in Telemark, southern Norway: Lithos, v. 93, p. 273-287.

Ayuso, R.A., and Bevier, M.L., 1991, Regional differences in Pb isotopic compositions of feldspars in plutonic rocks of the northern Appalachian Mountians, USA, and Canada: a geochemical method of terrane correlation: Tectonics, v. 10, p. 191-212.

Benkhelil, J., 1989, The origin and evolution of the Cretaceous Benue trough (Nigeria): Journal of African Earth Sciences, v. 8, p. 251-282.

Benkhelil, J., Mascle, J., and Guiraud, M., 1998, Sedimentary and structural characteristics of the Cretaceous along the Côte D'Ivoire-Ghana transform margin and the Benue trough: a comparison, in Mascle, J., Lohmann, GP., and Moullade, M. (Eds), Proceedings of the Ocean Drilling Program, Scientific Results, v. 159, p. 93-99.

Berquist, P.J., Fisher, C.M., Miller, C., Woodenk J.L., Fullagar, P.D., and Loewy, S.L., 2005, Geochemistry and U-Pb zircon geochronology of Blue Ridge basement, western North Carolina and eastern Tennessee: Implications for tectonic assembly, in Hatcher, R.D., and Merschat, A.J., eds, Blue Ridge Geology Geotraverse east of the Great Smoky Mountains National Park, western North Carolina: North Carolina Geological Survey, Carolina Geological Society Annual Field Trip Guidebook, p. 33-44.

Bettencourt, J.S., Tosdal, R.M., Leite, W.B., and Payolla, B.L., 1999, Mesoproterozoic rapakivi granites of Rondonia Tin province, southwest border of the Amazonian craton, Brazil, I: Reconnaissance U-Pb geochronology and regional implications: Precambrian Research, v. 95, p. 41-67.

Black, L.P., Kamo, S.L., Williams, I.S., Mundil., R., Davis, D.W., Korsch, R.J., and Foudoulis, C., 2003, The application of SHRIMP to Phanerozoic geochronology: a critical appraisal of four zircon standards: Chemical Geology, v. 200, p. 171-188.

Bodanova, S.V., Bingen, B., Gorbatschev, R., Kheraskova, T.N., Kozlow, V.I., Puchkov, V.N., Volozh, Y.A., 2008, The East European craton (Baltica) before and during the assembly of Rondinia: Precambrian Research, v. 160, p. 23-45.

Bond, G.C., Nickeson, P.A., and Kominz, M.A., 1984, Breakup of a supercontinent between 625 Ma and 555 Ma: New evidence and implications for continental histories: Earth and Planetary Science Letters, v. 70, p. 325-345.

Bond, G.C., Kominz, M.A., and Sheridan, R.E., 1995, Continental terraces and rises, *in* Busby, C.J., and Ingersoll, R.V., eds., Tectonics of sedimentary basins: Cambridge, Massachusetts, Blackwell Science, p. 149-178.

Bostock, H.H., 1983, Precambrian rocks of the Strait of Belle Isle area: in Blackadar, R.G., and Bruce, N. (eds), Geology of the Strait of Belle Isle area, northwestern insular Newfoundland, southern Labrador, and adjacent Quebec: Geological Survey of Canada Memoir, v. 400, 145 p.

Botsford, J., 1988, Stratigraphy and sedimentology of Cambro-Ordovician deep water sediments, Bay of Islands, western Newfoundland: Ph. D. thesis, Memorial University of Newfoundland, St. John's, Newfoundland, 534 p.

Boudette, E.L., Boone, G.M., and Goldsmith, R., 1989, The Chain Lakes Massif and its contact with a Cambrian ophiolite and a Caradocian granite (1989 Guidebook): New England Intercollegiat Geological Conference, 81st Annual Meeting, Farmington, Maine, p. 98-121.

Bouvier, A., Vervoort, J.D., and Patchett, P.J., 2008, The Lu-Hf and Sm-Nd isotopic composition of CHUR: Constraints from unequilibrated chondrites and

implications for the bulk composition of terrestrial planets: Earth and Planetary Science Letters, v. 273, p. 48-57.

Boyce, W.D., Knight, I., and Ash, J.S., 1992, The Weasel Group, Goose Arm area, western Newfoundland: Lithostratigraphy, biostratigraphy, correlation and implications: Current Research, Newfoundland Department of Mines and Energy, Geological Survey Branch, Report 92-1, p. 69-83.

Boyer, S.E., and Elliot, D., 1982, Thrust Systems: AAPG Bulletin, v. 66, p. 1196-1230.

Bradley, D.C, 1980, Taconic plate kinematics as revealed by foredeep stratigraphy, Appalachian orogen: Tectonics, v. 8, no. 5, p. 1037-1049.

Brem, A.G., Lin, S., and van Staal, C.R., 2003, Structural relationships south of Grand Lake, Newfoundland, Current Research, Newfoundland Department of Mines and Energy, Geological survey, Report 03-1, p. 1-15.

Brewer, T.S., Ahall, K.I., Darbyshire, D.P.F., and Menuge, J.F., 2002, Geochemistry of late Mesoproterozoic volcanism in southwest Scandinavia: implications for Sveconorwegian/Grenvillian plate tectonic models: Journal of the Geological Society, v. 159, p. 129-144.

Brooker, T., 2004, Final well report: Parsons Pond Well #1: Contact exploration, Inc., Newfoundland Department of Mines and Energy, Open File Report, 30 p.

Buck, W.R., Martinez, F., Steckler, M.S., and Cochran, J.R., 1988, Thermal consequences of lithospheric extension: Pure and simple: Tectonics, v. 7, p. 213–234, doi: 10.1029/TC007i002p00213.

Burke, K., and Dewey, J.F., 1973, Plume-generated triple junctions: key indicators in applying plate tectonics to old rocks: Journal of Geology, v. 81, p. 406-433.

Camire, G., La Fleche, M.R., and Jenner, G.A., 1995, Geochemistry of pre-Taconian mafic volcanism in the Humber Zone of the northern Appalachians, Quebec: Canadian: Chemical Geology, v. 119, p. 55–77, doi: 10.1016/0009-2541(94)00104-G.

Castonguay, S., Dietrich, J., Shinduke, R., and Laliberté, 2006, Nouveau regard sur l'architecture de la Plate-forme du Saint-Laurent et des Appalaches du sud du Quebec par le retraitement des profiles de sismique reflexion M-2001, M-2002, et M-2003: Commission Geologique du Canada, dossier public 5328, 19 p.

Calon, T., Buchanan, E., Burden, G., Feltham, G., and Young, J., 2002, Stratigraphy and structure of sedimentary rocks in the Humber Arm allochthon, southwestern Bay of Islands, Newfoundland: Current Research, Department of Mines and Energy, Geological survey, Report 02-1, p. 35-45.

Cawood, P.A., and Williams, H., 1986, Northern extremity of the Humber Arm allochthon in the Portland Creek area, western Newfoundland, and relationships to nearby groups: Current Research, Part A., Geological Survey of Canada, Paper 86-1A, p. 675-682.

Cawood, P.A., and Botsford, J.W., 1991, Facies and structural contrasts across Bonne Bay cross-strike discontinuity, western Newfoundland: American Journal of Science, v. 291, p. 737.

Cawood, P.A., and Suhr, G., 1992, Generation and obduction of ophiolites: constraints from the Bay of Islands complex, western Newfoundland: Tectonics, v. 11, p. 884-897.

Cawood, P.A., and van Gool, J.A.M., 1998, Geology of the Corner Brook-Glover Island region, Newfoundland: Geological Survey of Canada Bulletin, 96p.

Cawood, P.A., and Nemchin, A.A., 2001, Paleogeographic development of the east Laurentian margin: Constraints from U-Pb dating of detrital zircons in the Newfoundland Appalachians: Geological Society of America Bulletin, v. 113, no. 9, p. 1234-1246.

Cawood, P.A., and Pisarevsky, S.A., 2006, Was Baltica right-way up or upside down in the Neoproterozoic?: Journal of the Geological Society, v. 163, p. 753-759.

Cawood, P.A., Williams, H., and Grenier, R., 1987, Geology of Portland Creek area (12I/4), western Newfoundland: Geological Survey of Canada, Open File Map 1435, scale 1:50 000.

Cawood, P.A., Dunning, G.R., Lux, D., van Gool, J.A.M., 1994, Timing of peak metamorphism and deformation along the Appalachian margin of Laurentia in Newfoundland: Silurian not Ordovician: Geology, v. 16, p. 370-373.

Cawood, P.A., van Gool, J.A.M., and Dunning, G.R., 1995, Collisional tectonics along the Laurentian margin of the Newfoundland Appalachians, *in* Hibbard, J.P., van Staal, C., and Cawood, P.A., eds., New Developments in the Appalachian-Caledonian Orogen: Geological Association of Canada, Special Paper 41, p. 283-301.

Cawood, P.A., van Gool, J.A.M., and Dunning, G.R., 1996, Geological development of eastern Humber and western Dunnage Zones: Corner Brook-Glover Island region, Newfoundland: Canadian Journal of Earth Sciences, v. 33, p. 182-198.

Cawood, P.A., McCausland, P., and Dunning, G.R., 2001, Opening Iapetus: Constraints from the Laurentian margin in Newfoundland: Geological Society of America Bulletin, v. 113, no. 4, p. 443-453.

Cawood, P.A., Nemchin, A.A., Strachan, R., Prave, T., and Krabbendam, M., 2007, Sedimentary basin and detrital zircon record along east Laurentia and Baltica during assembly and breakup of Rodinia: Journal of the Geological Society, v. 164, p. 257-275.

Cherichetti, L., Doolan, B., and Mehrtens, C., 1998, The Pinnacle Formation: a late Precambrian rift valley fill with implications for Iapetus rift basin evolution: Northeastern Geology and Environmental Sciences, v. 20, p. 175–185.

Clark, T.H., 1934, Structure and stratigraphy of southern Quebec: Geological Society of America Bulletin, v. 45, p. 1-20.

Colman-Sadd, S.P., Hayes, J.P., and Knight, I., 1990, Geology of the island of Newfoundland: Newfoundland and Labrador Department of Mines and Energy, Geologic Survey Branch, Map 90–01, scale 1:1,000,000.

Condie, K.C., 2005, Earth as an Evolving Planetary System, Elsevier Academic Press, 447p.

Cooper, M., Weissenberger, J., Knight, I., Hostad, D., Gillespie, D., Williams, H., Burden, E., Porter-Chaudhry, J., Rae, D., and Clark, E., 2001, Basin Evolution in Western Newfoundland: New Insights from Hydrocarbon Exploration: American Association of Petroleum Geologists Bulletin, v. 85, p. 393–418.

Cordani, U.G., and Teixeira, W., 2007, Proterozoic accretionary belts in the Amazon craton, *in* Hatcher, R.D., Carlson, M.P., McBride, J.H., and Catalan, M., eds, 4-D framework of continental crust: Geological Society of America Memoir, v. 200, p. 297-320.

Corfu, F., and Davis, D.W., 1992, A U-Pb geochronological framework for the western Superior province, Ontario, in Thurston, P.C., et al., eds, The geology of Ontario: Toronto, Ontario, Ministry of Northern Development and Mines, p. 715-904.

Cousineau, P.A., and Longuépée, H., 2003, Lower Paleozoic configuration of the Quebec reentrant based on improved along-strike paleogeography: Canadian Journal of Earth Sciences, v. 40, p. 207–219, doi: 10.1139/e02-107.

Currie, K.L., and van Berkel, J.T., 1992, Notes to accompany a geologic map of the southern Long Range, southwestern Newfoundland: Geological Survey of Canada Paper 91-10, 10 p.

Dallmeyer, R.D., 1977, ^{40}Ar-^{39}Ar age spectra of mineral from the Fleur de Lys terrane in northwest Newfoundland: implications for the tectonic evolution of the Humber and Dunnage zones of the Appalachian orogen: Journal of Geology, v. 85, 89-103.

Dallmeyer, R.D., and Williams, H., 1975, ^{40}Ar-^{39}Ar ages from the Bay of Islands metamorphic aureole: their bearing on the timing of Ordovician ophiolite obduction: Canadian Journal of Earth Sciences, v. 12, p. 1685-1690.

Dalziel, I.W.D., 1994, Precambrian Scotland as a Laurentia-Gondwana link: origin and significance of cratonic promontories: Geology, v. 22, p. 589-592.

Dalziel, I.W.D., 1997, Neoproterozoic-Paleozoic geography and tectonics: Review, hypothesis, environmental speculation: Geological Society of America Bulletin, v. 109, p. 16-42.

Dalziel, I.W.D., Mosher, S., Gahagan, L.M., 2000, Laurentia-Kalahari collision and the assembly of Rodinia: Journal of Geology, v. 108, p. 499-513.

Davis, D.W., Amelin, Y., Nowell, G.M., and Parrish, R.R., 2005, Hf isotopes in zircon from the western Superior province, Canada: Implications for Archean crustal development and evolution of the depleted mantle reservoir: Precambrian Research, v. 140, p. 132-156.

De Broucker, G., 1987, Stratigraphie, pétrographie et structure de la boutonniére de Maquereau-Mictaw (Région de Port-Daniel, Gaspésie): Ministere de l'Energie et des Ressoures, Quebec, MM 86-03, 160 p.

DePaolo, D.J., and Wasserburg, G.J., 1976, Nd isotopic variations and petrogenetic models: Geophysical Research Letters, v. 3, p. 249-252.

Dewey, J.F., and Burke, K., 1974, Hot spots and continental break-up: implications for collisional orogeny: Geology, v. 2, p. 57-60.

Dickin, A.P., 2000, Crustal formation in the Grenville Province: Nd-isotope evidence: Canadian Journal of Earth Sciences, v. 37, p. 165-181.

Dickin, A.P., 2004, Mesoproterozoic and Paleoproterozoic crustal growth in the eastern Grenville Province: Nd isotope evidence from the Long Range inlier of the Appalachian orogen, in Tollo, R.P., Corriveau, L., McLelland, J.M., and Bartholomew, M.J., eds, Proterozoic tectonic evolution of the Grenville orogen in North America: Geological Society of America Memoir, v. 197, p. 495-503

Dix, G.R., Salad Hersi, O., and Nowlan, G.S., 2004, The Potsdam-Beekmantown Group boundy, Nepean Formation type section (Ottawa, Ontario): a cryptic sequence boundary, not a conformable transition: Canadian Journal of Earth Science, v. 41, p. 897-902.

Doig, R., 1970, An alkaline rock province linking Europe and North America: Canadian Journal of Earth Sciences, v. 7, p. 22-28.

Doig, R., and Barton, J.M., Jr., 1968, Ages of carbonatites and other alkaline rocks in Quebec: Canadian Journal of Earth Sciences, v. 5, p. 1401-1407.

Dubé, B., Dunning, G.R., Lauziére, K., and Roddick, J.C., 1996, New insights into the Appalachians orogen from geology and geochronology along the Cape Ray fault zone, southwest Newfoundland: Geological Society of America Bulletin, v. 108, p. 101-116.

Dunning, G.R., and Krogh, T.E., 1985, Geochronology of ophiolites of the Newfoundland Appalachians: Canadian Journal of Earth Sciences, v. 22, p. 1659-1670.

Dunning, G.R., and Cousineau, P., 1990, U/Pb ages of single zircons from Chain Lakes Massif and a correlative unit in ophiolitic melange in Quebec: Geological Society of America Abstracts with Programs, v. 22, no. 2, p. 13.

Dunning, G.R., Wilton, D.H.C., and Herd, R.K., 1989, Geology, geochemistry and geochronology of a Taconic calc-alkaline batholith, southwest Newfoundland: Transactions of the Royal Society of Edinburgh, Earth Sciences, v. 80, p. 159-168.

Dunning, G.R., O'Brien, S.J., Colman-Sadd, S.P., Blackwood, R.F., Dickson, W.L., O'Niell, P.P., and Krogh, T.E., 1990, The Silurian Orogeny in the Newfoundland Appalachians. Journal of Geology, v. 98, p. 895-913.

Elliot, D., and Johnson, M.R.W., 1980, Structural evolution in the northern part of the Moine thrust belt, NW Scotland: Transaction of the Royal Society of Edinburgh, Earth Sciences, v. 71, p. 69-96.

Eriksson, K, Campbell, I., Palin, J., and Allen, C., 2003, Predominance of Grenvillian magmatism recorded in detrital zircons from modern Appalachian rivers: Journal of Geology, v.111, p. 707-717.

Etheridge, M.A., Symonds, P.A., and Lister, G.S., 1989, Application of the detachment model to reconstruction of conjugate passive margins, *in* Tankard, A.J., and Balkwill, H.R., (eds), Extensional tectonics and stratigraphy of the North Atlantic margins: American Association of Petroleum Geologists Memoir, v. 46, p. 23-40.

Faure, G., and Mensing, T.M., 2005, Isotopes: Principles and Applications, 3rd Edition, John Wiley and Sons, Inc., Hoboken, New Jersey, 897p.

Fergusson, C.L., and Cawood, P.A., 1995, Structural history of the metamorphic sole of the Bay of Island Complex, western Newfoundland: Canadian Journal of Earth Sciences, v. 32, p. 533-544.

Francheteau, J., and Le Pichon, X., 1972, Marginal fracture zones as structural framework of continental margins in South Atlantic Ocean: American Association of Petroleum Geologists Bulletin, v. 56, p. 991-1007.

Geraldes, M.C., Van Schmus, W.R., Condie, K.C., Bell, S., Teixeira, W., and Babinski, M., 2001, Proterozoic geologic evolution of the SW part of the Amazonian craton in Mato Grosso State, Brazil: Precambrian Research, v. 111, p. 91-128.

Gillespie, R.T., 1983, Stratigraphic and structural relationships among rock groups at Old Man Pond, western Newfoundland: M.Sc. thesis, Memorial University of Newfoundland, St. John's, Newfoundland, 198 p.

Gorbatschev, R., and Bogdanova, S., 1993, Frontiers in the Baltic Shield, Precambrian Research, v. 64, p. 3-21.

Gower, C.F., and Krogh, T.E., 2002, A U-Pb geochronological review of the Proterozoic history of the eastern Grenville province: Canadian Journal of Earth Sciences, v. 39, p. 795-829.

Griffin, W., Pearson, N., Belousova, N., Jackson, E., van Achterbergh, E., O'Reilly, S., and Shee, S., 2000, The Hf isotope composition of cratonic mantle: LAM-MC-ICPMS analysis of zircon megacrysts in kimberlites: Geochimica et Cosmochimica Acta, v. 64, p. 133-147.

Griffin, W., Wang, X., Jackson, S., Pearson, N., O'Reilly, S., Xu, X., Zhou, X., 2002, Zircon chemistry and magma mixing, SE China: in situ analysis of Hf isotopes, Tonglu and Pingtam igneous complexes: Lithos, v. 61, p. 237-269.

Hamilton, W.B., 2003, An alternative Earth: GSA Today, v. 13, no. 11, p. 4-12.

Hartlaub, R.P, Heaman, L.M., Simonetti, A., and Bohm, C.O., 2006, Relicts of Earth's earliest crust: U-Pb, Lu-Hf, and morphological characteristics of >3.7 Ga detrital zircon of the western Canadian Shield, *in* Reimold, W.U., and Gibson, R.L., eds, Processes on the Earth Earth: Geological Society of America Special Paper, v. 405, p. 75-89.

Heaman, L.M., Philippe, E., and Owen, J.V., 2002, U-Pb geochronologic constraints on the crustal evolution of the Long Range Inlier, Newfoundland: Canadian Journal of Earth Sciences, v. 39, p. 845-865.

Hendricks, M., Jamieson, R., Zentilli, M., and Beaumont, C., 1990, Apatite fission track analysis on the Great Northern Peninsula, western Newfoundland: data and preliminary interpretation, in Hall, J., (ed), Lithoprobe East Transect Report 13, Memorial University of Newfoundland, p. 95-96.

Hibbard, J.P., 1983, Geology of the Baie Verte Peninsula, Newfoundland: Newfoundland Department of Mines and Energy, Mineral Development Division, Memoir, v. 2, 279 p.

Hibbard, J.P., 1988, Stratigraphy of the Fleur de Lys Belt, northwest Newfoundland, in Winchester, J.A., ed., Later Proterozoic Stratigraphy of the Northern Atlantic Regions: Blackie, London, p. 200-211.

Hibbard, J.P., van Staal, C.R., Rankin, D.W., and Williams, H., 2006, Lithotectonic map of the Appalachian Orogen, Canada-United States of America: Geological Survey of Canada, Map-2096A, scale 1:1,500,000.

Hibbard, J.P., van Staal, C.R., and Rankin, D.W., 2007, A comparative analysis of pre-Silurian crustal building blocks of the northern Appalachian and the southern Appalachian orogen: American Journal of Science, v. 307, p. 23-45.

Higgins, M.D., and van Breemen, O., 1998, The age of the Sept-Iles layered mafic intrusion, Canada: Implications for the late Neoproterozoic/Cambrian history of southeastern Canada: The Journal of Geology, v. 106, p. 421–431.

Hodych, J.P., and Cox, R.A., 2007, Ediacaran U-Pb zircon dates for the Lac Matapédia and Mt. St. Anselme basalts of the Quebec Appalachians: support for a long-lived mantle plume during the rifting phase of Iapetus opening: Canadian Journal of Earth Sciences, v. 44, p. 565–581, doi: 10.1139/E06-112.

Hoffman, P.F., 1988, United Plates of America, the birth of a craton: Annual Review of Earth and Planetary Sciences, v. 16, p. 543-603.

Hoffman, P.F., 1991, Did the breakout of Laurentia turn Gondwanaland inside-out? Science, v. 252, p. 1409-1412.

Hogdahl, K., Andersson, U.B., and Eklund, O., (Eds), 2004, The Transscandinavian Igneous Belt (TIB) in Sweden: a review of its character and evolution: Geological Survey of Finland Special Paper, v. 37, Espoo, 123 p.

Isnard, H., and Gariepy, C., 2004, Sm-Nd, Lu-Hf, and Pb-Pb signatures of gneisses and granitoids from the La Grande belt: Extent of late Archean crustal recycling in the northeastern Superior province, Canada: Geochimica et Cosmochimica Acta, v. 68, p. 1099-1113.

Jacobi, R.D., 1981, Peripheral bulge-A causal mechanism for the Lower-Middle Ordovician unconformity along the western margin of the northern Appalachians: Earth and Planetary Science Letters, v. 56, p. 245-251.

James, N.P., and Stevens, R.K., 1986, Stratigraphy and Correlation of the Cambro-Ordovician Cow Head Group, Western Newfoundland, Geological Survey of Canada Bulletin, 143 p.

James, N.P., Stevens, R.K., Barnes, C.R., and Knight, I., 1989, Evolution of a Lower Paleozoic continental margin carbonate platform, northern Canadian Appalachians, in Crevello, P.D., Wilson, J.L., Sarg, J.F., and Read, J.F., (eds) Controls on carbonate platform and basin development: Society of Economic Paleontologists and Mineralogists, Special Publication 44, p. 123-146.

Jamieson, R.A., 1990, Metamorphism of an early Paleozoic continental margin, western Baie Verte peninsula, Newfoundland: Journal of Metamorphic Petrology, v. 8, p. 269-288.

Jarvis, G.T., and McKenzie, D.P., 1980, Sedimentary basin formation with finite extension rates: Earth and Planetary Science Letters, v. 48, p. 42-52.

Jenner, G.A., Dunning, G.R., Malpas, J., Brown, M., and Brace, T., 1991, Bay of Islands and Little Port complexes, revisited: age, geochemical and isotopic evidence confirm suprasubduction-zone origin: Canadian Journal of Earth Sciences, v. 28, p. 1635-1652.

Kalsbeek, F., Thrane, K., Nutman, A.P., and Jepsen, H.F., 2000, Late Mesoproterozoic metasedimentary and granitic rocks in the King Oscar Fjord region, east Greenland Caledonides fold belt: evidence for Grenvillian orogenesis: Journal of the Geological Society, v. 157, p. 1215-1225.

Kamo, S.L., Gower, C.F., and Krogh, T.E., 1989, Birthdate for the Iapetus Ocean? A precise U-Pb zircon and baddeleyite age for the Long Range dikes, southeast Labrador: Geology, v. 17, p. 602-605.

Kamo, S.L., Krogh, T.E., and Kumarapeli, P.S., 1995, Age of the Grenville dyke swarm, Ontario-Quebec: implications for the timing of Iapetan rifting: Canadian Journal of Earth Sciences, v. 32, p. 273-280.

Karson, J.A., 1984, Variations in structure and petrology in the Coastal complex, Newfoundland: anatomy of an ocean fracture zone, *in* Glass, I.G., Lippard, S.J., and Shelton, A.W., (eds), Ophiolites and oceanic lithosphere: Geological Society of London Special Publication, v. 13, p. 131-146.

Karson, J.A., and Dewey, J.F., 1978, Coastal complex, western Newfoundland: an Early Ordovician oceanic fracture zone: Geological Society of America Bulletin, v. 89, p. 1037-1049.

Kennedy, D.P., 1981, Geology of the Corner Brook Lake area, western Newfoundland: M.Sc. thesis, Memorial University of Newfoundland, St. John's, Newfoundland, 370 p.

Keen, C.E., 1982, The continental margins of eastern Canada: A review, *in* Scrutton, R.A., (ed), Dynamics of passive margins: American Geophysical Union and Geological Society of America Geodynamics Series, v. 6, p. 45-58.

Keen, C.E., Kay, W.A., and Roest, W.R., 1990, Crustal anatomy of a transform continental margin: Tectonophysics, v. 173, p. 527-544.

Kerr, A., 2004, An overview of sedimentary rock hosted gold mineralization in western White Bay (NTS Map Area 12H/15): Current Research, Newfoundland Department of Mines and Energy, Report 04-1, p. 23-42.

Kerr, A., and Knight, I., 2004, Preliminary report on the stratigraphy and structure of Cambrian and Ordovician rocks in the Coney Arm in western White Bay (NTS Map Area 12H/15): Current Research, Newfoundland Department of Mines and Energy, Report 04-1, p. 127-136.

Ketchum, J.W.F., Nicholas, G.C., and Barr, S.M., 2002, Anatomy and orogenic history of a Paleoproterozoic accretionary belt: the Makkovik Province, Labrador, Canada: Canadian Journal of Earth Sciences, v. 39, p. 711-730.

Kindle, C.H., and Whittington, H.B., 1958, Stratigraphy of the Cow Head region, western Newfoundland: Geological Society of America Bulletin, v. 69, p. 315-342.

Knight, I., 1983, Geology of the Carboniferous Bay St. George Subbasin, western Newfoundland: Newfoundland Department of Mines and Energy, Mineral Development Divison, Memoir 1.

Knight, I., 1987, Geology of the Roddickton (12I/6) map area: Current Research, Newfoundland Department of Mines and Energy, Mineral Development Division, Report 87-1, p. 343-357.

Knight, I., 1992, Geology of marmorized lower Paleozoic platform carbonate rocks, "Pye's Ridge", Deer Lake: Current Research, Newfoundland Department of Mines and Energy, Report 92-1, p. 141-158.

Knight, I., 1991, Geology of Cambro-Ordovician rocks in the Port Saunders (NTS 12I/11), Castor River (NTS 12I/15), St. John Island (NTS 12I/14) and Torrent River (NTS 12I/10) map areas, St. John's, Newfoundland Department of Mines and Energy, Geological Survey Branch Report 91–4, 138 p.

Knight, I., 1994, Map 93-163 Pasadena 12H/4, Newfoundland and Labrador, Department of Natural Resources, Geological Survey, Open File 1276.

Knight, I., 1996, Geology of Cambro-Ordovician-shelf and coeval rocks, southwest of Corner Brook, western Newfoundland: Geological Survey, Newfoundland Department of Mines and Energy, Open File Report 2602.

Knight, I., 2003, Geology of the North Brook Anticline, Harrys River map area (NTS 12B/09): Current Research, Newfoundland Department of Mines and Energy, Geological Survey Branch, Report 03-1, p. 51-71.

Knight, I., 2006, The Blue Pond thrust stack – New mapping, re-evaluation of structural relationships and implications for allochthonous lower Paleozoic carbonate shelf rocks: Geological Survey, Newfoundland Department of Mines and Energy, Open File Report 2922, 21 p.

Knight, I., and Boyce, W.D., 1991, Deformed Lower Paleozoic platform carbonates, Goose Arm-Old Man's Pond: Current Research, Newfoundland Department of Mines and Energy, Geological Survey Branch, Report 91-1, p. 141-153.

Knight, I., and Cawood, P.A., 1991, Paleozoic geology of western Newfoundland: an exploration of a deformed Cambro-Ordovician passive margin and foreland basin, and Carboniferous successor basin: Center for Earth Resources Research, Short Course Field Guide, 403 p.

Knight, I., and Boyce, W.D., 2000, Geological notes on the Cambro-Ordovician rocks of the Phillips Brook anticline, north of Stephenville: Current Research, Newfoundland Department of Mines and Energy, Geological Survey, Report 2000-1, p. 197-215.

Knight, I., James, N.P., and Lane, T.E., 1991, The Ordovician St. George unconformity: the relationship of plate convergence at the St. Lawrence promontory to the Sauk/Tippecanoe sequence boundary: Geological Society of America Bulletin, v. 103, p. 1200-1225.

Krogh, T.E., and Kamo, S.L., 2006, Precise U-Pb zircon ID-TIMS ages provide an alternative interpretation to early ion microprobe ages and new insights into Archean crustal processes, northern Labrador, *in* Reimold, W.U., and Gibson, R.L., eds, Processes on the Earth Earth: Geological Society of America Special Paper, v. 405, p. 91-103.

Kurth, M., Sassen, A., Suhr, G., and Mezger, K., 1998, Precise ages and isotopic constraints for the Lewis Hills (Bay of Islands Ophiolite): preservation of an arc-spreading ridge intersection: Geology, v. 26, p. 1127-1130.

Kumarapeli, P.S., 1985, Vestiges of Iapetan rifting in the craton of the Northern Appalachians: Geoscience Canada, v. 12, p. 54–59.

Kumarapeli, P.S., 1993, A plume-generated segment of the rifted margin of Laurentia, southern Canadian Appalachians, seen through a completed Wilson Cycle: Tectonophysics, v. 219, p. 47-55.

Kumarapeli, P.S., Dunning, G.R., Pintson, H., and Shaver, J., 1989, Geochemistry and U-Pb zircon age of comenditic metafelsites of the Tibbit Hill Formation, Quebec Appalachians: Canadian Journal of Earth Sciences, v. 26, p. 1374–1383.

Lacelle, M.A., Hagadorn, J.W., and Groulx, P., 2008, The widespread distribution of Cambrian Medusae: Scyphomedusa strandings in the Potsdam Group of southwestern Quebec: Geological Society of America Abstracts with Programs, v. 40, p. 371.

Lavoie, D., and Asselin, E., 1998, Upper Ordovician facies in the Lac Saint-Jean outlier, Québec (eastern Canada): palaeoenvironmental significance for Late Ordovician oceanography: Sedimentology, v. 45, p. 817-832.

Lavoie, D., Burden, E., and Lebel, D., 2003, Stratigraphic framework for the Cambrian–Ordovician rift and passive margin successions from southern Quebec to western Newfoundland: Canadian Journal of Earth Sciences, v. 40, p. 177–205, doi: 10.1139/e02-078.

Lavoie, D., Chi, G., Brennan-Alpert, P., Desrochers, A., and Bertrand, R., 2005, Hydrothermal dolomitization in the Lower Ordovician Romaine Formation of the Anticosti Basin: significance for hydrocarbon exploration: Bulletin of Canadian Petroleum Geology, v. 53, p. 454-472.

Leeder, M.R., 1995, Continental rifts and proto-oceanic rift troughs, *in* Busby, C.J., and Ingersoll, R.V., eds., Tectonics of sedimentary basins: Cambridge, Massachusetts, Blackwell Science, p. 67-87.

Lemieux, Y., Tremblay, A., and Lavoie, D., 2003, Structural analysis of supracrustal faults in the Charlevoix area, Quebec; relation to impact cratering and the St-Laurent fault system: Canadian Journal of Earth Sciences, v. 40, p. 221-235.

Li, Z.X., Bogdanova, S.V., Collins, A.S., Davidson, A., De Waele, B., Ernst, R.E., Fitzsimons, I.C.W., Fuck, R.A., Gladkochob, D.P., Jacobs, J., Karlstrom. K.E., Lu, S., Natopov, L.M., Pease, V., Pisarevsky, S.A., Thrane, K., Vernikovsky, V., 2008, Assembly, configuration, and breakup of Rodinia: a synthesis: Precambrian Research, v. 160, p. 179-210.

Lillie, R.J., 1999, Whole Earth Geophysics: an introductory textbook for geologists and geophysicists: Prentice-Hall, Inc., Upper Saddle River, New Jersey, 361 p.

Lilly, H.D., 1963, Geology of the Hughes Brook-Goose Arm area: Memorial University of Newfoundland Department of Geology, Report 2, 123 p.

Lindholm, R.M., and Casey, J.F., 1990, The distribution and possible biostratigraphic significance of the ichnogenus Oldhamia in the shales of the Blow Me Down Brook Formation, western Newfoundland: Canadian Journal of Earth Sciences, v. 27, p. 1270-1287.

Lister, G.S., Etheridge, M.A., and Symonds, P.A., 1986, Detachment faulting and the evolution of passive continental margins: Geology, v. 14, p. 246–250, doi: 10.1130/0091-7613(1986)14<246:DFATEO>2.0.CO;2.

Lister, G.S., Etheridge, M.A., and Symonds, P.A., 1991, Detachment models for the formation of passive continental margins: Tectonics, v. 10, p. 1038–1064, doi: 10.1029/90TC01007.

Loewy, S.L., Connelly, J.N., Dalziel, I.W.D., and Gower, C.F., 2003, Eastern Laurentia in Rodinia: constraints from whole-rock Pb and U/Pb geochronology: Tectonophysics, v. 375, v. 169-197.

Longuépée, H., and Cousineau, P.A., 2005, Reapprasial of the Cambrian glauconite-bearing Anse Maranda Formation, Quebec Appalachians: from deep-sea turbidites to clastic shelf deposits: Canadian Journal of Earth Sciences, v. 42, p. 259–272, doi: 10.1139/e05-003.

Ludwig, K.R., 2003, Isoplot/Ex version 3.00, A geochronological toolkit for Microsoft Excel: Berkeley Geochronology Center Special Publication, v. 4, 74p.

Malo, M., Kirkwood, D., De Broucker, G., and St-Julien, P., 1992, A reevaluation of the position of the Baie Verte-Brompton Line in the Quebec Appalachians: the influence of Middle Devonian strike-slip faulting in Gaspé Peninsula: Canadian Journal of Earth Sciences, v. 29, p. 1265-1273.

Marquis, R., and Kumarapeli, P.S., 1993, An Early Cambrian deltaic-fluvial model for an Iapetan rift-arm drainage system, southeastern Quebec: Canadian Journal of Earth Sciences, v. 30, p. 1254–1261.

Marshak, S., 2004, Salients, recesses, arcs, oroclines, and syntaxes: a review of ideas concerning the formation of map-view curves in fold-thrust belts, *in* McClay, K.R., (ed), Thrust tectonics and hydrocarbon systems: AAPG Memoir, v. 82, p. 1-26.

Mascle, J., and Blarez, E., 1987, Evidence for transform margin evolution from the Ivory Coast-Ghana continental margin: Nature, v. 326, p. 378-381.

McCausland, P.J.A., and Hodych, J.P., 1998. Paleomagnetism of the 550 Ma Skinner Cove volcanics of western Newfoundland and opening of the Iapetus Ocean: Earth and Planetary Science Letters, v. 163, p. 15-29.

McClay, K.R., and Buchanan, P.G., 1992, Thrust faults in inverted extensional basins, *in* McClay, K.R., (ed), Chapman and Hall, London, p. 93-104.

McLelland, J., Daly, J. S., and McLelland, J. M., 1996, The Grenville orogenic cycle (ca. 1350-1000 Ma): an Adirondack perspective: Tectonophysics, v. 265, p. l-28.

McLelland, J., Hamilton, M., Selleck, B., McLelland, J.M., 2001, Zircon U-Pb geochronology of the Ottawan orogeny, Adirondack Highlands, New York: Regional and tectonic implications: Precambrian Research, v. 109, p. 39-72.

McKenzie, D.P., 1978, Some remarks on the development of sedimentary basins: Earth and Planetary Science Letters, v. 40, p. 25-32.

Miller, B.V., and Barr, S.M., 2000, Petrology and isotopic composition of a Grenvillian basement fragment in the northern Appalachian orogen: Blair River inlier, Nova Scotia, Canada: Journal of Petrology, v. 41, p. 1777-1804.

Moecher, D. and Samson, S., 2006, Differential zircon fertility of source terranes and natural bias in the detrital zircon record: Implications for sedimentary provenance analysis: Earth and Planetary Science Letters, v. 247, p. 252-266.

Moench, R.H., and Aleinikoff, J.N., 2003, Stratigraphy, geochronology, and accretionary terrane settings of two Bronson Hill arc sequences, northern New England: Physics and Chemistry of the Earth, v. 28, p. 113-160.

Mohr, P., 1982, Musings on continental rifts: American Geophysical Union Geodynamics Series, v. 8, p. 293-309.

Mueller, P.A., Heatherington, A.L., Wooden, J.L., Shuster, R.D., Nutman, A.P., Williams, I.S., 1994, Precambrian zircons from the Florida basement; a Gondwanan connection: Geology, v. 22, p. 119-122.

Mueller, P., Foster, D., Mogk, D., Wooden, J., and Vogl, J., 2007, Provenance of the Uinta Mountain Group from Pb and Hf isotopic compositions of detrital zircons: Geology, v. 35, p. 431-434.

Mueller, P.A., Kamenov, G.D., Heatherington, A.L., and Richards, J., 2008, Crustal evolution in the southern Appalachian orogen: evidence from Hf isotopes in detrital zircons: Journal of Geology, v. 116, p. 414-422.

Nance, R.D., and Linnemann, U., 2008, The Rheic Ocean: origin, evolution, and significance: GSA Today, v. 18, n. 12, p. 4-12.

Nowlan, G.S., and Barnes, C.R., 1987, Thermal maturation of Paleozoic strata in eastern Canada from conodont colour alteration index (CAI) data with implications for burial history, tectonic evolution, hotspot tracks and mineral and hydrocarbon potential: Geological Survey of Canada Bulletin, v. 369, 47 p.

Nutman, A.P., McGregor, V.R., Friend, C.R.L., Bennett, V.C., and Kinney, P.D., 1996, The Itsaq gneiss complex of southern west Greenland; the world's most extensive record of early crustal evolution (3900-3600 Ma): Precambrian Research, v. 78, p. 1-39.

Owen, 1991, Geology of the Long Range inlier, Newfoundland: Geological Survey of Canada Bulletin, v. 395, p. 1-89.

Osberg, P.H., 1969, Lower Paleozoic stratigraphy and structural geology, Green Mountain-Sutton Mountain Anticlinorium, Vermont and southern Quebec, in Kay, G.M., ed., North Atlantic—Geology and continental drift. A symposium on the origin of the Atlantic Ocean, Gander Newfoundland: American Association of Petroleum Geologists Memoir, v. 12, p. 687–700.

Paces, J.B., and Miller, J.D., 1993, Precise U-Pb ages for the Duluth Complex and related mafic intrusions, northeastern Minnesota: geochronological insights to physical, petrogenetic, paleomagnetic and tectonomagmatic processes associated with the 1.1 Ga Midcontinent Rift system: Journal of Geophysical Research, v. 98, p. 13,997-14,013.

Palmer, A.R., 1971, The Cambrian of the Appalachian and eastern New England regions, eastern United States, in Holland, C.H., ed., Cambrian of the New World: New York, Intersci., p. 169-217.

Palmer, S.E., Burden, E., and Waldron, J.W.F., 2001, Stratigraphy of the Curling Group (Cambrian), Humber Arm Allochthon, Bay of Islands: Current research, Newfoundland Department of Mines and Energy, Geological Survey Report 01–1, p. 105–112.

Palmer, S.E., Waldron, J.W.F., and Skilliter, D.M., 2002, Post-Taconian shortening, inversion and strike slip in the Stephenville area, western Newfoundland Appalachians: Canadian Journal of Earth Sciences, v. 39, p. 1393-1410.

Pinet, N., Duchesne, M., Lavoie, D., Bolduc, A., and Bernard, L., 2008, Surface and subsurface signatures of gas seepage in the St. Lawrence Estuary (Canada): Significance to hydrocarbon exploration: Marine and Petroleum Geology, v. 25, p. 271–288, doi: 10.1016/j.marpetgeo.2007.07.011.

Pisarevsky, S.A., Wingate, M.T.D., Powell, C.M., Johnson, S., and Evans, D.A.D., 2003, Models of Rodinia assembly and fragmentation, in Yoshida, M., Windley, B.F.,

and Dasgupta, eds, Proterozoic East Gondwana: Supercontinent assembly and breakup; Geological Society of London Special Publication, v. 206, p. 35-55.

Quinn, L.A., 1988, Distribution and significance of Ordovician flysch units in western Newfoundland: Current Research, Part B, Geological Survey of Canada, Paper 88-1B, p. 119-126.

Rankin, D.W., 1976, Appalachian salients and recesses: Late Precambrian continental breakup and the opening of the Iapetus Ocean: Journal of Geophysical Research, v. 81, p. 5605-5619.

Rankin, D.W., Drake, A. A., Jr, Glover, L. III, Goldsmith, R., Hall, L. M., Murray, D. P., Ratcliffe, N. M., Read, J. F., Secor, D. T., Jr, Stanley, R. S., 1989, Pre-orogenic terranes, in Hatcher, R. D., Jr, Thomas, W. A., Viele, G. W., (eds), The Appalachian-Ouachita Orogen in the United States: Geologic Society of America, Boulder, CO, F-2, p. 7-100.

Restrepo-Pace, P.A., Ruiz, J., Gehrels, G., and Cosca, M., 1997, Geochronology and Nd isotopic data of Grenville-age rocks in the Colombian Andes: New constraints for Late Proterozoic-early Paleozoic paleocontinental reconstructions of the Americas: Earth and Planetary Science Letters, v. 150, p. 427-441.

Rivers, T., 1997, Lithotectonic elements of the Grenville province: Review and tectonic implications: Precambrian Research, v. 86, p. 117-154.

Rivers, T., 2008, Assembly and preservation of lower, mid, and upper orogenic crust in the Grenville province-implications for the evolution of large hot long-duration orogens: Precambrian Research, v. 167, p. 237-259.

Rodgers, J., 1968, The eastern edge of the North American continent during the Cambrian and Early Ordovician, in Zen, E-an, White, W.S., Hadley, J.B., and Thompson, J.B., Jr., eds, Studies of Appalachian geology, northern and maritime: New York, Intersci., p. 141-149.

Rogers, J. J. W., and Santosh, M., 2004, Continents and Supercontinents: Oxford University Press, Inc, New York, New York, 289p.

Rosendahl, B.R., 1987, Architecture of continental rifts with special reference to East Africa: Annual Review of Earth and Planetary Sciences, v. 15, p. 445-503.

Rudnick, R.L., and Fountain, D.M., 1995, Nature and composition of the continental crust: a lower crustal perspective: Reviews of Geophysics: v. 33, p. 267-309.

Rudnick, R.L., and Gao, S., 2003, Composition of the continental crust, *in* Rudnick, R.L., ed, The Crust, Vol. 3 of Holland, H., and Turekian, K., eds, Treatise on geochemistry. Oxford, Pergamon, p. 1-64.

Sadowski, G.R., 2002, The fit between Amazonia, Baltica, and Laurentia during the Mesoproterozoic assemblage of the supercontinent Rodinia: Gondwana Research, v. 5, p. 101-107.

Sadowski, G.R., and Bettencourt, J.S, 1996, Mesoproterozoic tectonic correlations between eastern Laurentia and the western boarder of the Amazonian craton: Precambrian Research, v. 76, p. 213-227.

Santos, J.O.S., Rizzotto, G.J., Potter, P.E., McNaughton, N.J., Matos, R.S., Hartmann, L.A., Chemale, F., and Quadros, M.E.S., 2008, Age and autochthonous evolution of the Sunsas Orogen in west Amazon craton based on mapping and U-Pb geochronology: Precambrian Research, v. 165, p. 120-152.

Salad Hersi, O., Lavoie, D., Hilowle Mohamed, A., and Nowlan, G.S., 2002. Subaerial unconformity at the Potsdam – Beekmantown contact in the Québec Reentrant (southwestern Québec – eastern Ontario): regional significance for the Laurentian continental margin history: Bulletin of Canadian Petroleum Geology, v. 50, p. 419-440.

Salad Hersi, O., Lavoie, D., and Nowlan, G.S., 2003, Reappraisal of the Beekmantown Group sedimentology and stratigraphy, Montréal area, southwestern Québec: implications for understanding the depositional evolution of the Lower-Middle Ordovician Laurentian passive margin of eastern Canada: Canadian Journal of Earth Sciences, v. 40, p. 149-176.

Salad Hersi, O., Nowlan, G.S., and Lavoie, D., 2007, A revision of the stratigraphic nomenclature of the Cambrian-Ordovician strata of the Phillipsburg tectonic slice, southern Quebec: Canadian Journal of Earth Sciences, v. 44, p. 1775-1790.

Sanford, B.V., 1993, St. Lawrence Platform, in Scott, D.F., and Aitken, J.D., eds., Sedimentary Cover of the Craton in Canada, Geological Survey of Canada, Geology of Canada 5, p. 723–786.

Schmoker, J.W., and Halley, R.B., 1982, Carbonate porosity versus depth: a predictable relation for South Florida: AAPG Bulletin, v. 66, p. 2561-2570.

Schubert, C., and Dunbar, C.O., 1934, Stratigraphy of western Newfoundland: Geological Society of America, Memoir, v. 1, 123 p.

Sclater, J.G., and Christie, P.A.F., 1980, Continental stretching: An explanation of the post-mid-Cretaceous subsidence of the central North Sea basin: Journal of Geophysical Research, v. 85, no. B7, p. 3711-3739.

Scrutton, R.A., 1982, Passive continental margins: A review of observations and mechanisms, *in* Scrutton, R.A., (ed), Dynamics of passive margins: American

Geophysical Union and Geological Society of America Geodynamics Series, v. 6, p. 5-11.

Sleep, N.H., 1971, Thermal effects of the formation of Atlantic continental margins by continental breakup: The Geophysical Journal of the Royal Astronomical Society, v. 24, p. 325-350.

Spencer, C., Green, A., Morel-à-l'Huissier, P., Milkereit, B., Leutgert, J., Stewart, D., Unger, J., and Phillips, J., 1989, The extension of the Grenville basement beneath the northern Appalachians: results from the Quebec-Maine seismic reflection and refraction surveys. Tectonics, v. 8, p. 677-696.

Soderlund, U., Patchett, P., Vervoort, J., and Isachsen, C., 2004, The ^{176}Lu decay constant determined by Lu-Hf and U-Pb isotope systematics of Precambrian mafic intrusions: Earth and Planetary Science Letters, v. 219, p. 311-324.

Soderlund, U., Isachsen, C.E., Bylund, G., Heaman, L.M., Patchett, P.J., Vervoort, J.D., and Andersson, U.B., 2005, U-Pb baddeleyite ages and Hf, Nd, isotope chemistry constraining repeated mafic magmatism in the Fennoscandian Shield from 1.6 to 0.90 Ga: Contributions to Mineralogy and Petrology, v. 150, p. 174-194.

Stanley, R., and Ratcliffe, N., 1985, Tectonic synthesis of the Taconian orogeny in western New England: Geological Society of America Bulletin, v. 96, p. 1227-1250.

Stecker, M.A., and Watts, AB., 1978, Subsidence of Atlantic-type continental margins off New York: Earth and Planetary Science Letters, v. 41, p. 1-13.

Stenzel, S.R., Knight, I., and James, N.P., 1990, Carbonate platform to foreland basin: revised stratigraphy of the Table Head Group (Middle Ordovician), western Newfoundland: Canadian Journal of Earth Sciences, v. 27, p. 14-26.

Stevens, R.K., 1970, Cambro-Ordovician flysch sedimentation and tectonics in west Newfoundland and their possible bearing on a Proto-Atlantic Ocean, *in* Lajoie, J., (ed), Flysch Sedimentology in North America: Geological Association of Canada Special Paper, v. 7, p. 165-178.

Stewart, D.B., Wright, B.E., Unger, J.D., Phillips, J.D., Hutchinson, D.R., 1993, Global geoscience traverse 8: Quebec-Maine-Gulf of Maine transect, southeastern Canada, northeastern United States of America (with contributions by J.H. Luetgert, W.A. Bothner, K.D. Klitgord, L.M. Liberty, Carl Spencer), US Geological Survey Miscellaneous Investigations Series Map I-2329, 17 scale 1:1,000,000.

Stewart, J., Gehrels, G., Barth, A., Link, P., Christie-Blick, N., and Wrucke, C., 2001, Detrital zircon provenance of Mesoproterozoic to Cambrian arenites in the

western united States and northwestern Mexico: Geological Society of America Bulletin, v. 113, p. 1343-1356.

Stockmal, G.S., and Waldron, J.W.F., 1990, Structure of the Appalachian deformation front in western Newfoundland: implications from multichannel seismic reflection data: Geology, v. 18, p. 765-768.

Stockmal, G.S., and Waldron, J.W.F., 1993, Structural and tectonic evolution of the Humber Zone, western Newfoundland, Part 1. Implications of balanced cross sections through the Appalachian structural front, Port au Port peninsula: Tectonics, v. 12, no. 4, p. 1056-1075.

Stockmal, G.S., Waldron, J.W.F., and Quinlan, G.M., 1995, Flexural modeling of Paleozoic foreland basin subsidence: evidence for substantial post-Taconian thrust transport: Journal of Geology, v. 103, p. 653-671.

Stockmal, G.S., Slingsby, A., and Waldron, J.W.F., 1998, Deformation styles at the Appalachian structural front, western Newfoundland: implications of new industry seismic reflection data: Canadian Journal of Earth Sciences, v. 35, p. 1299-1306.

Stockmal, G.S., Slingsby, A., and Waldron, J.W.F., 2004, Basement-involved inversion at the Appalachian structural front, western Newfoundland; an interpretation of seismic reflection data with implications for petroleum prospectivity: Bulletin of Canadian Petroleum Geology, v. 52, p. 215-233.

Stukas, V., and Reynolds, P.H., 1974, 40Ar/39Ar dating of the Long Range dikes, Newfoundland: Earth and Planetary Science Letters, v. 22, p. 256-266.

Swinden, H.S., Jenner, G.A., and Szybinski, Z.A., 1997, Magmatic and tectonic evolution of the Cambrian-Ordovician Laurentian margin of Iapetus: geochemical and isotopic constraints from the Notre Dame Subzone, Newfoundland, in Sinha, K., Whalen, J.B., and Hogan, J., (eds), Magmatism in the Appalachian orogen: Geological Society of America Memoir, v. 191, p. 337-365.

Sylvester, A.G., 1988, Strike-slip faults: Geological Society of America Bulletin, v. 100, p. 1666-1703.

Theriault, R.J., and Ermanovics, I., 1997, Sm-Nd isotopic and geochemical characterisation of the Paleoproterozoic Torngat orogen, Labrador, Canada: Precambrian Research, v. 81, p. 15-35.

Thomas, W.A., 1977, Evolution of Appalachian-Ouachita salients and recesses from reentrants and promontories in the continental margin: American Journal of Science, v. 277, p. 1233.

Thomas, W.A., 1991, The Appalachian-Ouachita rifted margin of southeastern North America: Geological Society of America Bulletin, v. 103, p. 415–431, doi: 10.1130/0016-7606(1991)103<0415:TAORMO>2.3.CO;2.

Thomas, W.A., 1993, Low-angle detachment geometry of the late Precambrian-Cambrian Appalachian-Ouachita rifted margin of southeastern North America: Geology, v. 21, p. 921–924, doi: 10.1130/0091-7613(1993)021<0921:LADGOT>2.3.CO;2.

Thomas, W.A., 2006, Tectonic inheritance at a continental margin: GSA Today, v. 16, no. 2, p. 4-11.

Thomas, W.A., and Astini, R.A., 1999, Simple-shear conjugate rift margins of the Argentine Precordillera and the Ouachita Embayment of Laurentia: Geological Society of America Bulletin, v. 111, p. 1069–1079, doi: 10.1130/0016-7606(1999)111<1069:SSCRMO>2.3.CO;2.

Thomas, W.A., and Schenk, P.E., 1988, Late Palaeozoic sedimentation along the Appalachian orogen, *in* Harris, A.L., and Fettes, D.J., (eds), The Caledonian-Appalachian Orogen: Geological Society Special Publication, No. 38, p. 515-530.

Thomas, W.A., and Astini, R.A., 1999, Simple-shear conjugate rift margins of the Argentine Precordillera and the Ouachita Embayment of Laurentia: Geological Society of America Bulletin, v. 111, p. 1069–1079, doi: 10.1130/0016-7606(1999)111<1069:SSCRMO>2.3.CO;2.

Tohver, E., van der Pluijm, B.A., Van der Voo, R., Rizzotto, G., and Scandolara, J.E., 2002, Paleogeography of the Amazon craton at 1.2 Ga: early Grenvillian collision with the Llano segment of Laurentia: Earth and Planetary Science Letters, v. 199, p. 185-200.

Tohver, E., Bettencourt, J.S., Tosdal, R., Mezger, K., Leite, W.B., and Payolla, B.L., 2004, Terrane transfer during the Grenville orogeny: tracing the Amazonian ancestry of the southern Appalachian basement through Pb and Nd isotopes: Earth and Planetary Science Letters, v. 228, p. 161-176.

Trzcienski, W.E., Jr., Rodgers, J., and Guidotti, C.V., 1992, Alternative hypotheses for the Chain Lakes “Massif”, Maine and Quebec: American Journal of Science, v. 292, p. 508-532.

Tucker, R.D., and Gower, C.F., 1994, A U-Pb geochronological framework for the Pinware terrane, Grenville Province, southeast Labrador: Journal of Geology, v. 102, p. 67-78.

Tuke, M.F., 1968, Autochthonous and allochthonous rocks in the Pistolet Bay area in northernmost Newfoundland: Canadian Journal of Earth Sciences, v. 5, p. 501-513.

van Berkel, J.T., and Currie, K.L., 1988, Geology of the Puddle Pond (12A/5) and Little Grand Lake (12A/12) map areas, southwestern Newfoundland: Newfoundland Department of Mines, Mineral Development Division Report, v. 88-1, p. 99-107.

van der Pluijm, B.A., and Marshak, S., 2004, Earth Structure, 2nd Edition, W.W. Norton and Company, Inc., New York, New York, 656 p.

van Staal, C.R., 2005. Regional Geology of North America: Northern Appalachians: Encyclopedia of Geology, v. 4, Elsevier Publishers, London, p. 81-92.

van Staal, C.R., Sullivan, R.W., and Whelan, J., 1996, Provenance and tectonic history of the Gander Margin in the Caledonian/Appalachian Orogen: implications for the origin and assembly of Avalonia, in Nance, R.D., and Thompson, M.D., (eds), Avalonian and related terranes of the Circum-North Atlantic: Geological Society of America Special Paper, v. 304, p. 347-367.

van Staal, C.R., Dewey, J.F., MacNiocaill, C., and McKerrow, W.S., 1998, The Cambrian-Silurian tectonic evolution of the northern Appalachians and British Caledonides: history of a complex, west and southwest Pacific-type segment of Iapetus, *in* Blundell, D.J., and Scott, A.C., (eds), Lyell: the Past is the Key to the Present: Geological Society, London, Special Publications, v. 143, p. 199-242.

van Staal, C.R., Castonguay, S., McNicoll, V., Brem, A., Hibbard, J.P., Skulski, T., and Joyce, N., 2009, Taconic arc-continent collision confirmed in the Newfoundland Appalachians: Geological Society of America Abstracts with Programs, v. 41, no. 3, p. 4.

Vermeesch, P., 2004, How many grains are needed for a provenance study?: Earth and Planetary Science Letters, v. 224, p. 351-441.

Vervoort, J.D., and Patchett, P.J., 1996, Behavior of hafnium and neodymium isotopes in the crust: Constraints from Precambrian crustally derived granites: Geochimica et Cosmochimica Acta, v. 60, p. 3717-3733.

Vervoort, J.D., and Blichert-Toft, J., 1999, Evolution of the depleted mantle: Hf isotope evidence from juvenile rocks through time: Geochimica et Cosmochimica Acta, v. 63, p. 533-556.

Vervoort, J.D., Patchett, P.J., Soderlund, U., and Baker, M., 2004, Isotopic composition of Yb and the determination of Lu concentrations and Lu/Hf ratios by isotope dilution using MC-ICPMS: Geochemistry, geophysics, geosystems, v. 5, Q11002, doi:10.1029/2004GC000721.

Waldron, J.W.F., 1985, Structural history of continental margin sediments beneath the Bay of Islands Ophiolite, Newfoundland: Canadian Journal of Earth Sciences, v. 22, p. 1618-1632.

Waldron, J.W.F., and Stockmal, G.S., 1991, Mid-Paleozoic thrusting at the Appalachian deformation front: Port au Port Peninsula, western Newfoundland: Canadian Journal of Earth Sciences, v. 28, p. 1992-2002.

Waldron, J.W.F., and Stockmal, G.S., 1994, Structural and tectonic evolution of the Humber Zone, western Newfoundland, Part 2: a regional model for Acadian thrust tectonics: Tectonics, v. 13, p. 1498-1513.

Waldron, J.W.F., and Palmer, S.E., 2000, Lithostratigraphy and structure of the Humber Arm allochthon in the type-area, Bay of Islands, Newfoundland: Current Research, Newfoundland Department of Mines and Energy, Geological survey, Report 2000-1, p. 2790-290.

Waldron, J.W.F., and van Staal, C.R., 2001, Taconian orogeny and the accretion of the Dashwoods block: a peri-Laurentian microcontinent in the Iapetus Ocean: Geology, v. 29, no. 9, p. 811-814.

Waldron, J.W.F., Turner, D., and Stevens, K.M., 1988, Stratal disruption and development of mélange, western Newfoundland: effect of high fluid pressure in an accretionary terrain during ophiolite emplacement: Journal of Structural Geology, v. 10, p. 861-873.

Waldron, J.W.F., Stockmal, G.S., Corney, R.E., and Stenzel, S.R., 1993, Basin development and inversion at the Appalachian structural front, Port au Port peninsula, western Newfoundland Appalachians: Canadian Journal of Earth Sciences, v. 30, p. 1759-1772.

Waldron, J.W.F., Anderson, S.D., Cawood, P.A., Goodwin, L.B., Hall, J., Jamieson, R.A., Palmer, S.E., Stockmal, G.S., and Williams, P.A., 1998, Evolution of the Appalachian Laurentian margin: Lithoprobe results in western Newfoundland: Canadian Journal of Earth Science, v. 35, p. 1271-1287.

Waldron, J.W.F., Henry, A.D., and Bradley, J.C., 2002, Structure and polyphase deformation of the Humber Arm allochthon and related rocks west of Corner Brook, Newfoundland: Current Research, Department of Mines and Energy, Geological survey, Report 02-1, p. 47-52.

Waldron, J.W.F., Henry, A.D., Bradley, J.C., and Palmer, S.E., 2003, Development of a folded thrust stack: Humber Arm Allochthon, Bay of Islands, Newfoundland Appalachians: Canadian Journal of Earth Sciences, v. 40, p. 237-253.

Walsh, G.J., and Aleinikoff, J.N., 1999, U-Pb zircon age of metafelsite from the Pinney Hollow Formation: implications for the development of the Vermont Appalachians: American Journal of Science, v. 299, p. 157-170.

Wernicke, B., 1985, Uniform-sense normal simple shear of the continental lithosphere: Canadian Journal of Earth Sciences, v. 22, p. 108–125.

Whalen, J.B., van Staal., C.R., Longstaffe, F.J., Gariépy, C., and Jenner, G.A., 1997, Insights into tectonostratigraphic zone identification in southern Newfoundland based on isotopic (Nd, O, Pb) and geochemical data: Atlantic Geology, v. 33, p. 231-241.

Wardle, R.J., Ryan, B., Philippe, S., and Scharer, U., 1990, Proterozoic crustal development, Goose Bay region, Grenville Province, Labrador, Canada, *in* Gower, C.F., Rivers, T., and Ryan, A.B., eds, Mid-Proterozoic Laurentia-Baltica: Geological Association of Canada Special Paper, v. 38, p. 197-214.

Whitmeyer, S.J., and Karlstrom, K.E., 2007, Tectonic model for Proterozoic growth of North America: Geosphere, v. 3, p. 220-259.

Wilkerson, M.S., and Hsui, A. T.-K., 1989, Application of sediment backstripping corrections for basin analysis using microcomputers: Journal of Geological Education, v. 37, p. 337-340.

Williams, H., 1964, The Appalachians in northeastern Newfoundland: a two-sided symmetrical system: American Journal of Science, v. 262, p. 1137-1158.

Williams, H., 1979, Appalachian Orogen in Canada: Canadian Journal of Earth Sciences, v. 16, p. 792-807.

Williams, H., 1985, Geology of Gros Morne area, 12H/12, (west half) western Newfoundland: Geological Survey of Canada, Open File Map, 1134, scale 1:50,000

Williams, H., and Hatcher, R.D., 1983, Appalachian suspect terranes, *in* Contribution to the tectonics and geophysics of mountain chains, Hatcher, R.D., Williams, H., and Zietz, I., (Eds): Geological Society of America Memoir, v. 158, p. 35-53.

Williams, H., editor, 1995, Geology of the Appalachian-Caledonian orogen in Canada and Greenland: Ottawa, Geological Survey of Canada, Geology of North America, v. F-2, 944p.

Williams, H., and St. Julien, P., 1978, The Baie-Verte Brompton Line in Newfoundland and regional correlations in the Canadian Appalachians: Current Research, Part A, Geological Survey of Canada, Paper 78-1A, p. 225-229.

Williams, H., and Hatcher, R.D., 1983, Appalachian suspect terranes, *in* Contribution to the tectonics and geophysics of mountain chains, Hatcher, R.D., Williams, H., and Zietz, I., (Eds): Geological Society of America Memoir, v. 158, p. 35-53.

Williams, H., and Hiscott, R.N., 1987, Definition of the Iapetus rift-drift succession in western Newfoundland: Geology, v. 15, p. 1044-1047.

Williams, H., and Cawood, P.A., 1989, Geology of the Humber Arm allochthon, Newfoundland, Geological Survey of Canada, Ottawa, Ontario, Map 1678A.

Williams, H., Gillespie, R.T., and van Breemen, O., 1985, A late Precambrian rift-related igneous suite in western Newfoundland: Geology, v. 15, p. 1727-1735.

Williams, H., Cawood, P.A., James, N.P., and Botsford, J.W., 1986, Geology of the St. Pauls Inlet (12H/13), western Newfoundland: Geological Survey of Canada, Open File Map, 1238, scale 1:50,000

Williams, S.H., Burden, E.T., and Mukhopadhyay, P.K., 1998, Thermal maturity and burial history of Paleozoic rocks in western Newfoundland: Canadian Journal of Earth Sciences, v. 35, p. 1307-1322.

Wilson, J.T., 1966, Did the Atlantic close and then re-open?: Nature, v. 211, p. 676-681.

VITA

John Stefan Allen

Birthplace: Spartanburg, South Carolina

Birth date: July 2nd, 1981

Educational Background

M.Sc. (2003-2005) from the Department of Marine, Earth, and Atmospheric Sciences, North Carolina State University, Raleigh, North Carolina
Thesis Title: "The structure and kinematics of the Gold Hill fault zone in the vicinity of Waxhaw, North Carolina"
Thesis Supervisor: Dr. James P. Hibbard

B.Sc. (1999-2003) from the Department of Earth and Environmental Sciences, Furman University, Greenville, South Carolina.

Professional Experience:

Session co-organizer and co-chair (2009), Structural Geology and Tectonics, Technical sessions, SE Section, Geological Society of America meeting, St. Petersburg, Florida.

Field Trip Leader (2008), The Heart of Carolinia: Stratigraphic and Tectonic Studies in the Carolina Terrane of Central North Carolina: Geological Society of America, Southeastern Section Field Trip.

Volunteer Employee (2007), Geological Survey of Canada, Quebec Division, Dr. Denis Lavoie supervising.

Teaching Assistant (2006-2007), University of Kentucky
GLY 130: Dinosaurs and Disasters
GLY 235: Fundamentals of Geology (I) [Field Methods]

Field Trip Leader (2004), Geology of the Carolina Terrane and the Gold Hill fault zone in the vicinity of Waxhaw, NC and Van Wyck, SC: MS field defense.

Graduate Instructor (2003-2005), NC State University
MEA 110: Introduction to Geology Laboratory
MEA 110F: Introduction to Geology Laboratory/Field Geology
MEA 110H: Introduction to Geology Honors
MEA 451: Structural Geology

Peer Consultant (2000-2003), Furman University, Center for Collaborative Learning and Communication

Professional Affiliations.

Geological Society of America, student member (2006-current).

American Association of Petroleum Geologists, student member (2007-current).

AAPG Bluegrass Student Chapter: Founding member and Vice President, 2007-2008.

Grants and Awards

AAPG Arthur A. Meyerhoff Memorial Grant (2008), "The structure of the Iapetan rifted margin, western Newfoundland: An isotopic test for a new hypothesis"

Sigma Xi, Student Grant-in-aid of Research (2008), "Paleogeographic reconstruction of the eastern Laurentian rifted margin: an isotopic provenance test"

University of Kentucky Graduate School (2008), Dissertation Enhancement Award

Eastern Section AAPG (2007), Margaret Hawn Mirabile Best Student Paper Award; paper entitled: "Preliminary interpretation of syn-rift and early post-rift stratigraphy on the St. Lawrence promontory"

Geological Society of America (2007), "Palinspastic restoration of the northern Appalachian Iapetus rifted margin in western Newfoundland and the Gulf of St. Lawrence"

Geological Survey of Canada (2007), "Palinspastic restoration of the northern Appalachian Iapetus rifted margin in Newfoundland and Quebec"

University of Kentucky Department of Earth and Environmental Sciences (2006-2009), Pirtle Summer Research Fellowship

Furman University (2002), Furman Advantage Summer Research Grant

Publications.

Allen, J.S., Thomas, W.A., and Lavoie, D., (*submitted*), The Laurentian margin of northeastern North America; submitted to GSA Memoir special Appalachian volume.

Allen, J.S., Thomas, W.A., and Lavoie, D., 2009, Stratigraphy and structure of the Laurentian rifted margin in the northern Appalachians: a low-angle detachment rift system: Geology, v. 37, p. 335-338.

Allen, J.S., Hibbard, J.P., and Boland, I.B., 2008, Structure, kinematics, and timing of deformation of the Gold Hill fault zone in Hancock, South Carolina and Waxhaw, North Carolina: South Carolina Geology, v. 46, p.15-29.

Hibbard, J.P., Pollock, J., Allen, J.S., Brennan, M., 2008, The Heart of Carolinia: Stratigraphic and tectonic studies in the Carolina terrane of central North Carolina: Geological Society of America Geologic Field Trip Guide Book, Southeastern Section, 54 p.

Allen, J.S., Buffaloe, J. R., Lockery, J.R., Garihan, J.M., and Ranson, W.A., 2008, Geologic Map of the Dacusville 7.5-minute quadrangle, Greenville and Pickens Counties, South Carolina: South Carolina Department of Natural Resources, Geologic Map 42.

Abstracts.

Allen, J.S., Thomas, W.A., Mueller, P.A., Kamenov, G., and Hycinth, L., 2009, Paleogeographic provenance of Iapetan synrift detrital zircons from the St. Lawrence promontory, western Newfoundland: a U-Pb and Hf isotopic study: Geological Society of America Abstracts with Programs, v. 41, no. 1

Thomas, W.A., Mueller, P.A., McClelland, B., Kamenov, G., Allen, J.S., and Hycinth, L., 2009, Provenance of the Middle-Late Ordovician clastic wedge in the Argentine Precordillera: Geological Society of America Abstracts with Programs, v. 41, no. 1.

Allen, J.S., and Thomas, W.A., 2008, Palinspastic restoration of the eastern Laurentian margin on the St. Lawrence promontory, western Newfoundland: Preliminary results: American Association of Petroleum Geologists Student Expo, Houston, KY.

Allen, J.S., and Thomas, W.A., 2008; Does a low-angle detachment model apply to the eastern Laurentian rifted margin in the northern Appalachians?; GAC-MAC Joint Conference.

Allen, J.S., and Thomas, W.A., 2008, The Iapetan rifted margin in the northern Appalachians: A low-angle detachment model applied from south to north: Geological Society of America Abstracts with Programs, v. 40, no. 4, p. 10.

Allen, J.S., and Thomas, W.A., 2007, Preliminary interpretation of the Laurentian rifted margin on the St. Lawrence promontory: Geological Society of America Abstracts with Programs, v. 39, no. 6, p. 615.

Allen, J.S., and Thomas, W.A., 2007, Preliminary interpretation of syn-rift and early post-rift stratigraphy on the St. Lawrence promontory: American Association of Petroleum Geologists Annual Meeting, Eastern Section, Lexington, KY.

Allen, J.S., Miller, B.V., Hibbard, J.P., Boland, I.B., 2007, Significance of intrusive rocks along the Charlotte-Carolina terrane boundary: Evidence for the timing of deformation in the Gold Hill fault zone near Waxhaw, North Carolina: Geological Society of America Abstracts with Programs, v. 39, no. 2, p. 12.

Allen, J.S., and Hibbard, J.P., 2006, Evidence and implications of synkinematic contact metamorphism around the Waxhaw pluton, south-central North Carolina: Geological Society of America Abstracts with Programs, v. 38, no. 3, p. 73.

Box, G.H., Allen, J.S., and Hibbard, J.P., 2006, Structural character of the Smith River allochthon in central and south-central Virginia: Geological Society of America Abstracts with Programs, v. 38, no. 3, p. 77.

Allen, J.S., Hibbard, J.P., and Boland, I.B., 2005, Structure and Kinematics of the Gold Hill fault zone in south-central North Carolina: Geological Society of America Abstracts with Programs, v. 37, no. 2, p. 5.

Allen, J.S., Lockery, J.R., Garihan, J.M., and Ranson, W.A., 2003, Geology of the southern half of the Dacusville 7.5-minute quadrangle, Pickens County, South Carolina: Geological Society of America Abstracts with Programs, v. 35, no. 1, p. 23.

Plate 3.1 Balanced cross sections 1 to 4 perpendicular to structural strike across the deformed Laurentian margin exposed in the Appalachians of western Newfoundland. Datum is the top of the Early Cambrian (Unit 1). Cross sections 1 through 3 depict the geology of southwestern Newfoundland on Port au Port peninsula and in the Indian Head Range north of Stephenville. Cross section 4 displays the geology of the Humber Arm allochton through the Bay of Islands and east of Corner Brook. See Figure 3.11 for the location of each cross section. All four cross sections have been palinspastically restored using a combination of line-length and area balancing techniques (see text). Restored sections 2, 3, and 4 display the distance between the present position of the leading edge of the Humber Arm allochthon (i.e. Appalachian structural front of Stockmal and Waldron, 1993) and the restored trailing edge of the allochthon. Because there are no piercing points between rocks on the shelf in lines 2 and 3 and in the Humber Arm allochthon currently exposed in western Newfoundland, the leading edge of the Humber Arm allochthon is restored outboard of the trailing edge of the restored shelf.

Explanation

Structural cross sections

- Lithotectonic contact
- Projection of eroded lithotectonic contact
- Formation contact
- Fault
- Projection of eroded fault
- Apparent dip angle
- Apparent dip angle of overturned bedding
- Pin line
- Loose line
- Schematic break in section
- *Long Range Mountains* — Geographic location/Landmark
- **Round Head fault** — Exposed structure
- **(Round Head fault)** — Subsurface structure
- Undivided slope stratigraphy/Melange

Lithotectonic Units

shelf

not represented

5

4

3

2

1

Precambrian

Age

Lower Mississippian

Lower Devonian

Upper Silurian

Upper Ordovician

Middle Ordovician

Lower Ordovician

Upper Cambrian

Middle Cambrian

Lower Cambrian

Precambrian

General Shelf Stratigraphy

Codroy Gp

unconf.

Red Island Road Fm

Clam Bank Fm

unconf.

Long Point Gp — Miaty Point Fm; Winterhouse Fm; Lourdes Limestone

unconf.

Goose Tickle Gp

Table Head Gp — Cape Cormorant Fm (not); Table Cove Fm; Table Point Fm

unconf.

St. George Gp

Port au Port Gp

Reluctant Head Fm (Line 4 only)

Labrador Gp — Hawkes Bay Fm; Forteau Fm; Bradore Fm

unconf.

Crystalline basement

General Stratigraphy of the Humber Arm Supergroup (Line 4 only)

Corner Brook Thrust Sheet

Lithotectonic Units

top of exposure

Eagle Island Fm

Middle Arm Point Fm

Cooks Brook Fm

unconf.

Irishtown Fm

Summerside Fm

base unexposed

Northern Head Gp

Curling Gp

Watsons Brook Thrust Sheet

Lithotectonic Units

top of exposure

Goose Tickle Gp

Pinchgut Lake Gp

base unexposed

Woods Island Thrust Sheet

Lithotectonic Units

top of exposure

Blow Me Down Brook Fm

base unexposed

Corner Brook Lake terrane (Line 4 only)

Lithotectonic Units

top of exposure

Breeches Pond Fm

South Brook Fm

base unexposed

Mount Musgrave Gp

km 0 2 4 6

Scale

PLATE 3.1

Plate 3.2 Balanced cross sections 5 to 9 perpendicular to structural strike across the deformed Laurentian margin exposed in the Appalachians of western Newfoundland. Datum is the top of the Early Cambrian (Unit 1). These five cross sections represent the geology of the Northern Peninsula north of Bonne Bay. See Figure 3.11 for the location of each cross section. All five cross sections have been palinspastically restored using a combination of line-length and area balancing techniques (see text). Restored sections 5, 6, and 7 display the distance between the present position of the leading edge of the Humber Arm allochthon (i.e. Appalachian structural front of Stockmal and Waldron, 1993) and the restored trailing edge of the allochthon. Because there are no piercing points between rocks on the shelf and in the Humber Arm allochthon currently exposed in western Newfoundland, the leading edge of the Humber Arm allochthon is restored outboard of the trailing edge of the restored shelf. Reduced, full-length, palinstically restored wire-frame cross sections are displayed below lines that contain schematic breaks (Lines, 5, 6, and 7).

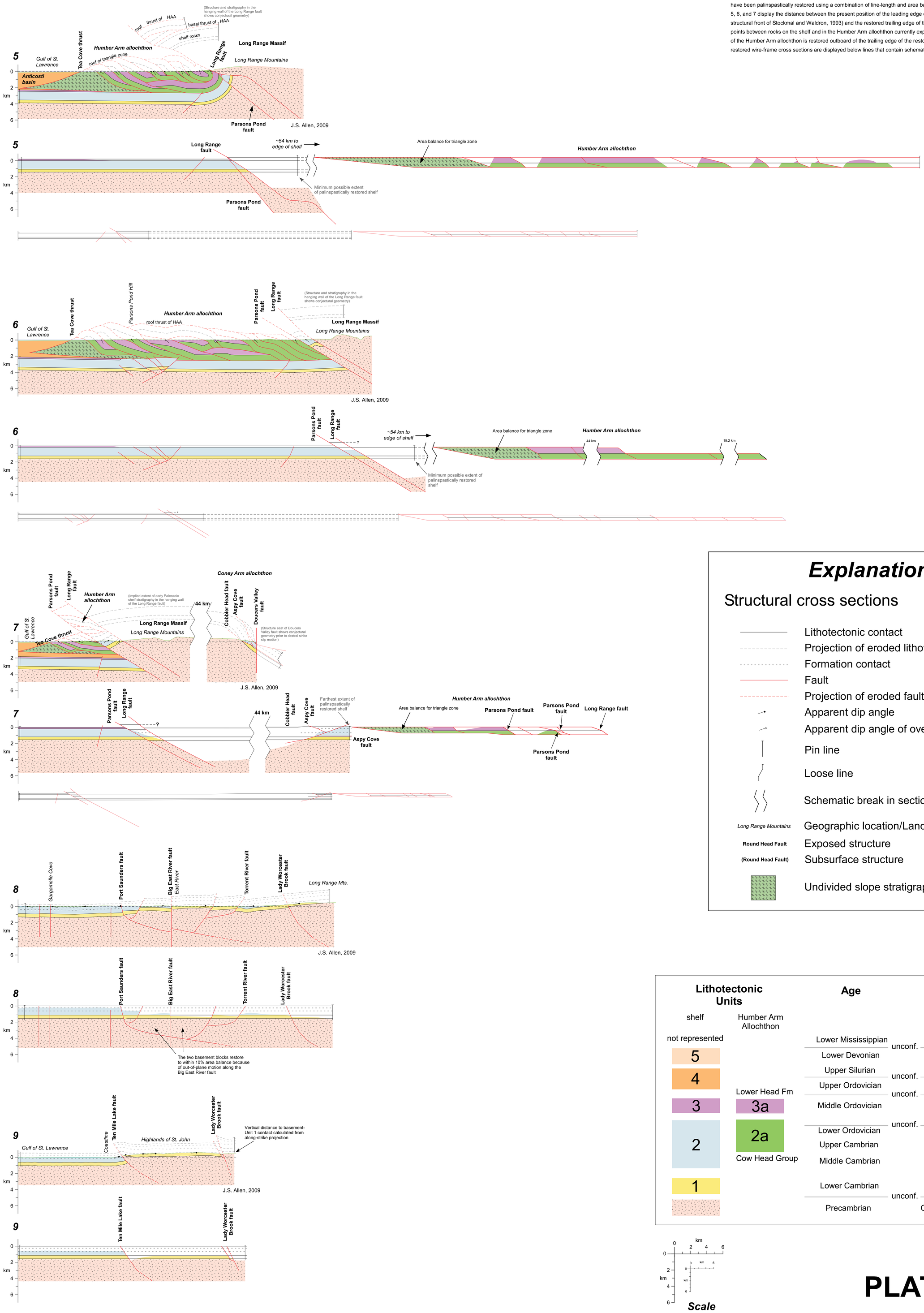

Explanation

Structural cross sections

- Lithotectonic contact
- Projection of eroded lithotectonic contact
- Formation contact
- Fault
- Projection of eroded fault
- Apparent dip angle
- Apparent dip angle of overturned bedding
- Pin line
- Loose line
- Schematic break in section
- *Long Range Mountains* — Geographic location/Landmark
- **Round Head Fault** — Exposed structure
- **(Round Head Fault)** — Subsurface structure
- Undivided slope stratigraphy/Melange

Lithotectonic Units		Age		General Shelf Stratigraphy
shelf	Humber Arm Allochthon			
not represented		Lower Mississippian	unconf.	Codroy Gp
5		Lower Devonian		Red Island Road Fm
4		Upper Silurian	unconf.	Clam Bank Fm
		Upper Ordovician	unconf.	Long Point Gp (- Misty Point Fm, - Winterhouse Fm, - Lourdes Limestone)
3	Lower Head Fm 3a	Middle Ordovician	unconf.	Goose Tickle Gp
2	2a	Lower Ordovician	unconf.	Table Head Gp (- Table Cove Fm, - Table Point Fm)
	Cow Head Group	Upper Cambrian		St. George Gp
		Middle Cambrian		Port au Port Gp
1		Lower Cambrian	unconf.	Labrador Gp (- Hawkes Bay Fm, - Forteau Fm, - Bradore Fm)
		Precambrian		Crystalline basement

Scale

PLATE 3.2